E-2338

FINAL REPORT

CONTRACT NAS 12-614

September 1968

INSTRUMENTATION LABORATORY

MASSACHUSETTS INSTITUTE OF TECHNOLOGY

Cambridge 39, Mass.

E-2338

FINAL REPORT

CONTRACT NAS 12-614

Prepared by

The Tactical Systems Group

for

The Electronics Research Center

National Aeronautics and Space Administration

September 1968

Instrumentation Laboratory
Massachusetts Institute of Technology
Cambridge, Massachusetts

Approved _____
R. B. Trueblood
Associate Director

Approved _____
J. B. Feldman
Executive Officer

ACKNOWLEDGMENT

This report was prepared in connection with DSR Project 55-30900 under NASA Contract NAS 12-614 by the Massachusetts Institute of Technology Instrumentation Laboratory, Cambridge, Massachusetts 02139.

Publication of this report does not constitute NASA approval of its contents.

CONTENTS

CONTENTS (contd.)

Chapter 1

Program Summary

1.1 Introduction

This report summarizes the services performed and the material prepared and compiled by the Tactical Systems Group of the Instrumentation Laboratory for the Electronics Research Center of the National Aeronautics and Space Administration under Contract NAS 12-614. The objective of the effort under this contract has been to provide the Center with background information and control system design data to support the Center's program for advanced avionics technology for V/STOL aircraft.

1.2 Scope of Effort

The work under this contract was carried out under the six tasks described below. The descriptions presented here paraphrase the more lengthy wording of the contractual work statement.

1. Conduct a series of helicopter flight control system seminars for ERC personnel including the following topics
    a. Helicopter Dynamics
    b. Helicopter Flight Control System Design and Simulation
    c. Flight Test Equipment and Procedures.

2. Prepare data packages covering the following topics

   a. Analysis Package to include equations of motion, trim parameters and stability derivatives for selected flight conditions, control linkage characteristics, etc. for the YHC-1A helicopter serial #85514.

   b. Simulation Package to include equations of motion and the simulator mechanization used by MIT/IL in prior simulation work.

3. Assist ERC in developing a simulation of the YHC-1A helicopter serial #85514 on the analog computer at ERC.

4. Perform an analytical design of a digital advanced flight control system for the YHC-1A helicopter serial #85514. Design to be based on prior work at MIT/IL under U. S. Army Contract DA 44-177-TC-757. (This task was cancelled after preliminary work including determination of Laplace, z plane and w plane transforms had been completed.)

5. Assist ERC by planning the design of an experimental guidance and control installation for the YHC-1A helicopter serial #85514. (This task was cancelled after preliminary work including general equipment block diagrams had been completed.)

6. Assist ERC in the design and implementation of certain interface equipment for the ERC fixed base helicopter cockpit simulator.

1.3 Utilization of Effort

The approximate fractional utilization of the technical effort for the above tasks was as follows:

Task 1	16%
Task 2	16%
Task 3	16%
Task 4	13%
Task 5	21%
Task 6	18%
	100%

1.4 Organization of Report

For convenience of reference, the material of this report is presented under four subject headings rather than in chronological order of preparation. Specific material of importance from the seminars (Task 1) has been included under the subject headings as appropriate. Aside from this, the relation between the subject headings and the contract tasks is as follows:

Chapter No.	Subject	Tasks Included
2.	Analytical System Design	2a, 4
3.	Helicopter Simulation	2b, 3
4.	Experimental Guidance and Control Equipment	5
5.	Simulation Interface Equipment	6

Since most of the detailed material consists of equation derivations data tabulations, block diagrams, and similar items, it appeared desirable to place it in a series of appendices rather than in the main text. In addition, the printout of the s-, z-, and w- transforms computed for the YHC-1A was physically too large for inclusion in the present document. It is, therefore, supplied in the form of an addendum.

Chapter 2

Analytical System Design

2.1 Development of Linearized Equations of Motion

The equations of motion which form the mathematical model of the aircraft were the principal subject of the first seminar. At this seminar, notes entitled "The Development of Linearized Equations of Motion and Performance Functions for VTOL Aircraft" were distributed to ERC personnel. This material, which was adapted from previous MIT/IL reports, is included in this report as Appendices A and B.

2.2 Development of Linearized Performance Functions

A section of the notes distributed at Seminar I was concerned with the development of linearized performance functions. This material is included as Appendix C.

Digital computer programs available at MIT have been used to calculate the Laplace, z- and w- transform performance functions for the YHC-1A for flight condition 1 (normal C.G., 13,400 lb. gross weight, zero rate of climb, sea level) at air speeds of 0, 40, 80, and 140 knots. The z- and w- transforms were computed for a sampling rate of 20/second. These performance functions in the form of a computer print out are furnished as an addendum to this report.

2.3 Definition of Symbols

The symbols used in the equations of motion are not the conventional ones used by NASA. These symbols and their definitions are tabulated in Appendix D. Where an equivalent NASA symbol exists, it is given.

2.4 Sequence Diagrams for the Analytical Design Process

A general sequence diagram for the flight control system design process is shown in Figure 2-1. A more detailed sequence diagram applicable to the analytical design of a longitudinal flight control system is presented in Figure 2-2.

2.5 Helicopter Operating Limits

A representative helicopter flight envelope is shown in Figure 2-3. The various factors that limit the maximum true airspeed at different altitudes are plotted on the figure.

An example of the so-called "dead man's" curve associated with engine failure in a helicopter is shown in Figure 2-4. Flight in the cross-hatched regions on this plot is unsafe in that a crash will result if there is a total engine failure.

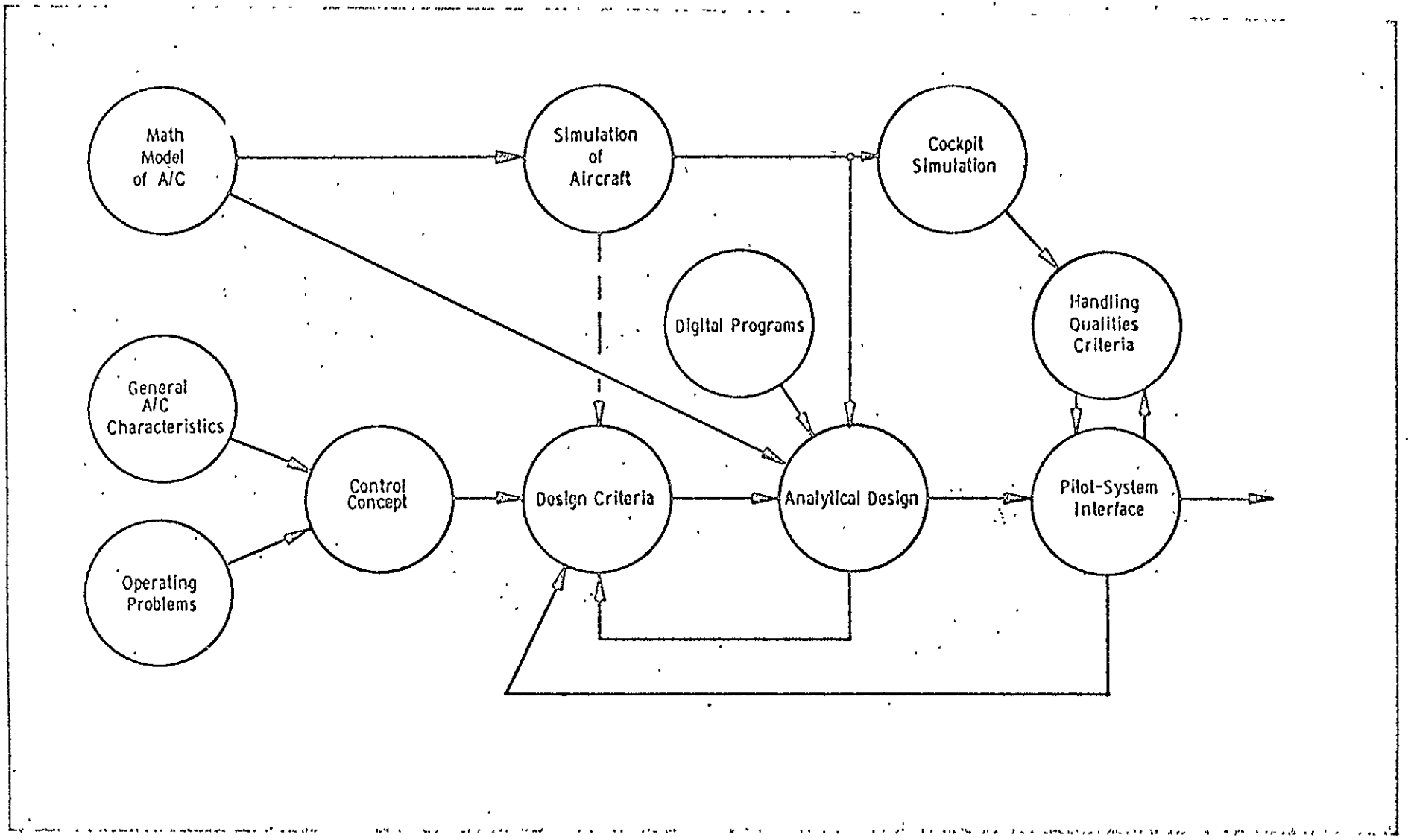

Fig. 2-1 Sequence Diagram of Flight Control System Design Process

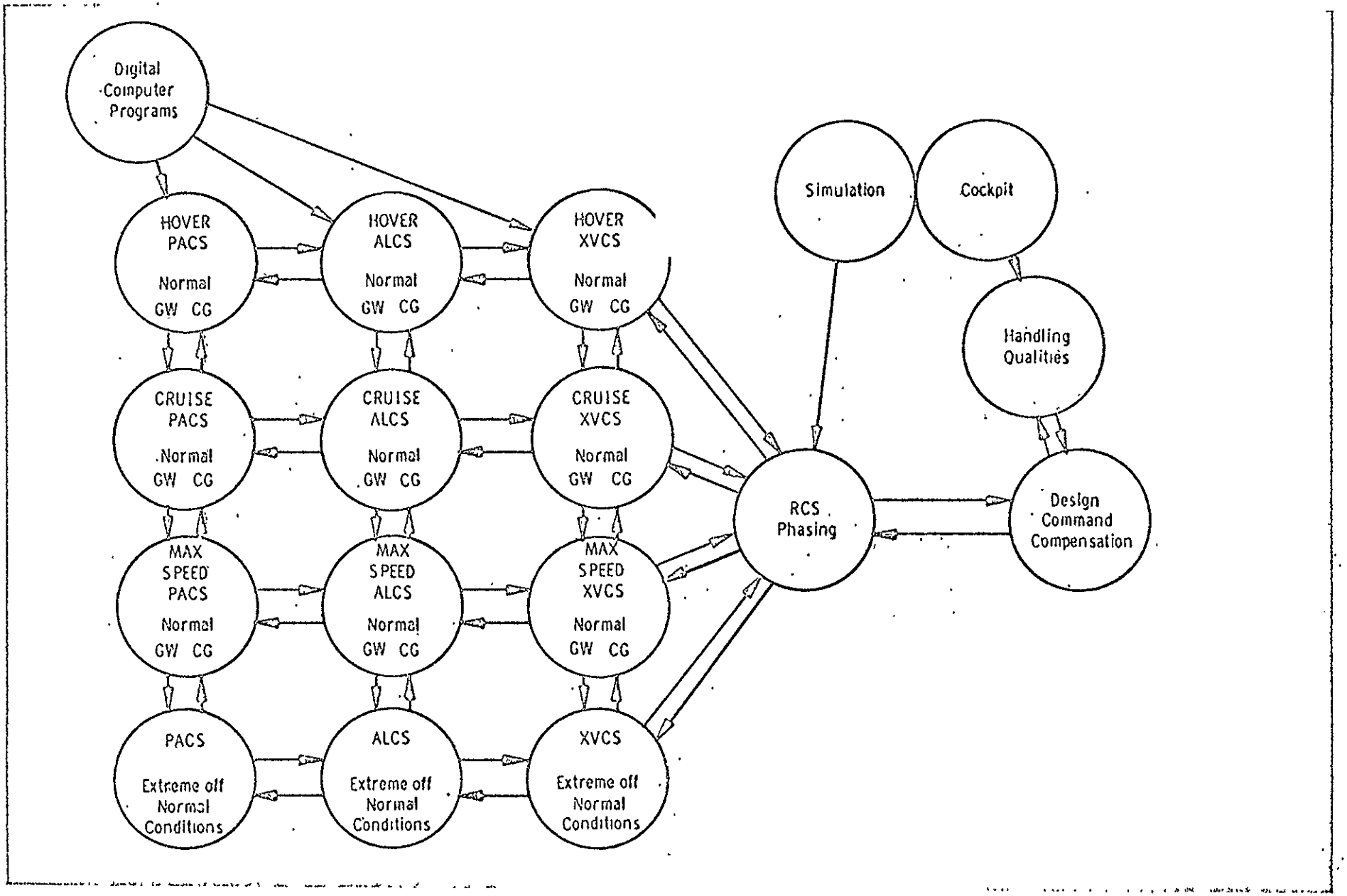

Fig. 2-2 Sequence Diagram for Analytical Design of the Longitudinal System

CH-113 HELICOPTER
MAX TRUE AIRSPEED VS ALTITUDE

ROTOR RPM = 264 (100%)
GW = 18700 LBS
STD DAY

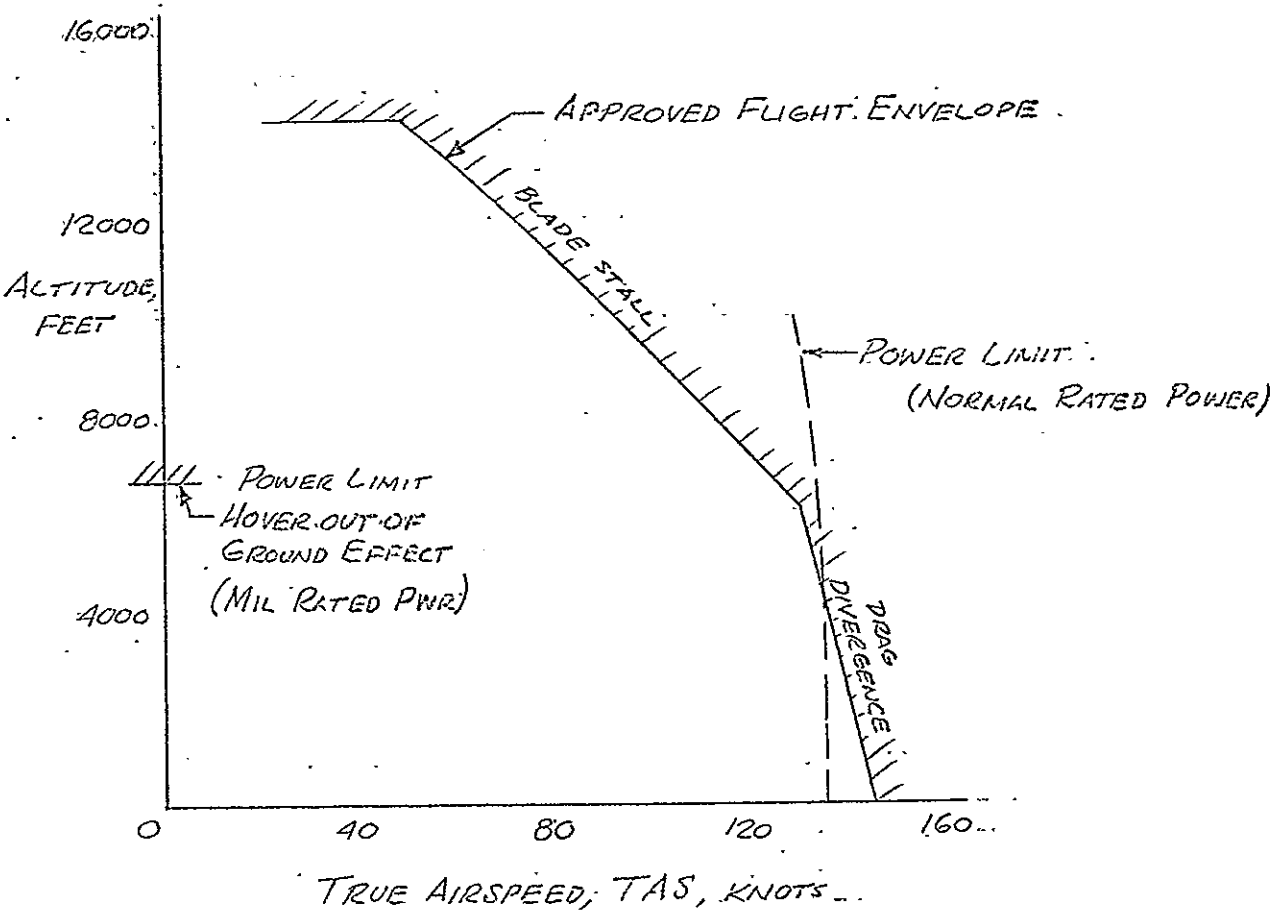

SOURCE: VERTOL REPORT # 107-AD-008

Fig. 2-3 Example of a Flight Envelope

BOEING VERTOL 107-II HELICOPTER
HEIGHT AND INDICATED AIRSPEEDS FOR SAFE
LANDING AFTER AN ENGINE FAILURE

VALID FOR DENSITY ALTITUDE UP TO +2600 FEET
OPERATION AT AIRSPEEDS AND HEIGHTS WITHIN THE
SHADED AREAS IS NOT APPROVED

NOTES: FOR ALLOWABLE WEIGHT SEE MAXIMUM TAKEOFF GROSS WEIGHT TABLE, PAGE 1-1

HARD SURFACE RUNWAY OR WATER, WIND--CALM

AT HEIGHTS ABOVE 90 FEET, ONE SECOND DELAY DEMONSTRATED DURING LEVEL FLIGHT OPERATION (100% ROTOR RPM)

POINT "A" INDICATES ROTATION IAS (REFER TO AIRSPEED CALIBRATION, FIGURES 4-5 and 4-6)

OVER WATER OPERATION

ENTRY INTO WATER AT AIRSPEEDS IN EXCESS OF 30 KNOTS NOT APPROVED

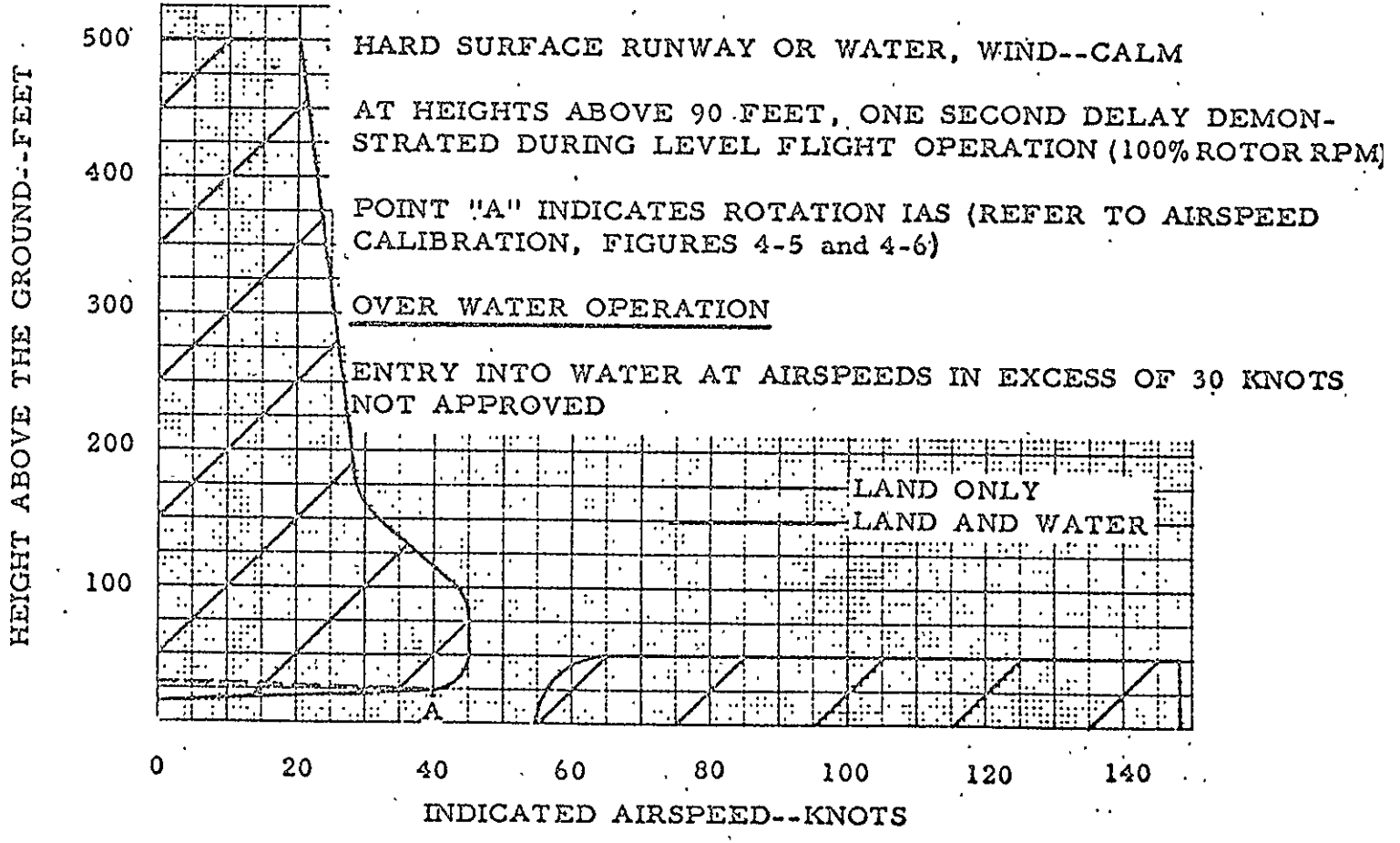

FAA APPROVED REISSUED MAY 9, 1966

Fig. 2-4 Example of "Dead Man's" Curve

Chapter 3

Helicopter Simulation

3.1 Summary of the MIT/IL Simulation of the CH-46C

In order to assist ERC in achieving an early start on the analog computer simulation of the helicopter, the details of the MIT/IL simulation of the CH-46C were transmitted to ERC as Addendum #2 to the Monthly Technical Progress Report of February 1968. This material is presented in Tables I and II, Figure 3-1 and Appendix I. Table I gives the equations of the airframe and the transfer functions of the servos and of the aircraft's control system. Table II gives the coordinate transformations involving the Euler angles (H, E, ϕ) used to describe the orientation of the aircraft. The airframe equations were derived from Equations 86-91 in Appendix B.

The approach used in the development of the simulation is in part similar to the conventional linearization procedure. However, all important stability derivatives are varied with airspeed and provisions for generating trim conditions have been made. The resulting simulation thus accounts for the variation of airframe trim and dynamic characteristics with forward speed. Gross weight, C.G. position, and altitude are treated as constants during any given computer run.

The stability derivatives that are varied with airspeed are shown in Figure 3-1. These plots were obtained from the data tabulated in Appendix G. Derivatives other than the eight shown in Figure 3-1 are treated as constants in the simulation and their hover values are used over the entire speed range. The mechanization of the equations of motion on the MIT/IL Pace computer was accomplished according to the connection diagrams in Appendix I. The computer component assignment sheets including potentiometer settings are also included in Appendix I.

The primary assumptions made in the variable airspeed simulation are that the airspeed changes relatively slowly compared to the natural periods and time constants of the airframe modes and that airspeed is the only important variable in producing non-linear affects. These assumptions lead to the quasi-linearized force expressions on the right side of the equations in Table I. Use of these equations leads to the generation of trim values of E, δ_e, and δ_z in reasonable agreement with the correct values of the NCH-46C aircraft.

3.2 Description of Alternate Simulation Scheme for Generating Trim Values.

Although the initial ERC simulation was based on the same trim mechanization used by MIT in order to facilitate a comparison of the simulations, an alternate trim generating scheme was recommended for subsequent utilization. This alternate method, which was described in Seminar II on 13 February 1968, is shown schematically in Figure 3-2. The steady state flight path for the generalized perturbation analysis is assumed to be straight and level with zero sideslip. Thus the unperturbed flight path is characterized by only a single non-zero quantity namely $V_{(AM-A)x_c}$. This quantity is obtained by subtracting the wind velocity

(including gusts), $\vec{V}_{(E-AM)_A}$, from the aircraft velocity $\vec{V}_{(E-A)_A}$ to give the vector airspeed $\vec{V}_{(AM-A)_A}$. The horizontal component of airspeed is then obtained by means of the A- to C- frame transformation (first equation in Table II). This quantity is the independent parameter from which the trimmed control deflections δ_{z_o} and δ_{e_o}, the trimmed pitch angle, E_o, and selected stability derivatives are computed. Since the equations of motion are expressed in the A- frame, it is necessary to resolve the steady state velocity into the A- frame corresponding to the trimmed condition. The difference between the output of this resolution and the vector airspeed is the incremental velocity, $\Delta\vec{V}_{(AM-A)_A}$, needed to compute force and moment increments in the perturbed equations of motion.

Figure 3-3 shows the curves of δ_{e_o}, δ_{z_o}, and E_o as functions of TAS that must be mechanized in the "Control Trim" and "Euler Angle Trim" boxes respectively. Approximate empirical equations for δ_{z_o} and E_o are given. A constant value of δ_{e_o} may be used in view of the small variations in the trim value relative to the total stick travel. (This assumption is predicated on the use of the LCT schedule without which the δ_e trim may be quite large at high speeds)

The equations of motion of the helicopter needed to implement the trim generating scheme of Figure 3-2 are slightly different from those given in the previous simulation data package. A sample derivation of one of the equations is shown in Figure 3-4 and the complete set of six equations of motion for the helicopter are summarized in Figure 3-5. Geometry and wind relations are presented in Figure 3-6.

INSTRUMENTATION LABORATORY
MASSACHUSETTS INSTITUTE OF TECHNOLOGY
CAMBRIDGE MASS.

TABLE I

PREPARED BY: RMac
DATE: 8Mar68

EQUATIONS USED IN THE MIT/IL SIMULATION OF THE NCH-46C HELICOPTER

SHEET.
OF

LONGITUDINAL AIRFRAME EQUATIONS

X-FORCE:
$$\dot{V}_{XA} = \frac{1}{m}\{\int X_{V_X}\dot{V}_{XA}\,dt + X_{VZ}\Delta V_{ZA} + X_q\,\omega_{YA} + X_{\delta e}\Delta\delta_e + X_{\delta z}\Delta\delta_z + X_{GX}\Delta G_{XA} + X_{GZ}\Delta G_{ZA} - W\cos E_o\,\Delta E\} - \omega_{YA}(V_{ZA_o} + \Delta V_{ZA})$$

Z-FORCE:
$$\dot{V}_{ZA} = \frac{1}{m}\{\int Z_{V_X}\dot{V}_{XA}\,dt + Z_{VZ}\Delta V_{ZA} + Z_q\,\omega_{YA} + Z_{\delta e}\Delta\delta_e + Z_{\delta z}\Delta\delta_z + Z_{GZ}\Delta G_{ZA} + W\cos\phi\cos E - W\cos E_o\} + \omega_{YA}(V_{XA_o} + \Delta V_{XA}) - \omega_{XA}\Delta V_{YA}$$

PITCHING MMT:
$$\dot{\omega}_{YA} = \frac{1}{I_Y}\{\int M_{V_X}\dot{V}_{XA}\,dt + M_{VZ}\Delta V_{ZA} + M_q\,\omega_{YA} + M_{\delta e}\Delta\delta_e + M_{\delta z}\Delta\delta_z + M_{GX}\Delta G_{XA} + M_{GZ}\Delta G_{ZA}\}$$

LATERAL AIRFRAME EQUATIONS

Y-FORCE:
$$\dot{V}_{YA} = \frac{1}{m}\{Y_{V_Y}\Delta V_{YA} + Y_p\,\omega_{XA} + Y_r\,\omega_{ZA} + Y_{\delta a}\Delta\delta_a + Y_{\delta r}\Delta\delta_r + Y_{GY}\Delta G_{YA} + W\cos E_o\,\Delta\phi\} + \omega_{XA}\Delta V_{ZA} - \omega_{ZA}(V_{XA_o} + \Delta V_{XA})$$

ROLLING MMT:
$$\dot{\omega}_{XA} = \frac{1}{I_X}\{L_{V_Y}\Delta V_{YA} + L_p\,\omega_{XA} + L_r\,\omega_{ZA} + L_{\delta a}\Delta\delta_a + L_{\delta r}\Delta\delta_r + L_{GY}\Delta G_{YA} + J_{ZX}\,\dot{\omega}_{ZA}\}$$

YAWING MMT:
$$\dot{\omega}_{ZA} = \frac{1}{I_Z}\{N_{V_Y}\Delta V_Y + N_p\,\omega_{XA} + N_r\,\omega_{ZA} + N_{\delta a}\Delta\delta_a + N_{\delta r}\Delta\delta_r + N_{GY}\Delta G_{YA} + J_{ZX}\,\dot{\omega}_{XA}\}$$

SERVO, ROTOR, AND BOOST UNIT TRANSFER FUNCTIONS

$$\dot{\delta}_{(\,)} = \frac{\delta_{(\,)_c}}{(T_S + T_R)p + 1}$$

WHERE SUBSCRIPT ( ) SPECIFIES THE CONTROL INVOLVED (e, a, r, OR z)

AND $T_S = .066$ SEC = TIME CONSTANT OF THE MIT SERVO

$T_R = .070$ SEC = TIME CONSTANT OF ROTOR & BOOST UNITS

INSTRUMENTATION LABORATORY
MASSACHUSETTS INSTITUTE OF TECHNOLOGY
CAMBRIDGE MASS.

TABLE II

PREPARED BY: RMoe
DATE: 13Mar68

COORDINATE TRANSFORMATIONS USED IN THE MIT/IL SIMULATION OF THE NCH-46C HELICOPTER

SHEET
OF

EXACT EXPRESSION	AS MECHANIZED
$\Delta V_{X_C} = \Delta V_{X_A}\cos E + \Delta V_{Y_A}\sin E\sin\phi + \Delta V_{Z_A}\sin E\cos\phi$	$\Delta V_{X_C} = \Delta V_{X_A}\cos E + \Delta V_{Z_A}\sin E$
$\Delta V_{Y_C} = \Delta V_{Y_A}\cos\phi - \Delta V_{Z_A}\sin\phi$	$\Delta V_{Y_C} = \Delta V_{Y_A}$
$\Delta V_{Z_C} = -\Delta V_{X_A}\sin E + \Delta V_{Y_A}\cos E\sin\phi + \Delta V_{Z_A}\cos E\cos\phi$	$\Delta V_{Z_C} = V_{Z_C} = -\dot{h} = -\Delta V_{X_A}\sin E + \Delta V_{Z_A}\cos E - V_{X_{C_0}}\Delta E$
$\dot{H} = \omega_{Y_A}\left(\frac{\sin\phi}{\cos E}\right) + \omega_{Z_A}\left(\frac{\cos\phi}{\cos E}\right)$	EXACT
$\dot{E} = \omega_{Y_A}\cos\phi - \omega_{Z_A}\sin\phi$	EXACT
$\dot{\phi} = \omega_{X_A} + \dot{H}\sin E$	EXACT
$H \cong \Delta H = \int \dot{H}\,dt \quad (H_0 = 0)$	EXACT
$E = E_0 + \Delta E$ $= E_0 + \int \dot{E}\,dt$	EXACT
$\phi \equiv \Delta\phi = \int \dot{\phi}\,dt \quad (\phi_0 = 0)$	EXACT

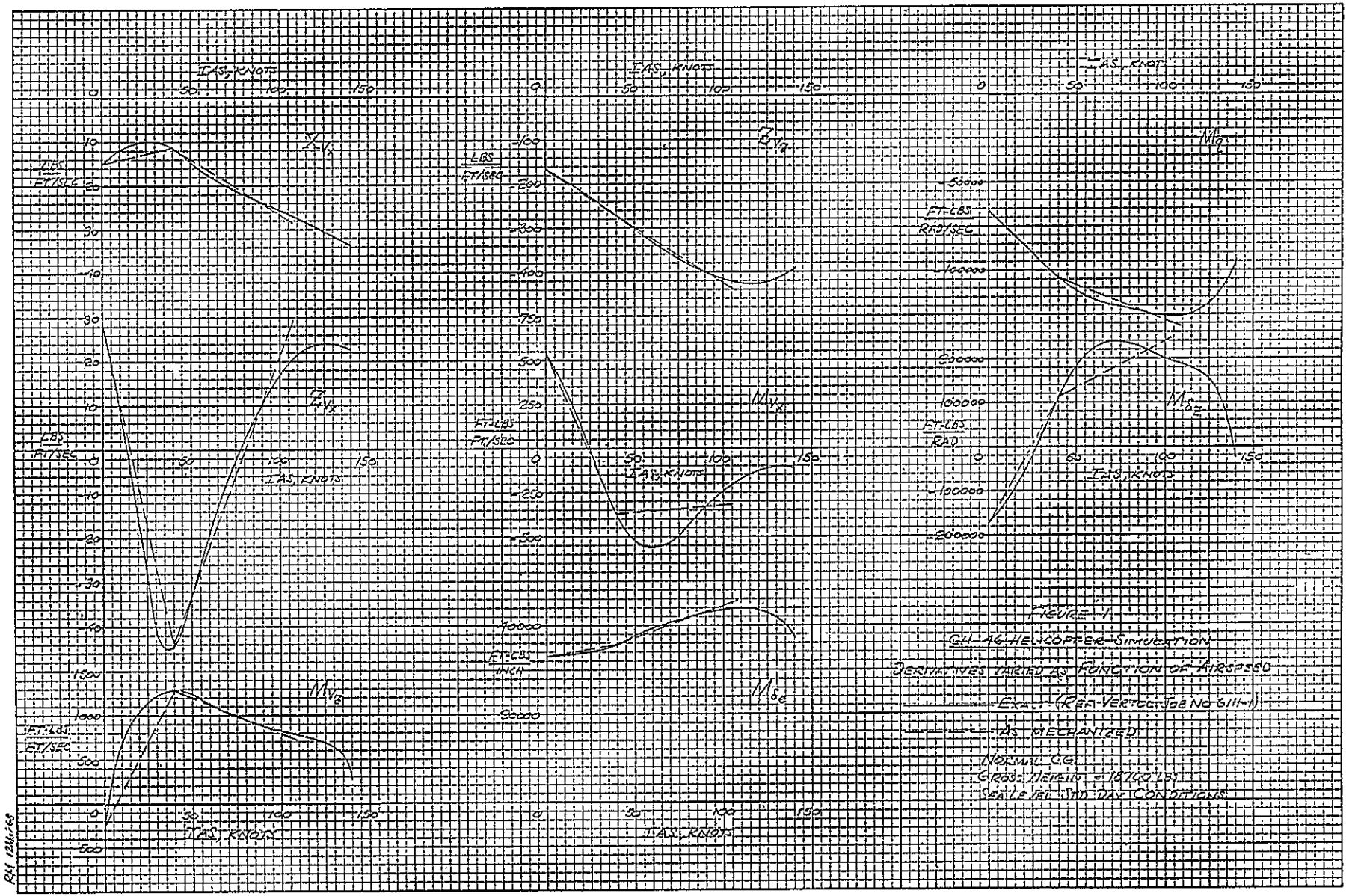

Fig. 3-1 Stability Derivatives Varied as a Function of Airspeed

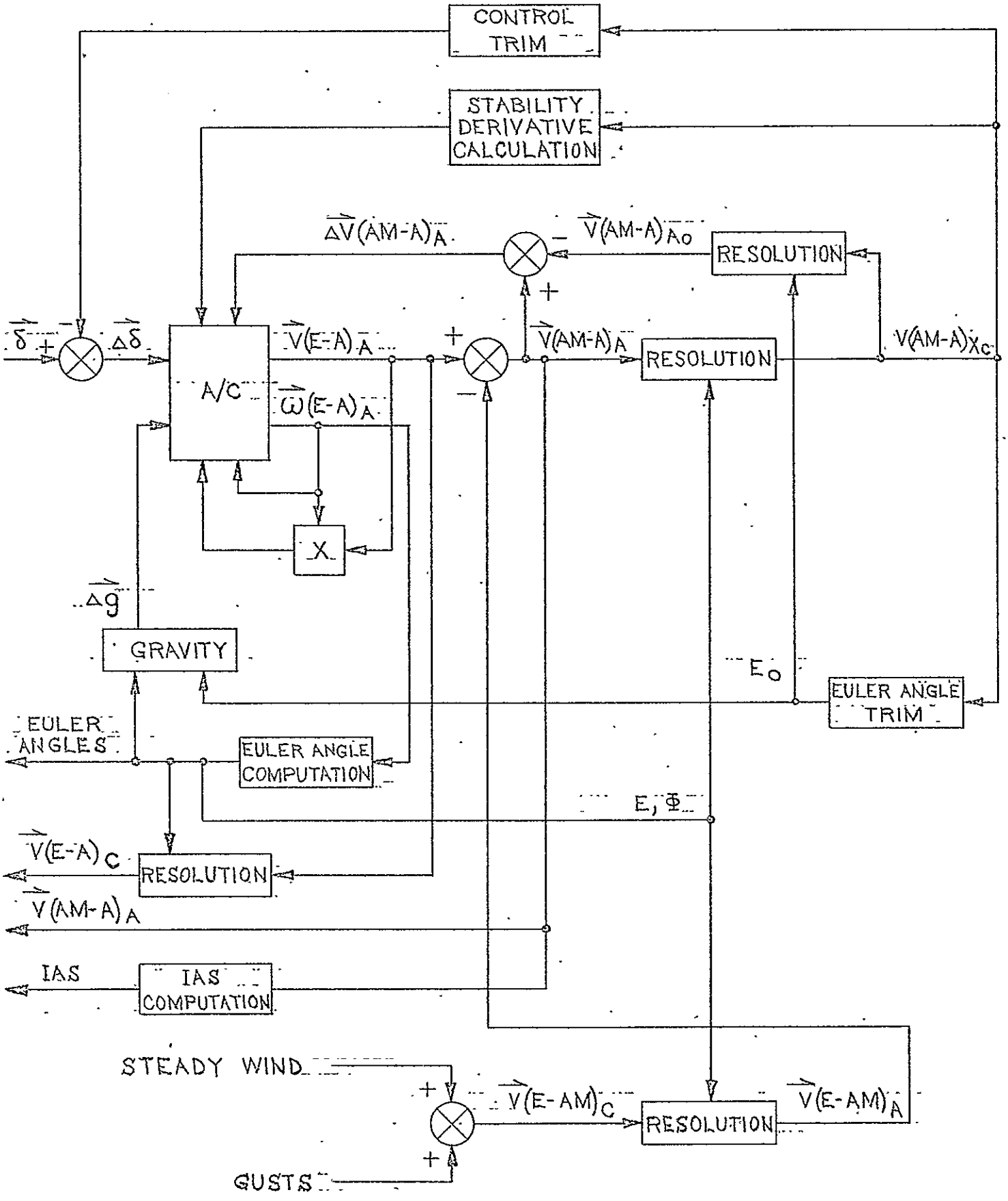

Fig.3-2 BLOCK DIAGRAM OF THE AIRCRAFT SIMULATION SHOWING GENERATION OF TRIM QUANTITIES

CH-46 HELICOPTER.

TRIMMED PITCH ANGLE, LONGITUDINAL STICK POSITION AND COLLECTIVE STICK POSITION VS FORWARD SPEED

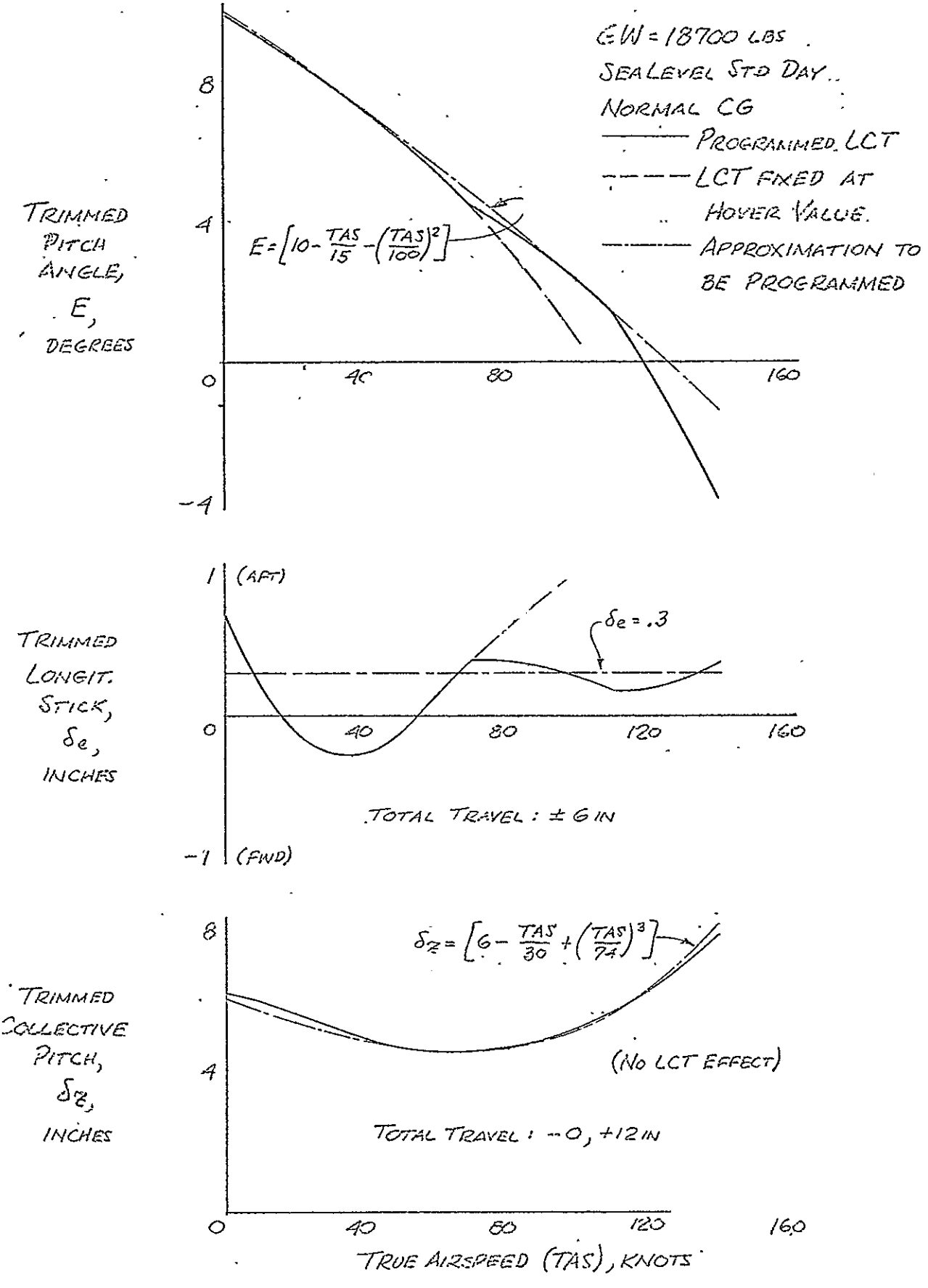

Fig. 3-3 Trim Pitch Angle and Control Deflections

Sample derivation of the simulation equations

From the previous derivation of the equations of motion

$$m[\dot{V}_{X_A} + \omega_{y_A} V_{z_A} - \omega_{z_A} V_{y_A}] + mg \sin E = F_{X_A \text{ non-gravity}}$$

$$F_{X_A \text{ non-gravity}} = f_{X_A}\left(\vec{V}_{(AM-A)}, \vec{\omega}_{(AM-A)}, \vec{\delta}\right)$$

$$= f_{\substack{X_A \\ trim}}\left(\vec{V}_{(AM-A)_o}, \vec{\omega}_{(AM-A)_o}, \vec{\delta}_o\right) + \Delta f_{X_A}\left(\Delta\vec{V}_{(AM-A)}, \Delta\vec{\omega}_{(AM-A)}, \Delta\vec{\delta}\right)$$

Define trim as non-accelerating, straight, and level flight at the current velocity

Thus

$$F_{\substack{X_A \\ non-gravity}} = f_{\substack{X_A \\ trim}}\left(V_{(AM-A)_{X_c}}\right) + \Delta f_{X_A}\left(\Delta\vec{V}_{(AM-A)}, \Delta\vec{\omega}_{(AM-A)}, \Delta\vec{\delta}\right)$$

At trim $\dot{V}_{X_A} = \omega_{y_A} = \omega_{z_A} = 0$ and the X equation becomes

$$mg \sin E_o = f_{X_A}\left(V_{(AM-A)_{X_o}}\right)$$

Subtracting from the general X force equation

$$m[\dot{V}_{X_A} + \omega_{y_A} V_{z_A} - \omega_{z_A} V_{y_A}] + mg(\sin E - \sin E_o) = \Delta f_{X_A}\left(\Delta\vec{V}_{(AM-A)}, \vec{\omega}_{(AM-A)}, \Delta\vec{\delta}\right)$$

Where (neglecting lateral cross coupling terms)

$$\Delta f_{X_A} = X_{V_{X_A}} \Delta V_{X_A} + X_{V_{z_A}} \Delta V_{z_A} + X_{\omega_{y_A}} \Delta \omega_{y_A} + X_{\delta e} \Delta \delta e + X_{\delta z} \Delta \delta z$$

Fig. 3-4 Sample Derivation of the Simulation Equations

X Force

$$\dot{V}_{X_A} + \omega_{y_A} V_{z_A} - \omega_{z_A} V_{y_A} + g(\sin\Theta - \sin\Theta_o) = X_{V_{X_A}} \Delta V_{X_A} + X_{V_{Z_A}} \Delta V_{Z_A} + X_{\omega_{y_A}} \Delta \omega_{y_A} + X_{\delta e} \Delta \delta e + X_{\delta z} \Delta \delta z$$

Y Force

$$\dot{V}_{y_A} + \omega_{z_A} V_{X_A} - \omega_{X_A} V_{z_A} - g(\cos\Theta \sin\phi) = Y_{V_{y_A}} \Delta V_{y_A} + Y_{\omega_{X_A}} \Delta \omega_{X_A} + Y_{\omega_{z_A}} \Delta \omega_{z_A} + Y_{\delta a} \Delta \delta a + Y_{\delta r} \Delta \delta r$$

Z Force

$$\dot{V}_{z_A} + \omega_{X_A} V_{y_A} - \omega_{y_A} V_{X_A} - g(\cos\Theta \cos\phi - \cos\Theta_o) = Z_{V_{z_A}} \Delta V_{z_A} + Z_{V_{X_A}} \Delta V_{X_A} + Z_{\omega_{y_A}} \Delta \omega_{y_A} + Z_{\delta e} \Delta \delta e + Z_{\delta z} \Delta \delta z$$

Pitch Moment

$$\dot{\omega}_{y_A} + \left(\frac{I_x - I_z}{I_y}\right) \omega_{z_A} \omega_{X_A} - \frac{J_{zx}}{I_y} \left(\omega_{z_A}^2 - \omega_{X_A}^2\right) = M_{V_{X_A}} \Delta V_{X_A} + M_{V_{z_A}} \Delta V_{z_A} + M_{\omega_{y_A}} \Delta \omega_{y_A} + M_{\delta e} \Delta \delta e + M_{\delta z} \Delta \delta z$$

Roll Moment

$$\dot{\omega}_{X_A} + \left(\frac{I_z - I_y}{I_x}\right) \omega_{y_A} \omega_{z_A} - \frac{J_{zx}}{I_x} \left(\dot{\omega}_{z_A} + \omega_{X_A} \omega_{y_A}\right) = L_{V_{y_A}} \Delta V_{y_A} + L_{\omega_{X_A}} \Delta \omega_{X_A} + L_{\omega_{z_A}} \Delta \omega_{z_A} + L_{\delta a} \Delta \delta a + L_{\delta r} \Delta \delta r$$

Yaw Moment

$$\dot{\omega}_{z_A} + \left(\frac{I_y - I_x}{I_z}\right) \omega_{X_A} \omega_{y_A} - \frac{J_{zx}}{I_z} \left(\dot{\omega}_{X_A} - \omega_{y_A} \omega_{z_A}\right) = N_{V_{y_A}} \Delta V_{y_A} + N_{\omega_{X_A}} \Delta \omega_{X_A} + N_{\omega_{z_A}} \Delta \omega_{z_A} + N_{\delta a} \Delta \delta a + N_{\delta r} \Delta \delta r$$

Fig. 3-5 Helicopter Simulation Equations of Motion

Geometry

$$V_{X_c} = V_{X_A} \cos E + V_{y_A} \sin E \sin\phi + V_{z_A} \sin E \cos\phi$$

$$V_{y_c} = V_{y_A} \cos\phi - V_{z_A} \sin\phi$$

$$V_{z_c} = -V_{X_A} \sin E + V_{y_A} \cos E \sin\phi + V_{z_A} \cos E \cos\phi$$

$$\dot{H} = \omega_{y_A} \left(\frac{\sin\phi}{\cos E}\right) + \omega_{z_A} \left(\frac{\cos\phi}{\cos E}\right)$$

$$\dot{E} = \omega_{y_A} (\cos\phi) - \omega_{z_A} (\sin\phi)$$

$$\dot{\phi} = \omega_{X_A} + \dot{H} \sin E$$

Winds

(Steady Wind, Gusts)

$$W_{Xc} = W_{Xc_o} + \Delta W_{Xc}$$

$$W_{y_c} = W_{y_{c_o}} + \Delta W_{y_c}$$

$$W_{z_c} = W_{z_{c_o}} + \Delta W_{z_c}$$

} Components of $\vec{V}_{(E-AM)_c}$

$$W_{X_A} = W_{Xc} \cos E - W_{z_c} \sin E$$

$$W_{y_A} = W_{X_c} \sin E \sin\phi + W_{y_c} \cos\phi + W_{z_c} \cos E \sin\phi$$

$$W_{z_A} = W_{X_c} \sin E \cos\phi - W_{y_c} \sin\phi + W_{z_c} \cos E \cos\phi$$

} Components of $\vec{V}_{(E-AM)_A}$

$$V_{X_{A-AM}} = V_{X_A} - W_{X_A}$$

$$V_{y_{A-AM}} = V_{y_A} - W_{y_A}$$

$$V_{z_{A-AM}} = V_{z_A} - W_{z_A}$$

Fig. 3-6 Geometry and Wind Equations

Chapter 4

Experimental Guidance and Control Equipment

4.1 Introduction

This chapter describes the preliminary design of experimental equipment necessary to permit in-flight evaluation of guidance and control systems in the Langley YHC-1A helicopter. This design was developed under the following general guidelines: (a) the aircraft would not be assigned full time to the program for which this equipment was intended so that it would be desirable, if not actually necessary that the equipment be easily and quickly removable from the aircraft, (b) operations might be conducted at a remote sight which would require a mobile van to house all necessary GSE, engineering test and software modification equipment and the system equipment when not in the aircraft and (c) the airborne equipment should be capable of implementing multi axis control systems ranging from the most elementary type through the most sophisticated conceived to date. To satisfy this last guideline the design is based on the use of a powerful easily programmed digital computer for the majority of the data processing required in the various systems to be studied. The aircraft experimental installation and the ground support van installation are discussed in section 4.2 and 4.3.

4.2 Aircraft Experimental Installation

A block diagram of the aircraft experimental installation indicating the interrelationship of the various units of equipment is shown in Fig. 4-1. As can be seen from the diagram the equipment is subdivided into the following major groupings:

1. Pallet Mounted Equipment
2. System A/C J-Box.
3. Observers' Station
4. Cockpit Station

A pictorial diagram indicating the location envisioned for the major groupings of equipment in the Langley YHC-1A helicopter is shown in Fig. 4-2. The pallet mounted equipment could be readily removed as an integral unit through the ramp exit, at the rear of the cabin area, and installed in a ground support van (as discussed in section 4.3) for test purposes and when the aircraft is being utilized for other research activities.

The system A/C J-box in Fig. 4-1 provides the interface between the pallet mounted equipment and the remaining aircraft equipment. The J-box is the focal point for the distribution of analog and digital signals in the aircraft experimental installation. Analog signal distribution is accomplished as shown in Fig. 4-3. Input/output signals associated with the analog data source/receiver units and the data conversion unit plus inputs to the recording control panel are available at jacks located in the analog signal J-box. The desired interconnections are made by means of patching cords. Digital signal distribution is carried out as shown in Fig. 4-4. Digital signals from various aircraft

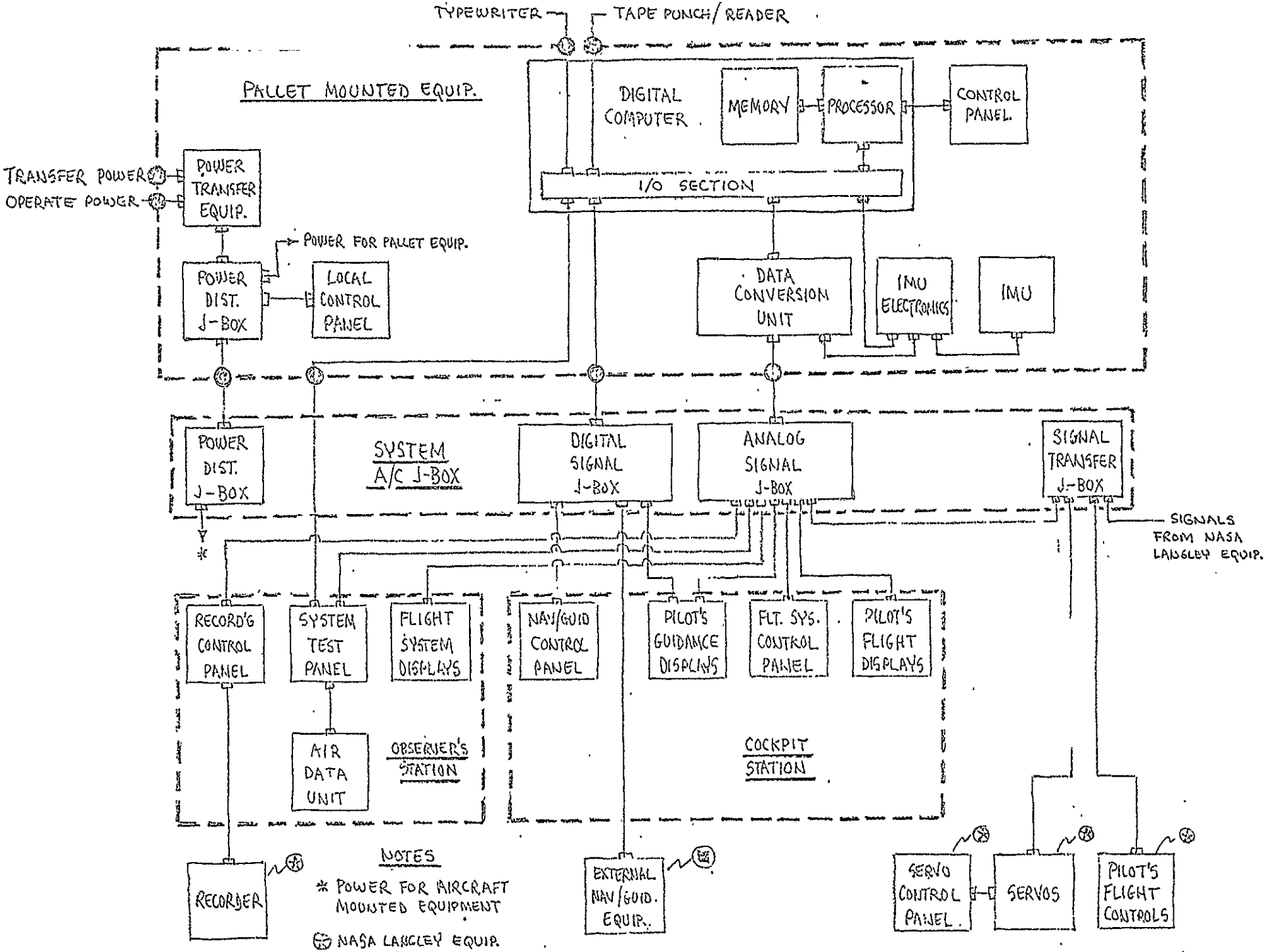

FIG. 4-1 A/C EXPERIMENTAL INSTALLATION DIAGRAM.

MITIL
12 APRIL '68

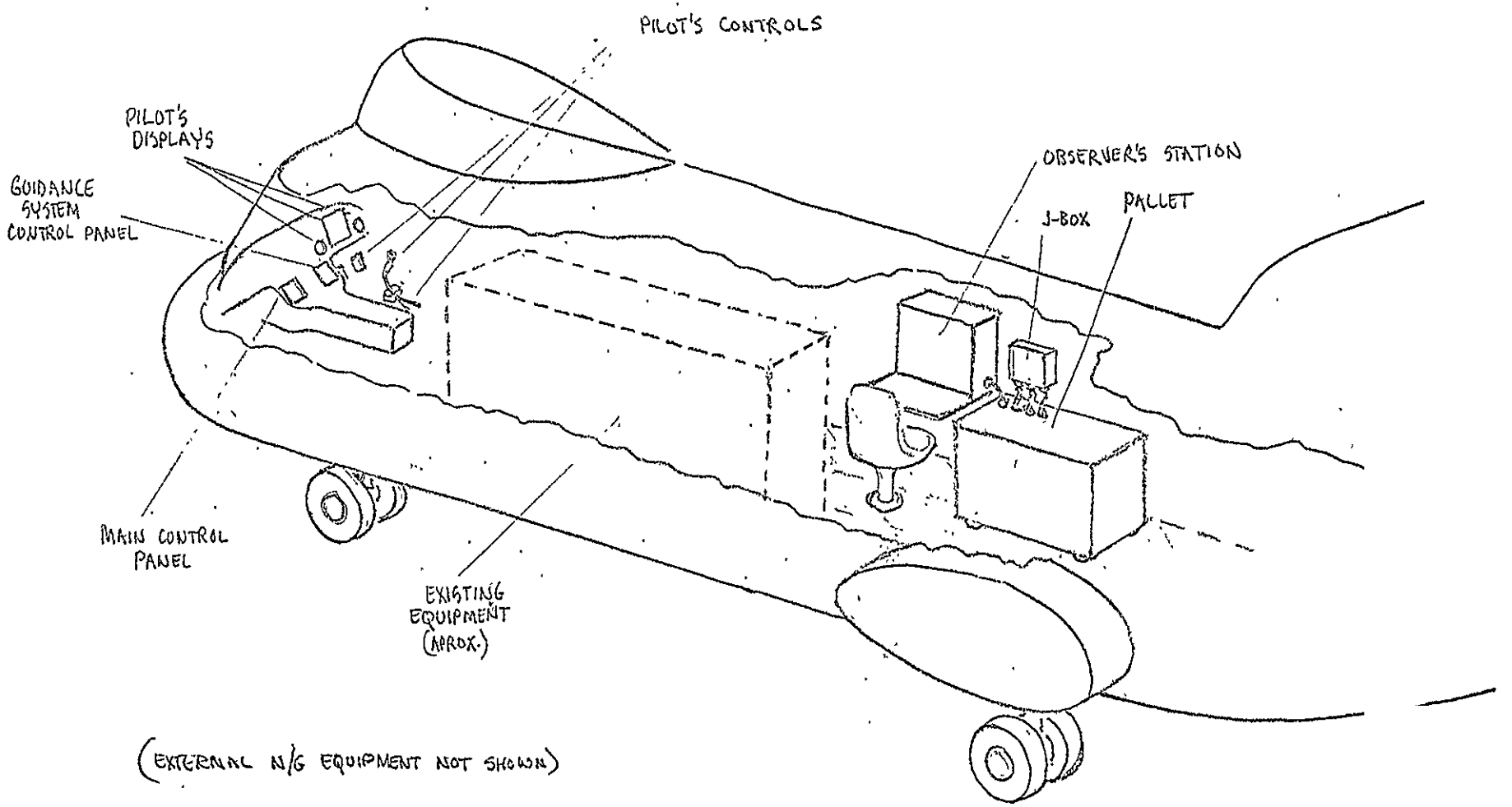

FIG. 4-2 EXPERIMENTAL EQUIPMENT INSTALLATION (SERIAL # 58814)

MITIL
11 APR. 1968

equipment data sources are gated sequentially on to the number transfer bus for transmission to the input data bus of the pallet mounted equipment. Digital data from the pallet mounted equipment is transmitted to the aircraft mounted digital display units in a similar manner.

The observers station would contain the equipment permitting an engineering flight observer to introduce test inputs to the system under evaluation and to observe and/or record the responses of selected system parameters to the test input. Pilot control panels and displays associated with the guidance and control system under test would be located in the cockpit area (the displays on the instrument panel) and hence would be an integral part of the aircraft cockpit installation.

4.3 Ground Support Van Installation

A block diagram of the ground support van installation is shown in Fig. 4-5. A pictorial diagram of the layout of equipment in the ground support van is shown in Fig. 4-6. The system van J-box provides the interface between the pallet mounted equipment and the van test equipment. The A/C equipment test jig would be used to simulated the load and signal sources of equipment not removed from the aircraft installation. The same jig would also permit interfacing aircraft equipment with the rest of the van installation for test and calibration purposes.

Other items of van equipment would include a digital computer (possibly the same as the pallet mounted computer) with paper tape handling equipment and a typewriter. Experience at MITIL with an airborne installation of the type discussed in section 4.2 has shown that this type of ground equipment is adequate for field support.

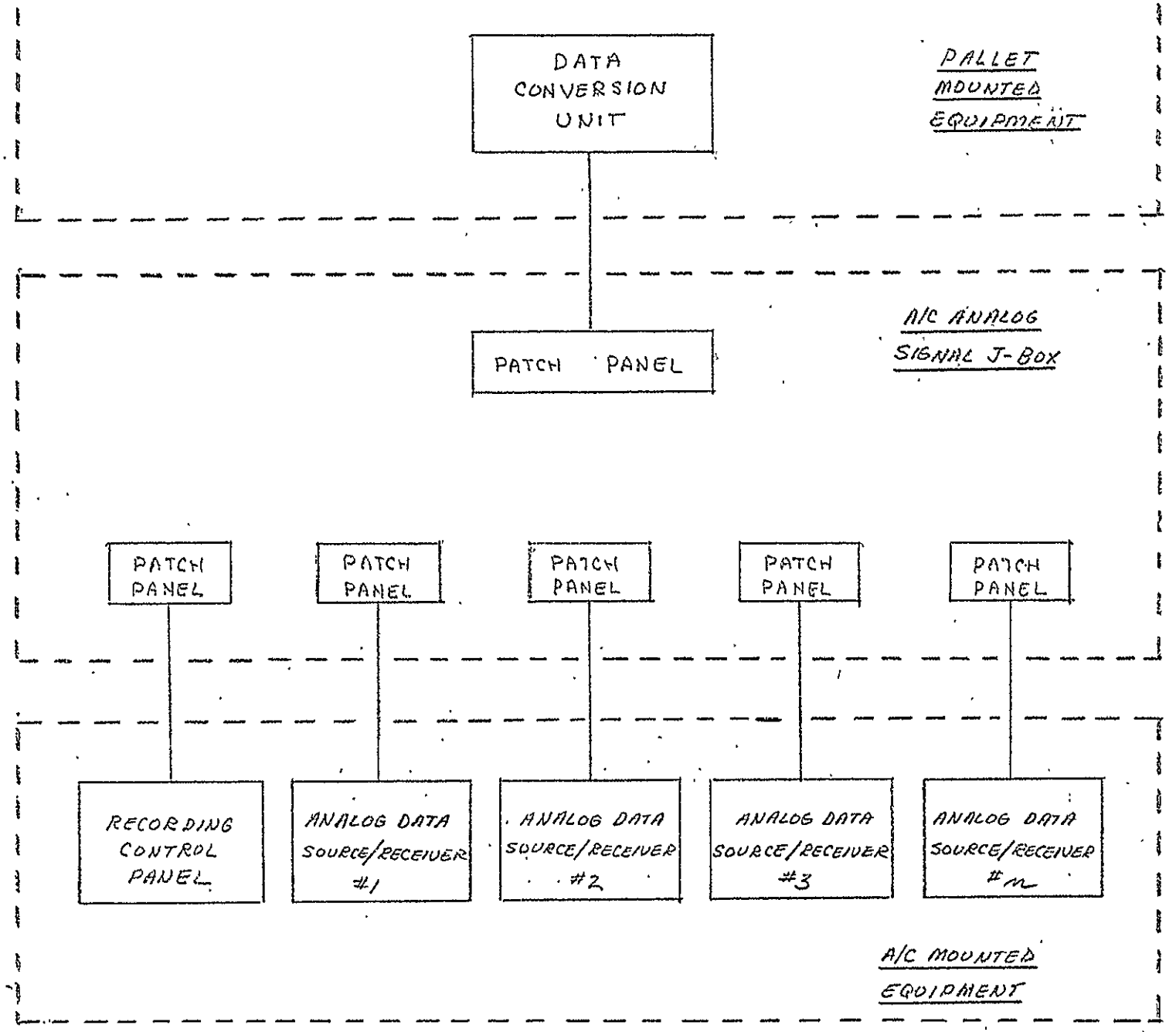

FIG. 4-3 EXPERIMENTAL SYSTEM ANALOG SIGNAL DISTRIBUTION

MITIL 16 APRIL '68

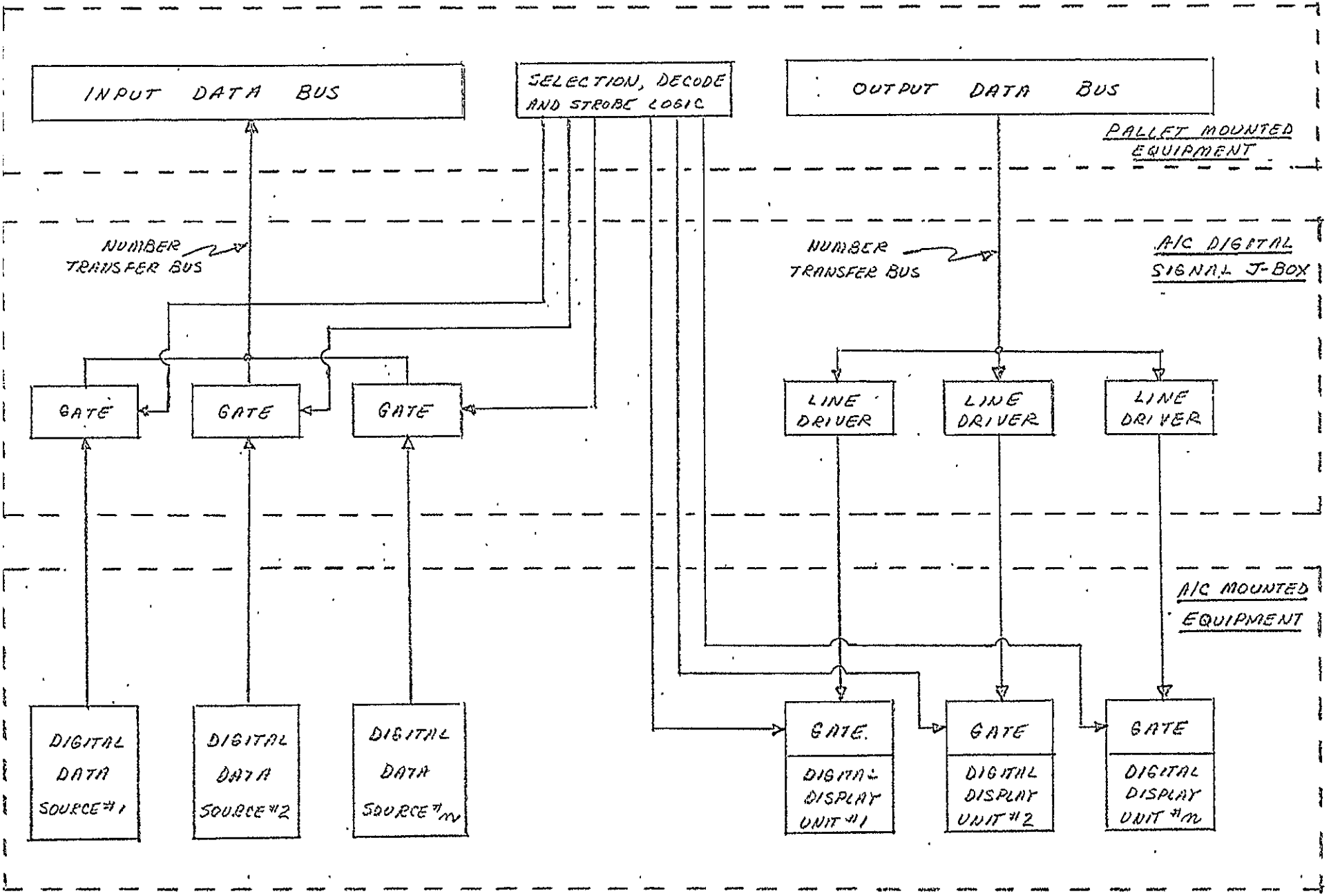

FIG. 44 EXPERIMENTAL SYSTEM DIGITAL SIGNAL DISTRIBUTION

MITIL 16 APRIL '68

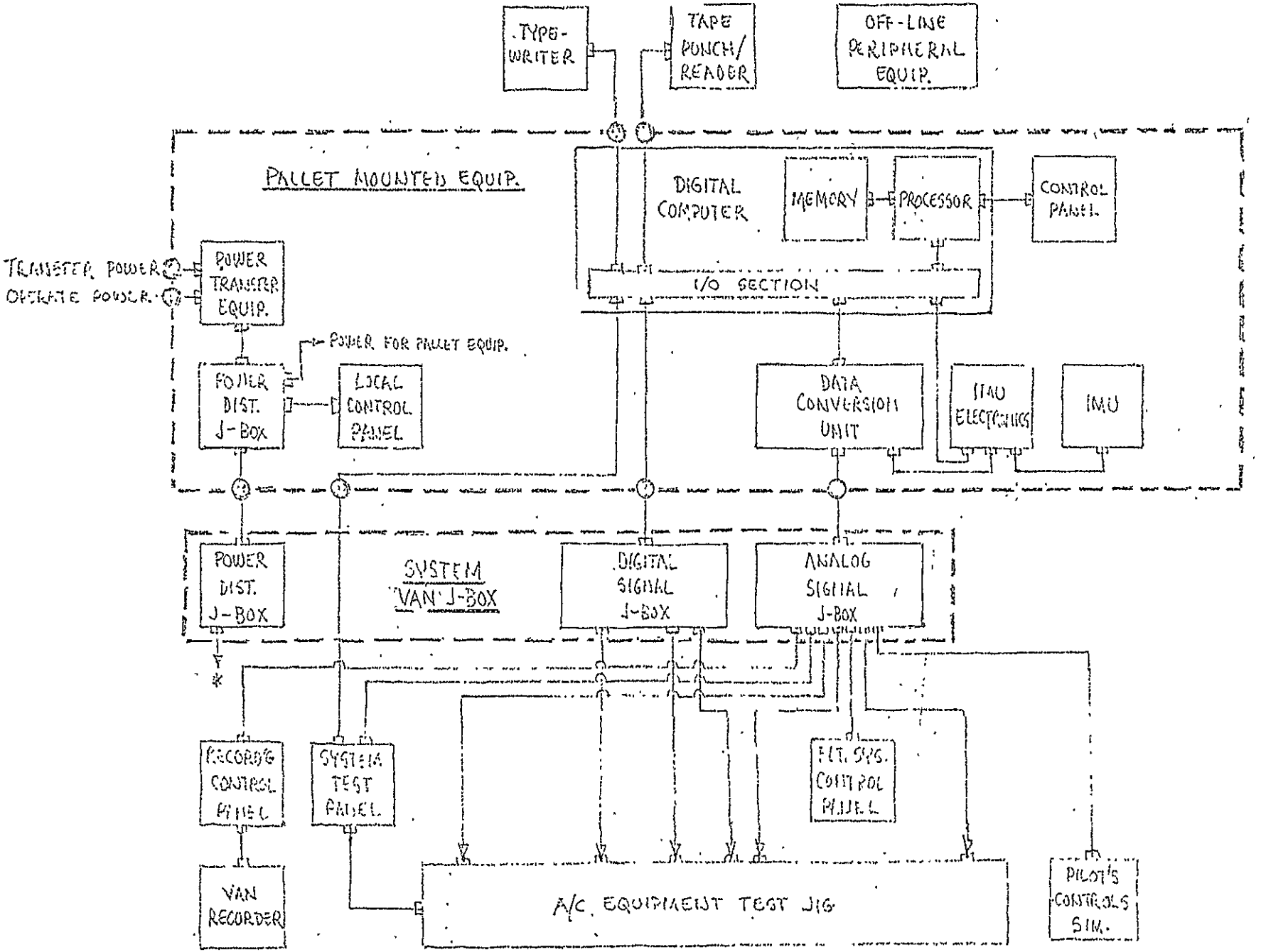

FIG. 4-5 SUPPORT VAN EXPERIMENTAL INSTALLATION DIAGRAM

INITIL
15 APRIL '68

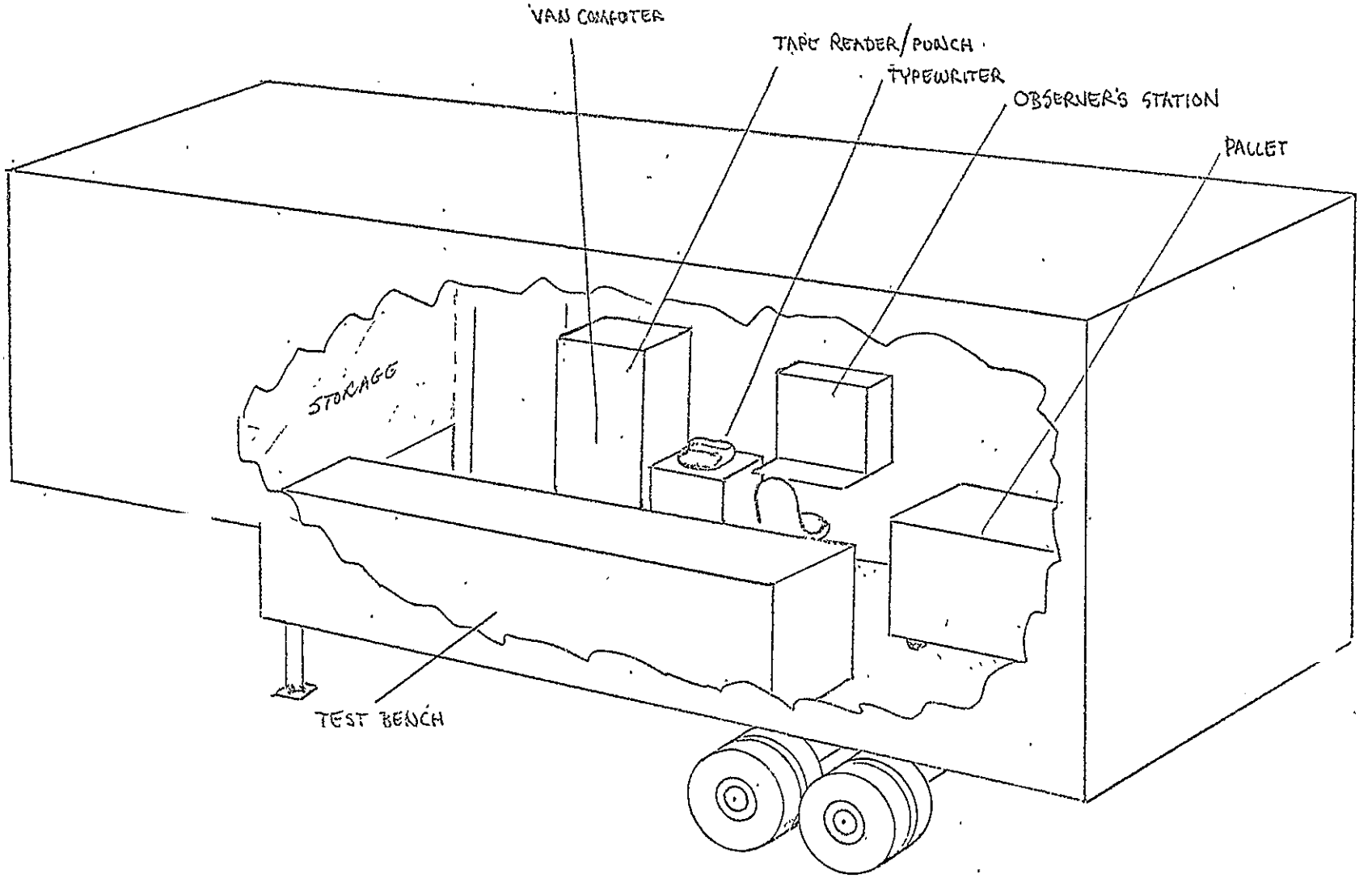

FIG. 4-6 EXPERIMENTAL SYSTEM SUPPORT VAN

MITIL
18 APR '68

Chapter 5

Simulation Interface Equipment

5.1 Description of Effort

In order to advance the operational date of ERC's fixed base cockpit simulator, MIT/IL assisted in the design and implementation of the interface unit between the cockpit flight instruments and the analog computer. At a joint meeting of ERC and MIT personnel, it was decided to use the Link Trainer attitude and turn-bank indicators with their associated electronics driven by analog computer electronic multipliers acting as 60 cycle signal modulators. Altitude, rate of climb, and indicated air speed were to be displayed on long scale (250^{o} arc) 3 inch DC meter movements driven in response to the DC outputs of the analog computer. The assembly of applicable Link Trainer components and fabrication of DC meter instrument dials was completed by MIT. After a laboratory checkout, the unit was delivered to the ERC Analog Computing Facility on 23 April 1968. An extended range altimeter display unit (0 - 7000 ft) was assembled from Link Trainer components as a replacement for the DC meter movement display. This unit was delivered to ERC on 1 July 1968. The schematic diagrams for these units, which were delivered as addenda to the monthly technical progress reports, are included in this report in Appendix J.

APPENDIX A

REFERENCE COORDINATE FRAMES AND NOTATION

A. 1 Introduction

The equations describing the motion of an aircraft are derived from Newton's second law, which relates the forces applied to the vehicle to the acceleration of the vehicle with respect to an inertial coordinate frame. It is generally convenient to sum the components of the applied force and moments in a reference frame fixed to the aircraft and hence rotating with respect to the inertial frame. The aerodynamic forces applied to the aircraft, on the other hand, depend upon the motion of the aircraft with respect to the air mass. Additionally, the motion which is frequently of greatest interest is that of the aircraft with respect to the Earth. Thus, several reference coordinate frames are necessary for the complete and accurate description of the forces applied to the aircraft, the resulting motions, and the physical quantities measured by the flight control system sensors.

The coordinate frames and notation used in the flight control studies are defined in sections A. 2 and A. 3 respectively. Insofar as possible, the axis systems have been selected so that the senses of rotation and translation are similar when small angles are used. When treated as vector quantities, positive force, moment, and motion components are defined to be in the positive sense of the axis. In general, notation using self-defining symbols is employed to facilitate distinguishing similar quantities in the various coordinate frames. Where applicable, the symbols are consistent with those in common usage in the guidance and control fields and with those used by NASA for aircraft stability and control work.

A. 2 Definition of Coordinate Frames

The principal reference frames needed for the analysis of VTOL aircraft and flight control systems dynamics are described below. Figure 99 shows the inertial, Earth-centered, Earth geocentric-vertical, and Earth local-vertical coordinate frames. Figure 100 shows the relationships between the Earth local-vertical, Earth-aircraft control, and aircraft body axes frames. Figure 101 shows the relation between the velocity of the aircraft with respect to the Earth, the velocity of the air mass with respect to the Earth, and the velocity of the aircraft with respect to the air mass.

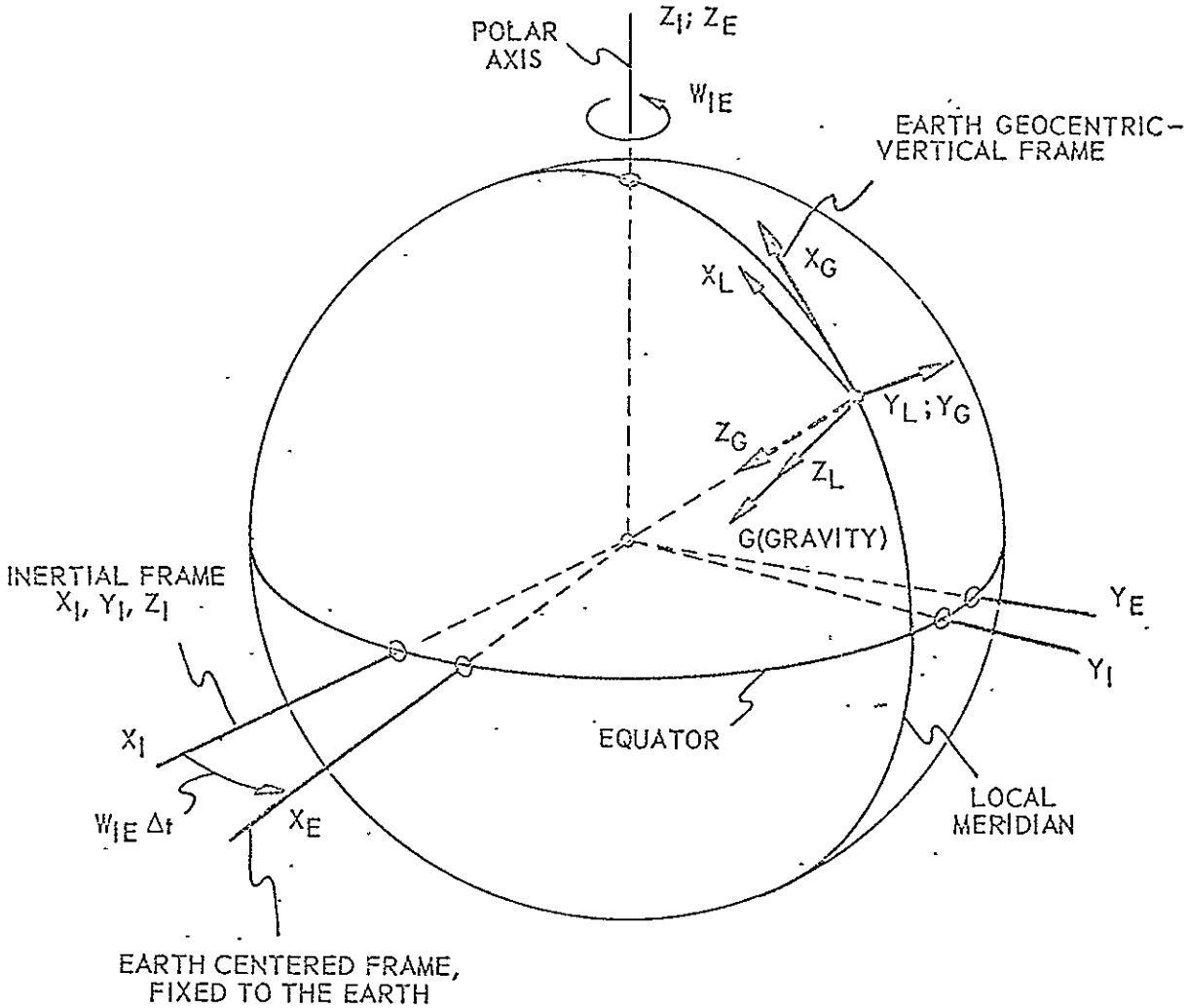

Figure 99. Reference Coordinate Frames – Inertial (I), Earth-Centered (E), Earth Local-Vertical (L), and Earth Geocentric-Vertical (G).

1. Inertial Coordinate Frame (I) X_I, Y_I, Z_I

This frame is nonrotating with respect to inertial space. The origin is the center of the Earth, with the Z_I axis coincident with the rotational axis of the Earth. The X_I and Y_I axes then lie in the equatorial plane. This placement of the axis system assumes that the linear and angular accelerations of the Earth with respect to inertial space in its orbit about the sun are negligible.

2. Earth-Centered Coordinate Frame (E) X_E, Y_E, Z_E

This frame is fixed with respect to the Earth, with its origin at the center of the Earth and with the Z_E axis coincident with the Z_I axis and

the Earth's rotational axis. The X_E and Y_E axes lie in the equatorial plane, intersecting the surface of the Earth at convenient points. The E-frame may be chosen to coincide with the I-frame at a particular instant of time.

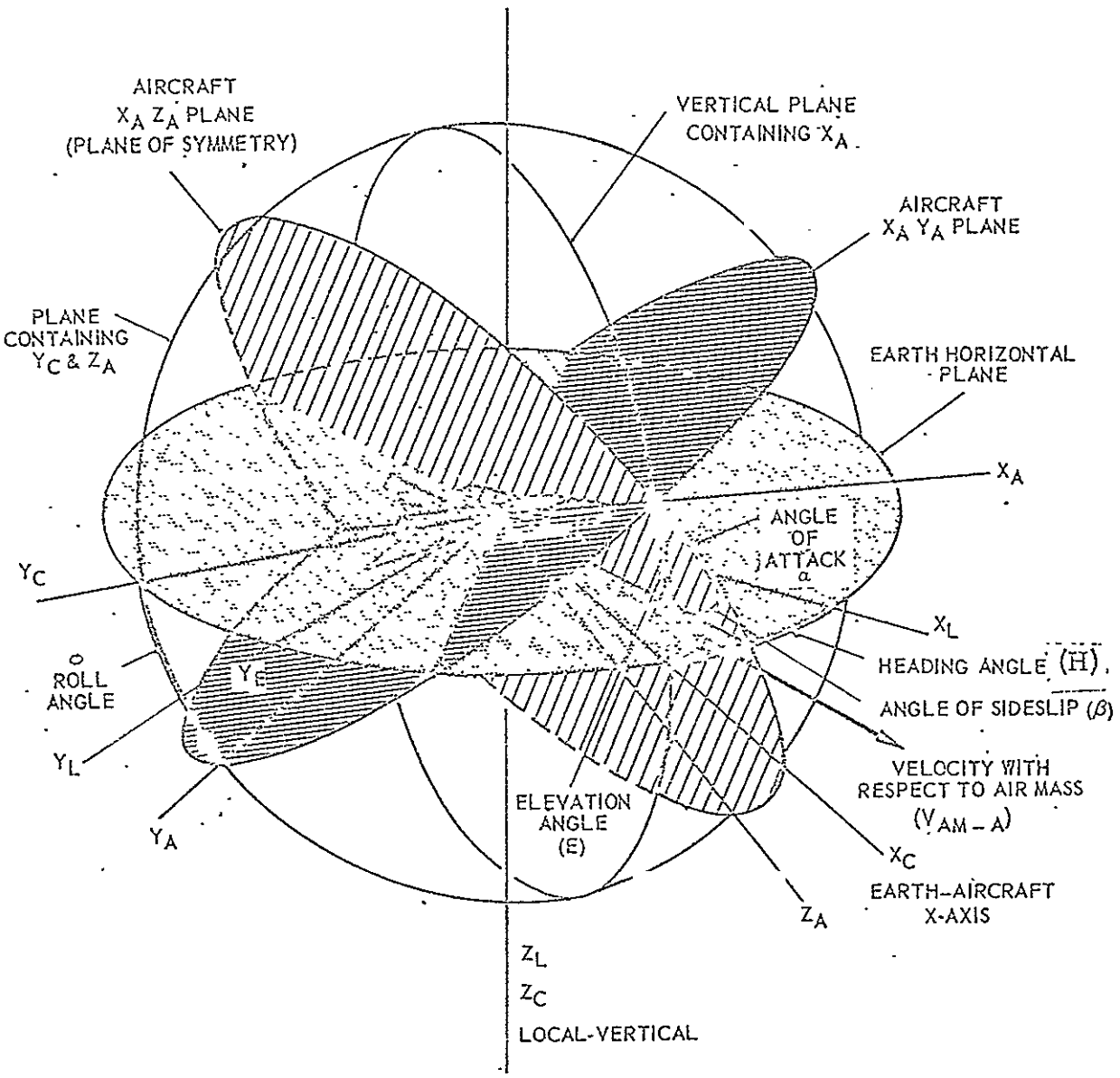

Figure 100. Coordinate Frames for Describing Motion of the Aircraft With Respect to the Earth.

3. Earth Local-Vertical Frame (L) X_L, Y_L, Z_L

The Earth local-vertical frame (L) is a local geographic frame. The origin of this frame is at the center of mass of the aircraft, with Z_L along

the vertical defined by the local gravity vector (positive downward), X_L parallel to geographic North (positive to the North), and Y_L parallel to geographic East (positive to the East). The L-frame is instrumented by the stable element of the experimental inertial velocity measuring system (IVMS).

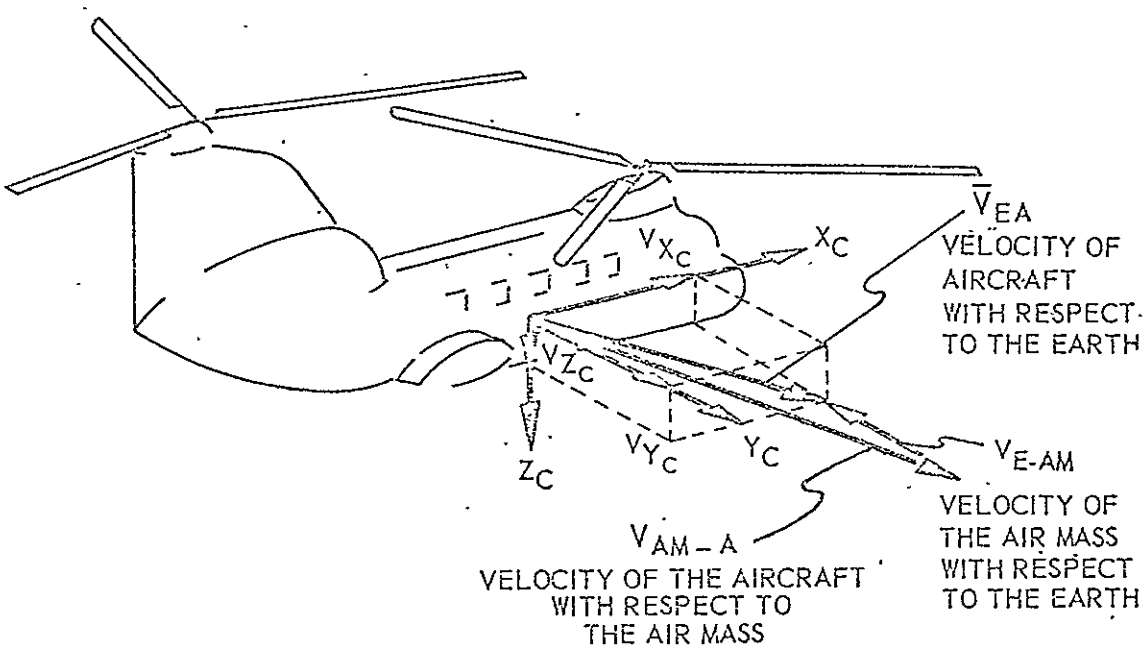

Figure 10.1. Aircraft Velocities With Respect to the Earth and the Air Mass.

4. Earth Geocentric-Vertical Frame (G) X_G, Y_G, Z_G

The Earth geocentric-vertical frame (G) is a geocentric latitude-longitude reference frame whose origin is at the center of mass of the aircraft, with Z_G (positive toward the Earth's center) in coincidence with a radius from the center of the Earth to the origin of the G-frame. X_G and Y_G form an orthogonal axis set with X_G and Y_G in directions similar to the North and East orientations of the X_L and Y_L axes. The difference between the G- and L-frames arises from the difference in the direction of the local gravity vector (which is approximately normal to the reference ellipsoid) and the direction of the geocentric radius vector.

5. Aircraft Body Coordinate Frame (A) X_A, Y_A, Z_A

The aircraft body coordinate frame is centered at the center of mass of the aircraft. The A-frame is fixed to the aircraft and rotates and translates with the aircraft. The X_A axis is chosen in a convenient forward direction in the plane of symmetry, the Y_A axis normal to the plane of symmetry (positive to the right), and the Z_A axis in the plane of symmetry

(positive down) forming an orthogonal right-hand system. The alignment used for the X_A axis of the tandem-rotor helicopter is a "waterline" axis approximately parallel to the floor. The exact alignment is shown in Appendix C with the development of the stability derivatives.

6. Earth-Aircraft Control Coordinate Frame (C) X_C, Y_C, Z_C

The earth-aircraft control coordinate frame is centered at the center of mass of the aircraft. The Z_C axis is along the local gravity vector (positive downward) and is coincident with the Z_L axis. The X_C axis is the intersection of the horizontal plane with the vertical plane containing the X_A axis. The Y_C axis forms a right-hand system. The C-frame is the intermediate frame for the definition of the Euler angles describing the relationship between the Earth local-vertical frame and the aircraft body axes frame. In their order of rotation, the Euler angles are defined as:

1. Heading (H) – angle of rotation about Z_L from X_L to X_C

$$H = A_{[X_L - X_C]Z_L}$$

2. Elevation (E) – angle of rotation about Y_C from X_C to X_A

$$E = A_{[X_C - X_A]Y_C}$$

3. Roll (ϕ) – angle of rotation about X_A from Y_C to Y_A

$$\phi = A_{[Y_C - Y_A]X_A}$$

7. Other Coordinate Frames

For the description of the measurements by particular instruments or for the derivation of aerodynamic effects, it is sometimes convenient to define additional coordinate frames. When necessary, these other frames are described in the applicable sections; in general, the results are then referred to one of the reference frames described above.

A. 3 Definition of Symbols

The general notation for the axis systems and the angle, angular velocity, acceleration, and velocity components in these various reference frames is defined as follows:

$X_{(\ )}$, $Y_{(\ )}$, $Z_{(\ )}$	Axes of the ( ) frame
$A_{[rf](\ )}$	Angular rotation from a reference frame (r) to another frame (f) about the ( ) axis

$W_{[rf]( )}$	Component about the ( ) axis of the angular velocity of frame (f) with respect to the reference frame (r)
$V_{[rf]( )}$	Component along the ( ) axis of the linear velocity of the frame (f) with respect to the reference frame (r)
$a_{[rf]( )}$	Component along the ( ) axis of the linear acceleration of the frame (f) with respect to the reference frame (r)
$\delta_{( )}$	Displacement of the ( ) primary flight control or the ( ) pilot's manual control

This complete self-defining notation is used in Appendix B for the derivation of the equations of motion in order to facilitate distinguishing similar quantities in the various coordinate frames. The results are, in general, reduced to the working, shorthand notation for the most used components of forces, moments, and motions in the three principal axis systems that is presented in Table VIII.

TABLE VIII

SUMMARY OF NOTATION FOR THE COMPONENTS OF FORCES AND MOTIONS IN THE VARIOUS COORDINATE FRAMES

Quantity		Aircraft Body Frame			Earth Reference Frame			Earth–Aircraft Frame		
Coordinate Frame Axes		X_A	Y_A	Z_A	X_L	Y_L	Z_L	X_C	Y_C	Z_C
Aircraft Body Axis Moments		L	M	N						
Applied Forces		F_X	F_Y	F_Z	F_{X_L}	F_{Y_L}	F_{Z_L}	F_{X_C}	F_{Y_C}	F_{Z_C}
Aircraft Angular Velocity with respect to Inertial Space	$\overline{W}_{(IA)}$	W_{X_A}	W_{Y_A}	W_{Z_A}						
Aircraft Acceleration with respect to Inertial Space	$\overline{a}_{(IA)}$	a_{X_A}	a_{Y_A}	a_{Z_A}						
Aircraft Velocity with respect to Inertial Space	$\overline{V}_{(IA)}$	V_{X_A}	V_{Y_A}	V_{Z_A}						
Aircraft Acceleration with respect to the Earth	$\overline{a}_{(EA)}$				a_{X_L}	a_{Y_L}	a_{Z_L}	a_{X_C}	a_{Y_C}	a_{Z_C}
Aircraft Velocity with respect to the Earth	$\overline{V}_{(EA)}$				V_{X_L}	V_{Y_L}	V_{Z_L}	V_{X_C}	V_{Y_C}	V_{Z_C}
Velocity of Air Mass with respect to the Earth	$\overline{V}_{(E-AM)}$				$\overline{V}_{(E-AM)X_L}$	$\overline{V}_{(E-AM)Y_L}$	$\overline{V}_{(E-AM)Z_L}$			
Velocity of Aircraft with respect to the Air Mass	$\overline{V}_{(AM-A)}$	V_X	V_Y	V_Z						
Euler Angles	Heading $A_{[X_L - X_C]Z_L}$						H			
	Elevation $A_{[X_C - X_A]Y_C}$								E	
	Roll $A_{[Y_C - Y_A]X_A}$	ϕ								
Moment Control Displacements	Pitch		δ_e							
	Roll	δ_a								
	Yaw			δ_r						

APPENDIX B

GENERALIZED KINEMATIC EQUATIONS OF MOTIONS

The generalized body axis equations of motion and the coordinate transformations needed to relate the components of forces and motions in the various reference coordinate frames are presented in this appendix. Also discussed are some of the approximations which have been used to make the analysis using these equations more tractable. Because of the capability of VTOL aircraft for hover, transition, and slow steep approaches where winds may produce a large difference between the aircraft's velocity with respect to the ground and with respect to the air mass, considerable emphasis is placed upon distinguishing between these two velocities.

B.1 Generalized Equations of Motion in Aircraft Axes-(A-Frame)

The generalized equations of motion are obtained by equating the forces and moments applied to the vehicle with the rates of change of the linear and angular momentum of the aircraft with respect to inertial space. Since the aircraft axis equations are written for an axis system that is rotating with respect to inertial space, the following two equations must be used:

$$\bar{F} = m\bar{a}_{(IA)} = m\left[\frac{d\bar{V}_{(IA)}}{dt}\right]_I = m\left[\frac{d\bar{V}_{(IA)}}{dt}\right]_A + m\left[\bar{W}_{(IA)} \times \bar{V}_{(IA)}\right] \tag{61}$$

$$\bar{M} = \left[\frac{d\bar{H}}{dt}\right]_I = \left[\frac{d\bar{H}}{dt}\right]_A + \bar{W}_{(IA)} \times \bar{H} \tag{62}$$

where $\bar{H}$ = Aircraft angular momentum

These equations of motion are completely rigorous. However, the quantities in these equations related to the inertial coordinate frame (I-frame) are not easily determined in the practical sense. Fortunately, for most stability and control analyses, it is sufficiently accurate to consider the rotating Earth to be an inertial frame, thus permitting the substitution of

$\overline{W}_{(EA)}$ for $\overline{W}_{(IA)}$ and $\overline{V}_{(EA)}$ for $\overline{V}_{(IA)}$

Except where noted otherwise, this assumption is basic to all analytical design work described in this report.

The above substitutions are employed in expanding equations 61 and 62 to obtain A-frame (body-axis) components of aircraft translational and angular acceleration with respect to the Earth. In this expansion, it is assumed that the Y_A axis is a principal axis. In this manner, we have

Force Equations

$$F_X = m\, a_{(IA)X_A} = m\left[\dot{V}_{(IA)X_A} + W_{Y_A} V_{(IA)Z_A} - W_{Z_A} V_{(IA)Y_A}\right] \tag{63}$$

$$F_Y = m\, a_{(IA)Y_A} = m\left[\dot{V}_{(IA)Y_A} + W_{Z_A} V_{(IA)X_A} - W_{X_A} V_{(IA)Z_A}\right] \tag{64}$$

$$F_Z = m\, a_{(IA)Z_A} = m\left[\dot{V}_{(IA)Z_A} + W_{X_A} V_{(IA)Y_A} - W_{Y_A} V_{(IA)X_A}\right] \tag{65}$$

Moment Equations

Rolling Moment:

$$L = I_X \dot{W}_{X_A} + (I_Z - I_Y) W_{Y_A} W_{Z_A} - J_{ZX}\left(\dot{W}_{Z_A} + W_{X_A} W_{Y_A}\right) \tag{66}$$

Pitching Moment:

$$M = I_Y \dot{W}_{Y_A} + (I_X - I_Z) W_{Z_A} W_{X_A} - J_{ZX}\left(W_{Z_A}^2 - W_{X_A}^2\right) \tag{67}$$

Yawing Moment:

$$N = I_Z \dot{W}_{Z_A} + (I_Y - I_X) W_{X_A} W_{Y_A} - J_{ZX}\left(\dot{W}_{X_A} - W_{Y_A} W_{Z_A}\right) \tag{68}$$

The forces (F_X, F_Y, F_Z) and moments (L, M, N) are the A-frame components of all external forces and moments applied to the aircraft. Before these forces are discussed further, however, the coordinate transformations that will be required in their development must be introduced.

B.2 Euler Angle Coordinate Transformation

Frequent use must be made of the transformation which relates a vector quantity in the A-frame to its components in the L- or C-frame and vice versa. In general, a vector $\overline{R}$ can be resolved into its A-frame, L-frame, or C-frame components:

$$\overline{R} = R_{X_A} i_A + R_{Y_A} j_A + R_{Z_A} k_A$$

$$= R_{X_C} i_C + R_{Y_C} j_C + R_{Z_C} k_C$$

$$= R_{X_L} i_L + R_{Y_L} j_L + R_{Z_L} k_L$$

where i, j, k are unit vectors in the indicated frames. The L-, A-, and C-frames are related by the Euler angles defined in Figure 100:

H = Heading Angle

E = Elevation Angle

ϕ = Roll Angle

Accordingly, the A-frame components of $\overline{R}$ can be expressed in terms of L-frame components as shown in equations 69 through 71:

$$R_{X_A} = R_{X_L} (\cos H \cos E) + R_{Y_L} (\sin H \cos E) + R_{Z_L} (-\sin E) \tag{69}$$

$$R_{Y_A} = R_{X_L} (\cos H \sin E \sin \phi - \sin H \cos \phi) + R_{Y_L} (\sin \phi \sin E \sin H + \cos \phi \cos H) + R_{Z_L} (\cos E \sin \phi) \tag{70}$$

$$R_{Z_A} = R_{X_L} (\cos H \sin E \cos \phi + \sin H \sin \phi) + R_{Y_L} (\sin H \sin E \cos \phi - \cos H \sin \phi) + R_{Z_L} (\cos E \cos \phi) \tag{71}$$

Conversely, the L-frame component of any vector R can be expressed in terms of A-frame components as shown in equations 72 through 74:

$$R_{X_L} = R_{X_A} (\cos H \cos E) + R_{Y_A} (\cos H \sin E \sin \phi - \sin H \cos \phi) + R_{Z_A} (\cos H \sin E \cos \phi + \sin H \sin \phi) \tag{72}$$

$$R_{Y_L} = R_{X_A}(\sin H \cos E) + R_{Y_A}(\cos H \cos \phi + \sin H \sin E \sin \phi) + R_{Z_A}(\sin H \sin E \cos \phi - \cos H \sin \phi) \quad (73)$$

$$R_{Z_L} = R_{X_A}(-\sin E) + R_{Y_A}(\cos E \sin \phi) + R_{Z_A}(\cos E \cos \phi) \quad (74)$$

Expressions for A-frame components in terms of C-frame components and vice versa can be readily obtained from the above sets of equations by setting H = 0 and replacing the subscript L by C. For example,

$$R_{X_A} = R_{X_C} \cos E + R_{Z_C}(-\sin E)$$

and

$$R_{X_C} = R_{X_A}(\cos E) + R_{Y_A}(\sin E \sin \phi) + R_{Z_A}(\sin E \cos \phi)$$

A-frame components of the aircraft's angular velocity in terms of the rates of change of Euler angles are

$$W_{(EA)X_A} = -\dot{H} \sin E + \dot{\phi} \quad (75)$$

$$\boxed{W_{(EA)Y_A}} = \dot{H} \cos E \sin \phi + \dot{E} \cos \phi \quad (76)$$

$$\boxed{W_{(EA)Z_A}} = \dot{H} \cos E \cos \phi - \dot{E} \sin \phi \quad (77)$$

Alternatively, the rates of change of the Euler angles may be expressed in terms of the A-frame components of the aircraft's angular velocity with respect to the Earth,

$$\dot{H} = \boxed{W_{(EA)Y_A}}\left(\frac{\sin \phi}{\cos E}\right) + W_{(EA)Z_A}\left(\frac{\cos \phi}{\cos E}\right) \quad (78)$$

$$\dot{E} = W_{(EA)Y_A}(\cos \phi) - W_{(EA)Z_A}(\sin \phi) \quad (79)$$

$$\dot{\phi} = W_{(EA)X_A} + \dot{H} \sin E \quad (80)$$

The angular velocities determined by equations 75 through 77 are those of the aircraft with respect to the Earth. However, an angular velocity with respect to the Earth may be approximated by the angular velocity with respect to inertial space. Thus, the solution of the equations of motion (equations 66, 67, and 68) may be used in the above equations to obtain the Euler angles.

B.3 Forces and Moments in Generalized Equations of Motion

The A-frame forces (F_X, F_Y, F_Z) and moments (L, M, N) of equations 63 through 68 represent all of the external forces and moments acting upon the aircraft. These include forces and moments due to aerodynamic loads, control and propulsion systems, and gravity.

Gravitation Forces – The gravity force is a vector quantity of magnitude mg* acting along the positive Z_L (or Z_C) axis. The A-frame components of this force can be obtained using equations 69 through 71 as

$$(F_X)_g = -mg \sin E \tag{81}$$

$$(F_Y)_g = mg \cos E \sin \phi \tag{82}$$

$$(F_Z)_g = mg \cos E \cos \phi \tag{83}$$

No moments are produced by the gravity force because the A-frame origin is located at the aircraft's center of gravity.

Non-Gravitational Forces and Moments – The remaining forces and moments are due primarily to aerodynamic, control, and propulsive effects.

The aerodynamic forces, by definition, are those generated by motions of the aircraft with respect to the air mass. The motions – translational and rotational – are

$$V_{(AM-A)} = V_{(E-A)} - \overline{V}_{(E-AM)} \tag{84}$$

$$\overline{W}_{(AM-A)} = \overline{W}_{(E-A)} - \overline{W}_{(E-AM)} \tag{85}$$

*g includes the gravitational acceleration G plus the centrifugal acceleration due to the Earth's rotation.

It is assumed herein that any rotational velocity of the air mass with respect to the Earth can be neglected; thus,

$$\overline{W}_{(AM-A)} = \overline{W}_{(E-A)} .$$

Control and propulsive forces are generated by control surface deflections or power plant settings. The appropriate control inputs may be represented in general by $\delta_1, \delta_2, \ldots \delta_n$.

Non-gravitational forces and moments can therefore be expressed symbolically:

$$\overline{F}_{non\text{-}gravity} = \overline{F}\,(\overline{V}_{(AM-A)}, \overline{W}_{(E-A)}, \delta_1, \delta_2, \ldots \delta_n) .$$

In general, the aerodynamic and control/propulsive forces cannot be considered independently of one another. For example, the force and moment produced by a command δ_i will be a function of flight condition as defined by $\overline{V}_{(AM-A)}$. Conversely, the aerodynamic forces and moments generated by vehicle motion relative to the air mass will depend upon the vehicle configuration established by $\delta_1, \delta_2, \ldots \delta_n$.

B.4 Nonlinear Six-Degree-of-Freedom Airframe Equations

The expressions for the A-frame forces and moments can be inserted in equations 63 through 68 to obtain the nonlinear equations of motion for a rigid aircraft in terms of body-fixed axes with origin at the C. G. The abbreviated notation

$$W_{(E-A)X_A} \equiv W_{X_A}, \text{ etc.},$$

$$V_{(E-A)X_A} \equiv V_{X_A}, \text{ etc.},$$

is used in the equations.

Force Equations

$$m[\dot{V}_{X_A} + W_{Y_A} V_{Z_A} - W_{Z_A} V_{Y_A} + g \sin E] = (F_X)_{non\text{-}gravity} \qquad (86)$$

$$m[\dot{V}_{Y_A} + W_{Z_A} V_{X_A} - W_{X_A} V_{Z_A} - g \cos E \sin \phi] = (F_Y)_{\text{non-gravity}} \quad (87)$$

$$m[\dot{V}_{Z_A} + W_{X_A} V_{Y_A} - W_{Y_A} V_{X_A} - g \cos E \cos \phi] = (F_Z)_{\text{non-gravity}} \quad (88)$$

Moment Equations

$$I_X \dot{W}_{X_A} + (I_Z - I_Y) W_{Y_A} W_{Z_A} - J_{ZX} (\dot{W}_{Z_A} + W_{X_A} Y_A) = (L)_{\text{non-gravity}} \quad (89)$$

$$I_Y \dot{W}_{Y_A} + (I_X - I_Z) W_{Z_A} W_{X_A} - J_{ZX} (W_{Z_A}^2 - W_{X_A}^2) = (M)_{\text{non-gravity}} \quad (90)$$

$$I_Z \dot{W}_{Z_A} + (I_Y - I_X) W_{X_A} W_{Y_A} - J_{ZX} (\dot{W}_{X_A} - W_{Y_A} W_{Z_A}) = (N)_{\text{non-gravity}} \quad (91)$$

These six equations are an almost exact description of the motions of a rigid aircraft operating near the Earth's surface. They can be developed further along any one of several paths depending on the needs of the user. In this case they will be manipulated into the form generally used for linearized aircraft stability and control studies.

APPENDIX C

DEVELOPMENT OF LINEARIZED PERFORMANCE FUNCTIONS

C.1 Linearized Equations of Motion for the CH-46C Helicopter

Equations 86 through 91 were linearized by expressing each independent variable as the sum of a steady-state value plus a small perturbation, expanding the nongravitational forces and moments as Taylor's series about the steady-state operating point and dropping all but first-order terms, and introducing small-angle approximations. The linearized equations may be separated into lateral and longitudinal sets by equating the steady-state longitudinal motions to zero when studying the perturbed lateral motions and vice versa. Steady-state values are denoted by subscript zero, e.g., $V_{x_{A_0}}$; perturbation quantities are prefixed by Δ, e.g., ΔV_{x_A}. The sum of the two quantities represents the total variable in each case.

In the equations, the abbreviated notation

$$G_{X_A} = V_{(E\text{-}AM)X_A}; \text{ etc.}$$

is used to represent A-frame wind velocities. Terms involving wind velocities are retained on the right-hand side of the equations as forcing terms.

The Laplacian operator p replaces d/dt in the equations.

Longitudinal

x-force:

$$\left[-x_{V_X} + p\right] \Delta V_{X_A} + \left[g + (V_{Z_{A_o}} - x_q)\, p\right] \Delta \Xi + \left[-x_{V_Z}\right] \Delta V_{Z_A} =$$
$$\left[x_{\delta_e}\right] \Delta \delta_e + \left[x_{\delta_z}\right] \Delta \delta_z + \left[-x_{V_X}\right] \Delta G_{X_A} + \left[-x_{V_Z}\right] \Delta G_{Z_A} \qquad (92)$$

z-force:

$$[-z_{V_X}]\Delta V_{X_A} + [-(V_{X_{A_o}} + z_q)p]\Delta E + [-z_{V_Z} + p]\Delta V_{Z_A} =$$

$$[z_{\delta_e}]\Delta_{\delta_e} + [z_{\delta_z}]\Delta_{\delta_z} + [-z_{V_X}]\Delta G_{X_A} + [-z_{V_Z}]\Delta G_{Z_A} \quad (93)$$

pitching moment:

$$[-m_{V_X}]\Delta V_{X_A} + [-m_q p + p^2]\Delta E + [-m_{V_Z}]\Delta V_{Z_A} =$$

$$[m_{\delta_e}]\Delta_{\delta_e} + [m_{\delta_z}]\Delta_{\delta_z} + [-m_{V_X}]\Delta G_{X_A} + [-m_{V_Z}]\Delta G_{Z_A} \quad (94)$$

Lateral

y-force:

$$[-y_{V_Y} + p]\Delta V_{Y_A} + [-g - y_p p]\Delta\phi + [V_{X_{A_o}} - y_r]\Delta\omega_{Z_A} =$$

$$[y_{\delta_a}]\Delta_{\delta_a} + [y_{\delta_r}]\Delta_{\delta_r} + [-y_{V_y}]\Delta G_{Y_a} \quad (95)$$

rolling moment:

$$[-\ell_{V_Y}]\Delta V_{Y_\ell} + [-\ell_p p + p^2]\Delta\phi + \left[-\ell_r \frac{J_{ZX}}{I_X} p\right]\Delta\omega_{Z_A} =$$

$$[\ell_{\delta_a}]\Delta_{\delta_a} + [\ell_{\delta_r}]\delta_r + [-\ell_{V_Y}]G_{Y_A} \quad (96)$$

yawing moment:

$$[-n_{V_Y}]\Delta V_{Y_A} + \left[-n_p p \frac{J_{ZX}}{I_Z} p^2\right]\Delta\phi + [-n_r + p]\Delta\omega_{Z_A}$$

$$[n_{\delta_a}]\Delta_{\delta_a} + [n_{\delta_r}]\Delta_{\delta_r} + [-n_{V_Y}]G_{Y_A} \quad (97)$$

C.2 Stability and Control Derivatives

Longitudinal and lateral stability and control derivatives are defined as follows:

X_{V_X}, Z_{V_X}, M_{V_X}	Aircraft longitudinal force, vertical force, and pitching moment derivative with respect to aircraft longitudinal velocity.
X_{V_Z}, Z_{V_Z}, M_{V_Z}	Aircraft longitudinal force, vertical force, and pitching moment derivative with respect to aircraft vertical velocity.

X_q, Z_q, M_q	Aircraft longitudinal force, vertical force, and pitching moment derivative with respect to aircraft pitching velocity.
X_{δ_e}, Z_{δ_e}, M_{δ_e}	Aircraft longitudinal force, vertical force, and pitching moment derivative with respect to longitudinal stick motion (δ_e positive aft).
X_{δ_z}, Z_{δ_z}, M_{δ_z}	Aircraft longitudinal force, vertical force, and pitching moment derivative with respect to collective stick motion (δ_z positive upward).
Y_{V_Y}, L_{V_Y}, N_{V_Y}	Aircraft lateral force, rolling moment, and yawing moment derivative with respect to aircraft lateral velocity.
Y_p, L_p, N_p	Aircraft lateral force, rolling moment, and yawing moment derivative with respect to aircraft rolling velocity.
Y_r, L_r, N_r	Aircraft lateral force, rolling moment, and yawing moment derivative with respect to aircraft yawing velocity.
Y_{δ_a}, L_{δ_a}, N_{δ_a}	Aircraft lateral force, rolling moment, and yawing moment derivative with respect to lateral stick motion (δ_a positive to right).
Y_{δ_r}, L_{δ_r}, N_{δ_r}	Aircraft lateral force, rolling moment, and yawing moment derivative with respect to rudder pedal motion (δ_r) positive right pedal forward).

It is noted that aerodynamic forces and moments experienced by the aircraft result from motion relative to the air mass. Thus, for example, the derivative X_{V_X} should more properly be written as $X_{V_{(AM-A)}X_A}$. The shorter notation is used herein for convenience.

Force derivatives may be normalized by dividing by aircraft mass; moment derivatives, by dividing by the appropriate moment of inertia. For example,

$$x_{V_x} = \frac{X_{V_x}}{m} \quad \frac{\text{ft/sec}^2}{\text{fps}}$$

C.3 Performance Functions

Performance functions are obtained from the simultaneous solution of equations 92-94 (for longitudinal modes) and equations 95-97 (for lateral modes). For a helicopter, performance functions of interest are those relating the inputs and outputs shown in the sketch:

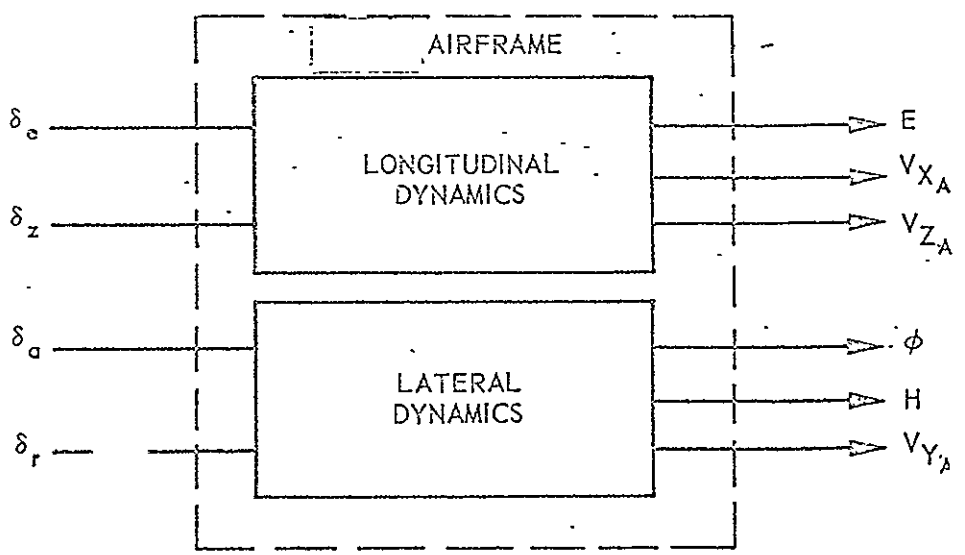

For example, the response of the helicopter in pitch (E) to a differential collective stick input (δ_e) is defined by the performance function

$$PF_{H[\delta_e;E]} = \frac{\Delta E}{\Delta \delta_e}(p) \tag{98}$$

Simultaneous solution of the linearized longitudinal equations of section C.1 for this performance function gives a ratio of polynomials in p:

$$PF_{H[\delta_e;E]} = \frac{N_{H[\delta_e;E]}}{\Delta_{XZM}} \frac{\text{deg}}{\text{in}} \tag{99}$$

where

$$N_{h[\delta_e;E]} = \left[a_o + a_1 p + a_2 p^2 + \cdots\right]_{[\delta_e;E]} \tag{100}$$

Δ_{XZM} = characteristic equation of longitudinal modes at a given forward velocity

$$= \left[b_o + b_1 p + b_2 p^2 + b_3 p^3 + b_4 p^4\right] \tag{101}$$

and the constants a_n and b_n are functions of the stability derivatives. Equation 98 can be written in factored form as

$$PF_{H[\delta_e;E]} = \left[K \frac{(1 + p/z_1)(1 + p/z_2)(\cdots)}{(1 + p/p_1)(1 + p/p_2)(1 + p/p_3)(\cdots)}\right]_{[\delta_e;E]} \tag{102}$$

where

z_n = the n^{th} zero of the performance function

p_n = the n^{th} pole of the performance function

$K = a_o/b_o$.

APPENDIX D

Comparison of NASA and MIT/IL Notation

MIT/IL Symbol	Meaning	NASA Symbol
A	Angle	
a	Acceleration	
CG	Center of gravity	
D	Drag	
E	Elevation (pitch) angle	
EAS	Equivalent airspeed = TAS $\sqrt{\sigma}$	
$\bar{F}$	Force vector	
$F_{( )}$	Component of $\bar{F}$ along the ( ) axis	
G	Gravitational acceleration	
$G_{( )}$	Wind component along ( ) axis $=V_{[E-AM]( )}$	
g	Acceleration due to gravity = G plus centrifugal acceleration due to Earth's rotation	
H	Heading angle	
$\bar{H}$	Angular momentum vector	
h	Altitude	
$\dot{h}$	Rate of change of altitude	
$i_{( )}$	Unit vector along the $X_{( )}$ axis	
IAS	Indicated airspeed = EAS plus measurement inaccuracies	
I_x, I_y, I_z	Moment of inertia in roll, pitch, and yaw respectively	A, B, C
$j_{( )}$	Unit vector along the $Y_{( )}$ axis	

MIT/IL Symbol	Meaning	NASA Symbol
J_{zx}	Product of inertia	E
$k_{( )}$	Unit vector along the $Z_{( )}$ axis	
L	Aircraft rolling moment	
$L_{( )}$	Aircraft rolling moment derivative with respect to ( ) = dL/d( )	
$\ell_{( )}$	Normalized aircraft rolling moment derivative with respect to ( ) = $L_{( )}/I_x$	
M	Aircraft pitching moment	
m	Mass = W/g	
$\bar{M}$	Moment vector	
$M_{( )}$	Aircraft pitching moment derivative with respect to ( ) = dM/d( )	
$m_{( )}$	Normalized aircraft pitching moment derivative with respect to ( ) = $M_{( )}/I_y$	
N	Aircraft yawing moment	
$N_{( )}$	Aircraft yawing moment derivative with respect to ( ) = dN/d( )	
$n_{( )}$	Normalized aircraft yawing moment derivative with respect to ( ) = $N_{( )}/I_z$	
p	Laplace operator	
$PF_{(a;b)}$	Frequency-dependent performance function of the system element whose input is quantity a and whose output is quantity b	
$\bar{R}$	Displacement vector	
$R_{( )}$	Component of $\bar{R}$ along the ( ) axis	
TAS	True airspeed = $V_{[AM-A]}$	
V	Linear velocity	

MIT/IL Symbol	Meaning	NASA Symbol
$V_{X_A}, V_{Y_A}, V_{Z_A}$	Linear velocity along the X_A, Y_A, and Z_A axes, respectively	U, V, W
$\Delta V_{X_A}, \Delta V_{Y_A}, \Delta V_{Z_A}$	Perturbations of V_{X_A}, V_{Y_A}, and V_{Z_A}, respectively	u, v, w
W	Angular velocity	
W	Weight	
$W_{X_A}, W_{Y_A}, W_{Z_A}$	Angular velocity components along the X_A, Y_A, Z_A axes., respectively	P, Q, R
X	Longitudinal Axis, force or displacement (with subscript to denote axis system)	
$X_{( )}$	Aircraft longitudinal force derivative with respect to ( ) = dX/d( )	
$x_{( )}$	Normalized aircraft longitudinal force derivative with respect to ( ) = $X_{( )}/m$	
Y	Lateral axis, force or displacement (with subscript to denote axis system)	
$Y_{( )}$	Aircraft lateral force derivative with respect to ( ) = dY/d( )	
$y_{( )}$	Normalized aircraft lateral force derivative with respect to ( ) = $Y_{( )}/m$	
Z	Vertical axis, force or displacement (with subscript to denote axis system)	
$Z_{( )}$	Aircraft vertical force derivative with respect to ( ) = dZ/d( )	
$z_{( )}$	Normalized aircraft vertical force derivative with respect to ( ) = $Z_{( )}/m$	
α	Angle of attack	
β	Sideslip angle	
$\Delta( )$	Incremental change in ( ) from a reference value	

MIT/IL Symbol	Meaning	NASA Symbol
δ	Control displacement (with subscript to identify control)	
ζ	Damping ratio	
ρ	Atmospheric mass density	
σ	Atmospheric mass density ratio = ρ / ρ_o	
ϕ	Roll angle	
ω	Frequency or angular velocity in radians per second	

Subscripts

A	Aircraft body coordinate frame
a	Rolling moment ("aileron") control; e.g., δ_a
AM	Air mass
C	Earth-aircraft control coordinate frame
c,com	Command or commanded
E	Earth-centered coordinate frame
e	Pitching moment ("elevator") control
G	Earth geocentric-vertical frame
g	Due to gravity
I	Inertial coordinate frame.
L	Earth local-vertical frame
o	Trim value; sea level value
p	Aircraft roll rate
q	Aircraft pitch rate
r	Aircraft yaw rate
r	Yawing moment ("rudder") control
z	Vertical control

APPENDIX E

FLIGHT CONDITIONS FOR WHICH YHC-1A STABILITY AND TRIM DATA ARE TO BE REQUESTED

GW, lbs	CG Position	Altitude, ft	Rate of Climb, fpm	Fwd Speed, knots
13400	normal	0	0	0,40,60,80,100,120,140
"	most fwd	0	0	"
"	most aft	0	0	"
"	normal	10000	0	40,60,80,100
"	most aft	10000	0	"
15500	normal	0	0	0,40,60,80,100,120,140
"	most aft	0	0	"
13400	normal	0	+1500	0,40,60,80
"	normal	0	-1500	

Total number of flight conditions: 51

APPENDIX F

STABILITY DERIVATIVE DATA FOR THE LANGLEY YHC-1A

The data in this appendix is a reproduction of the tabulations by ERC personnel from the stability data supplied by Boeing/Vertol.

Operating Conditions:
- Gross Wt. = 13,400
- c.g. Position = 10.0% ā
- I_{yy} = 75,914 slug-ft²
- Rate of Descent = 0 fpm
- Altitude = sea level

Longitudinal Stability Derivatives

Forward velocity	kts		0	20	40	60	80	100	120	140	
u	ft/sec		0.0	33.76	67.52	101.28	135.04	168.80	202.56	236.32	
α_o	deg		0.0	7.79286	6.24538	4.33124	1.95915	1.34498	-2.32062	-6.70362	
θ_o	deg		8.98247	7.85991	6.30389	4.39564	1.99886	1.39503	-2.30329	-6.65586	
X_u/m	$\frac{ft/sec^2}{ft/sec}$		-.02493	-.00110	-.02275	-.03752	-.04765	-.05661	-.06428	-.07333	
X_w/m	$\frac{ft/sec^2}{ft/sec}$		.05444	.06882	.08376	.09073	.08680	.10490	.08542	.05598	
X_q/m	$\frac{ft/sec^2}{rad/sec}$		.47278	.55272	.60550	.56542	.41751	.86280	.47079	-.01182	
$X_{\delta e}/m$	$\frac{ft/sec^2}{in}$		.16867	.14466	.14875	.18508	.21903	.00654	.01268	.00927	
$X_{\delta c}/m$	$\frac{ft/sec^2}{in}$		1.19776	.96257	.87920	.80702	.69438	.89060	.71347	.47301	
Z_u/m	$\frac{ft/sec^2}{ft/sec}$		.09728	-.13227	-.08444	-.01892	.01727	.06281	.06627	.05181	
Z_w/m	$\frac{ft/sec^2}{ft/sec}$		-.36903	-.48373	-.64000	-.80500	-.92252	-1.00337	-1.04679	-1.10586	
Z_q/m	$\frac{ft/sec^2}{rad/sec}$		.01643	-.01657	-.16377	-.18063	.07086	-.20274	-.18242	-.23794	
$Z_{\delta e}/m$	$\frac{ft/sec^2}{in}$		.05155	.25933	.52725	.54601	.48526	.41256	.33578	.27515	
$Z_{\delta c}/m$	$\frac{ft/sec^2}{in}$		-7.42981	-7.16977	-7.58999	-8.48846	-9.46673	-10.2528	-11.0633	-11.6945	
M_u/I_{yy}	$\frac{rad/sec^2}{ft/sec}$		.00589	.00715	-.00660	-.00731	-.00664	-.00308	-.00270	-.00214	
M_w/I_{yy}	$\frac{rad/sec^2}{ft/sec}$		.00159	.01613	.02374	.02296	.02246	.02199	.02101	.02094	
M_q/I_{yy}	$\frac{rad/sec^2}{rad/sec}$		-.79522	-.96234	-1.31160	-1.47449	-1.53709	-1.63302	-1.60451	-1.55425	
$M_{\delta e}/I_{yy}$	$\frac{rad/sec^2}{in}$		.35489	.35223	.39700	.44308	.47379	.51070	.52775	.54186	
$M_{\delta c}/I_{yy}$	$\frac{rad/sec^2}{in}$		.03284	.03478	.14221	.17395	.18611	.18021	.18517	.19008	
Trim δ_{e_o}	in		-.36082	-1.09382	-1.11713	-.54350	-.00194	-.73354	-.54753	-.33376	
Trim δ_{c_o}	in		5.02277	4.44246	3.71503	3.53057	3.86946	4.65598	6.03707	8.01568	

YHC-1A
Lateral Stability Derivatives

Operating Conditions:
- Gross Wt. = 13,400 lbs
- c.g. Position = 15.1" F.S.
- I_{xx} = 9203 slug-ft²
- I_{zz} = 71,736 slug-ft²
- I_{xz} = 7114 slug-ft²
- Rate of Descent = 0 f.p.m.
- Altitude = sea level

Fwd. velocity	kts		0	20	40	60	80	100	120	140	
"	ft/sec		0.0	33.76	67.52	101.28	135.04	168.80	202.56	236.32	
Y_v/m	$\frac{ft/sec^2}{ft/sec}$		-.26638	-.05403	-.07186	-.11823	-.15121	-.18040	-.14766	-.23442	
Y_p/m	$\frac{ft/sec^2}{rad/sec}$		-.76514	-.95618	-1.15991	-1.24324	-1.23341	-1.02245	-.76619	-.29372	
Y_r/m	$\frac{ft/sec^2}{rad/sec}$		-.12517	-.18179	-.20032	-.12813	-.05819	.13380	.12514	.22125	
$Y_{\delta L}/m$	$\frac{ft/sec^2}{in}$		.99794	.99700	.97673	.96426	.96465	.97123	1.01613	1.10225	
$Y_{\delta R}/m$	$\frac{ft/sec^2}{in}$		.14652	.13634	.11652	.10583	.07849	.11641	.13582	.15262	
L_v/I_{xx}	$\frac{rad/sec^2}{ft/sec}$		-.00778	-.01305	-.01998	-.01720	-.02442	-.03188	-.04724	-.05080	
L_p/I_{xx}	$\frac{rad/sec^2}{rad/sec}$		-.50730	-.57483	-.64045	-.65271	-.62549	-.52243	-.41134	-.23476	
L_r/I_{xx}	$\frac{rad/sec^2}{rad/sec}$		-.02297	-.04571	-.05943	-.02270	.01172	.09531	.11659	.19955	
$L_{\delta L}/I_{xx}$	$\frac{rad/sec^2}{in}$		.46536	.46558	.45954	.45575	.45805	.45820	.47354	.50528	
$L_{\delta R}/I_{xx}$	$\frac{rad/sec^2}{in}$		-.12638	-.13096	-.13422	-.13544	-.13910	-.13266	-.13248	-.14433	
N_v/I_{zz}	$\frac{rad/sec^2}{ft/sec}$		.00013	.00037	-.00123	-.00240	-.00415	-.00536	-.00377	-.00060	
N_p/I_{zz}	$\frac{rad/sec^2}{rad/sec}$		-.01831	-.02076	-.02598	-.03147	-.05341	-.06864	-.07797	-.07471	
N_r/I_{zz}	$\frac{rad/sec^2}{rad/sec}$		-.05847	-.05450	-.04597	-.05020	-.05438	-.06078	-.08642	-.12617	
$N_{\delta L}/I_{zz}$	$\frac{rad/sec^2}{in}$		.03001	.02923	.02764	.02663	.02633	.02646	.02857	.02170	
$N_{\delta R}/I_{zz}$	$\frac{rad/sec^2}{in}$		.17534	.17578	.17261	.17032	.17141	.17146	.17433	.19536	
δ_{L_0}	in		.12983	.08462	.07191	.13466	.17931	.29754	.44164	.47785	
δ_{R_0}	in		-.17764	-.04701	-.08508	-.32705	-.61293	-.75347	-1.04713	-1.14123	

Operating Conditions:
- Gross Wt. = 13,450 lbs
- c.g. Position = 133.0" fwd
- I_{yy} = 75,914 slug-ft²
- Rate of Descent = 0 ft/sec
- Altitude = sea level

YHC-1A
Longitudinal Stability Derivatives

Forward Velocity	kts		0	20	40	60	80	100	120	140	
u_1	ft/sec		0.0	33.76	67.52	101.28	135.04	168.80	202.56	236.32	
α_o	deg		0.0	8.29949	6.73454	4.79661	2.45742	1.34525	-2.34020	-6.69659	
θ_o	deg		9.47577	8.36019	6.79477	4.86329	2.47042	1.37417	-2.31055	-6.65579	
X_u/m	$\frac{ft/sec^2}{ft/sec}$		-.02612	-.00238	-.02127	-.03559	-.04563	-.05574	-.06492	-.07218	
X_w/m	$\frac{ft/sec^2}{ft/sec}$		.05434	.06828	.08185	.08878	.09500	.10302	.08599	.06243	
X_q/m	$\frac{ft/sec^2}{rad/sec}$		.63123	.64128	.98879	.99607	.88651	1.57142	.94491	.36629	
$X_{\delta e}/m$	$\frac{ft/sec^2}{in}$		.19175	.13644	.11150	.12523	.13583	-.08439	-.06606	-.03277	
$X_{\delta c}/m$	$\frac{ft/sec^2}{in}$		1.20560	.98307	.88235	.79909	.63085	.83900	.73600	.52023	
Z_u/m	$\frac{ft/sec^2}{ft/sec}$		.06322	-.12192	-.08184	-.02401	.01008	.05916	.06479	.04906	
Z_w/m	$\frac{ft/sec^2}{ft/sec}$		-.36895	-.42482	-.63339	-.79968	-.91843	-.99750	-1.04458	-1.10393	
Z_q/m	$\frac{ft/sec^2}{rad/sec}$		-1.18736	-1.73629	-2.40197	-2.67851	-2.79395	-3.14971	-3.32893	-3.55192	
$Z_{\delta E}/m$	$\frac{ft/sec^2}{in}$		-.03599	.13967	.50720	.57104	.54874	.49763	.45179	.39978	
$Z_{\delta c}/m$	$\frac{ft/sec^2}{in}$		-7.42201	-7.25489	-7.69425	-8.54711	-9.48941	-10.2587	-11.0930	-11.7232	
M_u/I_{yy}	$\frac{rad/sec^2}{ft/sec}$		.00690	.00609	-.00546	-.00648	-.00499	-.00115	-.00050	-.00023	
M_w/I_{yy}	$\frac{rad/sec^2}{ft/sec}$		-.00513	.00653	.01248	.00884	.00580	.00309	.00095	-.00057	
M_q/I_{yy}	$\frac{rad/sec^2}{rad/sec}$		-.73807	-.97108	-1.31632	-1.47048	-1.53122	-1.64405	-1.60459	-1.53348	
$M_{\delta a}/I_{yy}$	$\frac{rad/sec^2}{in}$		.33342	.35404	.40329	.45335	.48472	.51899	.53702	.54734	
$M_{\delta c}/I_{yy}$	$\frac{rad/sec^2}{in}$		-.09841	-.08332	-.00505	.01134	.00485	-.02333	-.03606	-.04037	
δe_o	in		1.19853	.46617	.21725	.65370	1.16758	.32771	.50998	.70454	
δc_o	in		5.02981	4.48307	3.74980	3.54032	3.83774	4.72892	6.07823	8.02943	

Operating Conditions

Gross Wt = 13,400 Lbs
C.G. Position = 280" Fwd.
I_{xx} = 9203.0 Slug Ft²
I_{zz} = 71786.0 Slug Ft²
I_{xz} = 7114.0 Slug Ft²
Rate of Descent = 0 FPM
Altitude = Sea Level

YHC-1A
LATERAL STABILITY DERIVATIVES

Fwd. Velocity	KNTS.		0	20	40	60	80	100	120	140	
"	ft/sec		0.0	33.76	67.52	101.28	135.04	168.80	202.56	236.32	
Y_v/m	ft/sec² / ft/sec		-.26687	-.05404	-.08029	-.11861	-.15184	-.18091	-.19867	-.23471	
Y_p/m	ft/sec² / rad/sec		-.76215	-.97080	-1.1580	-1.2696	-1.2464	-1.0561	-.85751	-.21591	
Y_r/m	ft/sec² / rad/sec		-.13320	-.16429	-.16755	-.12970	-.04881	.00243	.34313	.45010	
$Y_{\delta L}/m$	ft/sec² / IN		1.0138	1.0108	.99098	.98180	.98230	.99101	1.0319	1.1176	
$Y_{\delta R}/m$	ft/sec² / IN		.26744	.25302	.23252	.20964	.21374	.23538	.24918	.26719	
L_v/I_{xx}	rad/sec² / ft/sec		-.00775	-.01288	-.01389	-.01713	-.02409	-.03223	-.04742	-.05093	
L_p/I_{xx}	rad/sec² / rad/sec		-.49155	-.56159	-.61826	-.64573	-.61171	-.51494	-.42903	-.21500	
L_r/I_{xx}	rad/sec² / rad/sec		-.01718	-.03337	-.03813	-.02025	.01948	.04699	.21651	.29767	
$L_{\delta L}/I_{xx}$	rad/sec² / IN		.40452	.40415	.45837	.45628	.45631	.45866	.47333	.50444	
$L_{\delta R}/I_{xx}$	rad/sec² / IN		-.08132	-.08649	-.09048	-.09745	-.09563	-.08616	-.09132	-.10153	
N_v/I_{zz}	rad/sec² / ft/sec		.00165	.00058	-.00091	-.00229	-.00339	-.00429	-.00259	.00096	
N_p/I_{zz}	rad/sec² / rad/sec		-.00348	-.00324	-.03752	-.04536	-.06214	-.07983	-.08725	-.06175	
N_r/I_{zz}	rad/sec² / rad/sec		-.06500	-.05691	-.05050	-.05120	-.05602	-.06814	-.08431	-.12644	
$N_{\delta L}/I_{zz}$	rad/sec² / IN		.02979	.02885	.02727	.02595	.02602	.02697	.02755	.02843	
$N_{\delta R}/I_{zz}$	rad/sec² / IN		.17455	.17407	.17033	.16971	.16970	.17194	.17795	.19374	
δ_{Lo}	IN.		.18106	.10490	.11642	.13118	.20698	.33670	.51408	.58327	
δ_{Ro}	IN.		-.3164	-.10163	-.18246	-.39680	-.69216	-.96310	-1.1998	-1.3329	

Operating Conditions
[illegible]
C.G. Position = 110.07 in
... = 75,414 ...
Rate of Descent = 0 ft/sec
Altitude = sea level

YHC-1A

Forward Velocity	kts		0	20	40	60	80	100	120	140
u	ft/sec		0.0	33.76	67.52	101.28	135.04	168.80	202.56	236.32
α_s	deg		0.0	3.79296	6.24538	4.33124	1.95915	1.34498	-2.32062	-6.70362
θ_s	deg		8.93247	7.85991	6.30389	4.39564	1.99836	1.39503	-2.30329	-6.65556
X_u/m	[illegible]		-.02473	-.0010	-.02275	-.03752	-.04765	-.05561	-.06428	-.07233
X_w/m	[illegible]		.05444	.06852	.08576	.09073	.05690	.10490	.08542	.05593
X_{is}/m	[illegible]		.47278	.55272	.50550	.56542	.41751	.86250	.47079	-.01152
X_{1s}/m	[illegible]		.16867	.14466	.14375	.12503	.21903	.00554	.01268	.00927
$X_{\theta c}/m$	[illegible]		1.14776	.96257	.97920	.80702	.69435	.89060	.71347	.47301
Z_u/m	[illegible]		.05728	-.13527	-.05444	-.01892	.01727	.06281	.06627	.05181
Z_w/m	[illegible]		-.35403	-.48973	-.64000	-.80500	-.92252	-1.00337	-1.04679	-1.10586
Z_q/m	[illegible]		.01643	-.01657	-.16377	-.18063	.07086	-.20274	-.15242	-.23794
Z_{1s}/m	[illegible]		.05155	.25933	.52725	.54601	.48526	.41256	.33578	.27515
$Z_{\theta c}/m$	[illegible]		-7.42951	-7.16977	-7.59993	-8.48846	-9.46673	-10.2528	-11.0633	-11.6945
M_u/I_{yy}	[illegible]		.00789	.00715	-.00560	-.00731	-.00664	-.00308	-.00270	-.00214
M_w/I_{yy}	[illegible]		.00159	.01613	.02974	.02296	.02246	.02199	.02101	.02094
M_q/I_{yy}	[illegible]		-.73522	-.96234	-1.31160	-1.47449	-1.53709	-1.63902	-1.60451	-1.55425
M_{is}/I_{yy}	[illegible]		.35469	.35223	.39700	.44308	.47379	.51070	.52775	.54136
$M_{\theta c}/I_{yy}$	[illegible]		.0034	.07478	.14221	.17395	.18611	.18021	.18517	.19005
δ_{Bs}	in		-.36092	-1.09382	-1.11713	-.54350	-.00194	-.73364	-.54753	-.33976
δ_{Cs}	in		5.02277	4.44246	3.71503	3.63057	3.86946	4.65548	6.03707	8.01568

Operating Conditions:
- Gross Wt. = 13,400 #
- c.g. Position = 110.0" aft
- I_{xx} = 4203 slug-ft²
- I_{zz} = 71,786 slug-ft²
- I_{xz} = 7114 slug-ft²
- Rate of Descent = 0 fpm
- Altitude = sea level

YHC-1A
Lateral Stability Derivatives

Fwd. Velocity	kts		0	20	40	60	80	100	120	140	
"	ft/sec		0.0	33.76	67.52	101.28	135.04	168.80	202.56	236.32	
Y_v/m	$\frac{ft/sec^2}{ft/sec}$		-.26657	-.05314	-.03037	-.11800	-.15031	-.17946	-.19624	-.23226	
Y_p/m	$\frac{ft/sec^2}{rad/sec}$		-.76150	-.95748	-1.17144	-1.24159	-1.18989	-1.00044	-.70098	-.11942	
Y_r/m	$\frac{ft/sec^2}{rad/sec}$		-.17598	-.21630	-.09120	-.14219	-.06046	-.04396	.05101	.10331	
$Y_{\delta L}/m$	$\frac{ft/sec^2}{in}$		.97274	.96771	.95283	.94157	.94110	.94483	.98767	1.07454	
$Y_{\delta R}/m$	$\frac{ft/sec^2}{in}$		-.07735	-.04021	-.10813	-.12550	-.13279	-.09264	-.08746	-.05750	
L_v/I_{xx}	$\frac{rad/sec^2}{ft/sec}$		-.00804	-.01327	-.01462	-.01789	-.02527	-.03194	-.04623	-.05016	
L_p/I_{xx}	$\frac{rad/sec^2}{rad/sec}$		-.55246	-.61900	-.68329	-.68350	-.64693	-.55556	-.42797	-.21699	
L_r/I_{xx}	$\frac{rad/sec^2}{rad/sec}$		-.05590	-.06586	-.01732	-.03768	.00165	.01286	.07665	.13713	
$L_{\delta L}/I_{xx}$	$\frac{rad/sec^2}{in}$		.46883	.46762	.46306	.46017	.46062	.46011	.47570	.50657	
$L_{\delta R}/I_{xx}$	$\frac{rad/sec^2}{in}$		-.21032	-.21491	-.21801	-.22321	-.22555	-.21035	-.21739	-.22255	
N_v/I_{zz}	$\frac{rad/sec^2}{ft/sec}$		-.00287	.000003	-.00200	-.00405	-.00566	-.00735	-.00601	-.00327	
N_p/I_{zz}	$\frac{rad/sec^2}{rad/sec}$		.01290	.00620	-.00675	-.02075	-.03427	-.04439	-.05053	-.03555	
N_r/I_{zz}	$\frac{rad/sec^2}{rad/sec}$		-.05254	-.05195	-.03292	-.04546	-.01884	-.05704	-.07878	-.11367	
$N_{\delta L}/I_{zz}$	$\frac{rad/sec^2}{in}$		.03011	.02915	.02773	.02634	.02584	.02769	.02902	.03261	
$N_{\delta R}/I_{zz}$	$\frac{rad/sec^2}{in}$		.17524	.17461	.17191	.17010	.16995	.17069	.17872	.19453	
δ_{L_0}	in		.09501	.10597	.12051	.12314	.16061	.30244	.37002	.38373	
δ_{R_0}	in		.07237	.16972	.05877	-.20105	-.47659	-.57237	-.79952	-.75904	

OPERATING CONDITIONS { Gross Wt = 13,400 lbs
C.G. POSITION = 15.1" F.S.M.
I_{YY} = 75,914 SLUG-ft²
RATE of DESCENT 0 ft/min.
ALTITUDE = 10,000 ft.

YHC - 1A

LONGITUDINAL STABILITY DERIVATIVES

FORWARD VELOCITY	KTS		20	40	60	80	100				
"	ft/sec		33.76	67.52			168.80				
α_o	$\alpha = \theta$		7.942261	6.403122	4.57937	2.5160	2.17555				
θ_o	deg.		8.002019	6.46507	4.68990	2.5707	2.26076				
X_u/m	$\frac{ft/sec^2}{ft/sec}$		-.00676	-.02011	-.03064	-.03842	-.04362				
X_w/m	$\frac{ft/sec^2}{ft/sec}$		.04854	.05402	.05667	.05294	.06463				
X_q/m	$\frac{ft/sec^2}{rad/sec}$		1.18274	1.27543	1.3245	1.14179	1.34635				
$X_{\delta e}/m$	$\frac{ft/sec^2}{in}$		.11731	.10497	.11476	.14261	-.01534				
$X_{\delta c}/m$	$\frac{ft/sec^2}{in}$		.73082	.60927	.49169	.38684	.55796				
Z_u/m	$\frac{ft/sec^2}{ft/sec}$		-.10428	-.08311	-.04109	-.01031	.02654				
Z_w/m	$\frac{ft/sec^2}{ft/sec}$		-.37109	-.46709	-.57995	-.66699	-.72864				
Z_q/m	$\frac{ft/sec^2}{rad/sec}$		-.78938	-.96557	-1.36562	-1.54962	-2.08103				
$Z_{\delta e}/m$	$\frac{ft/sec^2}{in}$		.11878	.22527	.38735	.36662	.33959				
$Z_{\delta c}/m$	$\frac{ft/sec^2}{in}$		-5.67725	-5.83751	-6.38311	-6.9735	-7.51348				
M_u/I_{yy}	$\frac{rad/sec^2}{ft/sec}$		.00596	-.00287	-.00476	-.00424	-.00137				
M_w/I_{yy}	$\frac{rad/sec^2}{ft/sec}$		.00590	.01208	.01053	.00256	.00773				
M_q/I_{yy}	$\frac{rad/sec^2}{rad/sec}$		-.74532	-.98098	-1.10175	-1.13867	-1.20757				
$M_{\delta e}/I_{yy}$	$\frac{rad/sec^2}{in}$		.27308	.29324	.32647	.34753	.37460				
$M_{\dot{w}}/I_{yy}$	$\frac{rad/sec^2}{in}$		-.03141	.02056	.04731	.05114	.03905				
$S_{\delta o}$	in.		.05+01719	-.34992	.06020	.53133	-.10811				
$S_{\delta c}$	in		5.950603	5.14708	4.79474	4.945	5.50703				

Gross Wt. 13,400 lb
c.g. Position 15.1" fwd
I_{xx} 9203 slug-ft²
I_{zz} = 71,786 slug-ft²
I_{xz} 7114 slug-ft²
Rate of Descent 0 fpm
Altitude 10,000 ft

Control Condition

YHC-1A
Lateral Stability Derivatives

Fwd. Velocity	kts.		20	40	60	80	100				
"	ft/sec										
Y_v/m	ft/sec²/ft/sec		-.05154	-.06694	-.09351	-.11708	-.13950				
Y_p/m	ft/sec²/rad/sec		-1.33143	-1.5574	-1.6660	-1.64439	-1.3864				
Y_r/m	ft/sec²/rad/sec		-.22077	-.24355	-.19212	-.10401	-.04258				
Y_{δ_L}/m	ft/sec²/in		1.00068	.98003	.97069	.96468	.96484				
Y_{δ_R}/m	ft/sec²/in		.14586	.10337	.08838	.06990	.10034				
L_v/I_{xx}	rad/sec²/ft/sec		-.01407	-.01428	-.01753	-.02225	-.02571				
L_p/I_{xx}	rad/sec²/rad/sec		-.79473	-.87323	-.88429	-.86718	-.74691				
L_r/I_{xx}	rad/sec²/rad/sec		-.05877	-.06495	-.04734	-.00437	.00036				
L_{δ_L}/I_{xx}	rad/sec²/in		.46831	.46156	.45907	.45956	.45648				
L_{δ_R}/I_{xx}	rad/sec²/in		-.11646	-.14031	-.14398	-.15117	-.13794				
N_v/I_{zz}	rad/sec²/ft/sec		.00038	-.00027	-.00206	-.00295	-.00412				
N_p/I_{zz}	rad/sec²/rad/sec		-.02177	-.02632	-.02628	-.05083	-.06622				
N_r/I_{zz}	rad/sec²/rad/sec		-.06559	-.05846	-.05641	-.06007	-.06532				
N_{δ_L}/I_{zz}	rad/sec²/in		.02844	.02707	.02577	.02512	.02637				
N_{δ_R}/I_{zz}	rad/sec²/in		.17277	.17349	.17206	.17250	.17075				
δ_{L_o}	in		.08287	.08326	.10213	.16207	.25359				
δ_{R_o}	in		-.07643	-.03372	-.22665	-.48305	-.54755				

OPERATING CONDITIONS
- Gross Wt = 13,420 LBS
- C.G. POSITION 10.0" AFT
- Iyy = 75,917 SLUG-ft²
- Rate of Descent 0 ft/min
- ALTITUDE = 10,000 ft.

YHC - 1A

LONGITUDINAL STABILITY DERIVATIVES

FORWARD VELOCITY	KTS		20	40	60	80	100				
"	ft/sec		33.76	67.52			168.80				
α_o	deg.		7.59508	6.06776	4.23889	2.17403	2.13143				
Θ_o	deg.		7.65085	6.13028	4.31979	2.24015	2.21989				
X_u/m	$\frac{ft/sec^2}{ft/sec}$		-.006699	-.02109	-.03204	-.03844	-.04409				
X_w/m	$\frac{ft/sec^2}{ft/sec}$		.049135	.05523	.05732	.054558	.06887				
X_q/m	$\frac{ft/sec^2}{rad/sec}$		1.04294	1.11325	1.14785	.97057	1.17891				
$X_{\delta e}/m$	$\frac{ft/sec^2}{in}$		.11601	.10943	.13364	.14429	-.006626				
$X_{\delta c}/m$	$\frac{ft/sec^2}{in}$		.72526	.61388	.502796	.40639	.55074				
Z_u/m	$\frac{ft/sec^2}{ft/sec}$		-.10802	-.08336	-.03657	-.00687	.02810				
Z_w/m	$\frac{ft/sec^2}{ft/sec}$		-.37024	-.47079	-.58311	-.66401	-.73036				
Z_q/m	$\frac{ft/sec^2}{rad/sec}$		-.00903	-.013117	.02822	-.12241	-.61277				
$Z_{\delta e}/m$	$\frac{ft/sec^2}{in}$		.15415	.32469	.34552	.31281	.28235				
$Z_{\delta c}/m$	$\frac{ft/sec^2}{in}$		-5.64127	-5.83899	-6.35464	-6.95598	-7.49086				
M_u/I_{yy}	$\frac{rad/sec^2}{ft/sec}$		.006816	-.003299	-.005	-.00469	-.002302				
$M_{\dot{u}}/I_{yy}$	$\frac{rad/sec^2}{ft/sec}$		.010772	.01275	.01862	.01751	.01715				
M_q/I_{yy}	$\frac{rad/sec^2}{rad/sec}$		-.74592	-.9975	-1.1227	-1.15832	-1.21618				
$M_{\delta e}/I_{yy}$	$\frac{rad/sec^2}{in}$		.27217	.29113	.32282	.34476	.371536				
$M_{\delta c}/I_{yy}$	$\frac{rad/sec^2}{in}$		.026320	.07502	.1305	.14306	.13884				
δ_{Bo}	in		-1.30706	-1.55155	-1.58896	-.49757	-1.16982				
δ_{Co}	in		5.94562	5.12954	4.81974	4.96928	5.4812				

Gross Wt. 13,400 lb
c.g. Position 10.0" aft
I_{xx} = 9203 slug-ft²
I_{zz} = 71,786 slug-ft²
I_{xz} = 714 slug-ft²
Rate of Descent 0 fpm
Altitude 10,000 ft

Tabular Section

YIIC-1A
Lateral Stability Derivatives

Fwd. Velocity	Note		20	40	60	80	100				
"	ft/sec										
$Y_{\dot{v}}/m$	$\frac{ft/sec^2}{ft/sec}$		-.05183	-.06713	-.09242	-.11642	-.13886				
Y_p/m	$\frac{ft/sec^2}{rad/sec}$		-1.3406	-1.5485	-1.6552	-1.5831	-1.3349				
Y_r/m	$\frac{ft/sec^2}{rad/sec}$		-.26074	-.26982	-.20445	-.12337	-.14663				
Y_{δ_L}/m	$\frac{ft/sec^2}{in}$		.97591	.95652	.95048	.94607	.93916				
Y_{δ_R}/m	$\frac{ft/sec^2}{in}$		-.11110	-.12006	-.09533	-.14783	-.11746				
$L_{\dot{v}}/I_{xx}$	$\frac{rad/sec^2}{ft/sec}$		-.01457	-.01469	-.01815	-.02304	-.02593				
L_p/I_{xx}	$\frac{rad/sec^2}{rad/sec}$		-.85066	-.91129	-.93257	-.93172	-.76654				
L_r/I_{xx}	$\frac{rad/sec^2}{rad/sec}$		-.08207	-.08967	-.05864	-.01904	-.02907				
L_{δ_L}/I_{xx}	$\frac{rad/sec^2}{in}$		.47209	.46529	.46415	.46281	.45436				
L_{δ_R}/I_{xx}	$\frac{rad/sec^2}{in}$		-.23497	-.22496	-.20130	-.23222	-.21972				
$N_{\dot{v}}/I_{zz}$	$\frac{rad/sec^2}{ft/sec}$		.00012	-.00073	-.00288	-.00399	-.00555				
N_p/I_{zz}	$\frac{rad/sec^2}{rad/sec}$		.00456	-.00957	-.02303	-.03759	-.04829				
N_r/I_{zz}	$\frac{rad/sec^2}{rad/sec}$		-.06240	-.05661	-.05572	-.05834	-.06328				
N_{δ_L}/I_{zz}	$\frac{rad/sec^2}{in}$		.02833	.02732	.02602	.02537	.02649				
N_{δ_R}/I_{zz}	$\frac{rad/sec^2}{in}$		.17624	.17272	.16628	.17064	.16989				
δ_{L_o}	in		.10679	.11760	.14024	.15073	.23158				
δ_{R_o}	in		.19307	.17090	-.06965	-.29560	-.27287				

OPERATING CONDITIONS:
- Gross Wt. = 15,500 LBS
- C.G Position = 15.1" fwd.
- I_{yy} = 75,414 SLUG-FT²
- Rate of Descent = 0 ft/min
- Alt. code = Sea level

YHC - 1A

LONGITUDINAL STABILITY DERIVATIVES

FORWARD VELOCITY	KTS		0	20	40	60	80	100	120	140	
"	ft/sec										
α_o	deg.		0.0	8.0504	6.48937	4.6720	2.46990	.85134	-1.45267	-5.43036	
ϵ_o	deg.		9.3025	6.12154	6.55685	4.74234	2.49749	1.89087	-1.43028	-5.38938	
X_u/m	$\frac{ft/sec^2}{ft/sec}$		-.02606	-.00453	-.02093	-.03291	-.04200	-.04984	-.05678	-.06212	
X_w/m	$\frac{ft/sec^2}{ft/sec}$		.0474	.05765	.06616	.07052	.06535	.06148	.06782	.05216	
X_q/m	$\frac{ft/sec}{rad/sec}$		.73514	.85115	.92.052	.93829	.85720	1.20014	.74836	-.01630	
$X_{\delta e}/m$	$\frac{ft/sec^2}{in}$		.15403	.12503	.11066	+.12831	.14787	-.03261	-.02290	+.01325	
$X_{\delta c}/m$	$\frac{ft/sec^2}{in}$		1.06019	.83650	.71598	+.61425	.49606	+.65738	+.52661	.39715	
Z_u/m	$\frac{ft/sec}{ft/sec}$		.05355	-.11291	-.08226	-.03288	.00092	.04264	.04743	.03835	
Z_w/m	$\frac{ft/sec}{ft/sec}$		-.32575	-.42254	-.54306	-.68247	-.78390	-.85240	-.87244	-.92855	
Z_q/m	$\frac{ft/sec}{rad/sec}$		-.59946	-.91194	-1.2063	-1.48572	-1.51634	-1.97566	-1.97216	-2.13191	
$Z_{\delta e}/m$	$\frac{ft/sec^2}{in}$		-.00163	.16095	.41157	+.46557	.43829	.39375	.34673	.30778	
$Z_{\delta c}/m$	$\frac{ft/sec^2}{in}$		-6.5475	-6.3799	-6.7015	-7.3539	-8.11777	-8.73413	-9.22694	-9.8802	
M_u/I_{yy}	$\frac{rad/sec}{ft/sec}$		.00619	.00716	-.00496	-.00649	-.00580	-.00186	-.00152	-.00117	
M_w/I_{yy}	$\frac{rad/sec}{ft/sec}$		-.00291	.0088	.01621	.01402	.01178	.00988	.00827	.00718	
M_q/I_{yy}	$\frac{rad/sec^2}{rad/sec}$		-1.7559	-1.95462	-1.2761	-1.44449	-1.50013	-1.5852	-1.56141	-1.50602	
$M_{\delta e}/I_{yy}$	$\frac{rad/sec^2}{in}$		.35863	.35707	.39455	+.44216	.47122	.50139	+.52310	.52557	
$M_{\delta c}/I_{yy}$	$\frac{rad/sec^2}{in}$		-.04965	-.04451	.03618	+.06291	.06576	.04317	.04388	.03912	
$\epsilon_{\delta e}$	in		.74095	.62785	-.26519	-.21841	.65591	-.14579	.08317	.28000	
$\epsilon_{\delta c}$	in		5.69163	5.16045	4.39169	4.11274	4.33541	5.03437	6.22.40	7.97623	

Gross Wt. 15,500 lbs
c.g. Position 115.1" Aft
I_{xx} = 9203 slug-ft²
I_{zz} = 71,786 slug-ft²
I_{xz} = 7114 slug-ft²
Rate of Descent 0 fpm
Altitude sea level

Operating

Vehicle A

Lateral Directional Derivatives

Fwd. Velocity	kts.		0	20	40	60	80	100	120	140	
"	ft/sec										
Y_v/m	$\frac{ft/sec^2}{ft/sec}$		-.26543	-.05222	-.07346	-.10503	-.13333	-.15939	-.17344	-.20344	
Y_p/m	$\frac{ft/sec^2}{rad/sec}$		-.88730	-1.0277	-1.2113	-1.2983	-1.2935	-1.1335	-.89466	-.31748	
Y_r/m	$\frac{ft/sec^2}{rad/sec}$		-.13899	-.04739	-.18509	-.16205	.07461	-.07225	.05917	.00712	
$Y_{\delta L}/m$	$\frac{ft/sec^2}{in}$		1.00031	.99710	.97654	.96870	.96646	.96343	.99430	1.05551	
$Y_{\delta R}/m$	$\frac{ft/sec^2}{in}$		.14443	.13450	.11584	.10177	.10188	.10894	.11521	.13537	
L_v/I_{xx}	$\frac{rad/sec^2}{ft/sec}$		-.00960	-.01522	-.01622	-.01953	-.02632	-.03242	-.04836	-.05233	
L_p/I_{xx}	$\frac{rad/sec^2}{rad/sec}$		-.60598	-.66759	-.73596	-.75278	-.72957	-.63596	-.51719	-.25436	
L_r/I_{xx}	$\frac{rad/sec^2}{rad/sec}$		-.02248	.01450	-.04562	-.03628	.07722	.01507	.10356	.04688	
$L_{\delta L}/I_{xx}$	$\frac{rad/sec^2}{in}$		.52066	.52017	.51266	.51017	.51087	.50879	.52112	.54599	
$L_{\delta R}/I_{xx}$	$\frac{rad/sec^2}{in}$		-.14990	-.15302	-.15714	-.16177	-.15372	-.15260	-.16121	-.16567	
N_v/I_{zz}	$\frac{rad/sec^2}{ft/sec}$		.00012	-.00045	-.00091	-.00285	-.00413	-.00552	-.00435	-.00150	
N_p/I_{zz}	$\frac{rad/sec^2}{rad/sec}$		-.02138	-.01935	-.02612	-.03928	-.05223	-.06879	-.07647	-.08705	
N_r/I_{zz}	$\frac{rad/sec^2}{rad/sec}$		-.07150	-.04773	-.06054	-.05867	-.01619	-.06401	-.04353	-.10462	
$N_{\delta L}/I_{zz}$	$\frac{rad/sec^2}{in}$		.03424	.03313	.03138	.03044	.02842	.02973	.03091	.03302	
$N_{\delta R}/I_{zz}$	$\frac{rad/sec^2}{in}$		.20337	.20300	.19946	.19814	.19499	.19652	.20360	.21616	
δ_{L_o}	in		.14008	.04373	.03581	.12261	.16838	.26984	.41799	.45688	
δ_{R_o}	in		-.18958	-.06631	-.06037	-.28616	-.56343	-.67419	-.95795	-1.0389	

OPERATING CONDITIONS
- GROSS WT. = 15,500 LBS
- C.G. POSITION = 310.0" AFT
- I_{YY} = 75,914 SLUG-FT²
- RATE OF DESCENT = 0 ft/min
- ALTITUDE = SEA LEVEL

YHC - 1A

LONGITUDINAL STABILITY DERIVATIVES

FORWARD VELOCITY	KTS		0	20	40	60	80	100	120	140	
"	ft/sec										
α_o	deg.		0.0	7.69356	6.15264	4.35535	2.11281	1.7837	-1.49016	-5.50694	
Θ_e	deg.		9.00779	7.7685	6.22388	4.40976	2.15831	1.83185	-1.46317	-5.45226	
X_u/m	$\frac{ft/sec^2}{ft/sec}$	----	-.02533	-.00408	-.02200	-.03430	-.04328	-.0493 7	-.05717	-.06064	
Y_w/m	$\frac{ft/sec^2}{ft/sec}$		.04745	.05814	.06759	.07205	.06660	.08223	.06795	.05177	
X_q/m	$\frac{ft/sec}{rad/sec}$		.60293	.72243	.72706	.69920	.57936	.95115	.57302	.09404	
$X_{\dot{w}}/m$	$\frac{ft/sec^2}{in}$		.14768	.13071	.13256	.16439	.19230	.00795	.02133	.00254	
$X_{\delta e}/m$	$\frac{ft/sec^2}{in}$		+1.0545	.82695	.71703	.62226	.49747	.65813	.51809	.38419	
Z_u/m	$\frac{ft/sec^2}{ft/sec}$		.04960	-.11815	-.08238	-.02953	.00446	.04372	.04970	.03701	
Z_w/m	$\frac{ft/sec^2}{ft/sec}$		-.32595	-.42223	-.54786	-.68611	-.78492	-.85288	-.89325	-.92729	
Z_q/m	$\frac{ft/sec^2}{rad/sec}$		.12677	-.05132	.03559	-.02297	.13032	-.19733	-.21448	-.39822	
$Z_{\dot{w}}/m$	$\frac{ft/sec^2}{in}$		+.04201	.19703	.41244	.42947	.37432	.03874	.27272	.21815	
$Z_{\delta e}/m$	$\frac{ft/sec^2}{in}$		-6.55037	-6.33758	-6.63704	-7.30926	-8.0866	-8.70262	-9.39757	-9.72681	
M_u/I_{yy}	$\frac{rad/sec^2}{ft/sec}$		.00614	.00815	-.00560	-.00710	-.00644	-.00315	-.00263	-.00229	
M_w/I_{yy}	$\frac{rad/sec^2}{ft/sec}$		.00171	.01593	.02366	.02349	.02328	.02259	.02157	.02109	
M_q/I_{yy}	$\frac{rad/sec^2}{rad/sec}$		-.75031	-.95588	-1.29310	-1.46145	-1.52768	-1.59224	-1.5855	-1.51087	
$M_{\dot{w}}/I_{yy}$	$\frac{rad/sec^2}{in}$		.35904	.35551	.39110	.43617	.46456	.49842	.51712	.53171	
$M_{\delta e}/I_{yy}$	$\frac{rad/sec^2}{in}$		.03115	.03512	.13519	.17373	.19120	.18455	.18730	.19178	
$\bar{c}_e$	in		-1.1030	-1.1947	-1.31662	-1.29754	-1.2026	-.96325	-.73252	-.51740	
$\bar{c}_{c_o}$	in		5.68575	5.14427	4.36750	4.10901	4.35452	5.03397	6.21071	7.97168	

Gross Wt. 15,500 lb.
c.g. Position 110.0" a.r.t
I_{xx} = 9203 slug-ft²
I_{zz} = 71,786 slug-ft²
I_{xz} = 7114 slug-ft²
Rate of Descent 0 fpm
Altitude sea level

YHC-1A
Lateral Stability Derivatives

Ind. Velocity	kts.		0	20	40	60	80	100	120	140	
"	ft/sec										
Y_v/m	$\frac{ft/sec^2}{ft/sec}$		-.26504	-.05233	-.07348	-.10462	-.13268	-.15866	-.17272	-.20268	
Y_p/m	$\frac{ft/sec^2}{rad/sec}$		-.86509	-1.0272	-1.2126	-1.2906	-1.2526	-1.0648	-.80571	-.36599	
Y_r/m	$\frac{ft/sec^2}{rad/sec}$		-.18178	-.22615	-.20130	-.15643	-.08640	-.04962	-.00525	.03705	
$Y_{\delta L}/m$	$\frac{ft/sec^2}{in}$		.47234	.96963	.95188	.94199	.94038	.94186	.96882	1.02314	
$Y_{\delta R}/m$	$\frac{ft/sec^2}{in}$		-.07733	-.09725	-.10843	-.13164	-.13814	-.10935	-.10201	-.08253	
L_v/I_{xx}	$\frac{rad/sec^2}{ft/sec}$		-.00413	-.01567	-.01660	-.02020	-.02736	-.03279	-.04817	-.05221	
L_p/I_{xx}	$\frac{rad/sec^2}{rad/sec}$		-.64712	-.71217	-.77872	-.79201	-.74964	-.64377	-.51722	-.34287	
L_r/I_{xx}	$\frac{rad/sec^2}{rad/sec}$		-.05326	-.06908	-.06305	-.04144	-.00306	.00718	.06353	.12367	
$L_{\delta L}/I_{xx}$	$\frac{rad/sec^2}{in}$		.52316	.52322	.51670	.51396	.51396	.51301	.52491	.54577	
$L_{\delta R}/I_{xx}$	$\frac{rad/sec^2}{in}$		-.24486	-.25306	-.25470	-.26285	-.26414	-.25272	-.25523	-.26023	
N_v/I_{zz}	$\frac{rad/sec^2}{ft/sec}$		-.00031	.00009	-.00151	-.00391	-.00558	-.00746	-.00654	-.00412	
N_p/I_{zz}	$\frac{rad/sec^2}{rad/sec}$		.01247	.00606	-.00536	-.01746	-.03654	-.05332	-.05584	-.03048	
N_r/I_{zz}	$\frac{rad/sec^2}{rad/sec}$		-.06677	-.06509	-.05712	-.05511	-.05837	-.06303	-.08712	-.12266	
$N_{\delta L}/I_{zz}$	$\frac{rad/sec^2}{in}$		.03452	.03305	.03147	.02969	.02915	.03067	.03133	.03506	
$N_{\delta R}/I_{zz}$	$\frac{rad/sec^2}{in}$		.20236	.20220	.19860	.19681	.19643	.19673	.20247	.21526	
ζ_{L_0}	in		.10521	.10438	.12754	.14089	.15969	.26998	.35070	.38744	
ζ_{R_0}	in		.08426	.17930	.10222	-.15347	-.42583	-.48124	-.65784	-.67194	

OPERATING CONDITIONS

- Gross Wt. - 13,400 lbs.
- C.G. Position = 15.1" fwd.
- I_{yy} 75.914 slug-ft²
- Rate of descent = 1500 ft/min.
- Altitude = sea level

YHC - 1A

LONGITUDINAL STABILITY DERIVATIVES

FORWARD VELOCITY	KTS		0	20	40	60	80				
"	ft/sec										
α_o	deg.		76.607	46.1704	27.2029	19.1121	13.7198				
Θ_o	deg.		8.9891	8.13867	6.99471	5.34340	3.21352				
X_u/m	$\frac{ft/sec^2}{ft/sec}$		.01143	.02237	-.01231	-.03179	-.04306				
X_w/m	$\frac{ft/sec^2}{ft/sec}$		.04368	.05111	.10637	.10919	.10653				
X_q/m	$\frac{ft/sec^2}{rad/sec}$		1.02536	.93903	1.55534	1.45965	1.37043				
$X_{\dot{w}}/m$	$\frac{ft/sec^2}{in}$		.16625	.12347	.08226	.12593	.14594				
$X_{\delta e}/m$	$\frac{ft/sec^2}{in}$		1.13428	.44352	.82126	.93028	.82702				
Z_u/m	$\frac{ft/sec^2}{ft/sec}$		-.13435	-.23640	-.12619	-.02151	.01777				
Z_w/m	$\frac{ft/sec^2}{ft/sec}$		-.23744	-.26321	-.82254	-.90575	-.99052				
Z_q/m	$\frac{ft/sec^2}{rad/sec}$		-.79039	.90060	-2.45731	-2.40516	-2.42975				
$Z_{\delta e}/m$	$\frac{ft/sec^2}{in}$		.00615	.19446	.94841	.77315	.71536				
$Z_{\dot{w}}/m$	$\frac{ft/sec^2}{in}$		-7.45251	-7.3825	-6.35173	-8.00701	-9.05358				
M_u/I_{yy}	$\frac{rad/sec^2}{ft/sec}$		.01308	.01863	-.00406	-.00996	-.00635				
M_w/I_{yy}	$\frac{rad/sec^2}{ft/sec}$		.00368	.03420	.00223	.00469	.00683				
M_q/I_{yy}	$\frac{rad/sec^2}{rad/sec}$		-.58241	-.81810	-1.48210	-1.56553	-1.62309				
$M_{\dot{w}}/I_{yy}$	$\frac{rad/sec^2}{in}$		.34363	.30612	.43861	.47166	.50338				
$M_{\delta e}/I_{yy}$	$\frac{rad/sec^2}{in}$		-.05571	-.16472	.15368	.11620	.10834				
C_{Lo}	in		.03060	-1.69234	-.56816	.11550	.60565				
C_{Do}	in		3.89872	3.25032	1.25071	.90347	1.15881				

Gross Wt. 13,400 lb
c.g. Position 115.1" fwd
I_{xx} = 9203 slug-ft²
I_{zz} = 71,726 slug-ft²
I_{xz} = 7114 slug-ft²
Rate of Descent 1500 fpm
Altitude - sea level

YHC-1A
Lateral Stability Derivatives

Fwd. Velocity	kts.	0	20	40	60	80
	ft/sec					
Y_v/m	(ft/sec²)/(ft/sec)	-.08635	-.04068	-.1126	-.15170	-.18262
Y_p/m	(ft/sec²)/(rad/sec)	-1.1044	-1.3027	-1.7854	-1.8623	-1.7327
Y_r/m	(ft/sec²)/(rad/sec)	-.13435	-.10793	-.30137	-.22815	-.14244
Y_{δ_L}/m	(ft/sec²)/in	.48054	.47047	.42561	.84687	.87675
Y_{δ_R}/m	(ft/sec²)/in	.14260	.11217	.09751	.07301	.07008
L_v/I_{xx}	(rad/sec²)/(ft/sec)	-.00476	-.00747	-.00448	-.00371	-.00281
L_p/I_{xx}	(rad/sec²)/(rad/sec)	-.63036	-.71654	-.86876	-.87455	-.74734
L_r/I_{xx}	(rad/sec²)/(rad/sec)	-.05234	-.02747	-.10477	-.07877	-.05688
L_{δ_L}/I_{xx}	(rad/sec²)/in	.45403	.45705	.44170	.43230	.42630
L_{δ_R}/I_{xx}	(rad/sec²)/in	-.12454	-.13516	-.13135	-.13554	-.13256
N_v/I_{zz}	(rad/sec²)/(ft/sec)	.00122	-.00016	-.00236	-.00456	-.00706
N_p/I_{zz}	(rad/sec²)/(rad/sec)	-.02085	-.01101	-.02424	-.04001	-.05921
N_r/I_{zz}	(rad/sec²)/(rad/sec)	-.04986	-.02575	-.03287	-.03316	-.03704
N_{δ_L}/I_{zz}	(rad/sec²)/in	.02925	.02744	.02520	.02385	.02313
N_{δ_R}/I_{zz}	(rad/sec²)/in	.17235	.17149	.16373	.15906	.15540
δ_{L_0}	in	.09255	.04445	.01404	.05177	.04882
δ_{R_0}	in	-.07415	.32428	.06418	-.14676	-.43185

Operating Conditions:
- Gross Wt. 13100 lb
- c.g. Position 15.1" fwd.
- I_{YY} = 75,914 slug-ft²
- Rate of Descent/Climb +1500 fpm
- Altitude sea level

YHC - 1A

LONGITUDINAL STABILITY DERIVATIVES

FORWARD VELOCITY	KTS		0	20	40	60	80				
"	ft/sec										
α_o	deg.		-58.654	-24.907	-13.823	-9.558	-8.7905				
Θ_o	deg.		9.09615	8.24561	6.51304	4.34680	1.74707				
X_u/m	$\frac{ft/sec^2}{ft/sec}$		-.02649	-.0935	-.03260	-.04491	-.05277				
X_w/m	$\frac{ft/sec^2}{ft/sec}$		.07505	.08122	.08209	.07521	.06568				
X_q/m	$\frac{ft/sec^2}{rad/sec}$		.15633	.20875	.26690	.17058	.09717				
$X_{\delta e}/m$	$\frac{ft/sec^2}{in}$		.17842	.16223	.14284	.16227	.18105				
$X_{\delta c}/m$	$\frac{ft/sec^2}{in}$		1.16942	1.04002	.90570	.73861	.62563				
Z_u/m	$\frac{ft/sec^2}{ft/sec}$		.04316	-.02959	-.00971	.00737	.02520				
Z_w/m	$\frac{ft/sec^2}{ft/sec}$		-.52217	-.60121	-.72925	-.85332	-.94171				
Z_q/m	$\frac{ft/sec}{rad/sec}$		-1.07268	-1.2001	-1.2501	-1.38662	-1.47826				
$Z_{\delta e}/m$	$\frac{ft/sec^2}{in}$		.05444	.16010	.36212	.41296	.41472				
$Z_{\delta c}/m$	$\frac{ft/sec^2}{in}$		-7.5865	-7.64041	-8.2477	-8.9541	-9.7090				
M_u/I_{yy}	$\frac{rad/sec}{ft/sec}$		.00251	.00163	.00321	-.00458	-.00467				
M_w/I_{yy}	$\frac{rad/sec^2}{ft/sec}$		-.00148	.00327	.00726	.00765	.00730				
M_q/I_{yy}	$\frac{rad/sec^2}{rad/sec}$		-.93433	-1.0302	-1.2404	-1.37426	-1.4243				
$M_{\delta e}/I_{yy}$	$\frac{rad/sec^2}{in}$		.37472	.37430	.40095	.43815	.46558				
$M_{\delta c}/I_{yy}$	$\frac{rad/sec^2}{in}$		-.04570	-.03113	.01909	.03637	.04212				
$\epsilon_{\alpha_{ss}}$	in		.56611	.45244	.38166	.63183	1.02115				
δ_{c_o}	in		6.51301	6.30131	5.94168	5.94845	6.38836				

Gross Wt. 13,400 lb.
c.g. Position 115.1" fwd.
I_{xx} = 9203 slug-ft²
I_{zz} = 71,786 slug-ft²
I_{xz} = 7114. slug-ft²
Rate of Descent -1500 fpm
Altitude sea level

YHC-1A
Lateral Stability Derivatives

Fwd. Velocity	kts.		0	20	40	60	80				
"	ft/sec										
Y_v/m	ft/sec²/ft/sec		-.20605	-.08482	-.10455	-.12256	-.14842				
Y_p/m	ft/sec²/rad/sec		-.40849	-.48197	-.63817	-.68143	-.63180				
Y_r/m	ft/sec²/rad/sec		-.04204	.04052	-.06921	-.04086	.01514				
$Y_{\delta L}/m$	ft/sec²/in		1.03950	1.04223	1.04064	1.04266	1.06287				
$Y_{\delta R}/m$	ft/sec²/in		.14982	.14802	.12884	.11875	.12938				
L_v/I_{xx}	rad/sec²/ft/sec		-.02127	-.01846	-.01978	-.02244	-.02864				
L_p/I_{xx}	rad/sec²/rad/sec		-.37496	-.40345	-.45470	-.46312	-.42405				
L_r/I_{xx}	rad/sec²/rad/sec		.02907	.05743	.02113	.03740	.07083				
$L_{\delta L}/I_{xx}$	rad/sec²/in		.48113	.48228	.48271	.48417	.49124				
$L_{\delta R}/I_{xx}$	rad/sec²/in		-.13312	-.12406	-.14131	-.13554	-.14455				
N_v/I_{zz}	rad/sec²/ft/sec		.00103	.00098	.00014	.00052	.00041				
N_p/I_{zz}	rad/sec²/rad/sec		-.02133	-.02182	-.02478	-.02754	-.03643				
N_r/I_{zz}	rad/sec²/rad/sec		-.07852	-.06348	-.07218	-.07150	-.08262				
$N_{\delta L}/I_{zz}$	rad/sec²/in		.03074	.03053	.02924	.02856	.02918				
$N_{\delta R}/I_{zz}$	rad/sec²/in		.18338	.18365	.18366	.18425	.18730				
δ_{L_o}	in		.16567	.15081	.14181	.15535	.20065				
δ_{R_o}	in		-.23383	-.21772	-.28003	-.42584	-.61869				

APPENDIX G

STABILITY DERIVATIVE DATA FOR THE MIT CH-46C

MASSACHUSETTS INSTITUTE OF TECHNOLOGY
DEPARTMENT OF AERONAUTICS AND ASTRONAUTICS
INSTRUMENTATION LABORATORY
CAMBRIDGE, MASS. 02139

C. S DRAPER
DIRECTOR

TO R. B. Trueblood
FROM R. A. MacDonald
DATE 4 January 1965
SUBJECT Revised Stability Derivatives for CH-46 Helicopter (Project 54-190)

Attached is a tabulation of longitudinal and lateral stability derivatives for the CH-46 helicopter. These derivatives have been revised on the basis of results from the new Vertol computer program transmitted to us as Jobs 6111-1 and 2 on 4 December 1964. For convenience, the derivatives are presented in both dimensional and non-dimensional forms.

Derivatives for both the "normal" and "most aft" center of gravity positions are included. These positions are defined in the table:

	WRT Centerline between rotors	Fuselage Structural Station
"Normal" CG position	13.5 in fwd	298.8 in
"Most Aft" CG position	16.0 in aft	327.2 in

Many derivatives do not change significantly with c.g. position. Therefore, only those which change markedly are tabulated for the "most aft" c.g. condition. The remaining ones are assumed to be invariant with c.g. position.

Cross-coupled derivatives (e.g. M_r, Y_{V_X}, etc.) are omitted from this tabulation since investigation showed that all were of minor importance. These derivatives are available, however, in the event that they are required for special-purpose studies.

The derivatives have been calculated for a gross weight of 18700 lbs. Some derivatives are "worse" at higher or lower gross weights; however it is felt that the effect of gross weight is small enough to warrant confining our analyses to this one weight only.

The derivatives have been calculated assuming that "longitudinal cyclic trim" is used. (With LCT, the longitudinal tilt of the rear rotor is changed linearly with speed between 70 and 110 knots from 0.5 degrees aft to 4.0° forward.) Our flight control system does not use LCT. The effect on longitudinal derivatives (and therefore on pitching stability) of removing LCT at speeds above 70 knots is not known, and therefore must be established. The derivatives presented herein at 90 and 140 knots are subject to this reservation.

RM/cm Encl.
cc: W.B.Bryant, J.J.Cattel, M.L.Todd

INSTRUMENTATION LABORATORY
MASSACHUSETTS INSTITUTE OF TECHNOLOGY
CAMBRIDGE, MASS.

PREPARED BY: RMac

DATE: 22 Dec 64

W = 18700 LB, m = 581.2 SLUGS
I_x = 13478 SL-FT²
I_y = 105777 SL-FT²
I_z = 99641 SL-FT²

W = 18700 LBS, m = 581.2 SLUGS
I_x = 13478 SL-FT²
I_y = 112000 SL-FT²
I_z = 106000 SL-FT²

JOB: ___ PROJECT ___ JOB ___ RUN

SOURCE: VERTOL JOB NOS 6111-1 & 2 SHEET ... OF ...

WITH LONGITUDINAL CYCLIC TRIM

	PARAMETER	UNITS	NORMAL C.G POSITION V, KNOTS 0	40	90	140	AFT CG POSITION V, KNOTS 0	40	90	140
LONGITUDINAL	$X_{V_x}-g_{\theta_x}$	LBS/FPS	-15.1	-11.4	-24.0	-33.8				
	$X_{V_z}-X_{\alpha_z}$	LBS/FPS	+24.8	+34.8	+36.0	+10.9				
	X_q	LBS/RAD/SEC	+645	+836	+1025	+1027				
	X_{δ_e}	LBS/INCH	+105.1	+79.9	+42.0	-10.3	+102.1	+100.3	+97.0	+92.4
	X_{δ_z}	LBS/RAD	+25400	+17500	+12000	-2220				
	$Z_{V_x}-Z_{\theta_x}$	LBS/FPS	+28.7	-44.5	+10.5	+22.5				
	$Z_{V_z}-Z_{\theta_z}$	LBS/FPS	-165	-269	-400	-395				
	Z_q	LBS/RAD/SEC	-108.	-451	-1030	-3040	+210	+88	-80	-2027
	Z_{δ_e}	LBS/INCH	+7.1	+224	+243	+287	+29.4	+209.1	+155.0	-492.6
	$Z_{\dot{\alpha}_z}$	LBS/RAD	-150200	-153200	-164500	-179800				
	$M_{V_x}-M_{\dot{\theta}_x}$	FT-LBS/FPS	+530	-371	-333	-116				
	$M_{V_z}-M_{\dot{\alpha}_z}$	FT-LBS/FPS	-230	+1293	+880	+295	+199	+1967	+2010	+2835
	M_q	FT-LBS/RAD/SEC	-66500	-104900	-124000	-94800				
	M_{δ_e}	FT-LBS/INCH	+33100	+35650	+42900	+37450				
	M_{δ_z}	FT-LBS/RAD	-172000	+110700	215000	-23600	+170000	+531000	+790000	+1412000
	E_θ	DEG // RAD	-//-	7.15 // .1250	3.30 // .0576	-3.71 // -.0648	-//-	6.70 // .1170	3.00 // .0524	-4.02 // -.0702
	V_{X_θ}	FPS	0	67.6	152.0	236.5	0	67.6	152.0	236.5
	V_{Z_θ}	FPS	0	8.45	8.76	-15.32	0	7.91	7.96	-16.60
LATERAL	$Y_{V_x}-Y_{\theta_x}$	LBS/FPS	-10.6	-36.7	-71.8	-97.6				
	Y_p	LBS/RAD/SEC	-771	-1029	-1045	-631				
	Y_r	LBS/RAD/SEC	-115.8	-162.6	-101.5	+39.3				
	Y_{δ_L}	LBS/INCH	+586	+574	+560	+598				
	Y_{δ_r}	LBS/INCH	+72.0	+50.2	+43.0	+37.2	-62.8	-85.3	-89.8	-83.9
	$L_{V_x}-L_{\theta_x}$	FT-LBS/FPS	-121	-179	-280	-564				
	L_p	FT-LBS/RAD/SEC	-11740	-13750	-13220	-9480				
	L_r	FT-LBS/RAD/SEC	-975	-1344	-710	+1250				
	L_{δ_L}	FT-LBS/INCH	+6710	+6640	+6530	+6890				
	L_{δ_r}	FT-LBS/INCH	-1612	-1748	-1700	-1939	-2766	-2917	-2910	-2991
	$N_{V_x}-N_{\theta_x}$	FT-LBS/FPS	-26.5	-65.7	-129.0	-258.4				
	N_p	FT-LBS/RAD/SEC	-2213	-3387	-6280	-9815	+1340	-219	-3630	-4357
	N_r	FT-LBS/RAD/SEC	-6328	-5568	-5430	-9683				
	N_{δ_L}	FT-LBS/INCH	+2002	+1722	+1600	+1550				
	N_{δ_r}	FT-LBS/INCH	+15810	+15500	+15150	+16170				

CH-46 HELICOPTER
DIMENSIONAL STABILITY
DERIVATIVES

INSTRUMENTATION LABORATORY
MASSACHUSETTS INSTITUTE OF TECHNOLOGY
CAMBRIDGE MASS

PREPARED BY: RNA

DATE: 31 Dec 64

CH-46 HELICOPTER

NONDIMENSIONAL STABILITY DERIVATIVES (WITH LONGITUDINAL CYCLIC TRIM)

JOB ____ — ____ — ____
PROJECT JOB RUN

SOURCE: VERTOL JOB NOS 6111-1 & 2

SHEET ... OF ...

PARAMETER	UNITS	NORMAL CG POSITION — V, KNOTS				AFT CG POSITION — V, KNOTS			
		0	40	90	140	0	40	90	140
X_{G_1}, X_{V_X}	1/SEC	-.02592	-.01966	-.04130	-.05815				
X_{G_2}, X_{V_Z}	1/SEC	.04265	.05979	.06200	.01873				
X_q	FT/SEC	1.109	1.440	1.765	1.765				
X_{S_C}	$\frac{FT}{SEC^2}$/INCH	.1809	.1372	.07230	-.01773	.1756	.1725	.1680	.1589
X_{S_Z}	$\frac{FT}{SEC^2}$/RAD	43.72	30.09	20 64	-3.819				
$\bar{Z}_{G_1}, \bar{Z}_{V_X}$	1/SEC	.04938	-.07660	.01810	.03873				
$\bar{Z}_{G_2}, \bar{Z}_{V_Z}$	1/SEC	-.2834	-.4624	-.6890	-.6602				
$\bar{Z}_q$	FT/SEC	-.1854	-.7763	-1.772	-5.227	.3610	.1510	-.1330	-3.483
$\bar{Z}_{S_C}$	$\frac{FT}{SEC^2}$/INCH	.01221	.3854	.4180	.4935	.05060	.3597	.2670	-.8475
$\bar{Z}_{S_Z}$	$\frac{FT}{SEC^2}$/RAD	-258.6	-264.0	-317.5	-309.7				
M_{G_X}, M_{V_X}	SEC^{-2}/FPS	.005014	-.003507	-.003150	-.001094				
M_{G_Z}, M_{V_Z}	SEC^{-2}/FPS	-.002185	.001220	.0008320	.002792	.001773	.01756	.01793	.02532
M_q	$SEC^{-2}/\frac{RAD}{SEC}$	-.6286	-.9921	-1.173	-.8961				
M_{S_C}	SEC^{-2}/IN	.3135	.3374	.4060	.3544				
M_{S_Z}	SEC^{-2}/RAD	-1.629	1.047	2.033	-.2232	1.512	4.746	7.054	12.61
E_0	DEG // RAD	9.15 // -	7.151/.1250	5.30 // .0576	-3.71 // .0648	- // -	6.70 // .1170	3.00 // .0524	-1.02 // -.0702
V_{X_e}	FPS	0	67.6	152.0	236.5	0	67.6	152.0	236.5
V_{Z_e}	FPS	0	8.45	8.76	-15.32	0	7.91	7.96	-16.60
Y_{G_1}, Y_{V_X}	1/SEC	-.01815	-.06309	-.1235	-.1678				
Y_p	FT/SEC	-1.327	-1.771	-1.798	-1.056				
Y_r	FT/SEC	-.1592	-.2797	-.1746	.06757				
Y_{δ_C}	$\frac{FT}{SEC^2}$/INCH	1.008	.9869	.9635	1.029				
Y_{S_Z}	$\frac{FT}{SEC^2}$/INCH	.1238	.08642	.07599	.06896	-.1081	-.1467	-.1545	-.1444
L_{G_X}, L_{V_X}	SEC^{-2}/FPS	-.008979	-.01325	-.02077	-.04185				
L_p	$SEC^{-2}/\frac{RAD}{SEC}$	-.8713	-1.020	-.9808	-.7032				
L_r	$SEC^{-2}/\frac{RAD}{SEC}$	-.07230	-.09969	-.05268	.09272				
L_{δ_C}	SEC^{-2}/INCH	.4980	.4926	.4845	.5108				
L_{S_Z}	SEC^{-2}/INCH	-.1196	-.1297	-.1261	-.1439	-.2052	-.2164	-.2159	-.2219
N_{G_X}, N_{V_X}	SEC^{-2}/FPS	-.0002667	-.0006591	-.004305	-.002593				
N_p	$SEC^{-2}/\frac{RAD}{SEC}$	-.02221	-.03399	-.0630	-.09650	.01264	-.002062	-.03425	-.04110
N_r	$SEC^{-2}/\frac{RAD}{SEC}$	-.06351	-.05588	-.05450	-.09718				
N_{δ_C}	SEC^{-2}/INCH	.02009	.01728	.01606	.01556				
N_{S_Z}	SEC^{-2}/INCH	.1587	.1556	.1520	.1623				

	NORMAL	AFT
C.G. POSIT		
W, LBS	18700	18700
m, SLUGS	581.2	581.2
I_x, SL-FT^2	13478	13478
I_y, SL-FT^2	105777	112000
I_z SL-FT^2	99641	106000

APPENDIX H

SUMMARY COMPARISON OF SELECTED PARAMETERS FOR SEVERAL BOEING/VERTOL HELICOPTERS

Summary Comparison of Selected Parameters for Several Vertol Helicopters

Parameter	Aircraft →	MIT NCH-46C (Ser. 58-5516)					NASA YHC-1A (Ser 58-5514)				
	Data Source →	Measured	Vertol Job G111-1,2	B-V Print L107C2001			NASA TN D-2847	B-V Report Aero Inv 111-41	B-V Print 107X2001	B-V Job Ⓑ #6377 Et Al	
Rotor Radius, Ft			25				24.17	24.17	24.17	24.167	
Blade Chord, Ft			1.5				1.5	1.5		1.5	
Blade Twist, Ctr of Rotation to Tip, Deg			-8.33				-8.05	-8.055		-8.055	
Flapping Hinge Offset, Ft			.425				.383	.383		.383	
Solidity = nb/πR			.0573				.0593	.0593			
Rotor Disc Area (Total 2 Rotors), Ft			3925 *				3670	3670			
Rotor Blade Weight, Lbs			-				≈130	-			
Rotor Blade Moment of Inertia About Flap Hinge, Sl-Ft²			970				-	646		646.25	
Distance Between Rotor Heads, Ft (Not ∥ X-Axis)			38.35				38.33	-	38.33		
Rotor Shaft Fwd Tilt (Wrt Fuse Ref Line), Deg	Front		9.5				9.5	9.5		9.5	
	Rear		7.0				7.0	7.0		7.0	
Normal Gross Weight, Lbs			18700				15500	15550		15500	
Overload Gross Weight, Lbs			-				16600	-			
Operating Gross Weight, Lbs			-				13000	-		13400	
Normal Rotor Speed, RPM			264 *				268	258		258 *	
Normal Rotor Tip Speed, FPS			690				678	653		653	
Most Fwd CG Position (Wrt C.L. Betw Rotors), In.			-				28 Fwd	28.0 Fwd Ⓐ		28.0" Fwd	
Most Aft CG Position ("), In			16 Aft				10 Aft	10.0 Aft Ⓐ		10.0" Aft	
Normal CG Position ("), In			13.5 Fwd	-			-	15.1 Fwd Ⓐ	16.4 Fwd	15.1" Fwd	
Distance ∥ X-Axis, Norm CG to Rotor Hub, Ft	Front		16.75				-	16.25	≈16.23 *	16.5	
	Rear		16.28				-	16.57	≈16.81 *	16.5	
Distance ∥ Z-Axis, Norm CG to Rotor Hub, Ft	Front		6.29				-	5.01	≈5.04 *	5.97	
	Rear		10.93				-	10.68	≈10.71 *	10.62	
Pitch Moment of Inertia at Norm GW & CG, Sl-Ft²			105777				75000	75914		75914	
Roll " " " " " , Sl-Ft²			13478				9200	9203		9203	
Yaw " " " " " , Sl-Ft²			99641				71000	71786		71786	
Product of Inertia, J_{zx}, at Norm GW & CG, Sl-Ft²			-				-	±7114		±7114	
Longitudinal Stick Travel, δ_e, In		±7.0		±6.0 @ 247.5R			±5.5	±5			
Differential Collective Pitch Travel, Deg		±4.2		±4			±3	±3			
|Ratio|, Deg/In		.600 *	.667	.667 *			.545 *	.600		.600	
Longitudinal Cyclic Trim, Front (Fixed), Deg				-2.82			-2 (Fwd)	-2		2.0° (Fwd)	
" " " " , Rear (Hover Value), Deg				±0.5			0.5 (Aft)	0.5		.5° (Aft)	
Lateral Stick Travel, δ_a, In		±5.25		±3.66 @ 247.5R			±3.6	±3.6			
Lateral Cyclic Pitch Travel Due to δ_a, Deg	Front	±8.25		±9.00			±6.15	±7.27			
	Rear	±7.00		±7.50			±4.60	±4.73			
|Ratio|, Deg/In	Front	1.571 *	1.845	2.500 *			1.708 *	2.019		2.02	
	Rear	1.333 *	1.540	2.083 *			1.278 *	1.314		1.31	
Pedal Travel, δ_r, In		±3.25		±2.3 @ 140R			±2.3	±2.3			
Directional Differential Lateral Cyclic, Deg	Front	±9.2		±9.50			±7.13	±7.13			
	Rear	±9.1		±9.50			±7.13	±7.13			
|Ratio|, Deg/In	Front	2.631 *	2.77	4.130 *			3.100 *	3.100		3.10	
	Rear	2.600 *	2.77	4.130 *			3.100 *	3.100		3.10	
Collective Stick Travel, δ_c, In		13.4		12.0 @ 18.19R			0 to 12.8	12			
Total Collective Pitch Blade Travel, Deg		16.35		16			1 to 17	1 to 17			
Ratio, Deg/In		1.220 *		1.333 *			1.250 *	1.333 *		1.333	

Date	Rev
23 Apr 68	Add column Ⓑ
29 Feb 68	Add Ⓐ

*: Value calculated from other parameters in same column

RH 21 Feb 68

APPENDIX I

DETAILS OF THE ANALOG SIMULATION OF THE CH-46C

I.1 Component assignment sheets and potentiometer settings for the simulation of the CH-46C

The component assignment sheets are included as pages I-2 and I-3 and the potentiometer settings as pages I-4 to I-7.

I.2 Computer Connection Diagrams

The computer connection diagrams are included as pages I-8 to I-11.

Enclosure 11

231-R AMPLIFIER ASSIGNMENT SHEET

AMPLIFIER NUMBER	FEEDBACK CONNECTION	OUTPUT FUNCTION, AND, OR, VARIABLE	CHECK POINT	STATIC TEST
00	∫	X_{Vx} COMPUTATION		10.00
01	∫	$+V_{XA}$		10.00
02		$-F_x$		-30.49
03		$+V_{Xc}$		+11.13
04		F_{XA} COMPONENT		+18.60
05				
06		$-\delta_e$		-10.00
07				
08		$+\delta_{ZC}$		0.00
09				
10	∫	Z_{Vx} COMPUTATION		10.00
11	∫	$+V_{ZA}$		10.00
12		$-F_z$		75.32±2.0
13				
14		$+P_{Sx}$		
15				
16				
17				
18				
19		IAS - 40 KNOTS		-22.65
20	∫	M_{Vx} COMPUTATION		10.00
21	∫	$+\omega_{YA}$		10.00
22		$-M$		-75.31
23		M COMPONENT		-2.24
24		P_{SY}		
25				
26				
27				
28				
29				
30		$+h$		
31	∫	$+V_{YA}$		10.00
32		$-F_y$		-0.66
33		Fy COMPONENT		+0.58
34		$+P_{SH}$		

AMPLIFIER NUMBER	FEEDBACK CONNECTION	OUTPUT FUNCTION, AND, OR, VARIABLE	CHECK POINT	STATIC TEST
35		$+\delta_a$		10.00
36		$-IAS$		
37		$+\delta_{ea}$		
38		$-\delta_{ac}$		
39		$-\delta_{rc}$		
40		$+\delta_r$		10.00
41		$-\omega_{XA}$		10.00
42		$+L$		35.45
43		$-V_{ZA}$ SINE		-1.71
44		L COMPONENT		-35.43
45		$+H$		10.00
46		$+\omega_{ZA}$		10.00
47		$-N$		-27.33
48		N COMPONENT		-0.18
49				
50		$-\delta_z$		-10.00
51				
52		$+\dot{h}$		-6.28±.20
53				
54				
55		$+V_{Kc}$ TO EDC		+0.73
56		$+\delta_z$		10.00
57				
58				
59				
60				
61				
62				
63				
64				

TP#4547 (Rev.7/64) Change RM 13 Mar 68

AMPLIFIER ASSIGNMENT SHEET

AMPLIFIER NUMBER	FEEDBACK CONNECTION	OUTPUT: FUNCTION, AND, OR, VARIABLE	CHECK POINT	STATIC TEST
65		$-P_{SX}$ TO EDC		
66		$-P_{SY}$ TO EDC		
67				
68				
69				
70				
71				
72				
73				
74				
75		$+V_{YA}$ TO EDC		+2.00
76		$+\phi$ TO EDC		− 2.50
77				
78				
79				
80				
81				
82				
83				
84				
85		$-H$		−10.00
86		$+\phi$		−10.00
87				
88				
89		$-\Delta E$		10.00
90		$+E$		10.00
91		$-\phi$		10.00
92		$+\dot{H}$		6.36
93				
94				
95		$g \cos\phi$		43.93
96		$\omega_{ZA} \sin\phi$		−3.42
97				
98				
99		$-\dot{H}$		−6.36

AMPLIFIER NUMBER	FEEDBACK CONNECTION	OUTPUT: FUNCTION, AND, OR, VARIABLE	CHECK POINT	STATIC TEST
F	60	$-V_{XC}$		−11.13
F	61	$-\dot{h}$		+1.13
F	62	IAS TO EDC		+0.73
F	63	$+H$ TO EDC		+1.12
F	64	$+\omega_{XA}$		−10.00
F	70	$+\delta_e$		+10.00
F	71	$+P_{SH}$ TO EDC		
F	72	$+\Delta E$ TO EDC		−3.32
F	73	$+\Delta E$		−10.00
F	74	$100 \cos\phi$		−94.00
M	06	$-\omega_{YA} V_{XA}$		−1.00
M	07	$-V_{XA}$		−10.00
M	16	$-\omega_{XA} V_{ZA}$		+1.00
M	17	$-V_{ZA}$		−10.00
M	26	$+\omega_{YA} V_{ZA}$		+1.00
M	27	$-\omega_{YA}$		−10.00
M	36	$+\omega_{XA} V_{YA}$		− 1.00
M	37	$-V_{YA}$		−10.00
M	46	$+\omega_{ZA} V_{XA}$		+1.00
M	47	$-\omega_{ZA}$		−10.00
M	56			
M	57			

A/C COEFFICIENTS I-4

POTENTIOMETER ASSIGNMENT SHEET

POT. NO.	SETTING RUN NO. ST. TEST	SETTING RUN NO. HOVER	SETTING RUN NO. 40 Kts	SETTING RUN NO. 90 KTS	NOTES	PARAMETER DESCRIPTION	POT. NO.
P 0	0563	0563	0730	0894		$8.7266\times10^{-5} X_q$	~~P15~~
Q 0	0196	—	—	—		11.4 /m	Q15
P 1	.0755	.0755	.0570	.1200		$X_{EX}/200$	P16
Q 1	.1270	.1270	.0875	0600		$5\times10^{-6} X_{\delta_E}$	Q16
P 2	0620	0620	0870	0900		$.0025 X_{V_E}$	~~P17~~
Q 2	3441	—	—	—		200 /m	~~Q17~~
P 3	1051	1051	0799	0420		$.001 X_{\delta_E}$	~~P18~~
Q 3	.1240	.1240	.1740	.1800		$X_{EZ}/200$	~~Q18~~
P 4	1610	1610	1619	1629		$.87266\times10^{-5} W\cos E_o$	~~P19~~
Q 4							~~Q19~~
P 5	1510	—	—	—			P20
Q 5	2241	—	—	—		130.26 /m	Q20
P 6							~~P21~~
Q 6	7756	—	—	—			~~Q21~~
P 7	3434	—	—	—			P22
Q 7	3728	—	—	—		216.70 /m	Q22
P 8							~~P23~~
Q 8	.1000						Q23
P 9							~~P24~~
Q 9							~~Q24~~
P 10	.8250	.8250	1.3450	1.0000		$Z_{EZ}/200$	P25
Q 10	.1934	—	—	—		M_q CALC	Q25
P 11	7510	7510	7660	9225	(.9100 = 4200 LBS/IN)	$-.5\times10^{-5} Z_{\delta_E}$	~~P26~~
Q 11	0071	0071	2240	2430		$.001 Z_{\delta_E}$	~~Q26~~
P 12	0.222	—	—	—		$5\times10^{-4} Z_{V_{X_o}}$	~~P27~~
Q 12	6882	—	—	—		400 /m	Q27
P 13	4611	4611	4639	4667	Balance C11	$.25\times10^{-4} W\cos E_o$	~~P28~~
Q 13	0094	0094	0394	0899		$-.87266\times10^{-4} Z_{E_o}$	~~Q28~~
P 14	.7647	—	—	—		Z_{V_E} CALC	~~P29~~
Q 14	6725	—	—	—		$.0025 Z_{V_{E_o}}$	~~Q29~~

TP #4547

— WINDS

* CHANGE FOR STATIC TEST

V " " DIFFERENT V_X — LONGITUDINAL RUNS

" LATERAL RUNS

POTENTIOMETER ASSIGNMENT SHEET

POT. NO.	SETTING RUN NO. ST. TEST	SETTING RUN NO. HOVER	SETTING RUN NO. 40 KTS	SETTING RUN NO. 90 KTS	NOTES	PARAMETER DESCRIPTION	POT. NO.
P15							P15
Q15							Q15
P16							P16
Q16							Q16
P17							P17
Q17							Q17
P18	6981	—	—	—			P18
Q18							Q18
P19							P19
Q19	0349	0000	2358	5306		.0034906 $V_{X_{19}}$	Q19
P20	5417	—	—	—		$5.7296 \times 10^{4} / I_Y$	P20
Q20	3491	—	—	—			Q20
P21	.0530	-.0530	+.0371	+.0333	into Σ23 for hover	$M_{Gx}/10000$	P21
Q21	0646	—	—	—		$5 \times 10^{5} M_{V_Z}$	Q21
P22	7130	—	—	—		$2 \times 10^{5} M_{\delta_E}$	P22
Q22	1107	—	—	—		$10^{6} M_{\delta_{E_2}}$	Q22
P23	0371	—	—	—		$10^{-4} m_{V_X}$	P23
Q23	1831	—	—	—		$1.7453 \times 10^{6} m_{I_Z}$	Q23
P24	+3379	+3378	0000	-4220			P24
Q24	.0230	-.0230	+.1293	+.0880	into Σ22 for hover	$M_{GZ}/10000$	Q24
P25							P25
Q25	0918	—	—	—		53.345 / m	Q25
P26							P26
Q26	0031	—	—	—		1.7999 / m	Q26
P27							P27
Q27							Q27
P28	0489	—	—	—		M_{IZ} CALC	P28
Q28	2254	—	—	—		M_{IZ} CALC	Q28
P29							P29
Q29	1745	—	—	—			Q29

TP #4547

POTENTIOMETER ASSIGNMENT SHEET

POT. NO.	SETTING RUN NO. ST. TEST	SETTING RUN NO. HOVER	SETTING RUN NO. 40 KTS	SETTING RUN NO. 90 KTS	NOTES	PARAMETER DESCRIPTION	POT. NO.
P30	6981	—	—	—			P30
Q30	.0789	—	—	—		M_q CALC	Q30
P31	1610	1610	1619	1629		$.87266\times10^{-3} W\cos E_o$	P31
Q31	0265	0265	0918	1795		$-2.5\times10^{-3} Y_{VT}$	Q31
P32	0180	0180	0126	0108		$2.5\times10^{-4} Y_{\delta r}$	P32
Q32	6982	—	—	—		400/m	Q32
P33	.0530	.0530	.1835	.3590		$Y_{G_y}/200$	P33
Q33	0673	0673	0898	0912		$-.87266\times10^{-4} Y_p$	Q33
P34	1465	1465	1435	1400		$2.5\times10^{-4} Y_{\delta a}$	P34
Q34	0101	0101	0142	0089		$-.87266\times10^{-4} Y_r$	Q34
P35							P35
Q35	0349	0000	2358	5306		$.0034907 V_{X_{A_o}}$	Q35
P36							P36
Q36	3491	—	—	—			Q36
P37	0513	—	—	—		29.840/m	P37
Q37	0188	—	—	—		10.953/m	Q37
P38							P38
Q38							Q38
P39							P39
Q39							Q39
P40							P40
Q40							Q40
P41	3355	3355	3320	3265		$.5\times10^{-4} L_{\delta a}$	P41
Q41	0806	0806	0874	0850		$-.5\times10^{-4} L_{\delta r}$	Q41
P42	0605	0605	0895	1400		$-.5\times10^{-3} L_{V_T}$	P42
Q42	2212	—	—	—		$4 I_{zx}/I_z$	Q42
P43	4251	—	—	—		$5729.6/I_x$	P43
Q43	.1210	.1210	.1790	.2800		$L_{G_y}/1000$	Q43
P44	0170	0170	0235	0124		$-1.7453\times10^{-5} L_r$	P44
Q44	2049	2049	2400	2307		$-1.7453\times10^{-5} L_p$	Q44

TP#4547

POTENTIOMETER ASSIGNMENT SHEET

POT. NO.	SETTING RUN NO. ST TEST	SETTING RUN NO. HOVER	SETTING RUN NO. 40 KTS	SETTING RUN NO. 90 KTS	NOTES	PARAMETER DESCRIPTION	POT. NO.
P45	0276	0276	0243	0237		$-.43633\times10^{-5}\ N_r$	P45
Q45	.0066	.0066	.0164	.1073		$N_{GY}/4000$	Q45
P46	0097	0097	0148	0274		$-.43633\times10^{-5}\ N_p$	P46
Q46	1976	1976	1938	1894		$.125\times10^{-4}\ N_{\dot{r}}$	Q46
P47	1494	—	—	—		$.25\ J_{ex}/I_x$	P47
Q47	0033	0033	0042	0526		$-.1125\times10^{-3}\ N_{V_T}$	Q47
P48	2300	—	—	—		$2.2918\times10^{-4}/I_z$	P48
Q48	.0250	.0250	0215	0200		$.125\times10^{-4}\ N_{\delta a}$	Q48
P49	1000	0473	0358	0165		$.005\ E_0$ (occ)	P49
Q49	4675	—	—	—		$.25\times10^{-4}\ W$	Q49
Q50							Q50
Q51							Q51
Q52							Q52
Q53	2470	—	—	—			Q53
Q54							Q54
Q55							Q55
Q56				—			Q56
Q57	0500	0000	1188	2656		$.0017453\ V_{X_{CO}}$	Q57
Q58	0873	0000	1478	1529		$.017453\ V_{Z_{H_0}}$	Q58
Q59	8369	—	—	—			Q59
Q60	1000	—	—	—		ST. TEST VOLTAGE	Q60
Q61	1000					ST. TEST VOLTAGE	Q61
Q62							Q62
Q63							Q63
Q64							Q64
Q65							Q65
Q66							Q66
Q67							Q67
Q68							Q68
Q69							Q69

TP #4547

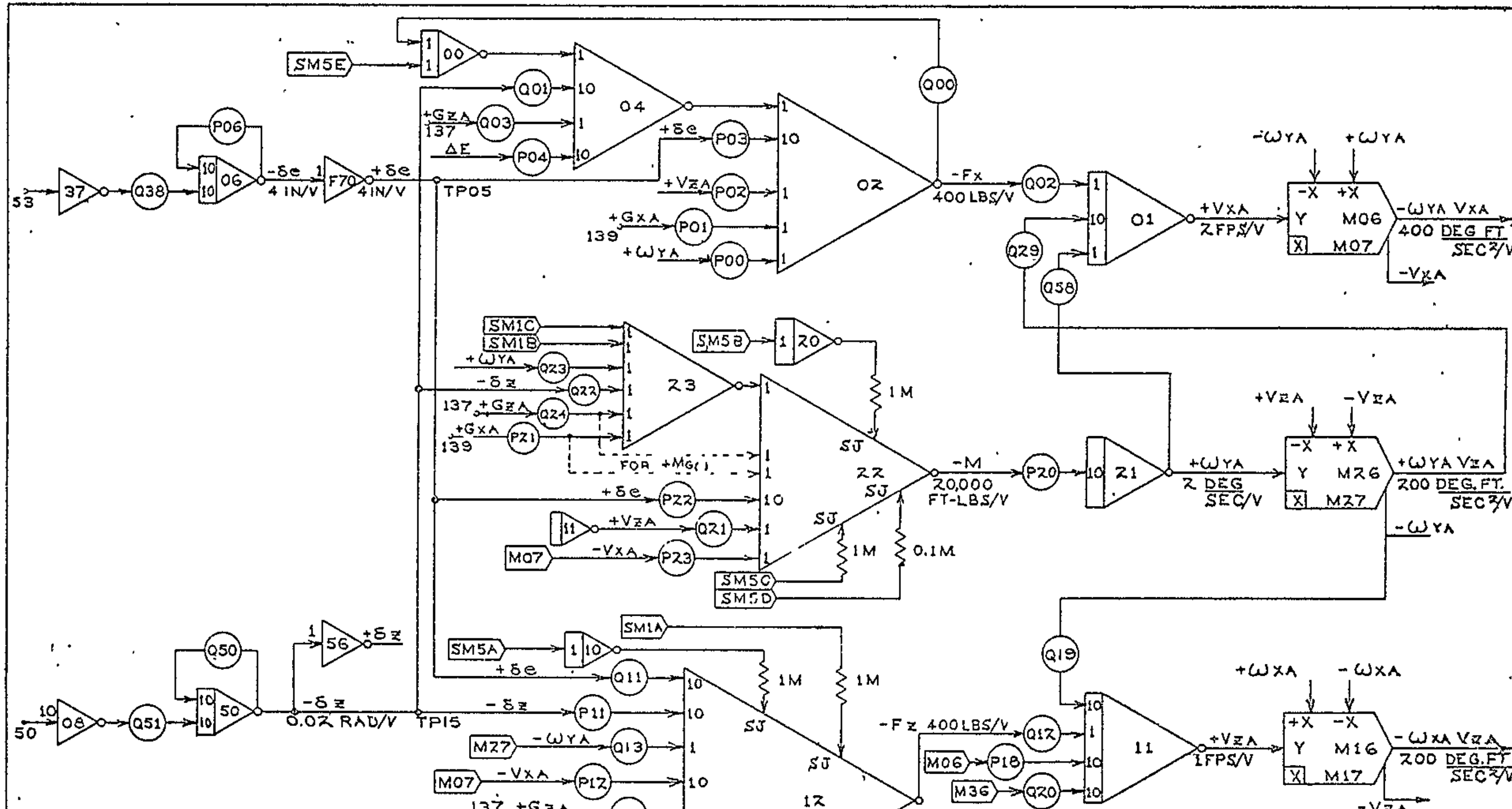

CH-46 HELICOPTER SIMULATION
PACE COMPUTER
LONGITUDINAL EQUATIONS

INSTRUMENTATION LABORATORY
MASSACHUSETTS INSTITUTE OF TECHNOLOGY
CAMBRIDGE, MASS.

SCALE —— X ACTUAL	DRAWN BY W.H.S.	3/12/65 DATE
CHECKED RMac 3-15-65 DATE	APPROVED	DATE
PROJECT NUMBER	DRAWING NUMBER	

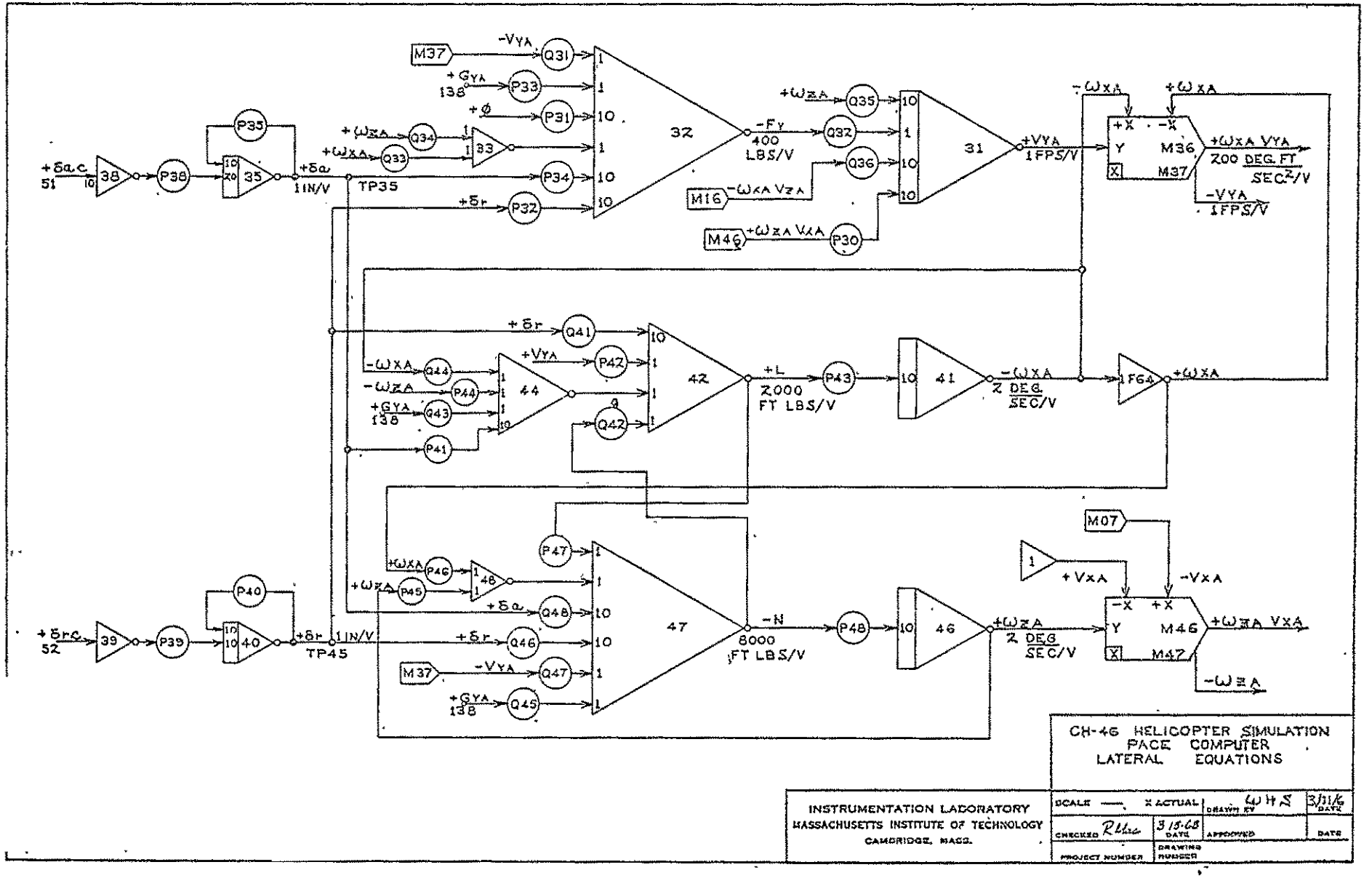
+δa.c.
51
38
P38
P35
35
+δa
1 IN/V
TP35
M37
-VYA
Q31
+GYA
138
P33
+ϕ
P31
+ωZA
Q34
33
+ωXA
Q33
P34
+δr
P32
32
-FY
400
LBS/V
+ωZA
Q35
Q32
Q36
10
1
10
10
31
+VYA
1 FPS/V
M16
-ωXA VZA
M46
+ωZA VXA
P30
-ωXA
+ωXA
+X
-X
Y
X
M36
M37
+ωXA VYA
200 DEG. FT
SEC²/V
-VYA
1 FPS/V
+δr
Q41
-ωXA
Q44
+VYA
P42
-ωZA
P44
44
+GYA
138
Q43
P41
42
Q42
+L
2000
FT LBS/V
P43
10
41
-ωXA
2 DEG.
SEC/V
1 FG4
+ωXA
+δrc
52
39
P39
P40
40
+δr
1 IN/V
TP45
P47
+ωXA
P46
46
+ωZA
P45
+δa
Q48
+δr
Q46
M37
-VYA
Q47
+GYA
138
Q45
47
-N
8000
FT LBS/V
P48
10
46
+ωZA
2 DEG
SEC/V
M07
1
+VXA
-VXA
-X
+X
Y
X
M46
M47
+ωZA VXA
-ωZA
CH-46 HELICOPTER SIMULATION
PACE COMPUTER
LATERAL EQUATIONS
INSTRUMENTATION LABORATORY
MASSACHUSETTS INSTITUTE OF TECHNOLOGY
CAMBRIDGE, MASS.
SCALE —— X ACTUAL
DRAWN BY
W H S
3/11/68
DATE
CHECKED
R Blue
3.15.68
DATE
APPROVED
DATE
PROJECT NUMBER
DRAWING NUMBER

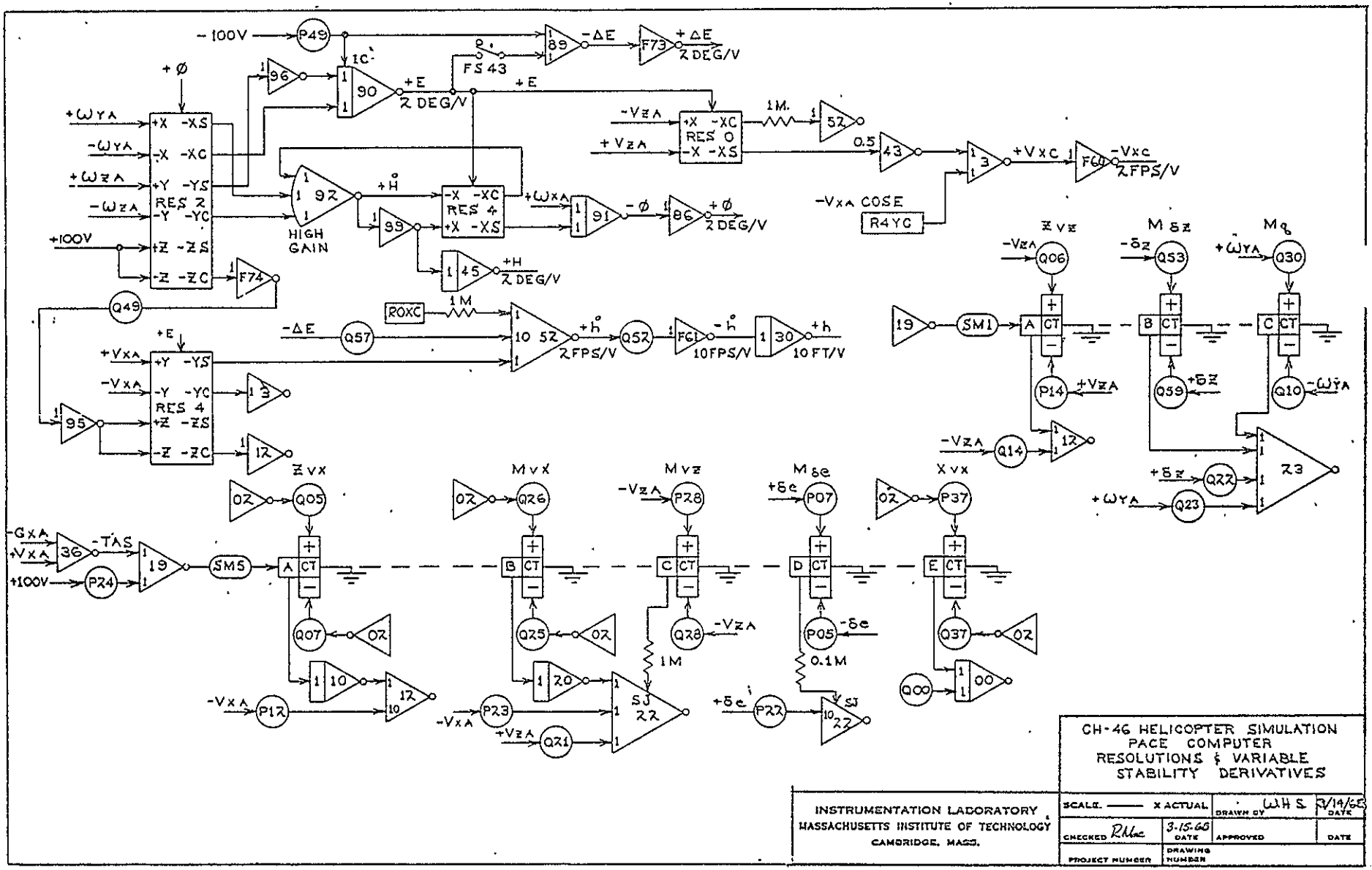

CH-46 HELICOPTER SIMULATION
PACE COMPUTER
RESOLUTIONS & VARIABLE
STABILITY DERIVATIVES

INSTRUMENTATION LABORATORY
MASSACHUSETTS INSTITUTE OF TECHNOLOGY
CAMBRIDGE, MASS.

SCALE —— X ACTUAL | DRAWN BY W.H.S. | 2/14/68 DATE
CHECKED RMac | 3-15-68 DATE | APPROVED | DATE
PROJECT NUMBER | DRAWING NUMBER

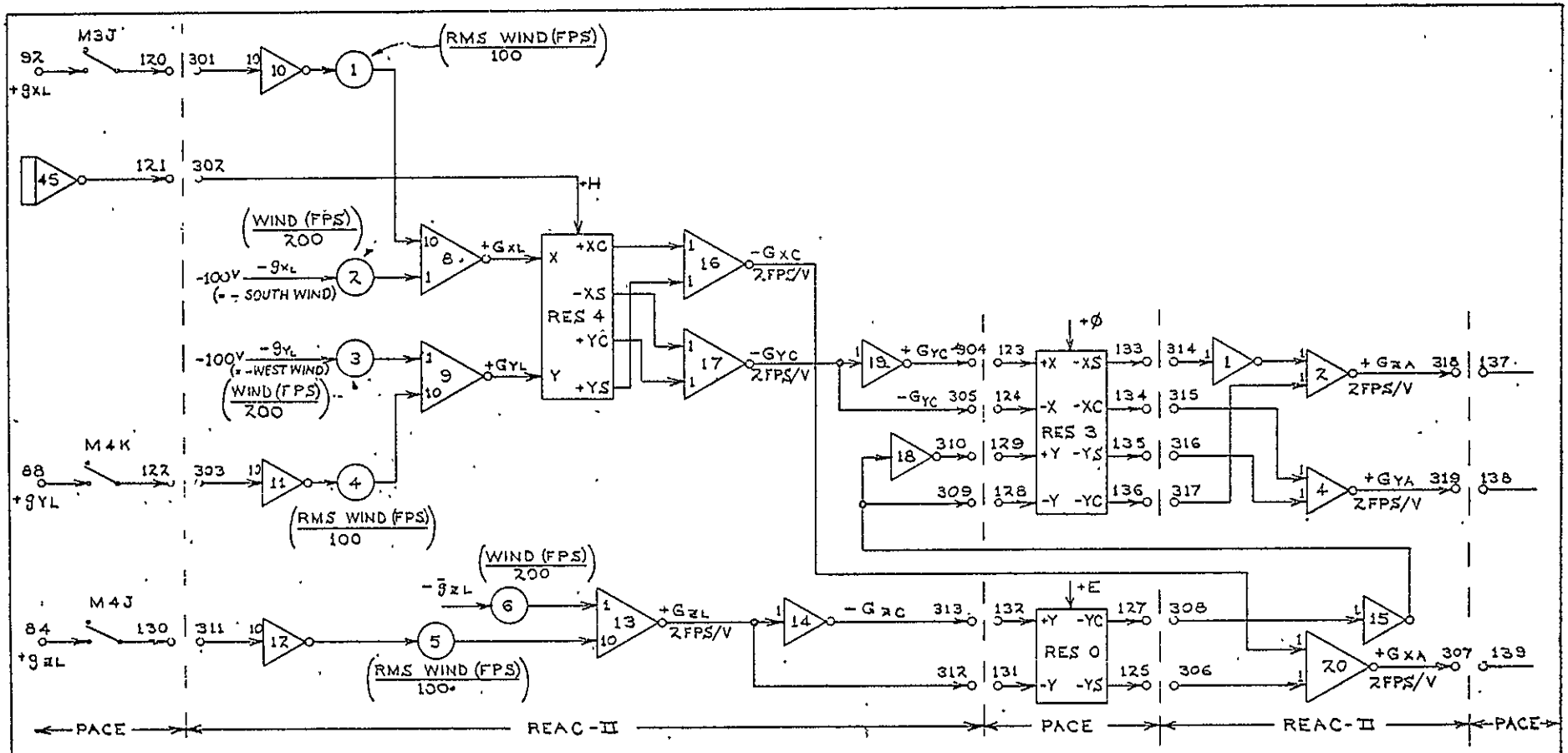

NOTE: $G = \bar{g} + g$ WHERE
G = TOTAL AIR MASS VELOCITY
$\bar{g}$ = STEADY STATE (MEAN) AIR MASS VELOCITY
g = AIR MASS VELOCITY DUE TO GUSTS (MEAN = 0)

CH-46 HELICOPTER SIMULATION
PACE & REAC II COMPUTERS
WIND RESOLUTIONS

INSTRUMENTATION LABORATORY
MASSACHUSETTS INSTITUTE OF TECHNOLOGY
CAMBRIDGE, MASS.

SCALE —— X ACTUAL | DRAWN BY W.H.S | DATE 3/14/68
CHECKED RMac | DATE 3-15-68 | APPROVED | DATE
PROJECT NUMBER | DRAWING NUMBER

APPENDIX J

Flight Instrument-Analog Computer Interface Unit
for NASA/ERC
Fixed Base Cockpit Simulator

Schematic Diagrams

Instrumentation Laboratory
Massachusetts Institute of Technology
Cambridge, Massachusetts

Table of Contents

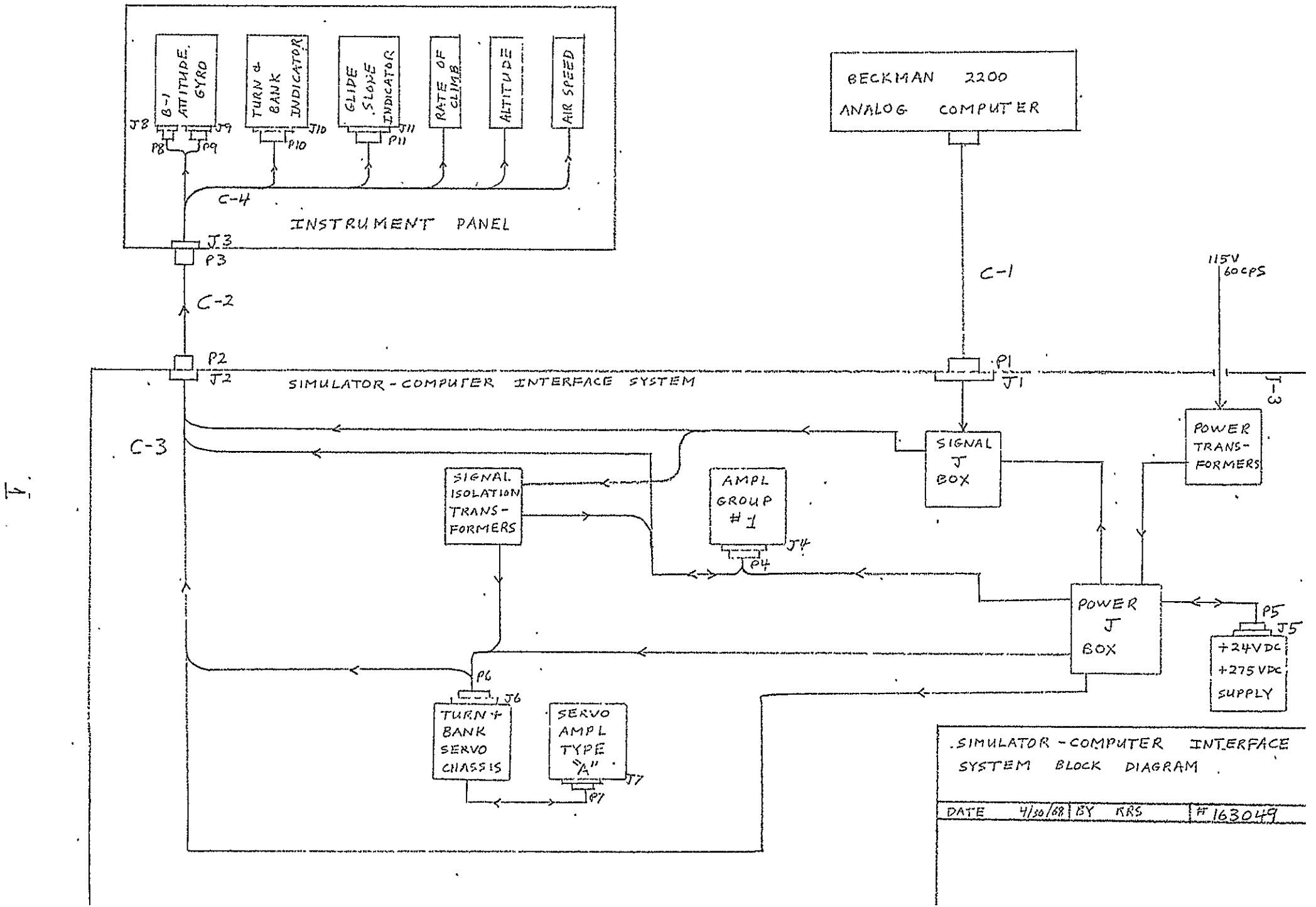

SIMULATOR - COMPUTER INTERFACE SYSTEM BLOCK DIAGRAM

DATE	4/30/68	BY	KRS	# 163049

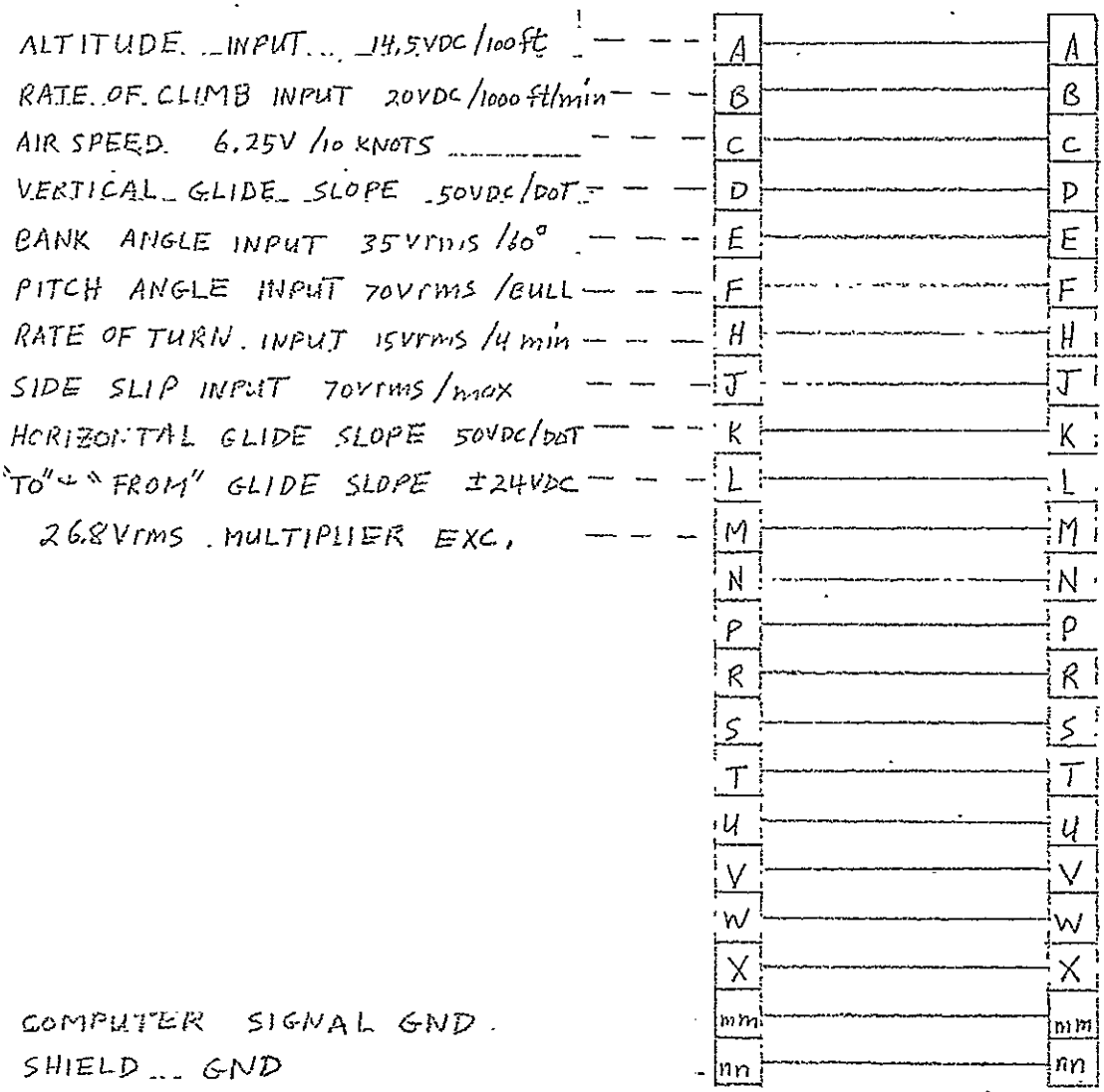

INPUT CABLE

C-1

DATE 5/3/68	BY RRS	# 163050

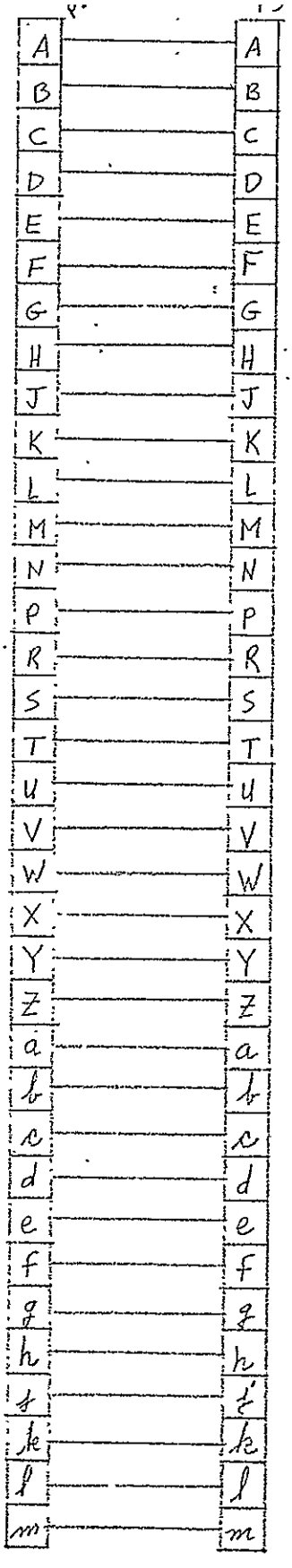

J-5

A	ISOLATED GND FROM TB8-5
B	P4-R
C	P4-m
D	ISOLATED GND FROM TB8-5
E	18.5V 60cps FROM TB1-1
F	COMPUTER GND FROM TB9-2
G	ISOLATED GND FROM TB8-6
H	45V 60cps L180° FROM TB5-7
J	P4-U
K	15V 60cps L0° FROM TB7-1
L	SPARE
M	15V 60cps L180° FROM TB7-2
N	ISOLATED GND FROM TB8-6
P	P4-W
R	+24V D.C. FROM TB2-2
S	P4-C
T	P4-S
U	P4-V
V	115V 60cps FROM TB3-2
W	P6-M
X	P6-N
Y	32V 60cps FROM TB6-5
Z	ISOLATED GND FROM TB8-7
a	TB7-9
b	P6-K
c	TB7-10
d	ALTITUDE INPUT FROM TB10-1
e	RATE OF CLIMB INPUT FROM TB10-2
f	AIRSPEED INPUT FROM TB10-3
g	VERTICAL LINE INPUT FROM TB10-4
h	HORIZONTAL LINE INPUT FROM TB10-9
j	"TO" + "FROM" INPUT FROM TB10-10
k	P4-k
l	+24V D.C. FROM TB2-3
m	ISOLATED GND FROM TB8-7

AN-3106A-28-15P

AN-3106A-28-15S

INTERFACE TO INSTRUMENT PANEL
INTERCONNECT CABLE C-2

DATE	BY	#
5/3/65	RRS	163051

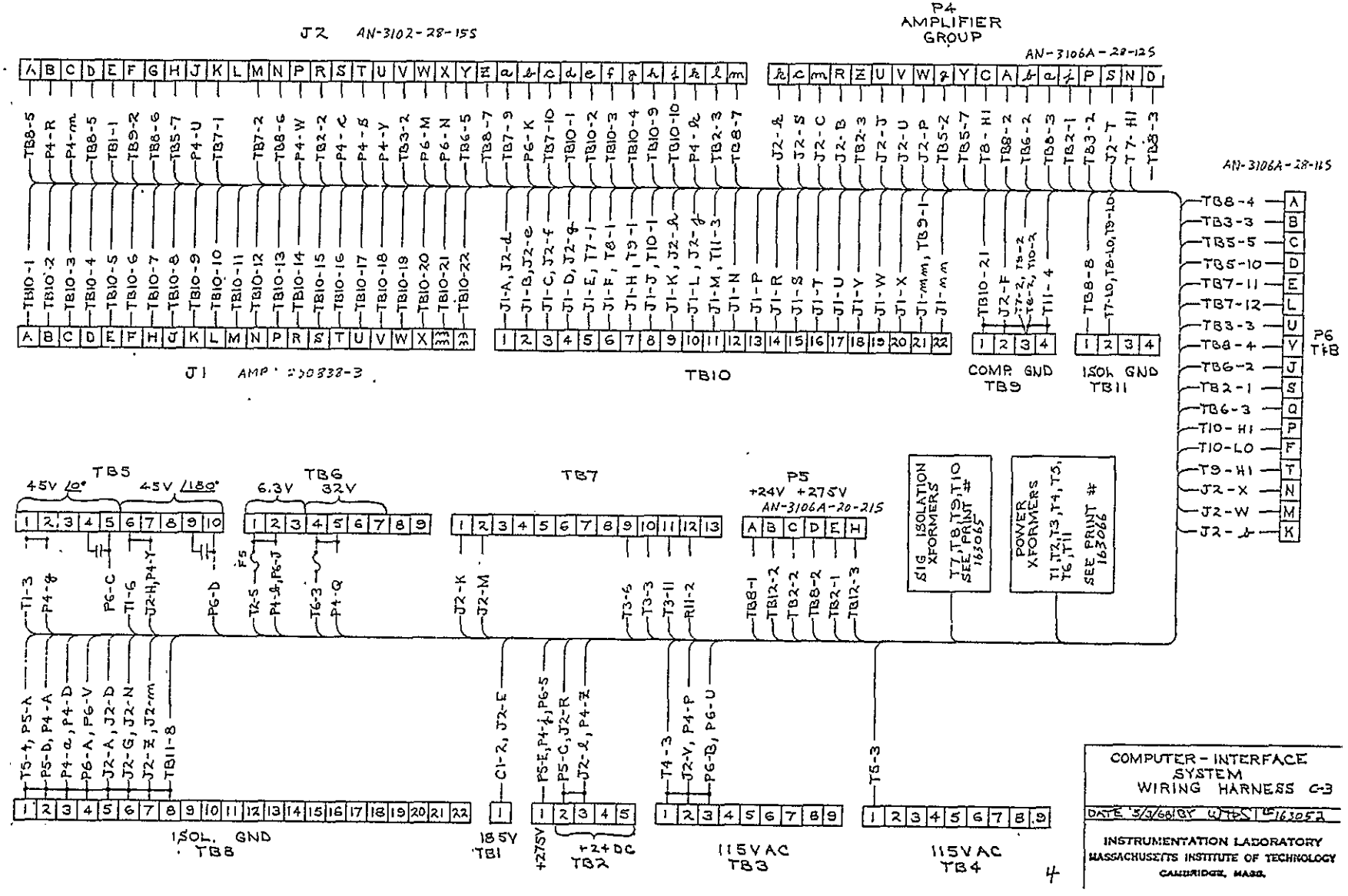
J2 AN-3102-28-15S
P4 AMPLIFIER GROUP
AN-3106A-28-12S
AN-3106A-28-11S
J1 AMP # 530838-3
TB10
COMP GND TB9
ISOL GND TB11
P6 TB
TB5
45V /0°
45V /180°
TB6
6.3V
32V
TB7
P5
+24V +27.5V
AN-3106A-20-21S
SIG ISOLATION XFORMERS
T7,T8,T9,T10 SEE PRINT # 163065
POWER XFORMERS
T1,T2,T3,T4,T5, T6,T11
SEE PRINT # 163066
ISOL. GND TB8
-18.5V TB1
+27.5V
+24 DC TB2
115VAC TB3
115VAC TB4
COMPUTER - INTERFACE SYSTEM WIRING HARNESS C-3
DATE 5/3/68 BY W.T.S. E 163052
INSTRUMENTATION LABORATORY
MASSACHUSETTS INSTITUTE OF TECHNOLOGY
CAMBRIDGE, MASS.

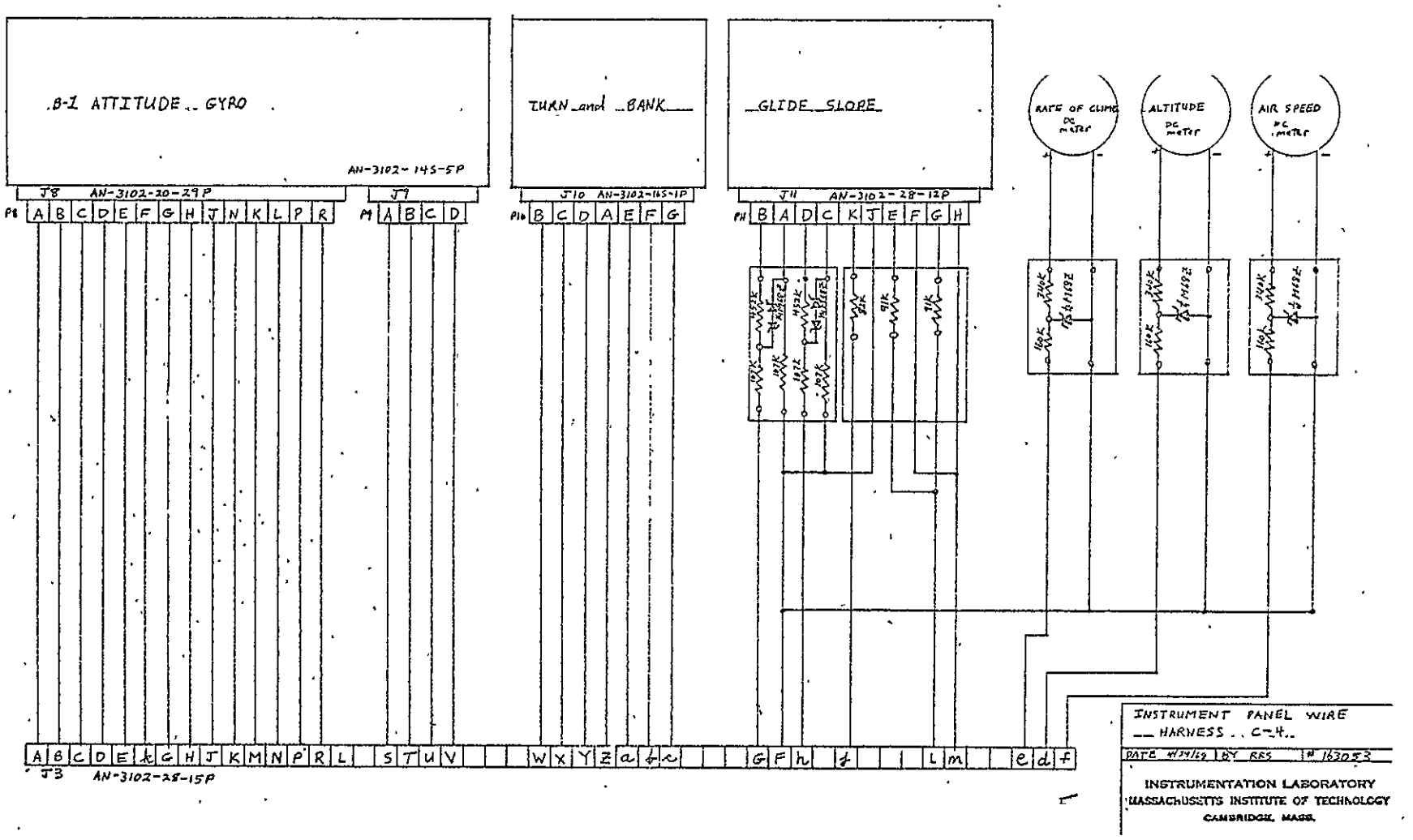
B-I ATTITUDE GYRO
AN-3102-14S-5P
J8 AN-3102-20-29P
P8 A B C D E F G H J N K L P R
J7
M A B C D
TURN and BANK
J10 AN-3102-16S-1P
P10 B C D A E F G
GLIDE SLOPE
J11 AN-3102-28-12P
P11 B A D C K J E F G H
RATE OF CLIMB DC METER
ALTITUDE DC METER
AIR SPEED DC METER
A B C D E k G H J K M N P R L S T U V W X Y Z a b c G F h j L m e d f
J3 AN-3102-28-15P
INSTRUMENT PANEL WIRE
HARNESS C-4
DATE 4/29/49 BY RRS M 163053
INSTRUMENTATION LABORATORY
MASSACHUSETTS INSTITUTE OF TECHNOLOGY
CAMBRIDGE, MASS.

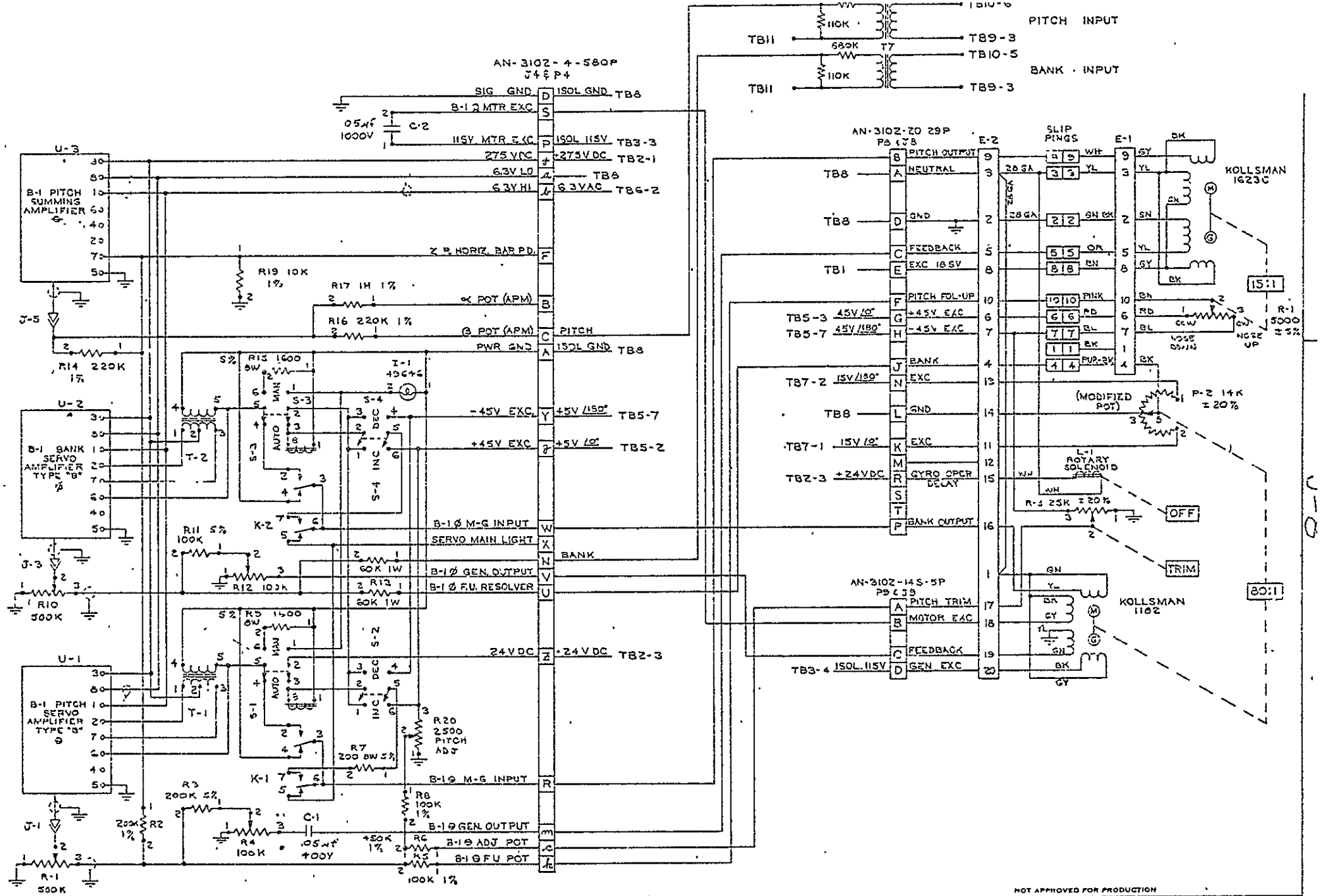
AN-3102-4-580P J4 & P4
SIG GND
B-1 Ø MTR EXC
.05µf 1000V C-2
115V MTR EXC
27.5 VDC
6.3V LO
6.3V HI
Z R HORIZ BAR PO.
R19 10K 1%
R17 1M 1%
∝ POT (APM)
R16 220K 1%
β POT (APM)
PWR GND
R14 220K 1%
ISOL GND TB8
ISOL 115V TB3-3
+27.5V DC TB2-1
TB8
6.3VAC TB6-2
PITCH
U-3
B-1 PITCH SUMMING AMPLIFIER
J-5
U-2
B-1 BANK SERVO AMPLIFIER TYPE "B"
J-3
R10 500K
R11 5% 100K
R12 100K
R13 60K 1W
T-2
S-3 AUTO MAN
S-4 INC DEC
R15 1600 5% 8W
I-1 40646
-45V EXC.
+45V EXC
+5V /150°
+5V /0°
TB5-7
TB5-2
K-2
B-1 Ø M-G INPUT
SERVO MAIN LIGHT
B-1 Ø GEN. OUTPUT
B-1 Ø F.U. RESOLVER
BANK
60K 1W
U-1
B-1 PITCH SERVO AMPLIFIER TYPE "B"
J-1
R1 500K
R2 200K 1%
R3 200K 1%
R4 100K
C-1 .05µf 400V
R5 1600 5% 8W
R7 200 8W 5%
R20 2500 PITCH ADJ
K-1
B-1 Ø M-G INPUT
R6 100K 1%
R8 450K 1%
R9 100K 1%
B-1 Ø GEN OUTPUT
B-1 Ø ADJ POT
B-1 Ø F.U POT
24V DC
+24V DC TB2-3
TB11
110K
680K
T7
TB10-6
TB10-5
TB9-3
PITCH INPUT
BANK INPUT
AN-3102-20 29P P8 & J8
E-2
SLIP RINGS
E-1
PITCH OUTPUT
NEUTRAL
GND
FEEDBACK
EXC 18 SV
PITCH FOL-UP
+45V EXC
-45V EXC
BANK
EXC
GYRO OPER DELAY
BANK OUTPUT
TB8
TB1
TB5-3 45V /0°
TB5-7 45V /180°
TB7-2 15V /180°
TB7-1 15V /0°
TB7-3 +24VDC
KOLLSMAN 1623C
15:1
R-1 5000 ± 5%
NOSE DOWN
NOSE UP
P-2 14K ± 20%
(MODIFIED POT)
L-1 ROTARY SOLENOID
R-3 25K ± 20%
OFF
TRIM
80:1
AN-3102-14S-5P P9 & J9
PITCH TRIM
MOTOR EXC
FEEDBACK
GEN EXC
TB3-4 ISOL 115V
KOLLSMAN 1182
NOT APPROVED FOR PRODUCTION
UNLESS OTHERWISE NOTED —
CAPACITOR VALUES ARE IN µf
RESISTOR VALUES ARE IN OHMS
ELECTRICAL TOLERANCES ±1%
K=x1000 M=x1 000 000
INSTRUMENTATION LABORATORY
MASSACHUSETTS INSTITUTE OF TECHNOLOGY
CAMBRIDGE MASS
B-1 ATTITUDE GYRO FUNCTION DIAGRAM
DRAWN BY JHS 5/1/63
CHECKED
APPROVED
PROJECT NUMBER
DRAWING NUMBER C-163054

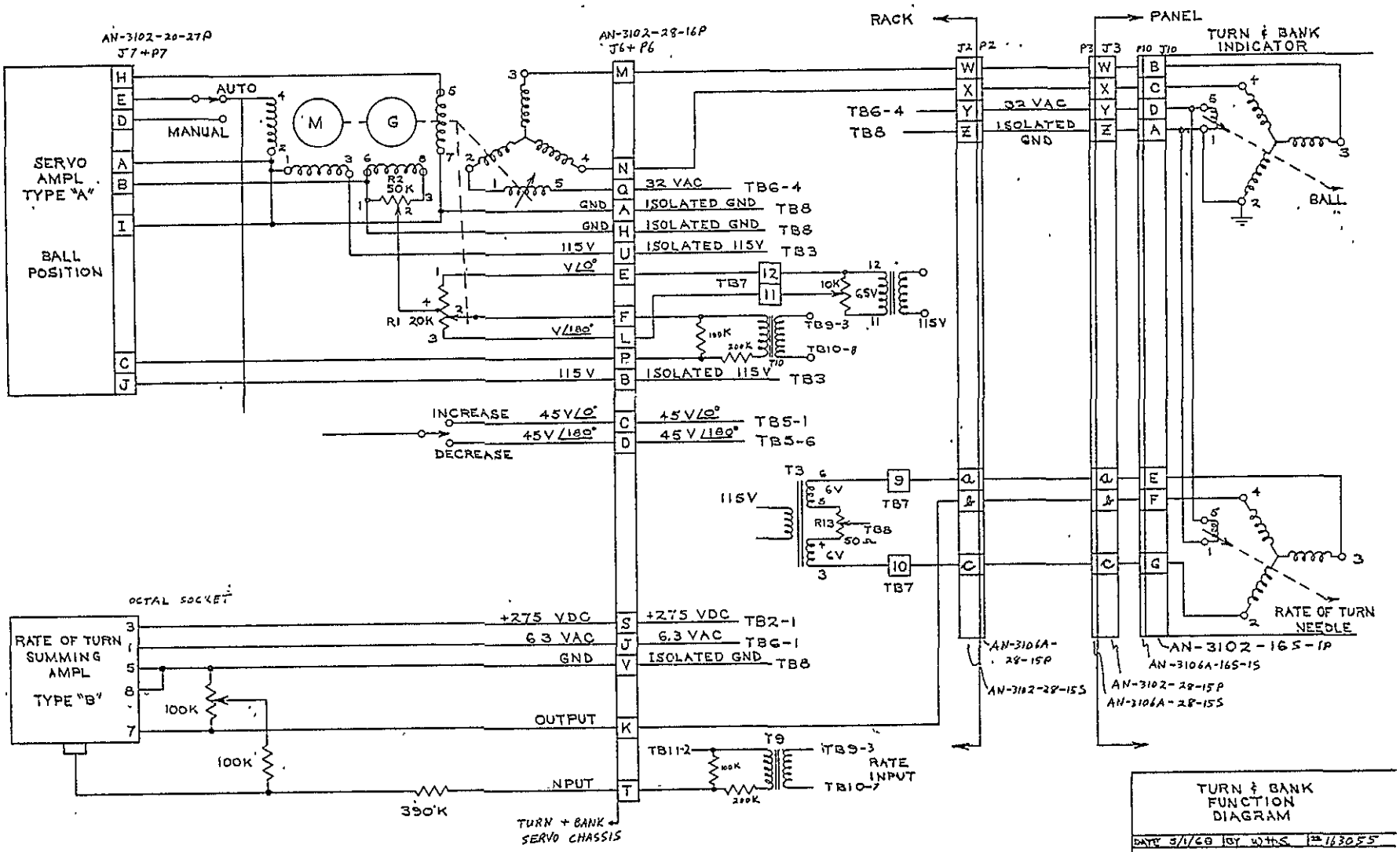

7

TURN & BANK FUNCTION DIAGRAM

DATE 5/1/68 BY WHS SK 1630S5

INSTRUMENTATION LABORATORY
MASSACHUSETTS INSTITUTE OF TECHNOLOGY
CAMBRIDGE, MASS.

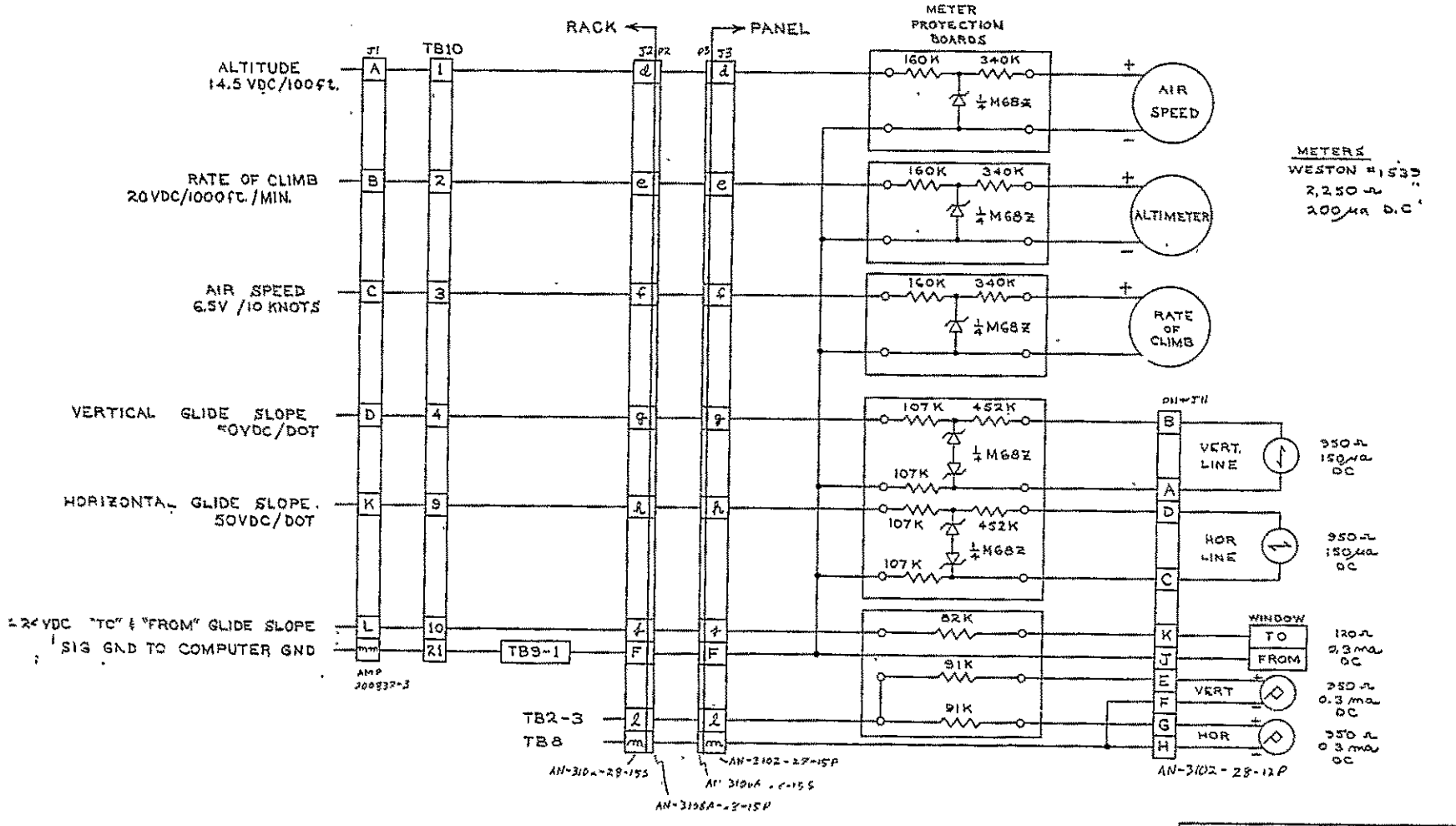

AIR SPEED ALTIMETER RATE OF CLIMB AND GLIDE SLOPE FUNCTION DIAGRAM

DATE 5/2/68 BY G.H.S. #183056

INSTRUMENTATION LABORATORY
MASSACHUSETTS INSTITUTE OF TECHNOLOGY
CAMBRIDGE, MASS.

8

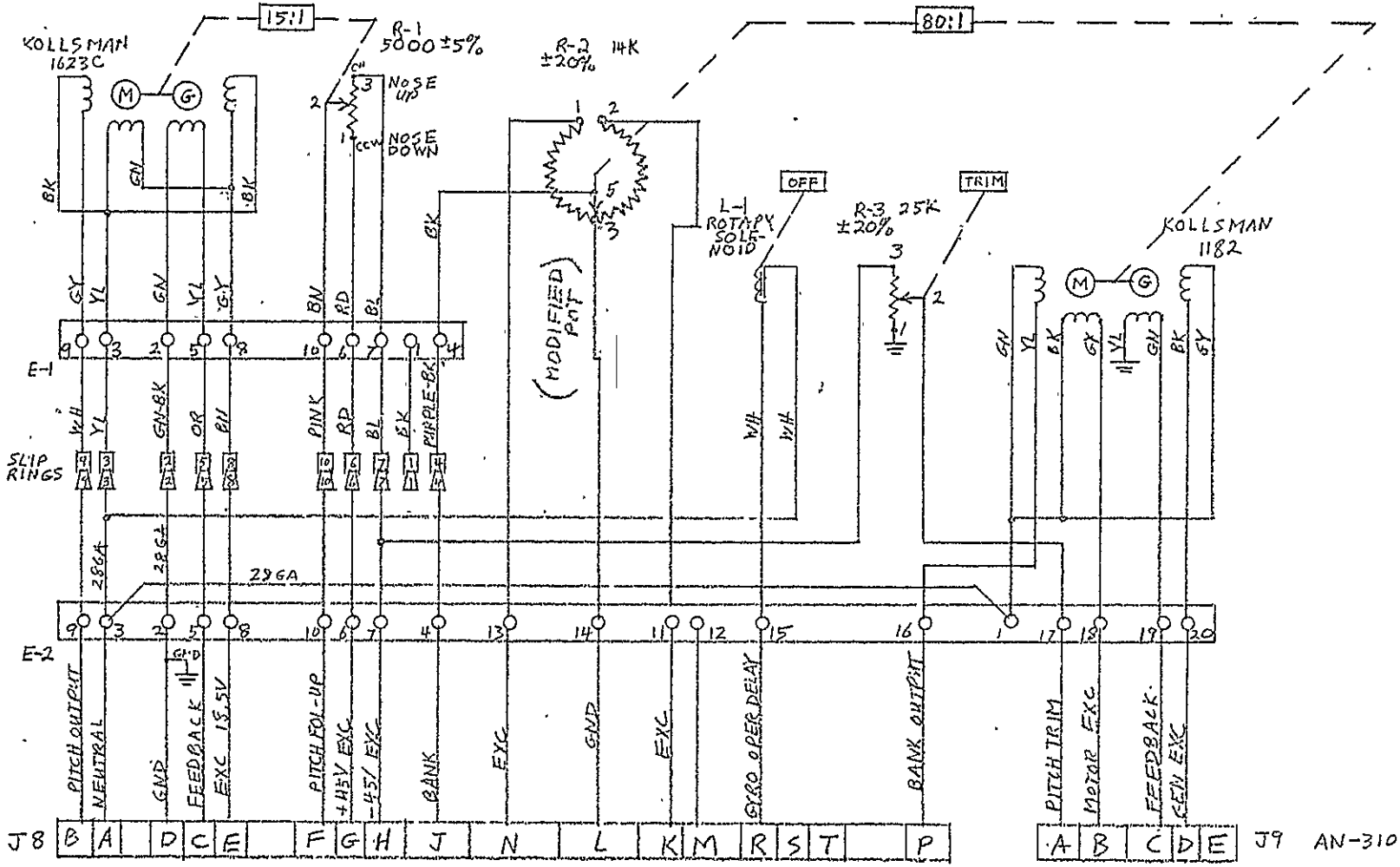

B-1 ATTITUDE . . GYRO

DATE	4/26/68	BY	RRS	#	163057

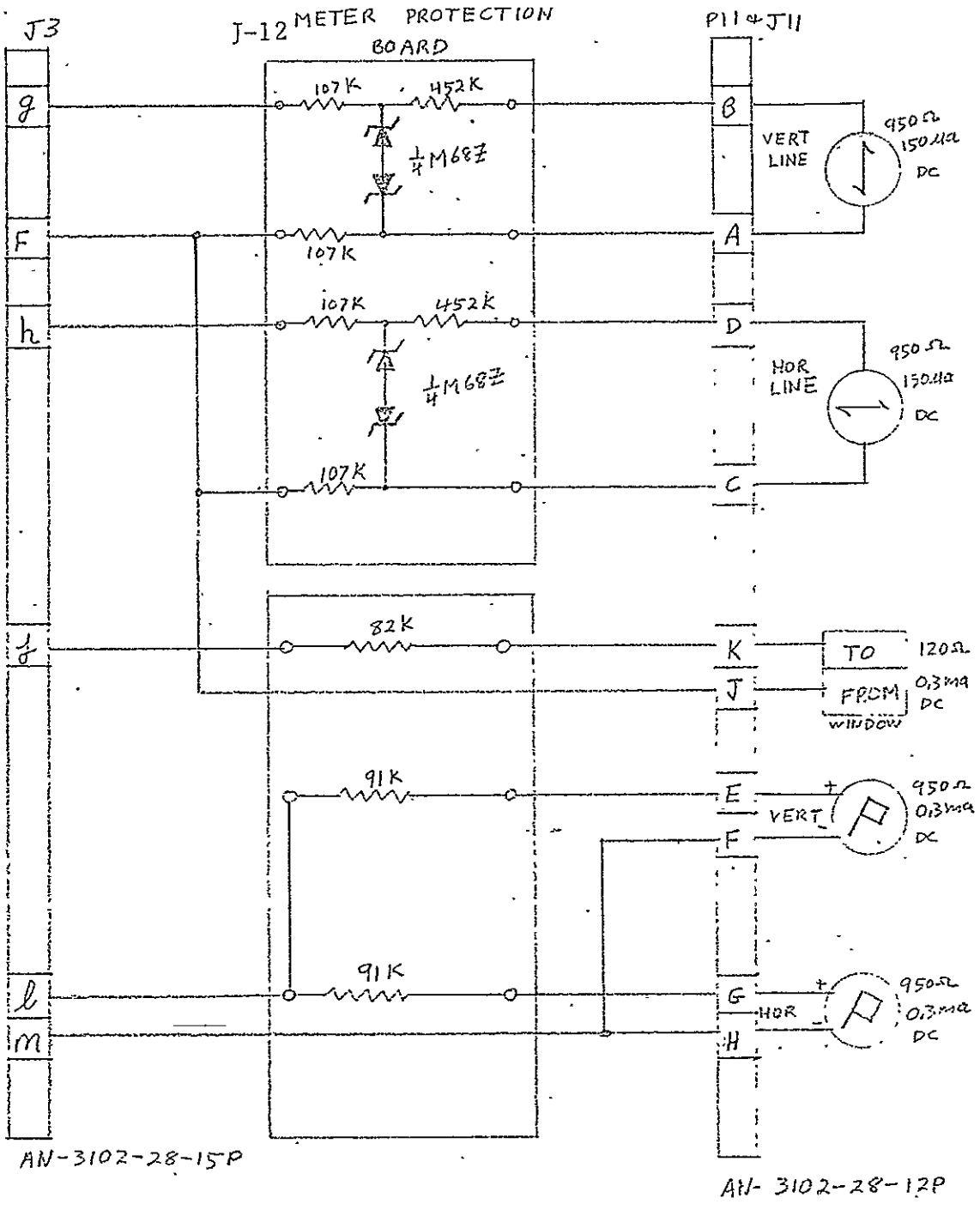

GLIDE SLOPE INDICATOR

DATE 4/25/68 | BY RRS | # 163058

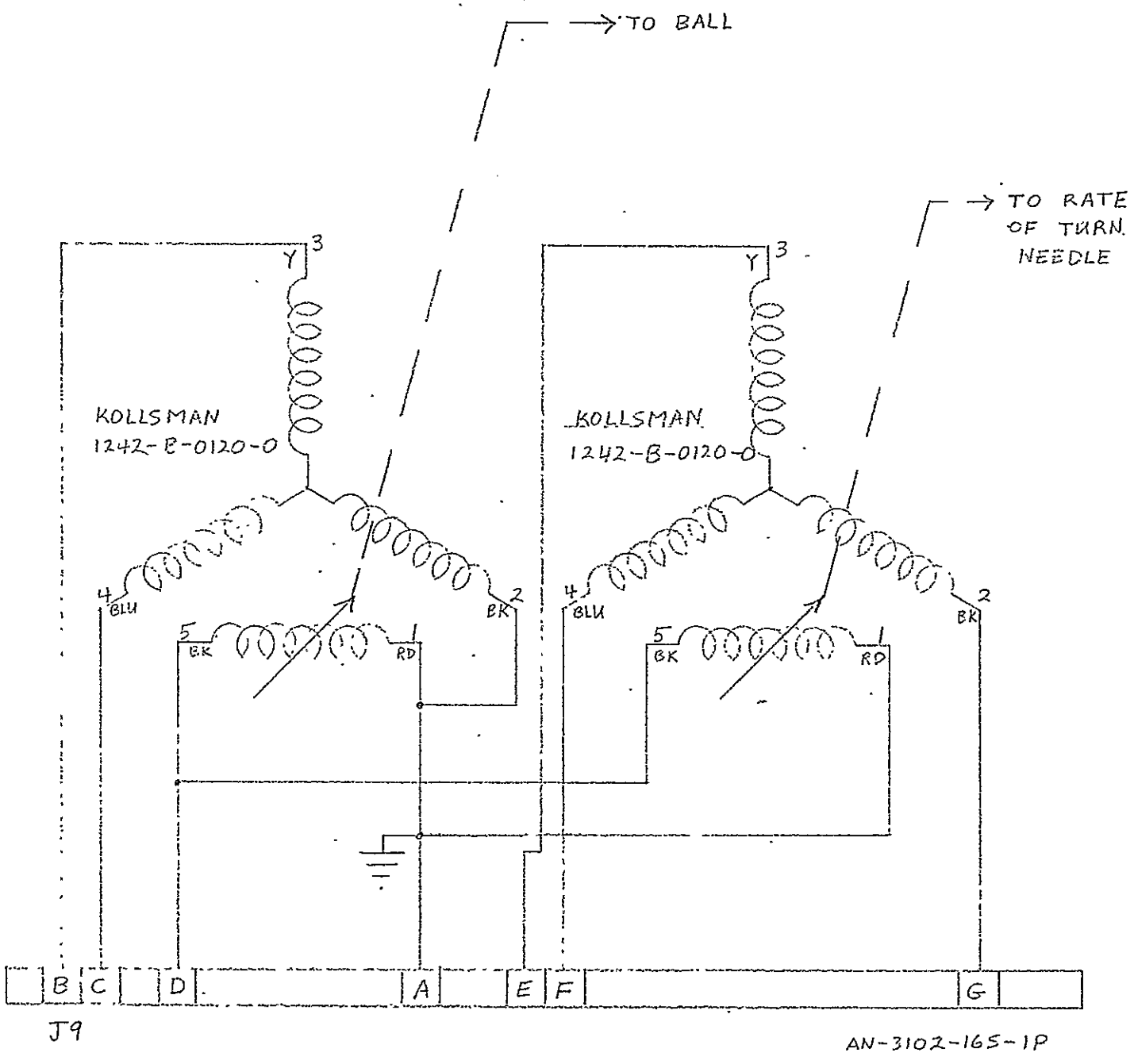

TURN AND BANK INDICATOR

DATE 4/24/68	BY RRS	# 163059

METER PROTECTION BOARDS

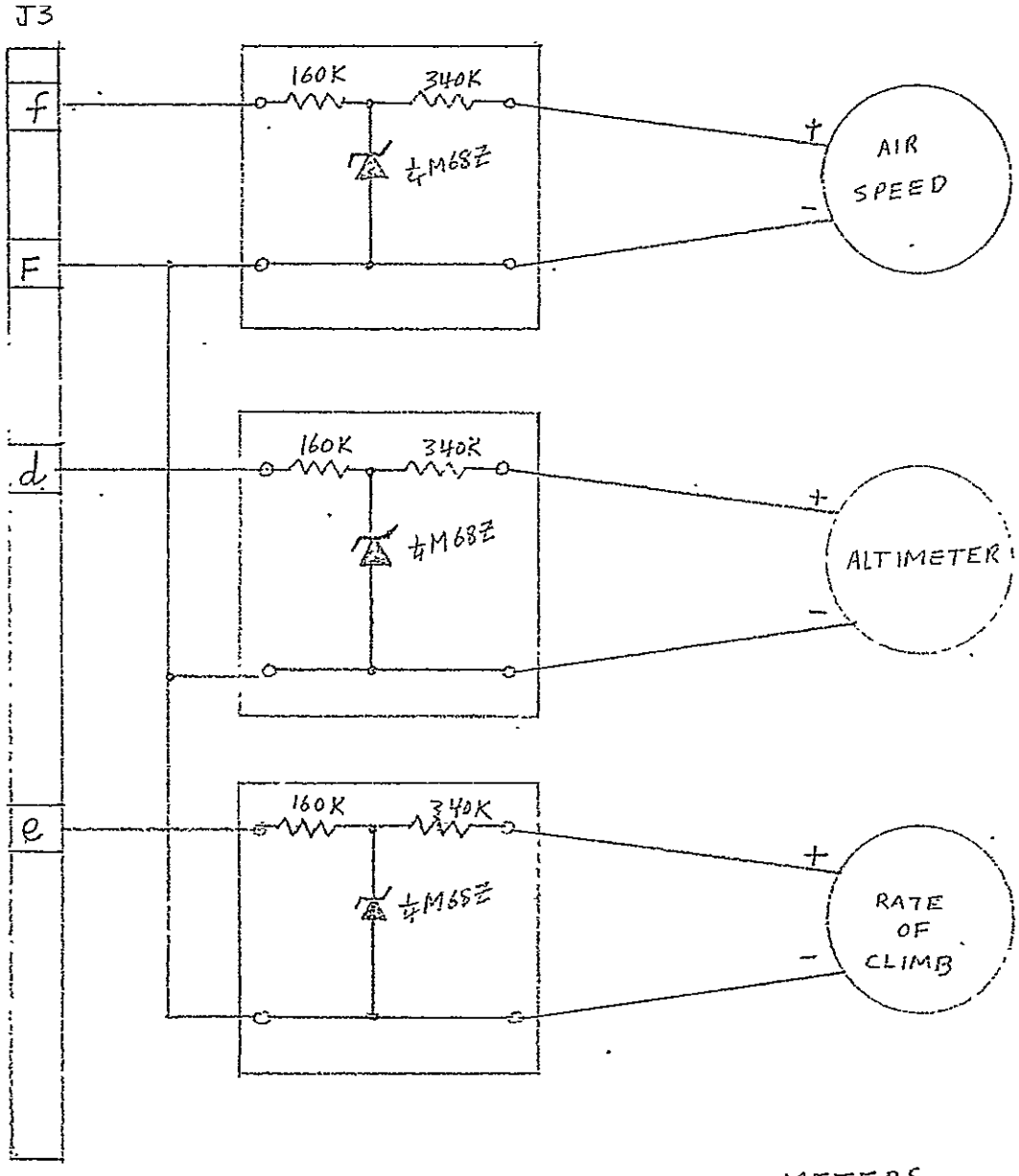

AN-3102-28-15P

METERS

WESTON #1539

2,250 Ω

200 μa D.C.

ALTITUDE, AIR SPEED and RATE OF CLIMB D.C. METERS

DATE 4/25/68	BY RRS	# 163060

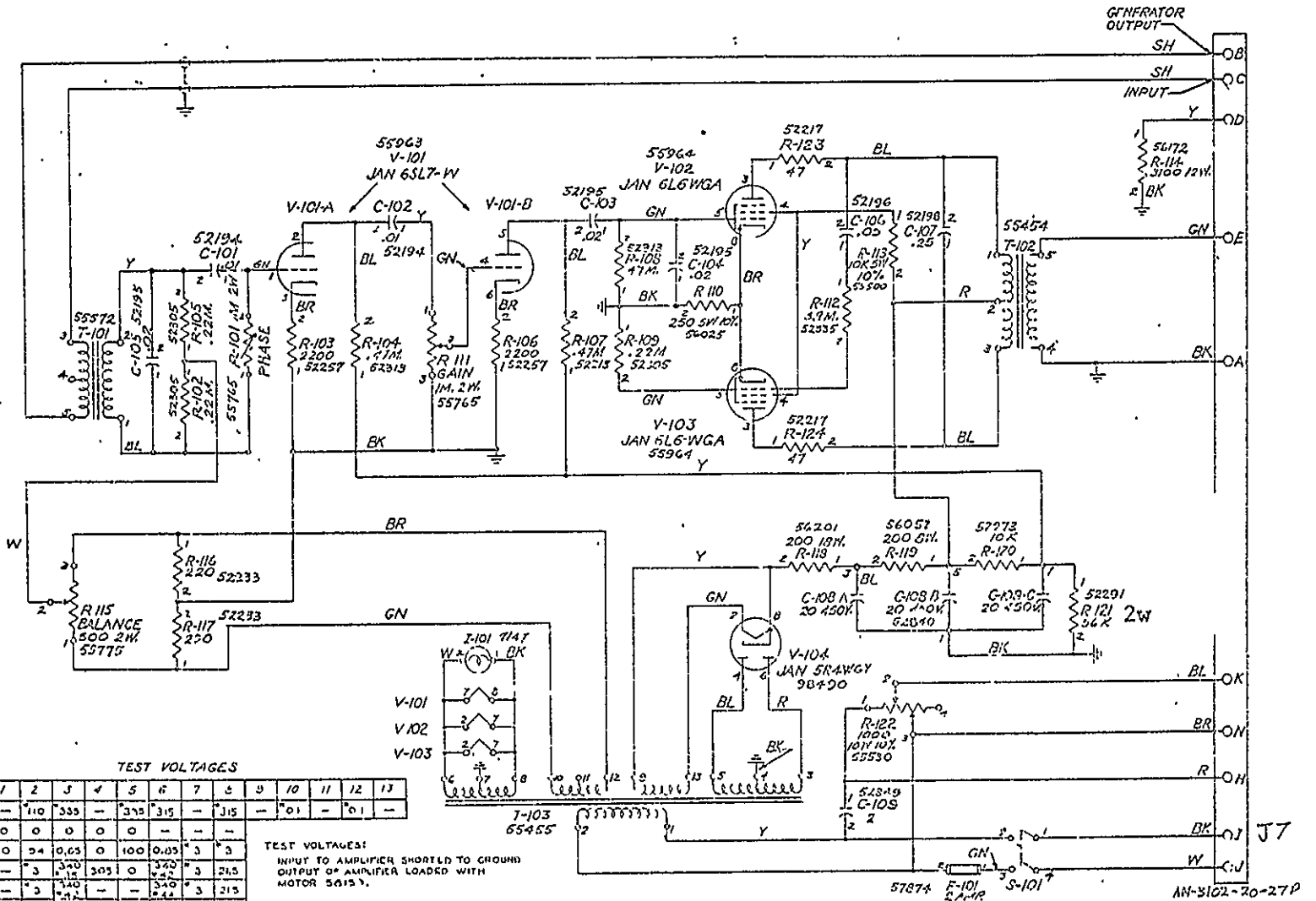

TEST VOLTAGES

	1	2	3	4	5	6	7	8	9	10	11	12	13
T 103	—	*110	*335	—	*315	*315	—	*315	—	*01	—	*01	—
T-102	0	0	0	0	0	—	—	—					
V 101	0	94	0.65	0	100	0.65	*3	*3					
V 102	—	*3	*340 *15	305	0	*340 *44	*3	215					
V 103	—	*3	*340 *44	—	—	*340 *44	*3	215					
V 104	—	365	—	335	—	335	—	365					
C 108	0	—	365	—	345	—	265	—					
R 114	265	94											
R 107	265	100											
R-113	0	*340 90.8											

TEST VOLTAGES:
INPUT TO AMPLIFIER SHORTED TO GROUND
OUTPUT OF AMPLIFIER LOADED WITH MOTOR 56151.

NOTE:
1-ALL VOLTAGES MEASURED WITH VAC. TUBE VOLTMETER TO GROUND (CHASSIS).
2-ALL VOLTAGES D.C. UNLESS OTHERWISE INDICATED
3-ALL VOLTAGES MARKED * ARE A.C.
ALL RESISTANCES IN OHMS ±5% 1W. ALL CAPACITANCES IN MF 600 V. UNLESS OTHERWISE NOTED

MOTOR CONNECTIONS

MOTOR NO.	GENERATOR EXCITATION	MOTOR CONTROL PHASE
KOLLSMAN 11112-0160600	CONNECT TO I & H	SHORT D TO E CONNECT TO A & B
KOLLSMAN 11150-0160610	SHORT K TO N CONNECT TO I & N	CONNECT TO A & B

SERVO AMPLIFIER TYPE "A"

DATE · 4/30/58 | BY RRS · | # 163061

J-15

13

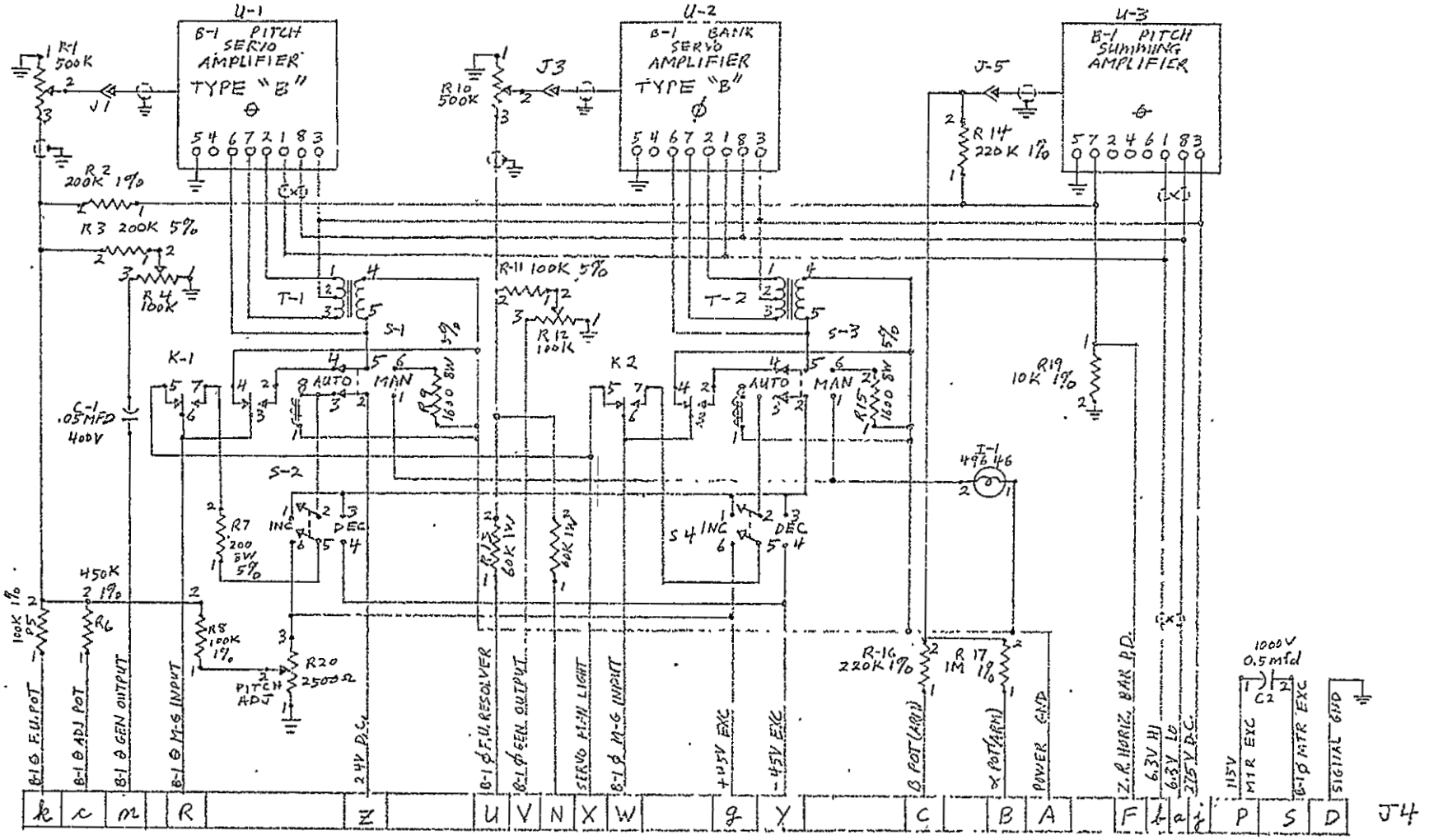

AN-3102-4-58DP

J-16

4/1

AMPLIFIER GROUP # 1		
DATE 4/30/68	BY RRS	# 163062

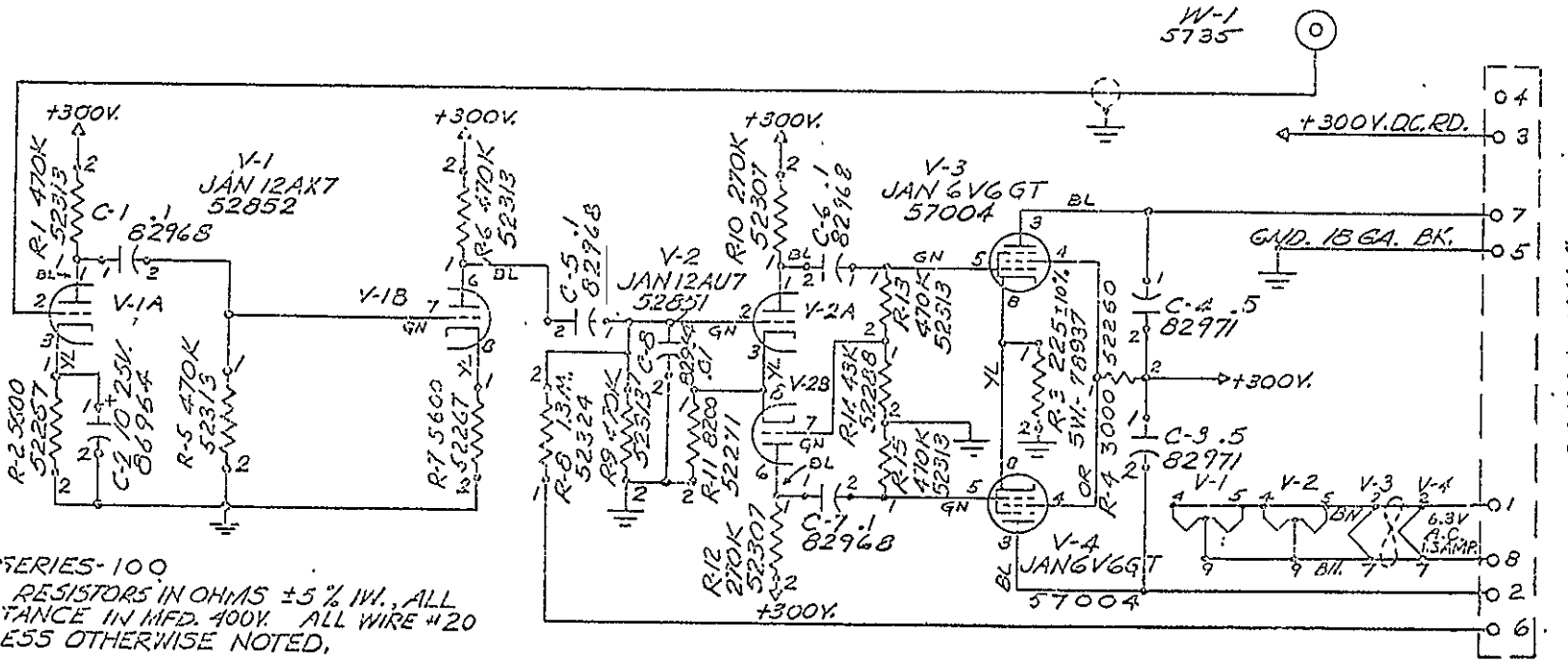

CODE SERIES-100

ALL RESISTORS IN OHMS ±5% 1W., ALL CAPACITANCE IN MFD. 400V. ALL WIRE #20 GA. UNLESS OTHERWISE NOTED,

ALL JUMPERS YELLOW
ALL +300 V. LEADS RED

J-17

SERVO AMPLIFIER TYPE "B".			
DATE 4/29/68	BY RRS	# 163063	

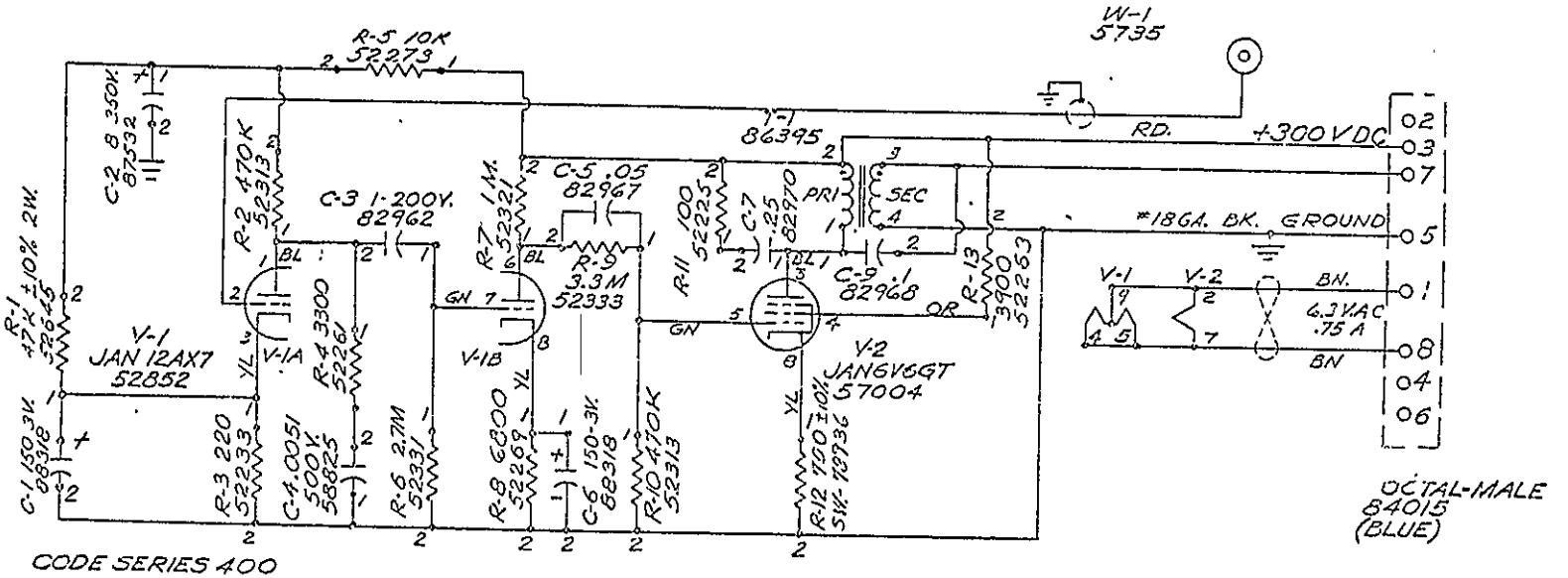

CODE SERIES 400
ALL RESISTORS IN OHMS ±5% 1W.,
ALL CAPACITANCE IN MFD. 400V. &
ALL WIRE #20GA. UNLESS OTHERWISE NOTED.

ALL JUMPERS YELLOW
ALL +300V. LEADS RED

SINGLE CHANNEL SUMMING AMPLIFIER			
DATE 1/30/68	BY RRS		# 163064

J-18

91

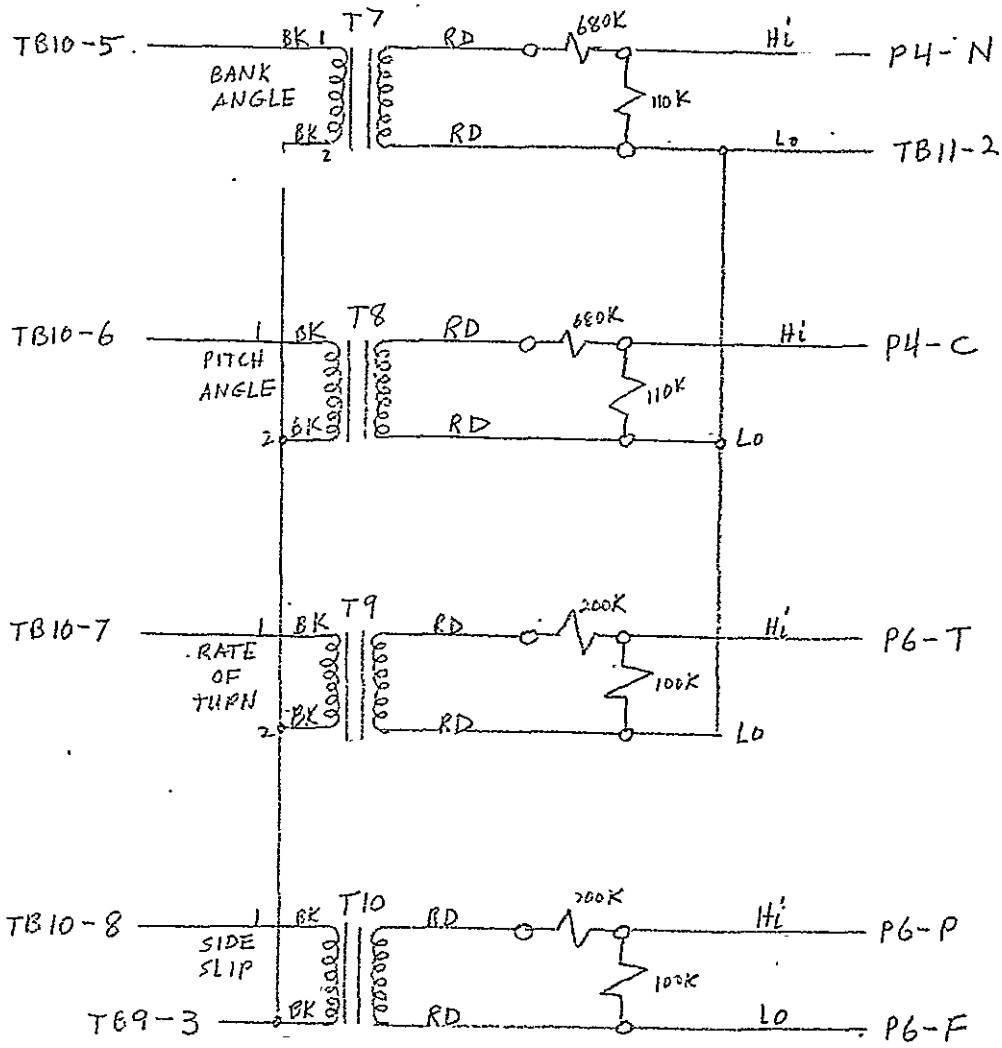

TRIAD
N-48X

SIGNAL ISOLATION TRANSFORMER ... WIRING DIAGRAM		
DATE 5/3/68	BY RRS	# 163065

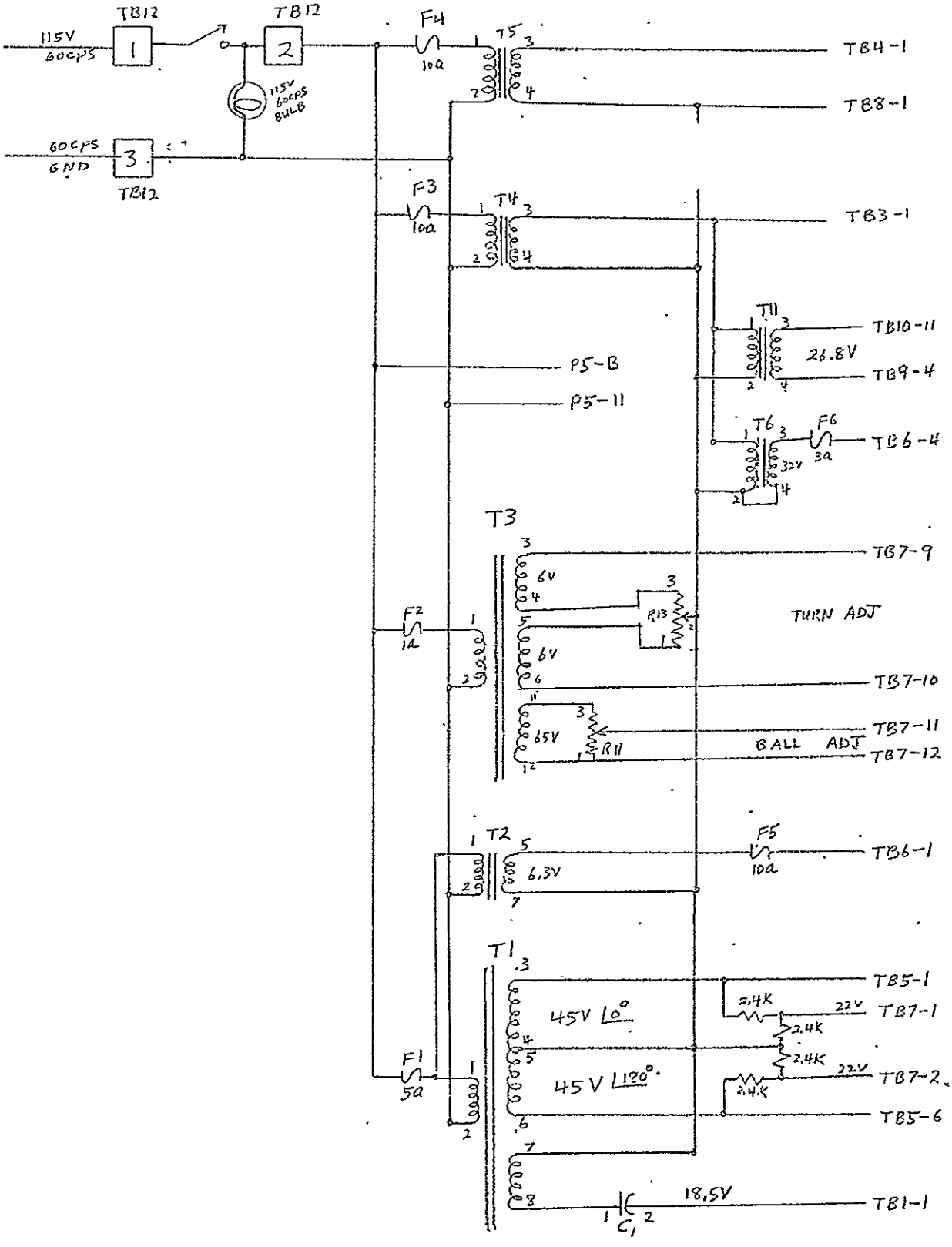

POWER TRANSFORMER
WIRING DIAGRAM.

DATE 5/3/68	BY KRS	# 163066

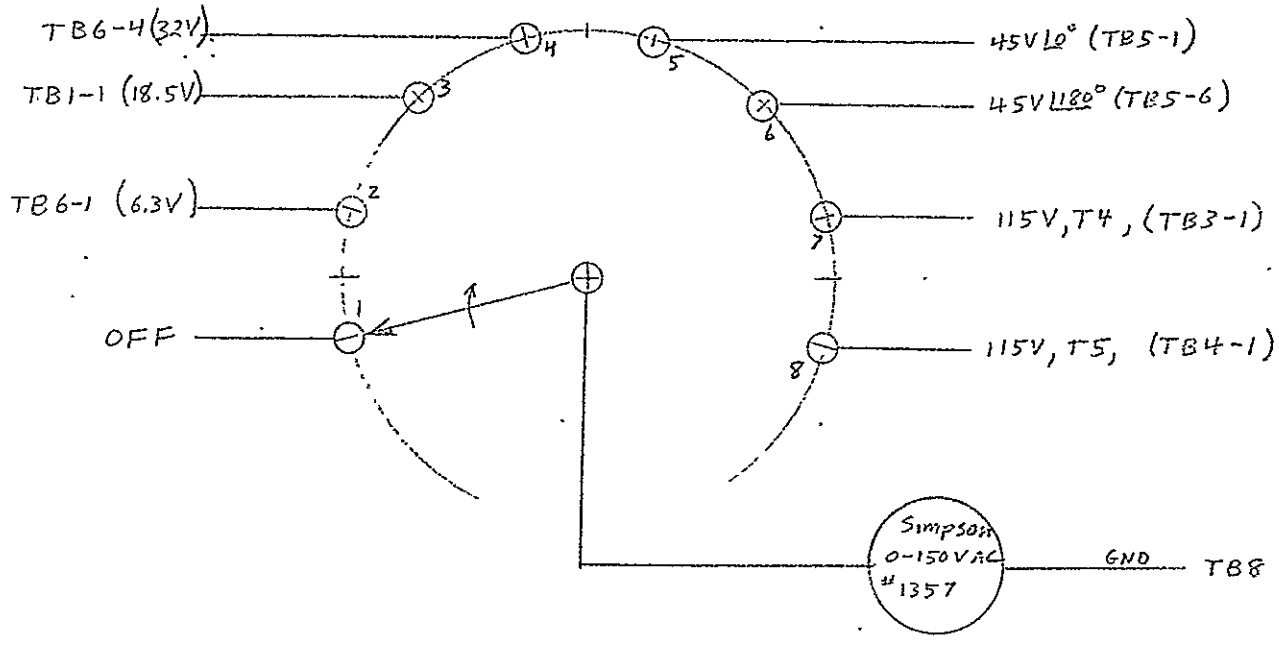

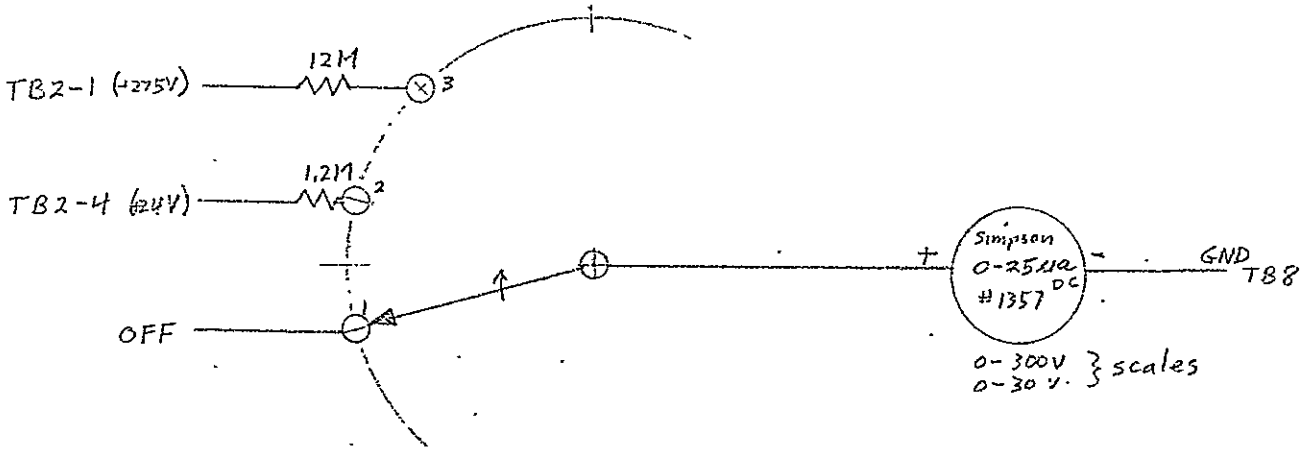

A.C. + D.C. VOLTAGE INDICATOR CIRCUITS

DATE	4/30/68	BY	RRS	# 163067

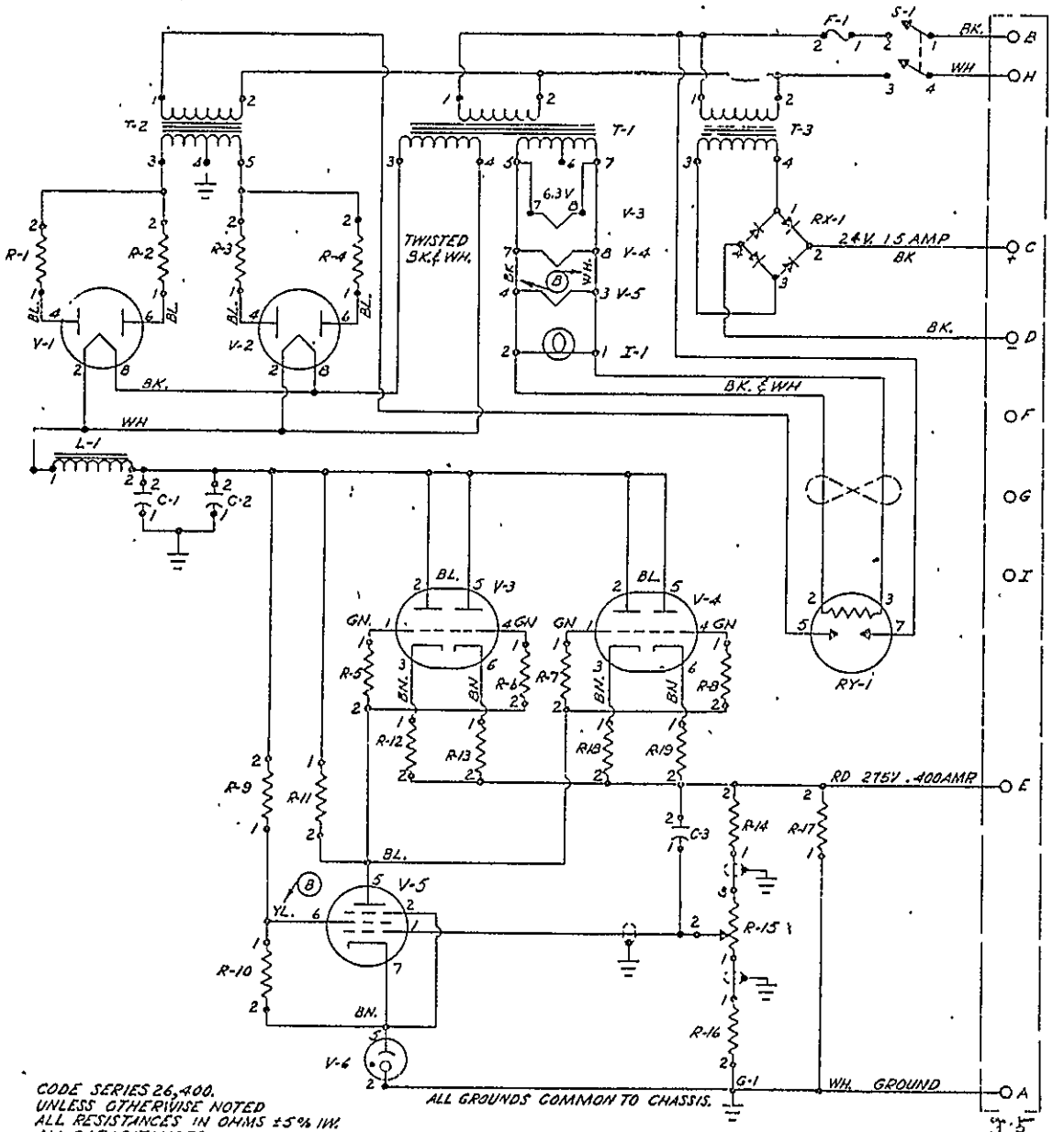

CODE SERIES 26,400.
UNLESS OTHERWISE NOTED
ALL RESISTANCES IN OHMS ±5% 1W.
ALL CAPACITANCES IN MFD. 600V
ALL GROUNDS WHITE.
ALL JUMPERS YELLOW.
300 VOLT LINE RED
USE #18 GA. WIRE EXCEPT FOR #20 GA. SHIELDED LEADS

AN-3102-20-21P

SYS.	DESCRIPTION	LINK#	JAN. #
C-1	CAP-10 MFD 600V.	52353	CP70BIEF106K
C-2	CAP-10 MFD 600V	52353	CP70BIEF106K
C-3	CAP-.25 MFD 600V	59043	CP54BIEF254K
F-1	FUSE-4 AMP.	59501	
I-1	LAMP-6.8 VOLT	7147	
L-1	CHOKE-5-25 HY 500MA	57632	
PL-1	CONN.-RECEPT. CHASSIS	52397	AN-3102-20 21P
R-1	RES-22 Ω 2W ±10%	52605	RC-40-AE-220K
R-2	RES-22 Ω 2W ±10%	52605	RC-40-AE-220K
R-3	RES.-22 Ω 2W. ±10%	52605	RC-40-AE-220K
R-4	RES.-22 Ω 2W. ±10%	52605	RC-40-AE-220K
R-5	RES.-10K Ω.	52273	RC-30-AE-103J
R-6	RES.-10K Ω.	52273	RC-30-AE-103J
R-7	RES.-10K Ω.	52273	RC-30-AE-103J
R-8	RES.-10K Ω.	52273	RC-30-AE-103J
R-9	RES-20K Ω 10W	56874	
R-10	RES.-4.5K Ω 5W	56936	
R-11	RES.-1MEG.	52321	RC-30-AE-105J
R-12	RES.-47 Ω 2W	52609	RC-40-AE-470K
R-13	RES-47 Ω 2W.	52609	RC-40-AE-470K
R-14	RES-75K Ω 1W ±5%	52294	RC-30-BF753J
R-15	POT-2.5K Ω LOCKING	55770	
R-16	RES.-47K Ω.	52289	RC-30-AE-473J
R-17	RES-50K Ω 10W	56882	
R-18	RES-47 Ω 2W	52609	RC-40-AE-470K
R-19	RES.-47 Ω 2W.	52609	RC-40-AE-470K
RX-1	RECT-SEL	66723	
RY-1	RELAY-DELAY	59736	
S-1	SW-TOGGLE D.P.S.T.	52160	ST52K
T-1	TRANS.-FILAMENT	57634	
T-2	TRANS-POWER	65957	
T-3	TRANS.-15 AMP.	66739	
V-1	TUBE-5R4WGY	98490	JAN5R4WGY
V-2	TUBE-5R4WGY	98490	JAN5R4WGY
V-3	TUBE-6AS7G	56993	JAN6AS7G
V-4	TUBE-6AS7G	56993	JAN6AS7G
V-5	TUBE-6AU6	52856	JAN6AU6
V-6	TUBE-VR-105	56997	JANOC3VR105

24 VOLT & 275 VOLT D.C. POWER SUPPLY CHASSIS

DATE 4/30/48 | BY RKS | # 163068

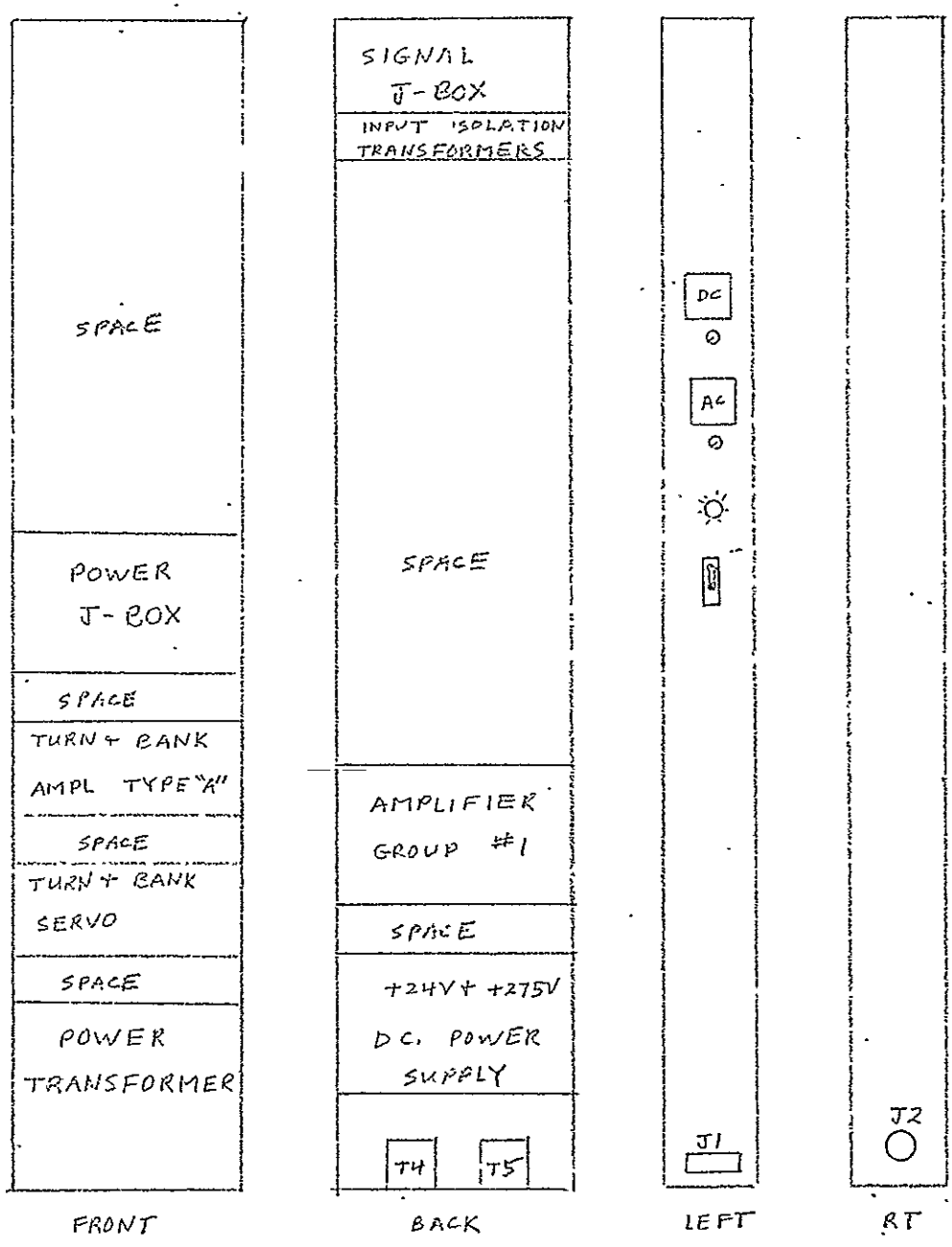

RACK ___ COMPONENT LAYOUT

DATE 5/2/68	BY RRS	# 163069

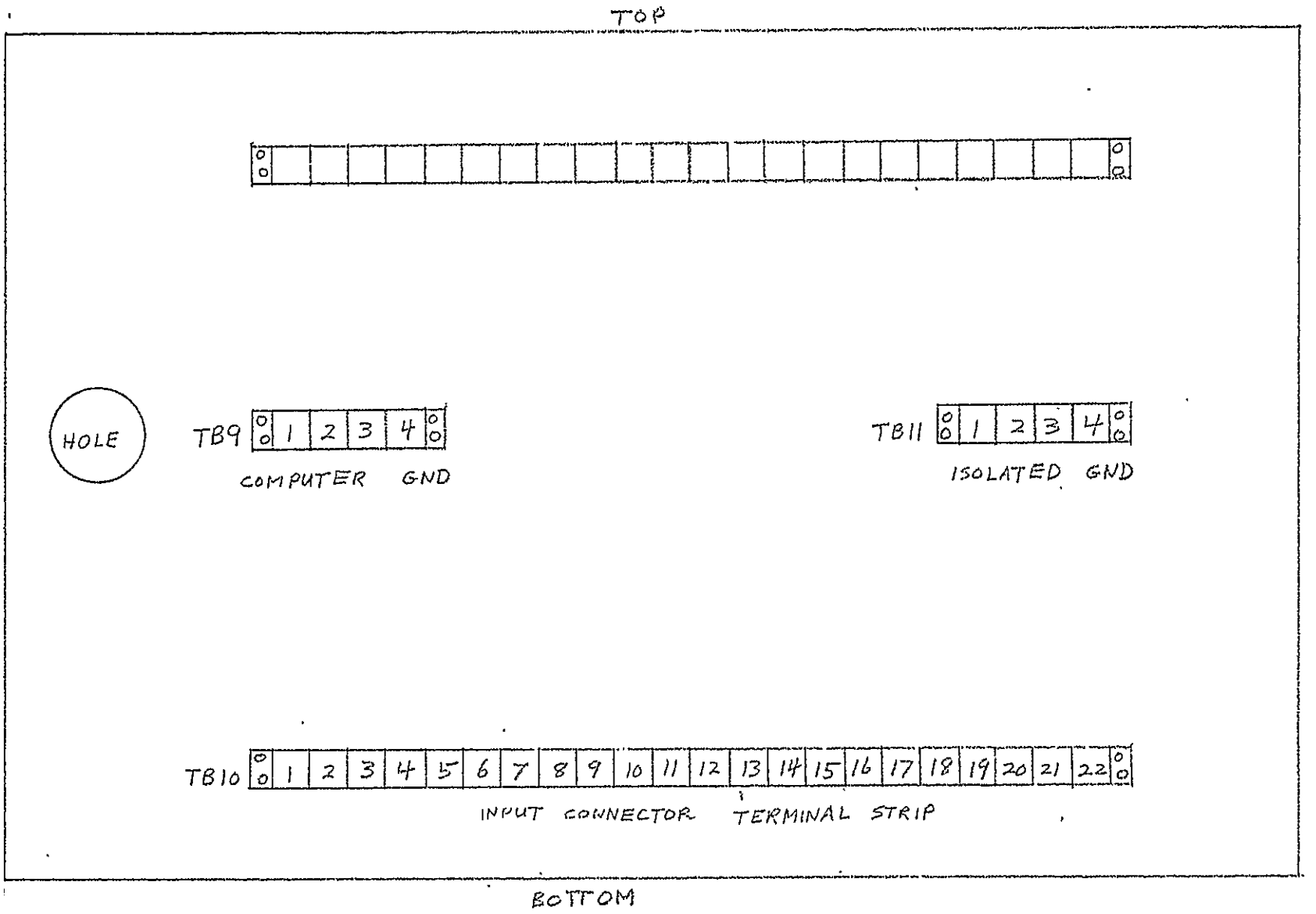

INPUT SIGNAL
J-BOX LAYOUT

DATE 5/11/68	BY RRS	# 163070

22

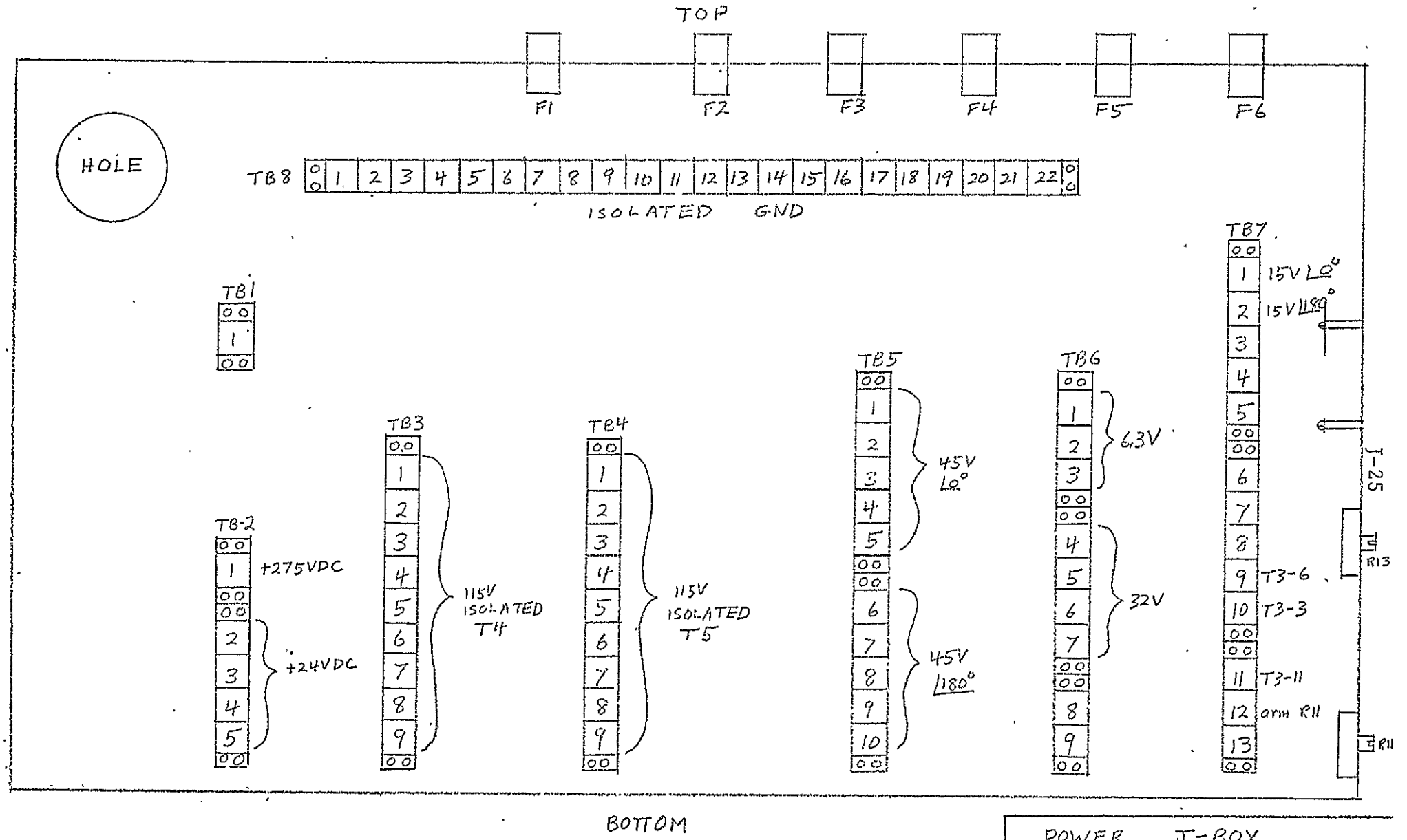

BOTTOM

POWER J-BOX LAYOUT

DATE 5/1/68 BY RRS # 16307J

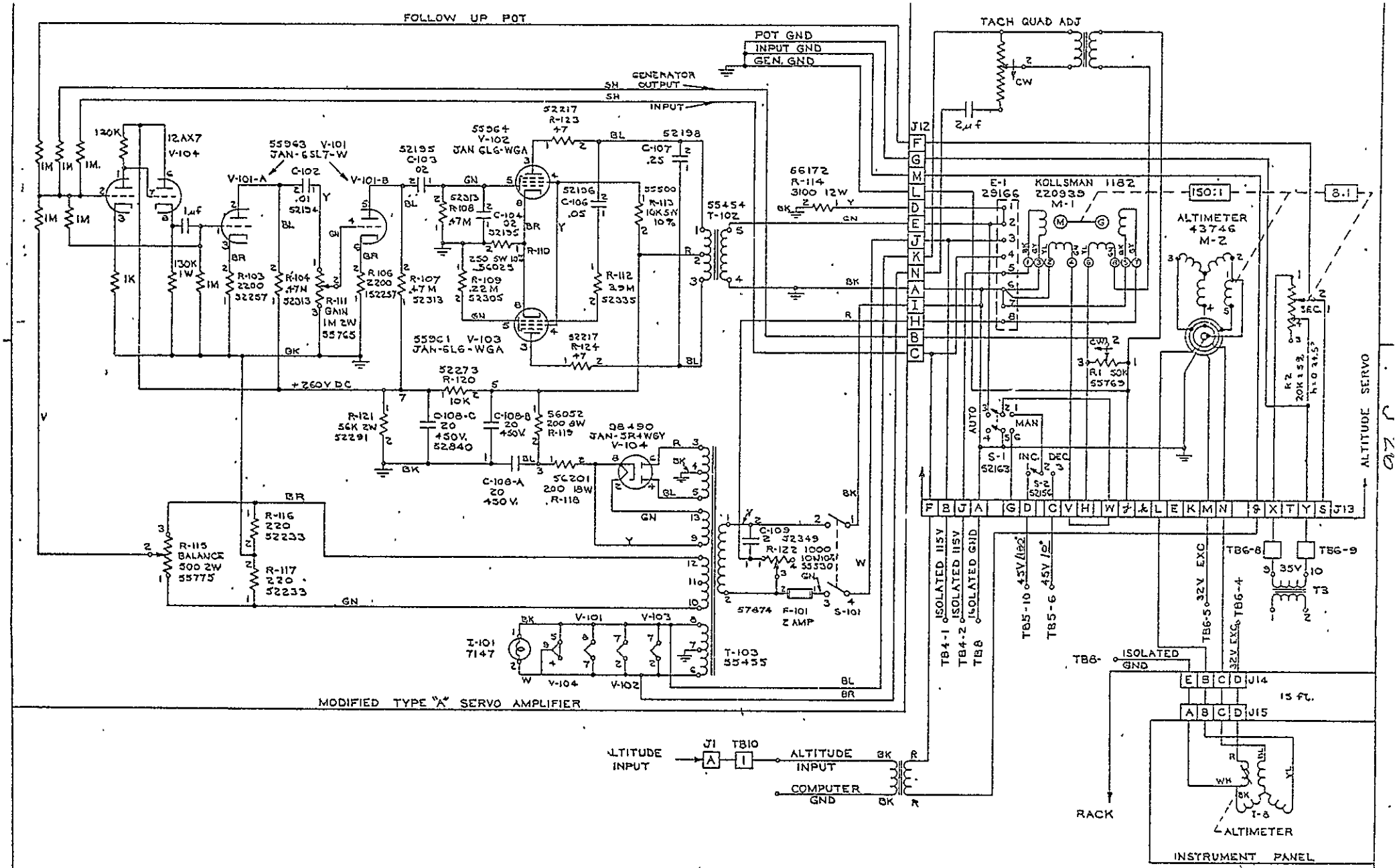

NOT APPROVED FOR PRODUCTION

UNLESS OTHERWISE NOTED —
CAPACITOR VALUES ARE IN μf
RESISTOR VALUES ARE IN OHMS
ELECTRICAL TOLERANCES—10%
K=X1000 M=X1,000 000

INSTRUMENTATION LABORATORY
MASSACHUSETTS INSTITUTE OF TECHNOLOGY
CAMBRIDGE MASS

0-7000 ft. ALTIMETER SERVO SYSTEM

DRAWN BY GMS

CHECKED | DATE | APPROVED | DATE

PROJECT NUMBER | DRAWING NUMBER C-163072

DATE	CHANGE	BY	APP

APPENDIX K

"VERTOL STABILITY AUGMENTATION SYSTEM DETAILS"

This report has been reproduced with the permission of Boeing/Vertol.

VERTOL STABILITY AUGMENTATION SYSTEM DETAILS

CONFERENCE ON CONTROL RESPONSE OF MANNED VEHICLES
SEATTLE, MARCH 15-16, 1962

BRUCE B. BLAKE

MILTON I. GERSTINE

I. INTRODUCTION

The purpose of the Vertol Stability Augmentation System (hereafter called SAS) is to make the flying qualities of the helicopter equivalent to those of a docile fixed wing aircraft. It is not an autopilot, since it uses rate damping and turn coordination signals only. It will not hold heading, altitude, or speed for long periods, though it allows hands off flight for a minute or two.

The first SAS was installed experimently on a test helicopter in 1957 and subsequently was fitted to the last nine Vertol 44's (military H-21) delivered to foreign governments.

Its success was such that the present generation of Vertol helicopters, the 107-II and the Army HC-1B, have a dual SAS installed as an inherent part of the basic aircraft, and depend to a large extent on these units to provide acceptable flying qualities.

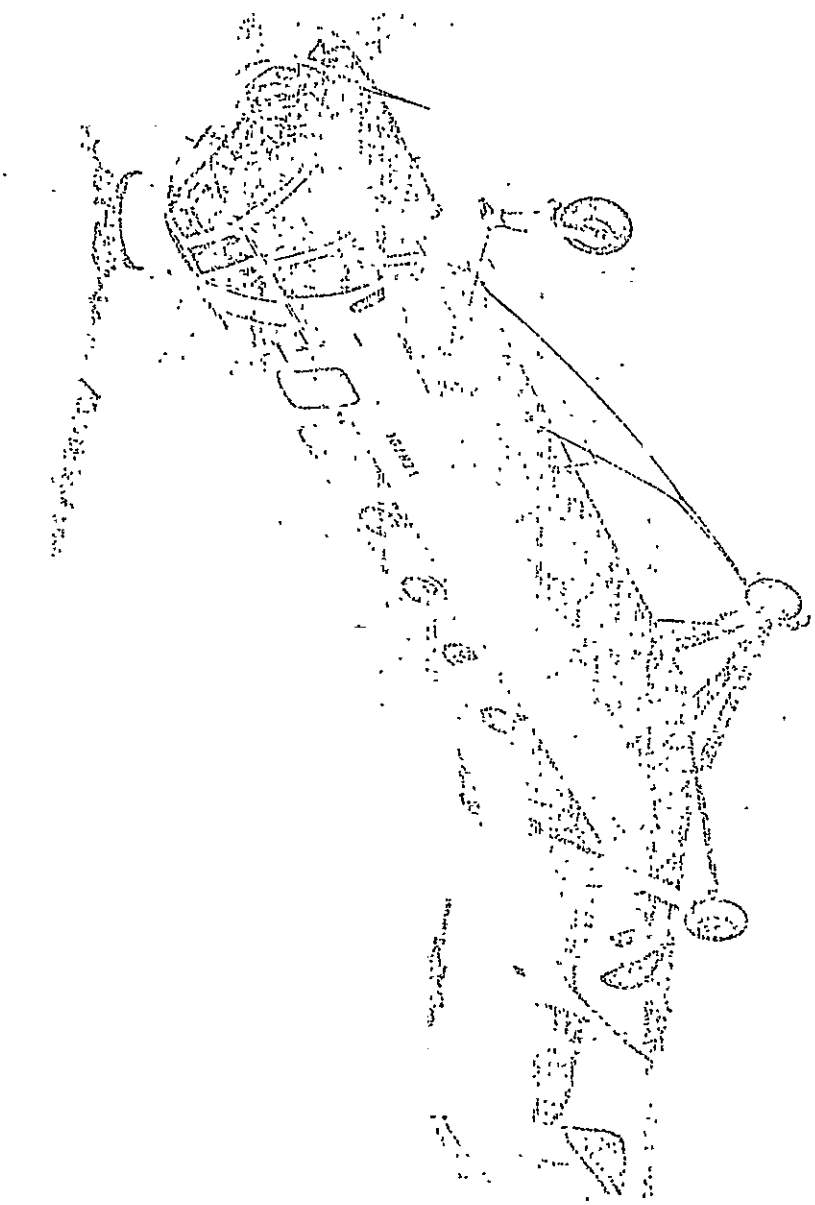

II. BACKGROUND

A. Helicopter Instability

As a background to the following system description it is helpful to describe the dynamic characteristics of the basic helicopter.

In hover, the dominant mode in both pitch and roll is an 8 to 20 sec oscillation which at least doubles amplitude every half cycle. In forward flight this degenerates to an almost pure divergence in pitch and in the coupled roll yaw mode, caused respectively by the longitudinal and directional static instability of the basic aircraft.

B. Previous Approaches to Helicopter Stabilization

These breakdown into three general classes - aerodynamic surfaces, large mechanical gyros, and autopilots.

Aerodynamic surfaces such as horizontal and vertical fins do not stabilize the aircraft in hover, but do however add considerable weight and drag at all times.

Large gyros such as the Bell stabilizer bar, are not adaptable for optimum stability about all axes, as well as having high drag and weight, particularly for a tandem helicopter.

Vertol was the first manufacturer to install an autopilot in a helicopter. Since then we have continually worked with advanced autopilot designs. Our experience has shown that helicopter autopilots are relatively expensive, heavy and complex, and are only required for certain missions. They are not in general suited to installation in every aircraft, nor can they be completely dualized within practical limitations.

Experience with all of these devices finally lead us to try the simple electronic system to be described. A review of tandem helicopter basic controls will, however, be helpful.

C. Aerodynamic Controls.

The four basic controls are;

1. Thrust - obtained by changing the blade pitch on both rotors simultaneously.
2. Pitch - obtained by changing the thrust differentially between the rotors.
3. Roll - obtained by tilting both rotor discs (and hence thrust vectors) laterally in the same direction.
4. Yaw - obtained by tilting the rotor discs oppositely.

PITCH AXIS RESPONSE

Flight - SAS off - YHC - 1A

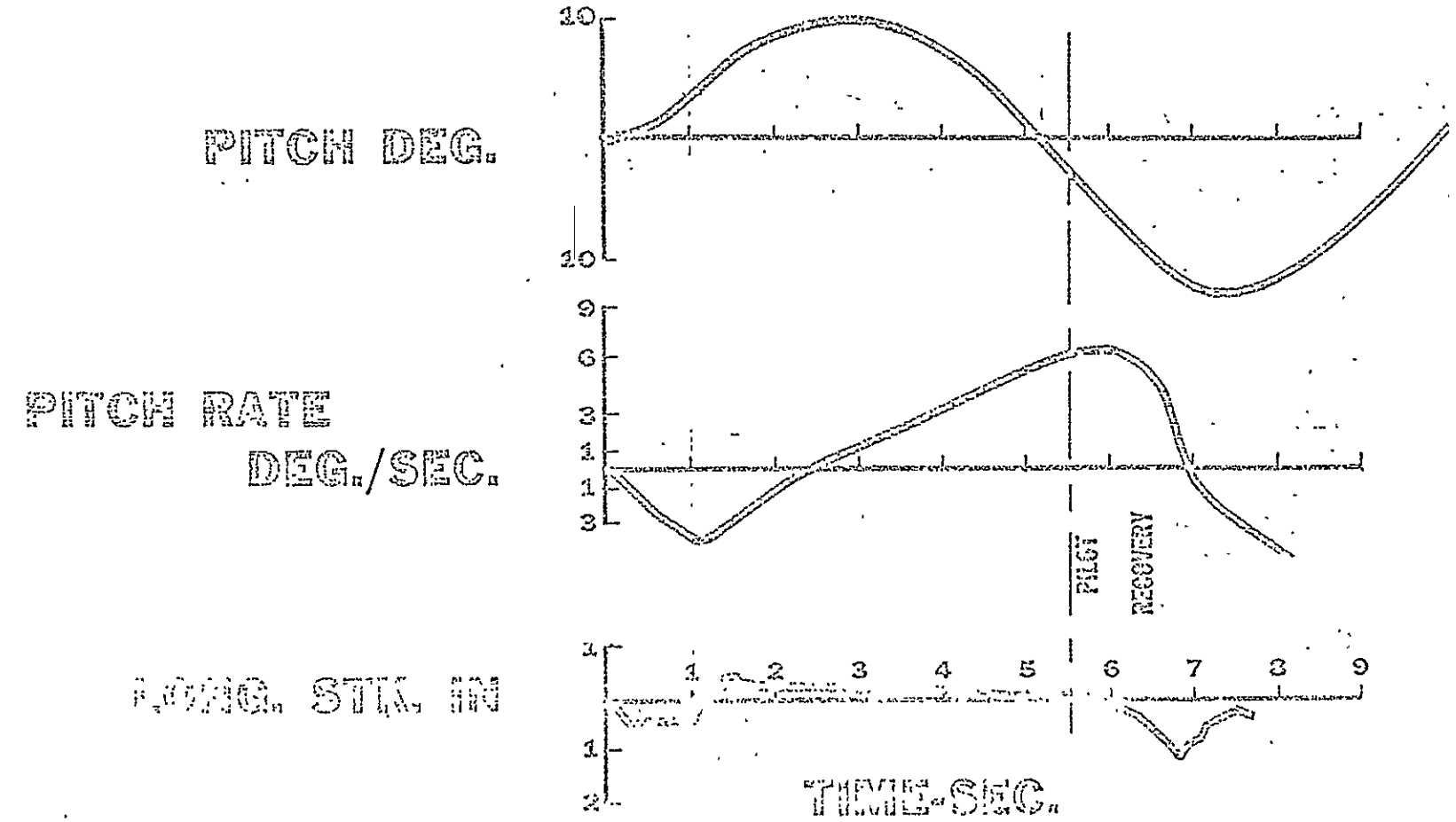

PITCH AXIS RESPONSE

Airspeed = 140 knots - SAS off - YHC - 1A

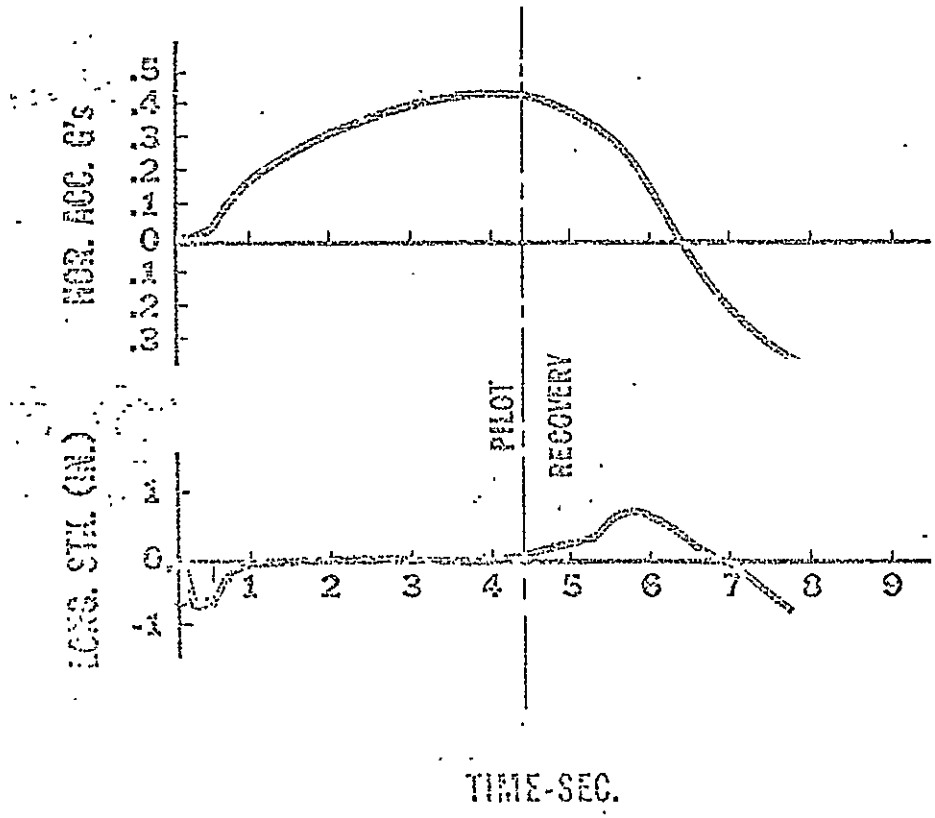

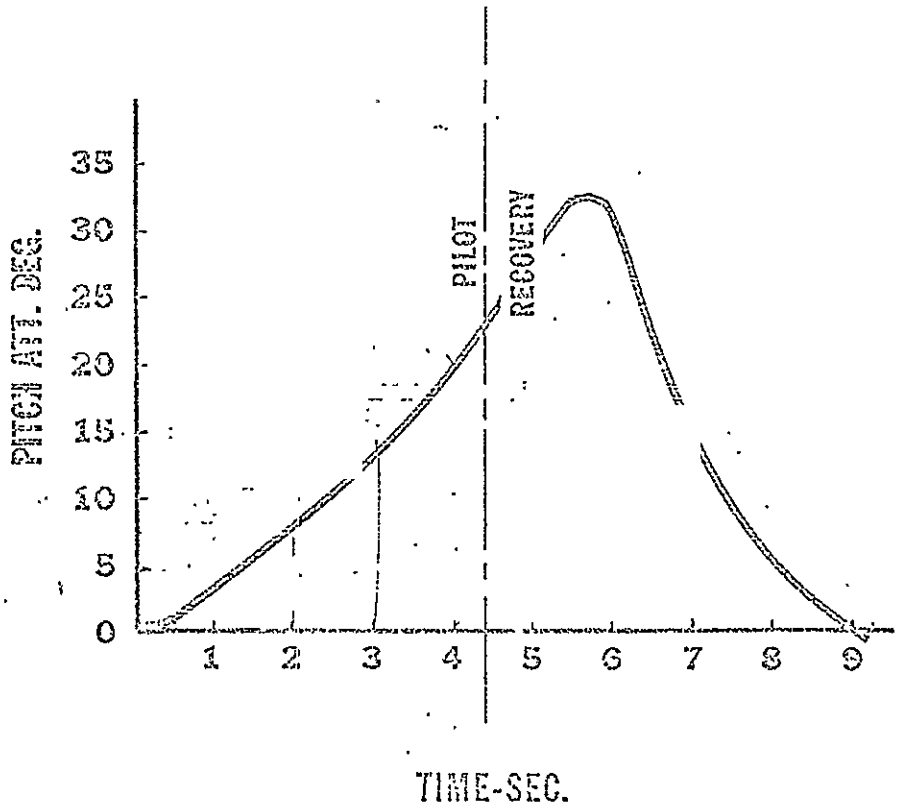

ROLL RATE DEG./SEC.
15
10
5
0
-5
-10
LAT. STK. IN.
0
-1
-2
1
2
3
4
5
6
7
8
9
PILOT
RECOVERY
TIME-SEC.

ROLL DEG.
20
15
10
5
0
-5
-10
1
2
3
4
5
6
7
8
9
PILOT
RECOVERY
TIME-SEC.

ROLL AXIS RESPONSE

Airspeed – 400 knots. SAS off. YHC : 1A

BASIC AERODYNAMIC CONTROLS

PITCH	THRUST	ROLL	YAW
LONGITUDINAL STICK DIFFERENTIAL COL- LECTIVE PITCH (DCP)	COLLECTIVE STICK	LATERAL STICK	RUDDERS

Mechanical Hydraulic Control System

All rotor controls are power operated by dual hydraulic actuators at the rotor heads. Each dual actuator consists of two pistons, arranged in parallel, supplied from separate hydraulic systems, and controlled by a tandem servo valve which is moved by mechanical linkage from the cockpit. At the cockpit is a second, though much lower power set of hydraulic actuator units. These serve a dual purpose. First, they prevent all friction, static weight, and inertia forces from the intermediate linkages from being felt by the pilot. Second, they provide a positive backup to react all forces from the SAS extensible link actuators which "float" in the intermediate controls without being tied to structure. The SAS actuators operate differentially with respect to the cockpit controls in that they move the rotor blades without moving the primary controls. For safety, then, the authority of the actuators is limited to the following nominal values...

Pitch	20%
Roll	20%
Yaw	40%

MECHANICAL AND HYDRAULIC CONTROL SYSTEM

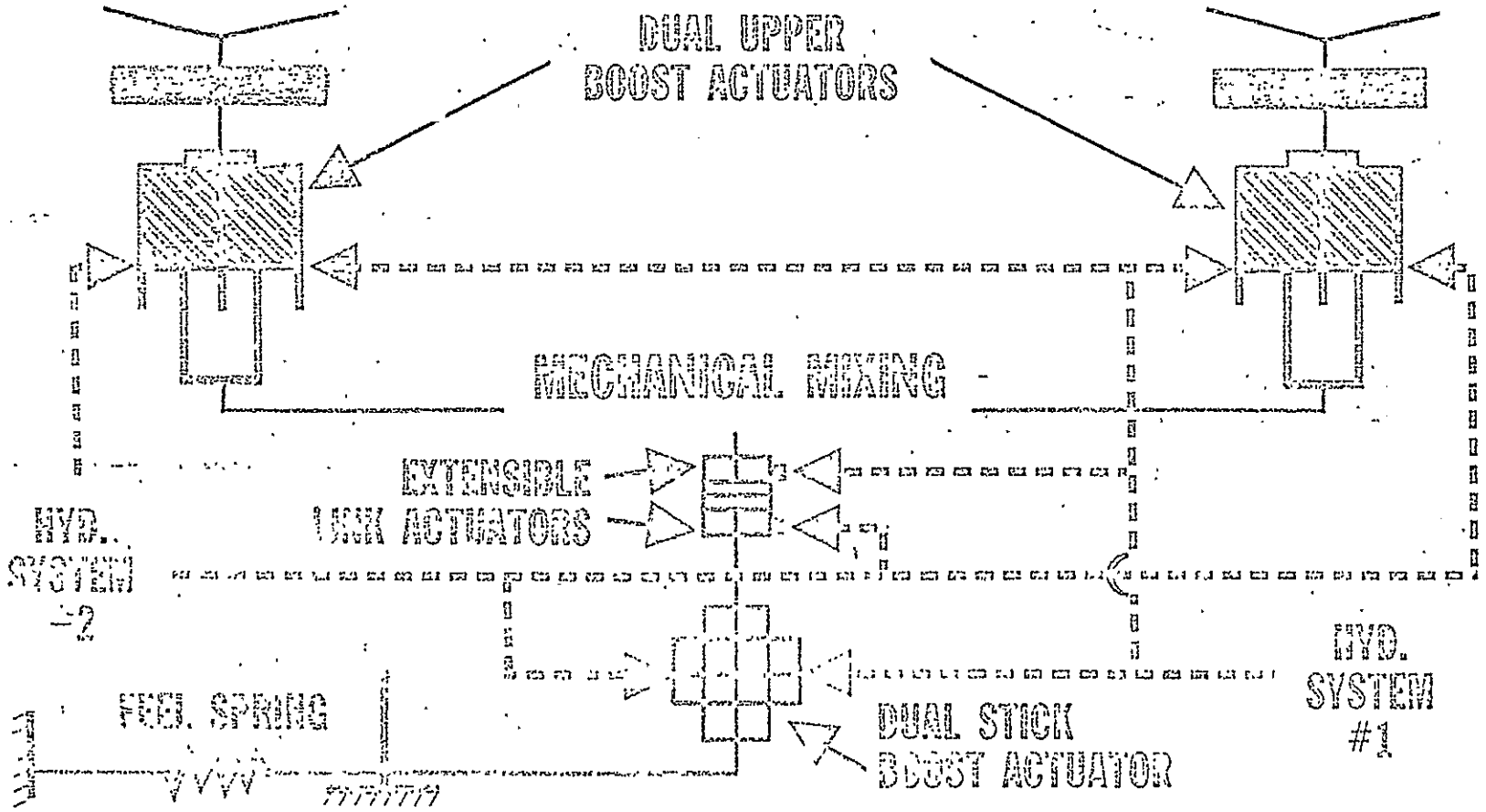

III. SAS DYNAMICS IN DETAIL (See Figure 1)

Before discussing the detailed dynamics, the general system functions and signal paths will be described. As was previously mentioned, the SAS uses only rate gyros for dampers, and sideslip sensors to obtain static directional stability with good turn coordination. Signals from these sensors are demodulated, filtered as required, remodulated, and used as the input signal to a servo amplifier hydraulic actuator loop. This results in a mechanical control input in either the pitch, roll or yaw axis as required. This in turn is hydraulically boosted and fed to the rotor, from which the appropriate corrective moments are applied to the aircraft.

A. Basic Control Dynamics in Detail (See Figure 2)

The Dynamic response common to all three SAS axes consists of a series of relatively high frequency lags. Values are shown for the 107-II as being typical. Taken in order, they are:

1. Rotor dynamics simplified - 0.06 sec.
2. SAS Hydraulic actuator. servo amplifier loop - 0.05 sec.
3. Upper Control Boost Actuator - 0.01 sec.

B. Pitch Axis (See Figure 3)

1. The static gain and 1 second lag time constant were predicted by analysis as giving good stability and response in all flight regimes This was confirmed by flight tests.

2. The 0.2 second lead was found necessary during flight test to eliminate "porpoising" of the aircraft, particularly at high airspeeds. Later analysis showed that this lead compensates in the critical frequency range for the phase lag introduced by servo loop and rotor dynamics.

3. The final lag was introduced on a cut and try basis to eliminate a ground handling effect in which pitch motion of the aircraft on its landing gear caused the longitudinal stick to move against its control feel spring. This in turn moved the controls and caused more aircraft pitch response. Since the natural frequency of the aircraft on its gear is much higher than the predominant in-flight mode, the SAS phase shift was such that it aggrevated the landing gear - stick coupling to the point where it became unstable. Since the pilot could naturally stop any motion by holding the stick, the whole problem was merely a nuisance which was cleaned up during test ground run up.

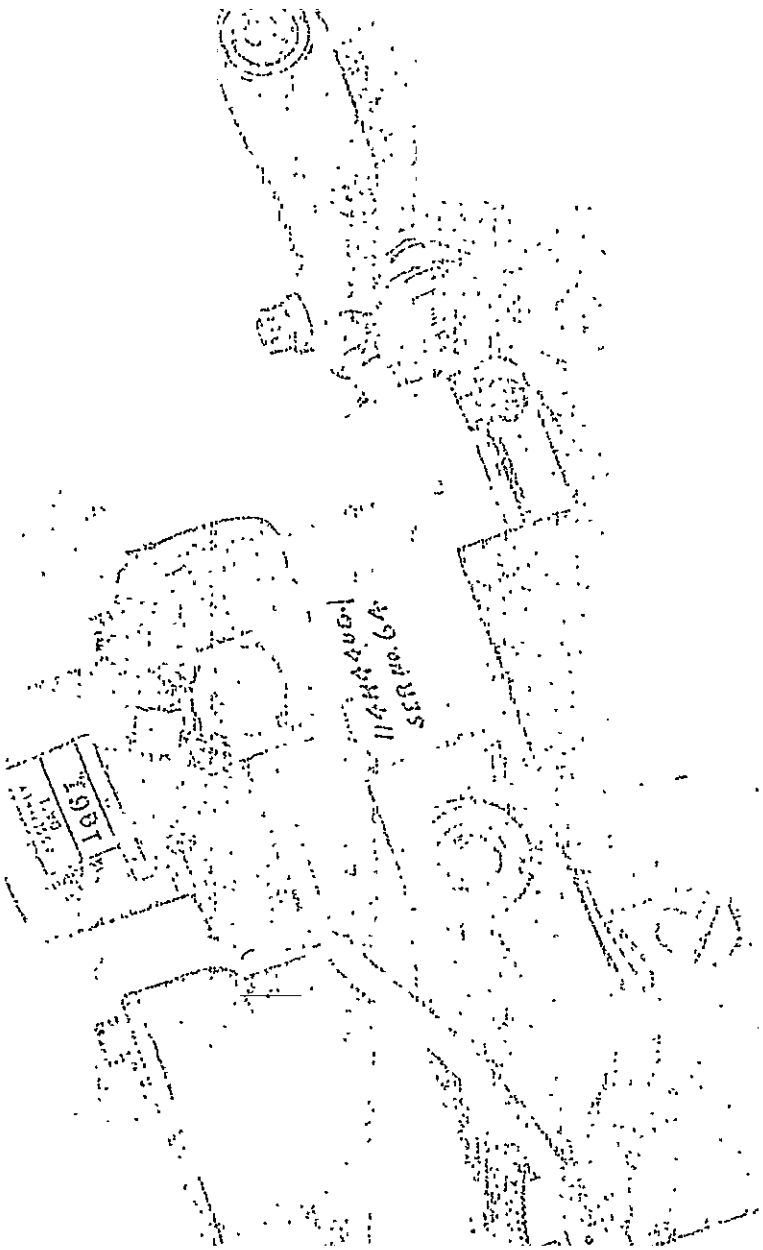

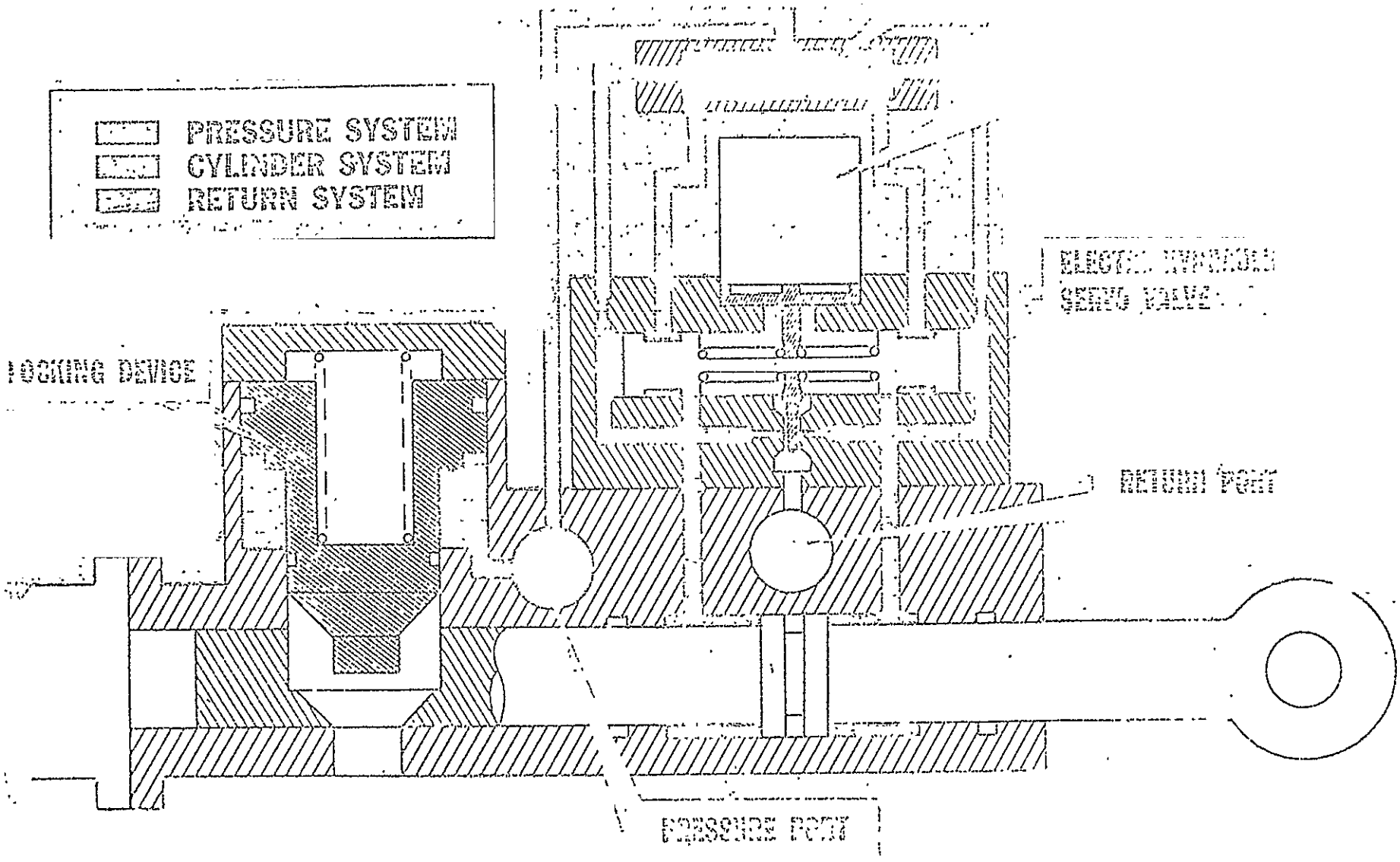
PRESSURE SYSTEM
CYLINDER SYSTEM
RETURN SYSTEM
RETURN PORT

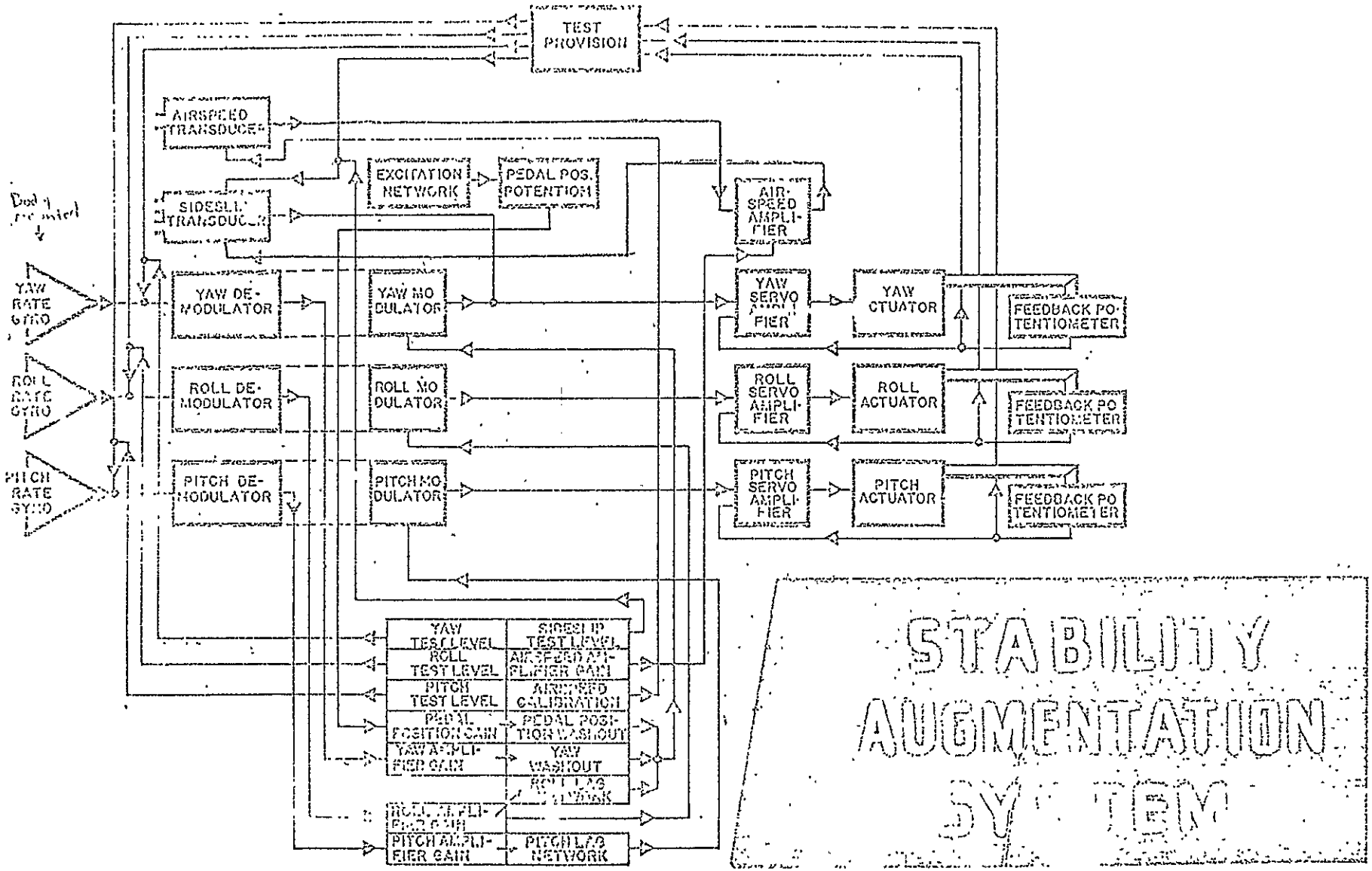
TEST PROVISION
AIRSPEED TRANSDUCER
SIDESLIP TRANSDUCER
EXCITATION NETWORK
PEDAL POS. POTENTION
AIR-SPEED AMPLI-FIER
YAW RATE GYRO
ROLL RATE GYRO
PITCH RATE GYRO
YAW DE-MODULATOR
ROLL DE-MODULATOR
PITCH DE-MODULATOR
YAW MO DULATOR
ROLL MO DULATOR
PITCH MO DULATOR
YAW SERVO AMPLI-FIER
ROLL SERVO AMPLI-FIER
PITCH SERVO AMPLI-FIER
YAW CTUATOR
ROLL ACTUATOR
PITCH ACTUATOR
FEEDBACK PO-TENTIOMETER
FEEDBACK PO TENTIOMETER
FEEDBACK PO TENTIOMETER
YAW TEST LEVEL
SIDESLIP TEST LEVEL
ROLL TEST LEVEL
AIRSPEED AMPLIFIER GAIN
PITCH TEST LEVEL
AIRSPEED CALIBRATION
PEDAL POSITION GAIN
PEDAL POSITION WASHOUT
YAW AMPLIFIER GAIN
YAW WASHOUT
ROLL LAG NETWORK
ROLL AMPLIFIER GAIN
PITCH AMPLIFIER GAIN
PITCH LAG NETWORK
STABILITY AUGMENTATION SYSTEM

INHERENT CONTROL SYSTEM RESPONSE

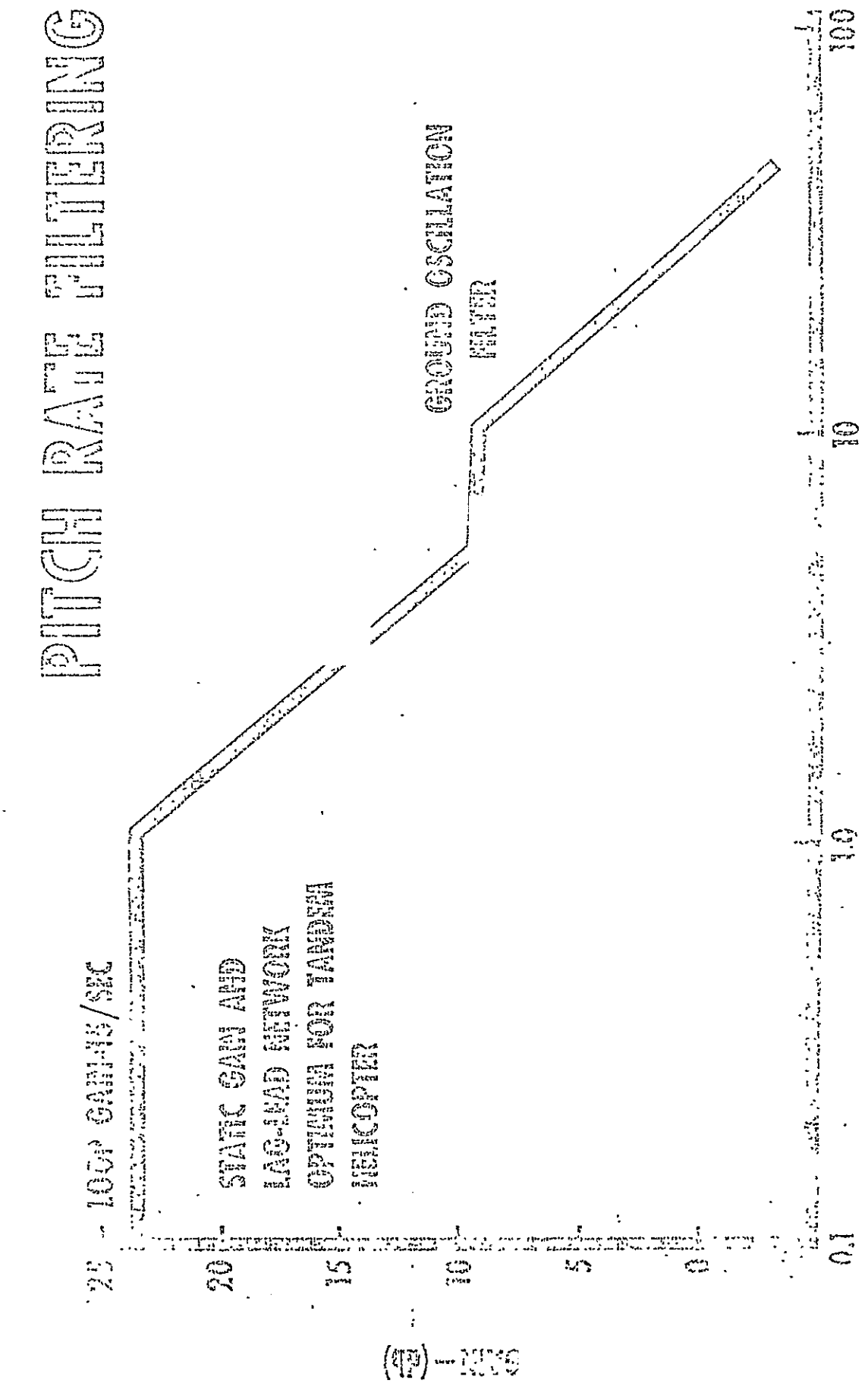
PITCH RATE FILTERING
20 - 10db GAIN/SEC
20
15
10
5
0
STATIC GAIN AND
MAGNAD NETWORK
OPTIMIZED FOR TANDEM
HELICOPTER
GROUND OSCILLATION
RIG STEP
0.1
1.0
10
100
ω (RAD/SEC)
GAIN (DB)

PITCH AXIS RESPONSE

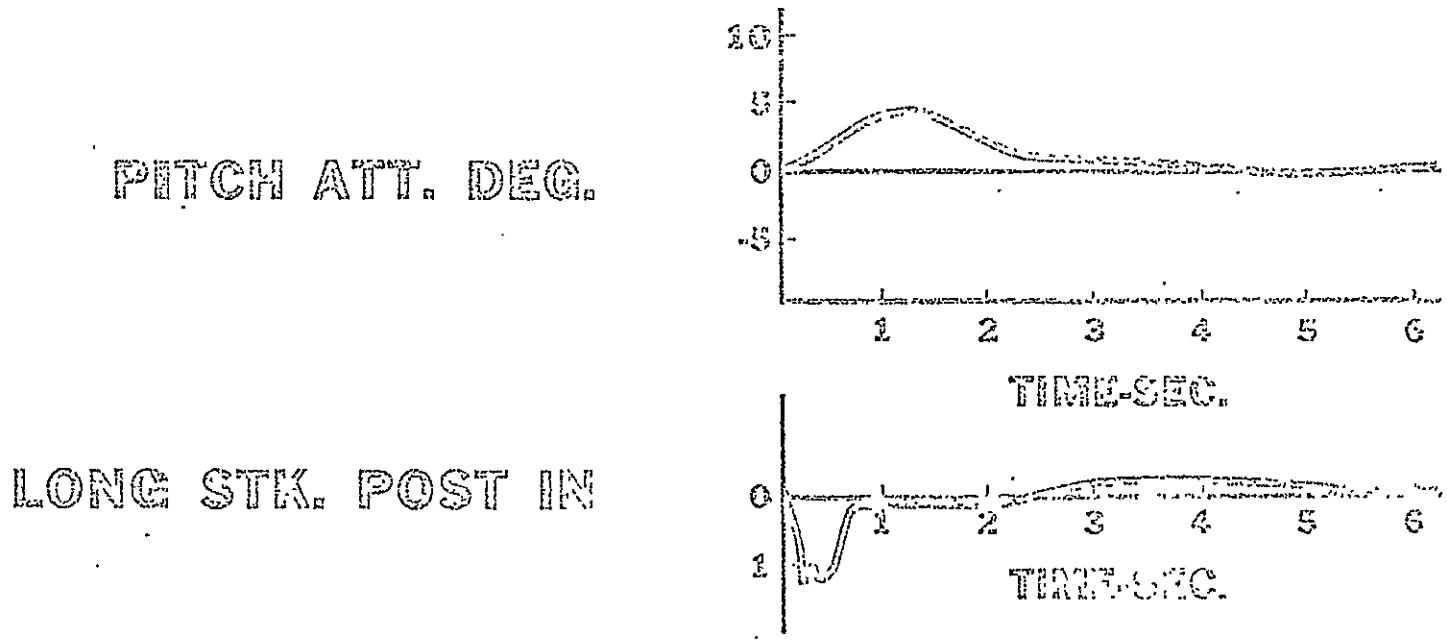

C. Roll Axis (See Figure 4)

A pure rate filtered roll damper is sufficient to provide dynamic stability in hover and forward flight. All articulated rotor helicopters are, however, subject to a potentially violent mechanical instability known as "ground resonance" involving the roll dynamics of the fuselage on the landing gear coupled with a center of gravity shift of the rotor mass due to in plane blade motion. The troublesome natural frequency usually falls at about 2/3 of rotor speed, or about 3 cps for the 107-II. During the normal "ground resonance" testing, it was found that the SAS sometimes increased the tendency to ground instability. The filtering shown eliminated the problem.

D. Yaw Axis

1. Yaw Rate Damper (See Figure 5

The middle frequency damper gain is set by the requirement of eliminating any yaw oscillation in forward flight.

The low frequency washout reduces the yaw rate signal to zero during a steady turn. This prevents bottoming the yaw differential actuator which might otherwise occur with its attendant loss in stability.

The high frequency lag attenuates undesirable vibration pick up from the gyros into the control system.

2. Sideslip (See Figure 6)

All current Vertol helicopters are statically unstable with respect to yawing moment due to sideslip. The sideslip sensor compensates for this, providing the static stability necessary to allow easy high speed flight, pedal fixed turn coordination, and to meet MIL spec requirements.

Sensing is accomplished by means of a pair of static pressure ports symmetrically located on the nose about 45° around from the aircraft center line. It has been found that the differential pressure between these ports is a linear function of sideslip angle, approximating that predicted by potential flow theory on an infinite cylinder in uniform flow. ($\Delta P = 4q\beta$)

From the above it is apparent that the gain of the sideslip loop in terms of inches of control per unit sideslip will increase with airspeed squared. Even though the aircraft instability follows a similar trend in the negative direction, the net total has been found to be too high at high airspeeds when set for good stability at intermediate speeds. This can be explained as follows. The increase in net static stability with airspeed can be looked upon as an increasingly stiff spring restraint in the yaw axis to directional disturbances. Since the damping is constant, and the natural frequency of the motion increases, the damping ratio (actual/critical) drops.

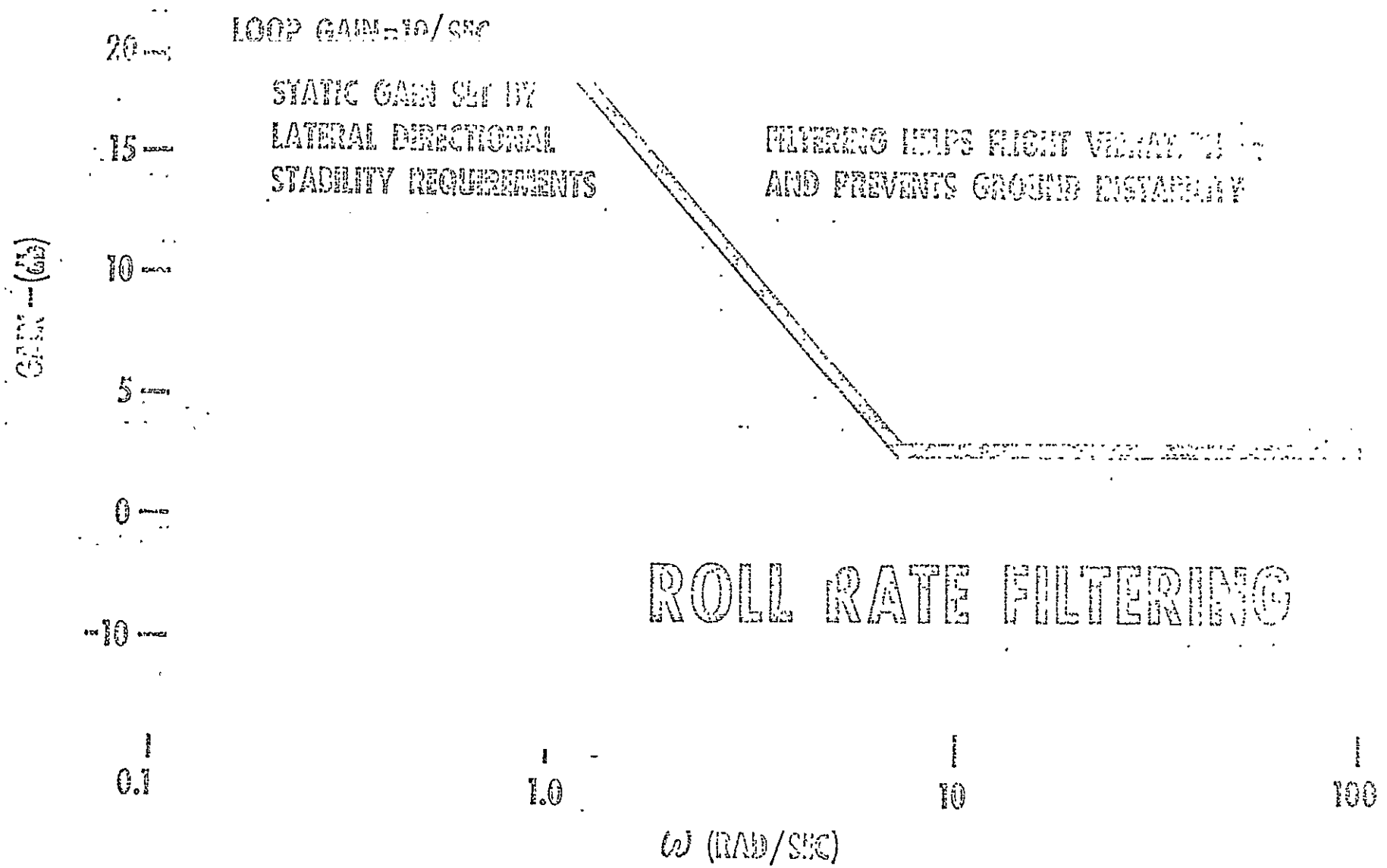

ROLL RATE FILTERING

YAW RATE FILTERING

AIRSPEED SYSTEM
DYNAMIC PRESSURE
AIRSPEED TRANSDUCER
STATIC PRESSURE
DIFFERENTIAL STATIC PRESSURE
SIDESLIP TRANSDUCER
AIRSPEED PROGRAM
SIDESLIP GAIN - f (FORWARD SPEED)
TO YAW SAS ACTUATOR

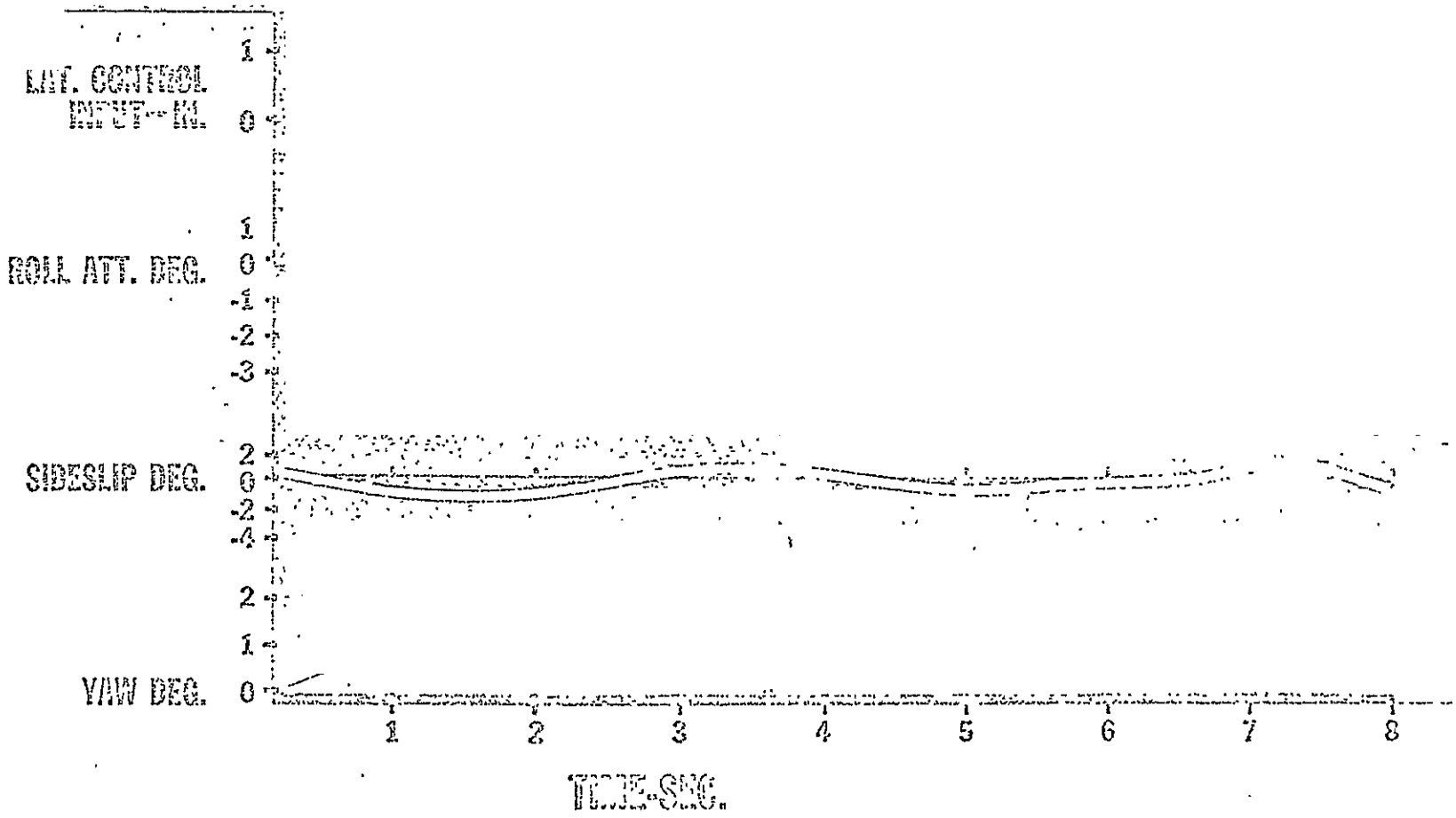
LAT. CONTROL INPUT--IN.
1
0
ROLL ATT. DEG.
1
0
-1
-2
-3
SIDESLIP DEG.
2
0
-2
-4
YAW DEG.
2
1
0
1
2
3
4
5
6
7
8
TIME-SEC.

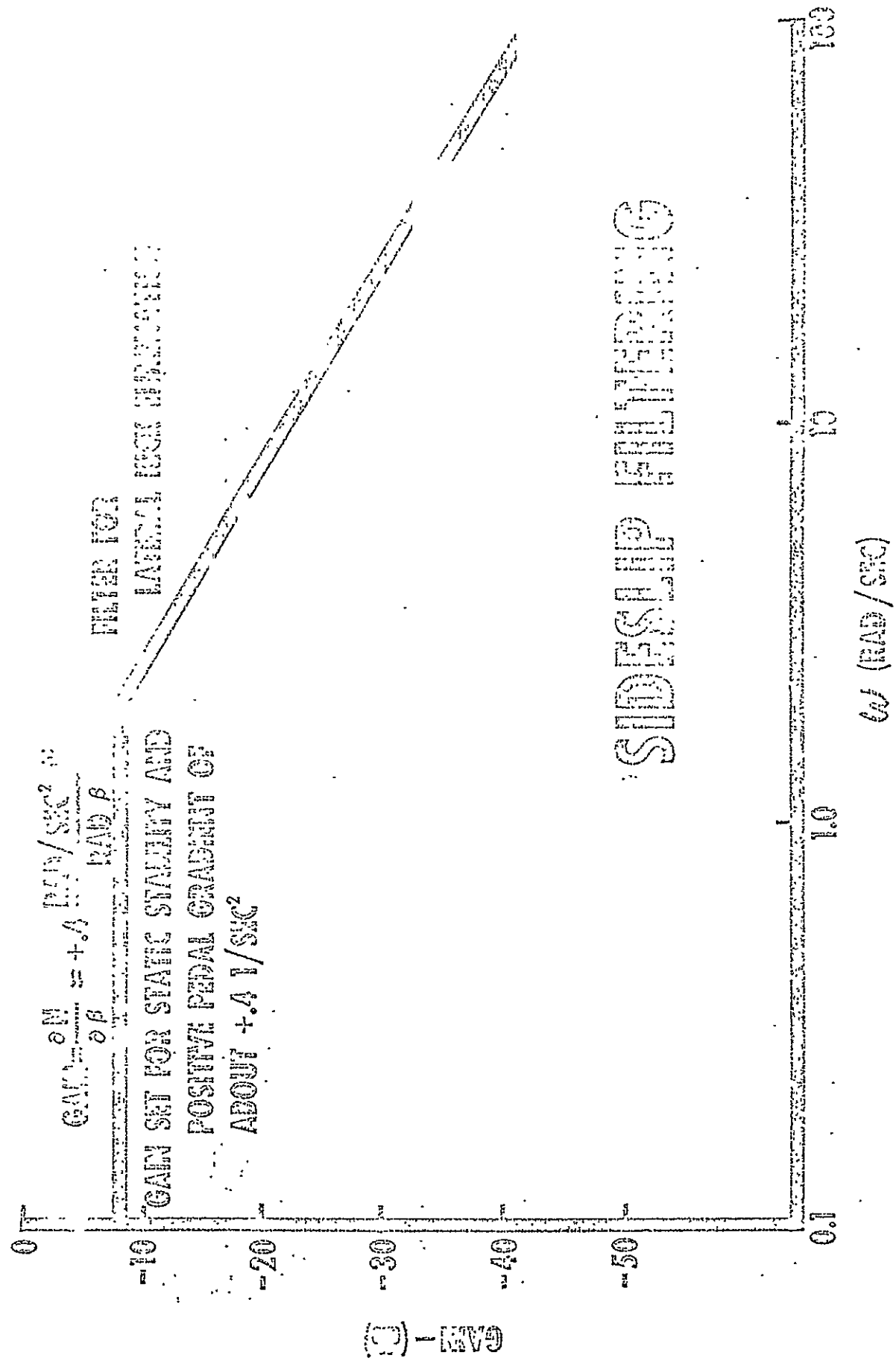
0
-10
-20
-30
-40
-50
0.1
1.0
10
100
SIDESLIP (DEG)
LATERAL ACCEL (FT/SEC²)
GAIN SET FOR STABILITY AND
POSITIVE PEDAL GRADIENT OF
ABOUT +4.1 LB/SEC²

...is ... e up as a characteristic 3 to 5 sec period fishtailing motion. ... to avoid this, the sideslip gain is reduced at higher speeds by ... airspeed signal.

Both sideslip differential pressure and airspeed electrical signals are obtained from Vertol designed pressure transducers.

3. Roll Rate Into Yaw (See Figure 7)

This cross coupling signal was added to the basic three axis damper in order to maintain good coordination during rapid entries into turns using stick commands and with pedals fixed. The lag is chosen long enough such that it approximately integrates the roll rate signal for short periods. The result is a roll angle signal which commands the required yaw rate for smooth turn entires.

Two disadvantages caused by this crosscoupling are:

(a) It decreases the spiral stability of the aircraft if the gain is slightly higher than necessary.

(b) Introduces the possibility of a simultaneous roll-yaw hardover signal through roll gyro failure.

4. Pedal Position (See Figure 8)

The yaw damper reduces the yaw control response of the aircraft to a degree which is undesirable in hover. To regain the original controllability, a washed out pedal position signal is used to cancel the yaw gyro into the servo amplifier. The washout prevents trim pedal displacements from affecting the system.

$$\text{GAIN} = 2\,\frac{\text{RAD/SEC}^2\ \dot{\psi}}{\text{RAD/SEC}\ \phi}$$

GAIN AND FILTER FOR
* COORDINATED TURN ENTRY

ROLL RATE INTO YAW FILTERING

FILTER TO MATCH
YAW RATE CLOSED
GAIN TO CANCEL YAW RATE
PEDAL PICKOFF FILTERING
40
30
20
10
0
-10
.01
0.1
1.0
10
100
ω (RAD/SEC)

IV. HARDWARE CONSIDERATIONS

A. Contamination

The hydraulic actuators and servo valves are protected against contamination by filtering. It was also found that the pneumatic system used to measure sideslip angle also required some definite foreign particle protection. The static ports and lines posed no problem due to their relatively large size. The transducer signal pickoff element was susceptable to dirt clogging. Since the commercial unit originally used could not be modified, Vertol designed, tested, and is now manufacturing transducers which overcome this through their mechanical design.

Sensitivity is such that full output signal is obtained for a differential pressure of 0.5 psi. Since a usable signal can be gotten for the altitude change from the floor to a desk top, these units are also used as barometric altitude sensors in the Vertol autopilot which is in early development testing.

B. Nonlinearities

The design of the amplifier actuator servo loop hardware was such that a hydraulic servo valve was chosen which had a higher gain than was required. In normal operation, only a small part of the value flow capability is utilized, resulting in a magnification of the nonlinearities around the null position.

In extremely calm air, a long period low amplitude limit cycle oscillation has been noticed in the pitch axis caused by excessive valve threshold.

A null shift, resulting in a slight "engage error" has also been noted in day to day operations.

A change to a low gain servo valve, with appropriate circuit adjustments is now in progress.

C. Unwanted Signal Pickup

Since the first experimental SAS installation, all rate signals have had intentional high frequency filtering, particularly to reject the predominant 13 cps vibration frequency.

As a matter of convenience, no filtering was included in the sideslip system of the 107-II SAS design since none had been found necessary for previous aircraft. During test flying, pilots complained of a random lateral "kick" which occurred SAS-on at high speeds. This proved to be an intermittant yaw oscillation which appeared to be a direct function of sideslip sensor gain. After some cut and try testing, a pair of one gallon cans to serve as pneumatic filters were tried and eliminated the problem.

Apparently the higher system gain required by higher speeds and poorer basic aircraft stability was sufficient to show up the problem on the 107-II. Subsequent experience on the HC-1B, has shown that a simple filter network as is used for rate signals, also solves the problem.

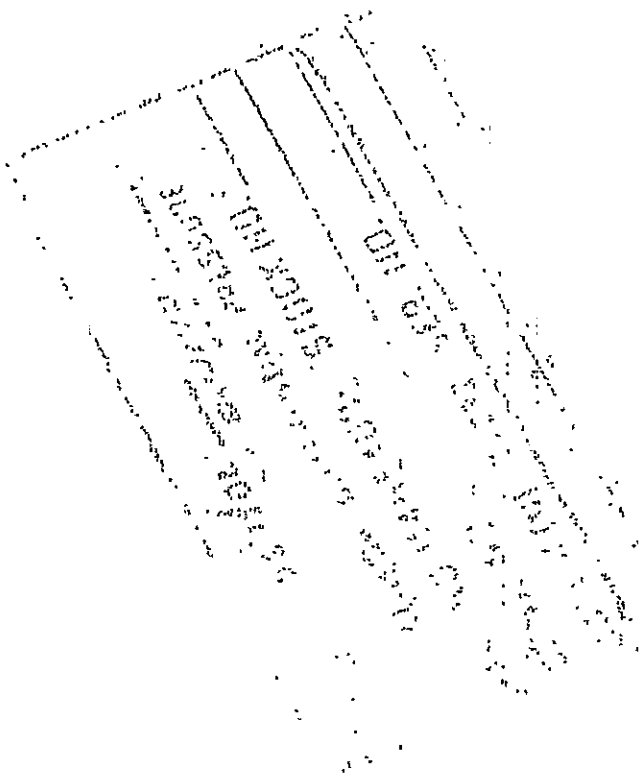

V. FAILURE CONSIDERATIONS

A. Dualization

In order to have fail safe reliability and to maintain aircraft stability following failure, two identical complete and independent SAS are installed in each aircraft. This dualization includes separate electric and hydraulic power supplies as well as black boxes and actuators. No single failure can lose both systems.

Normally both SAS operate each at half gain. If hydraulic or electric power to one system fails the other automatically is switched to full gain. If some other failure occurs, the pilot must manually switch to the remaining system.

B. Flight Tests

All possible system failures have been demonstrated in flight to show recovery capability, and to define flight limitations if any.

Early in .07 failure testing it was determined that a loss-of-actuator-feedback failure in which the actuator oscillated at maximum velocity between its limits, was so bad even in hover that a forward flight demonstration was inadvisable. After this experience, each individual actuator had its feedback loop dualized.

C. Overtravel

Sufficient control throw is available in the cockpit so that the pilot can still move the rotor controls to their limit stops following a full extend or retract SAS actuator failure. This insures that there will be no loss of controllability resulting from a single system failure.

OVERTRAVEL

NEUTRAL
CONTROL
THROW

NEUTRAL
CONTROL
THROW WITH
SHIFTED
NEUTRAL
POSITION

VI. SERVICE [illegible]

A single [illegible] SAS almost identical to that just described was installed in the last [illegible] commercial versions of the H-21 which were sold to foreign governments [illegible] 1959. Since then these have accumulated 2700 flight hours, and have had [illegible] discrepancies consisting of one gyro failure, one leaky actuator, one rough feedback potentiometer, and one circuit discrepancy.

VII. SUMMARY

This paper has attempted to give an overall picture of the SAS with regard to its purpose, method of operation and problems encountered during design.

Any means of stabilizing a basically unstable vehicle must be weighed in relation to mission requirements. For the large helicopter or VTOL, the most important factors are:

1. Reliability - failure rate per unit time, and consequences should one occur.

2. Quality of Stability - must consider both hover and forward flight.

3. Performance Penalties - weight and drag of fixed surfaces for example.

Considering these, we believe that the Dual SAS installation described herein represents a good solution to the problem for the present generation of aircraft.

APPENDIX L

"HELICOPTER AUTOMATIC CONTROL THROUGH INTEGRATION OF SEPARATE FUNCTIONAL UNITS"

HELICOPTER AUTOMATIC CONTROL THROUGH INTEGRATION OF SEPARATE FUNCTIONAL UNITS

M. I. Gerstine and B. B. Blake
Vertol Division
The Boeing Company

Summary

The trend in helicopter automatic stabilization has always been to combine functions of stabilization, trim and flight guidance in a single package. This evolved from the background of fixed wing autopilots which were first adapted to helicopters. The weight, cost and reliability of this approach has impeded operational suitability and brought about development of a different concept.

The requirement of providing excellent stabilization dictates the use of high frequency response actuators and other critical system components, without compromising flight safety or aircraft control feel. Such functions as guidance and navigational coupling of a stable aircraft can be accomplished by the installation of a simple memory unit utilizing slow acting low response hardware. The differences in duties and performance requirements logically leads up to a complete separation using different systems.

The concept of separation of function used in the 107-II leads to less cost, weight, and complexity, and greater reliability than standard systems.

I. Introduction

Confusion has existed in the past as a result of adapting fixed wing autopilots to helicopters. This has been reflected not only in terminology, but in the manner in which the functions have developed in the devices themselves. The majority of fixed wing autopilots primarily need to supply a long term reference to hold a basically stable aircraft on a fixed speed, heading and altitude. If such a system is simply adapted to helicopters, on the other hand, it must perform a fairly difficult stabilization task, as well as accomplishing flight guidance, and this stabilizing function must be accomplished with no loss in the maneuvering capabilities or deterioration in control feel. Considerable effort in attempting to cope with these diverse requirements of stabilization and of guidance have resulted in development of a new approach to the problem of helicopter automatic flight, which has been applied to the Boeing-Vertol 107-II shown in Figure 1. The concept, details, and performance of the new systems are described in this paper.

II. Concept of Separation of System Function

The design philosophy of the helicopter is to incorporate provisions for two types of automatic flight control systems. These are:

1. A Stability Augmentation System (S.A.S.) which is an integral part of the aircraft control system in both function and dependability.

2. Attitude and Altitude Lock System which is supplementary equipment employed as an automatic pilot and for automatic navigation control, and/or programmed missions. Figure 2 explains this principle, showing a damping loop composed of a dual S.A.S. installation to give completely reliable stability, and a trim function loop for long term reference or navigation.

A. S.A.S. Concept

The concept of the S.A.S. is based on the need for good stability characteristics at all speeds, without compromising the overall size and weight of the aircraft. These requirements apply, particularly, to low airspeeds and instrument approaches at steep angles of descent. Since optimum design is defined by installation of the simplest means of obtaining good stabilization as standard equipment inherent in every aircraft, then if good stability characteristics can be provided without the sophistication of the autopilot, and its consequent weight, complication, expense and problems of maintenance and reliability, it is mandatory that the autopilot be relegated to the role of optional equipment.

The many aerodynamic (fixed surface type) stability devices which have been developed in the past have suffered from several disadvantages. Probably the most important was their ineffectiveness at low airspeeds and in hover, where stabilization is needed as much, if not more, than during forward flight.

Another stabilization system which has been investigated was the damped gyro stabilizer bar mounted on the rotor hub. This gives rate damping similar to that obtained with a gyro. However, because the bar turns at rotor speed and acts directly on blade pitch, it must be heavy enough to generate sufficient control forces. In addition to this weight and the drag associated with a large exposed bar, it suffers from another deficiency. Since the gyro bar is part of the rotating rotor system, there can be only one stabilization gain for both roll and pitch unless a complex mechanical linkage is used. Since the requirements in these two axes are different, it follows that the gain setting is always a compromise resulting in sluggishness for one axis, and insufficient stability for the other.

After several years of intensive effort in stability augmentation and autopilot development, Vertol arrived at a S.A.S. based on internally mounted, high speed, rate gyroscopes. Since the gyro is an inertial device, it provides the same stabilization for all flight conditions. Further, being small and light and well suited to easy aircraft installation, it is feasible to use more than one to (1) optimize characteristics about all control axes and (2) duplicate systems for fail-safe features. The output of the S.A.S. utilizes limited authority differential-type control actuators. This means that the stability augmentation system does not move the pilot's controls. In effect he is flying a stable aircraft and thus needs only slow, fixed-wing type control motions to guide the helicopter.

3 Precise Attitude and Altitude Lock Concept

As the original S.A.S. test program was nearing its close, an interesting characteristic was noted. Instead of making normal helicopter-type control motions during flight, the pilot was merely holding the stick fixed in position and making very small trim corrections at several second intervals. This suggested that the addition of a simple automatic P.A.A.L. system would completely relieve the pilot of control effort during normal steady flight. Such a system was investigated more thoroughly, and offers many significant advantages for a relatively small cost increase.

Since the automatic P.A.A.L. system need only supply minor correction signals, it readily lends itself to a simple and consequently a cheap and reliable method of installation. Figure 3 shows schematically the layout of the system for either the longitudinal or lateral axis. The directional axis is similar except that a directional gyro replaces the vertical gyro. It can be seen that the S.A.S. operates independently of the P.A.A.L., to insure reliable stabilization even in the event of failure. The P.A.A.L. operates as follows: Any attitude error causes the vertical gyro to put out a voltage proportional to the error. This signal, after amplification, drives the attitude trim actuator which changes the zero force position of the preloaded centering springs. This causes movements of the control stick which in turn moves the entire control system. Details of the operation of the attitude and altitude lock are described in subsequent sections of this paper.

III. Description of S.A.S.

A. Development

The present S.A.S. was developed following an extensive analytical and flight test program. Various possible means of improving stability were first investigated on an analog computer, and the most promising systems from this analysis were then tested in an HUP-4 helicopter. Displacement, rate, acceleration and sideslip were all considered as possible parameters for sensing, and any combination of these could be fed into any axis or axes with or without a signal shaping. Eight of these systems were actually flight tested in the HUP. By installing a multiplicity of sensing devices and providing suitable rapid switching and in-flight adjustment of gain settings, it was possible to obtain a direct comparison of the stabilizing characteristics of these various systems.

The system finally selected for the HUP-4 used a lagged pitch rate damper in the longitudinal system, a roll rate damper without lag in the lateral system, and a yaw rate damper in the directional system. In addition, roll rate was fed into the yaw axis to improve dynamic stability and lateral stick turn capability. During the course of the HUP flight test program, the aircraft was frequently flown "hands off" for periods of four to five minutes. In addition, the helicopter successfully flew for two minutes "hands off" in a steady partial power descent at 750 feet/minute at 30 knots airspeed, as would be required for blind approaches. This test was limited to two minutes only by lack of altitude, and the stability would have been adequate to continue for a substantially longer period.

Initial tests of the HUP-4 "breadboard" system on the Vertol Model 107 prototype revealed a requirement for more stability in the yaw axis than that which can be obtained without the addition of a sideslip sensor. To avoid the installation of a boom in front of the aircraft for mounting a sideslip vane, a system was developed which sensed a sideslip by using a differential pressure transducer fed from a pair of static ports symmetrically disposed on the front of the forward pylon. This system gives a high degree of static and dynamic stability on the Model 107 in forward flight and allows "stick" turns up to maximum airspeed with excellent coordination.

The first three-axis production system was designed and produced for the YHC-1A. It embodied the operational features of the Model 107 system but was designed as a single electronic unit, with transistor amplifiers, printed wiring and other features to insure a high degree of reliability.

B. Hardware Operation

1. Servo Loop - The servo loop is the same for roll, pitch and yaw and consists of a transistor amplifier, the output of which is demodulated and fed to the torquemotor of a differential hydraulic actuator. The actuator motion is sensed with a differential transformer and a proportional voltage is fed back to the amplifier. This results in an actuator displacement proportional to the signal voltage applied to the amplifier.

The differential actuator system offers two basic advantages. First, it eliminates undesirable forces and motions from reaching the pilot's controls and, second, it permits the use of lim-

fted authority so that the S.A.S. can never move the controls by more than a fixed percentage of their total travel. This means that even in the event of a malfunction resulting in a hardover signal, sudden motions of the aircraft are minimized, and the pilot can easily override the S.A.S. In addition, the control system stops are arranged on the output side of the S.A.S. actuators so that in the event of a hardover signal the pilot still has available his normal full control plus a sufficient overtravel to counteract the full S.A.S. signal.

2. Stabilization Signals

Roll Axis - The signal applied to the roll amplifier is roll rate from a rate gyro.

Pitch Axis - The pitch axis is identical to the roll axis except for a network which performs a lag-lead on the demodulated rate gyro signal. This particular shaping is optimum for a tandem helicopter.

Yaw Axis - Four signals feed the yaw axis amplifier. One is a yaw rate signal from a rate gyro contained within the electronic unit. Another is lagged roll rate from the roll axis. This signal tends to cancel out any yaw rate signal during turn entry so that turns may be well coordinated. Since this cancellation lasts only during entry into the turn, the yaw gyro signal is fed to the servo amplifier through a "wash out" which eliminates any steady state yaw gyro signal. The third signal is sideslip which is detected by a differential pressure transducer fed by a pair of static ports, symmetrically placed on the nose of the aircraft. For optimum stability at all airspeeds the gain of this transducer is programmed as a function of airspeed so that precise coordination is obtained at all airspeeds between approximately 60 knots and V_{max}. A second differential pressure transducer supplies the necessary signal to accomplish this. For precise control in hover, a fourth signal is applied to the yaw axis. A rudder pedal pickoff signal is used to cancel the yaw gyro signal in turns.

The following figures illustrate explanations of this section.

Figure 3 Boeing-Vertol 107 Control System Schematic Showing Typical S.A.S. Installation

Figure 4 Boeing-Vertol 107 Electronic Block Diagram

Figure 5 Boeing-Vertol 107 Complete Control System Schematic

C. Flight Records

Flight records made during a YHC-1A test program are presented to show the stable qualities of the S.A.S. equipped aircraft. Because of the similarity of basic airframes, and the fact that the S.A.S. has much more powerful effect on dynamic response than aircraft aerodynamic characteristics these records are indicative of what is obtained on the 107-II. The following figures show the pertinent control input and resulting helicopter response for the various axes in hover and forward flight.

Figure 6 Pitch Axis Response - Hover
Figure 7 Roll Axis Response - Hover
Figure 8 Yaw Axis Response - Hover
Figure 9 Pitch Axis Response - Forward Flight
Figure 10 Roll Yaw Response - Forward Flight

D. Reliability

The S.A.S. is designed such that aircraft stability is as reliable as any critical mechanical component. This is accomplished in two ways:

1. Simplicity - A complete three (3) axis S.A.S. contains only about 1/4 the number of critical components as a modern helicopter ASE.

2. Dualization - The installation in the 107-II includes two complete and independent three (3) axis S.A.S.'s. Both of these are normally on at once, each supplying half the required control motion for stabilization. Should a failure occur, either system can take over the full load, and supply all stabilization. The two systems are run from identical but separate electrical and hydraulic power supplies which are standard in the aircraft. There is no single failure (other than catastrophic mechanical) which can result in a loss of both S.A.S.

IV. Description of P.A.A.L.

A. Development

As described in the Introduction, the principle of operation of the precise attitude and altitude lock, is based on flight test experience where it was noted that the pilot need make only small, infrequent control corrections when flying S.A.S. equipped aircraft. This can be done automatically using the scheme shown in Figure 3, where a slow-speed stabilization-synchronization unit repositions the stick as necessary by changing the zero force position on the preloaded centering springs which provide artificial feel to the aircraft controls. This system has several inherent advantages.

1. Since the system only trims the helicopter, there are no large rapid motions such as are associated with stabilization. The system moves the stick in the same way that the pilot does, so that stick motion is unobjectionable and most often even undetected by the pilot.

2. Maximum stick velocity necessary is only about one inch per second. By making maximum motor speed correspond to this velocity, a rapid "hardover" input is impossible, so that one objection to the usual "parallel" type of system is negated. Thus, the system may have 100% author-

ity, overcoming the need for the complex system necessary to keep a limited authority actuator centered.

3. In the event of a failure, the pilot only need overcome the normal centering spring force to completely overpower the system.

B Hardware Operation

The heart of the system is the stabilization-synchronization unit, which is shown schematically in Figure 11. It replaces the magnetic brake installation. The artificial force feel centering spring is attached to the unit output arm. System gain can be changed only by changing gear or linkage ratios, and is not a function of electronic adjustment. Figure 12 is a photograph of the breadboard stabilization-synchronization unit connected to a control mockup for lab checkout purposes.

Modes of Operation

1. P.A.A.L. Off - The brake is engaged and through the centering spring holds the stick or pedals in a trimmed position. The clutch is disengaged and the duplex clutch is in the OFF-SYNC position. In response to any changes in the gyro signal the amplifier will drive the motor so as to null the output of the synchro. Synchronization will be rapid (about 120° per second) since the gear reduction to the synchro will be small in this mode of operation. The pilot can manually retrim the stick or pedals by depressing the Mag. Brake button.

2. P.A.A.L. On (Stabilizing) - The brake is disengaged and the clutch is engaged so that the motor will drive the output arm of the actuator. The duplex clutch is in the STAB position and the motor drives the synchro through a somewhat greater gear reduction than in the OFF-SYNC position, the exact ratio being determined by the gain (output rotation per degree of synchro rotation) required for helicopter stabilization. The output arm is then rotated through an angle proportional to the gyro error signal.

3. P.A.A.L. On (Maneuvering) - The pilot may make temporary commands in pitch and roll by forcing the stick out of detent to change attitude manually. With the stick out of detent in either pitch or roll the power is removed from the motor in that axis and no motion occurs within the actuator. When the stick is released or returned to detent the actuator will return the helicopter to its original attitude.

4. P.A.A.L. On (Synchronizing) - Permanent attitude changes are made in pitch and roll by depressing the Mag. Brake button. This temporarily returns the system to the ASE OFF state in which the system is allowed to resynchronize. Upon release of the button, the system again stabilizes. All heading changes are permanent and are initiated by a pedal going out of detent in hover and by depressing the Mag. Brake switch or moving the stick out of lateral detent in forward flight.

V. Failure Considerations

A. S.A.S.

1. Actuators(See Figure 13) - The authority of the S.A.S. actuators is limited so that under normal operation they cannot provide more control travel than ± .90 inches of longitudinal stick, ± .52 inches of lateral stick and ± .78 inches of rudder pedal.

If there is a loss of hydraulic pressure or if the pilot wishes to turn one of the S.A.S. systems off, a spring loaded lock piston is driven down past the actuator output piston. The lock piston is tapered so that it centers the S.A.S. actuator and locks it in this position.

B. P.A.A.L.

As shown schematically in Figure 3, this function is applied to the pilot's controls through the feel spring. Any normal function encountered therefore, could be overcome by pilot effort with no more than 7.90 lb maximum force in longitudinal stick, 4.53 lb lateral stick, 17.1 lb in rudder pedal and 16.1 lb in collective pitch stick.

VI. Conclusions

1. A new concept of helicopter automatic flight control has been developed, tested, and applied to the Boeing-Vertol 107-II.

2. Stabilization requirements are best satisfied by a simple damper system, dualized for reliability, acting through limited authority differential actuators.

3. Flight guidance of a stable aircraft can best be done using large authority, slow-moving control inputs. Since these are very similar to pilot control motions, it is feasible to move the basic cockpit controls with parallel actuators to accomplish this. Safety requirements are satisfied by putting in control movements through the force feel spring, thereby positively limiting the maximum control force.

4. Detailed analysis and test experience has shown that no single failure can result in a loss of aircraft control or stability.

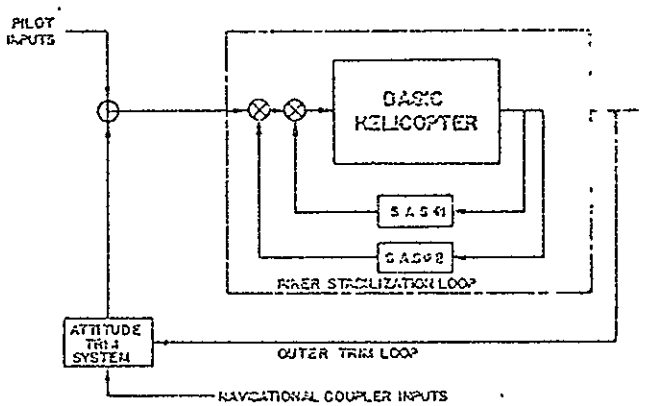

FIGURE 2
INNER AND OUTER LOOP PRINCIPLE

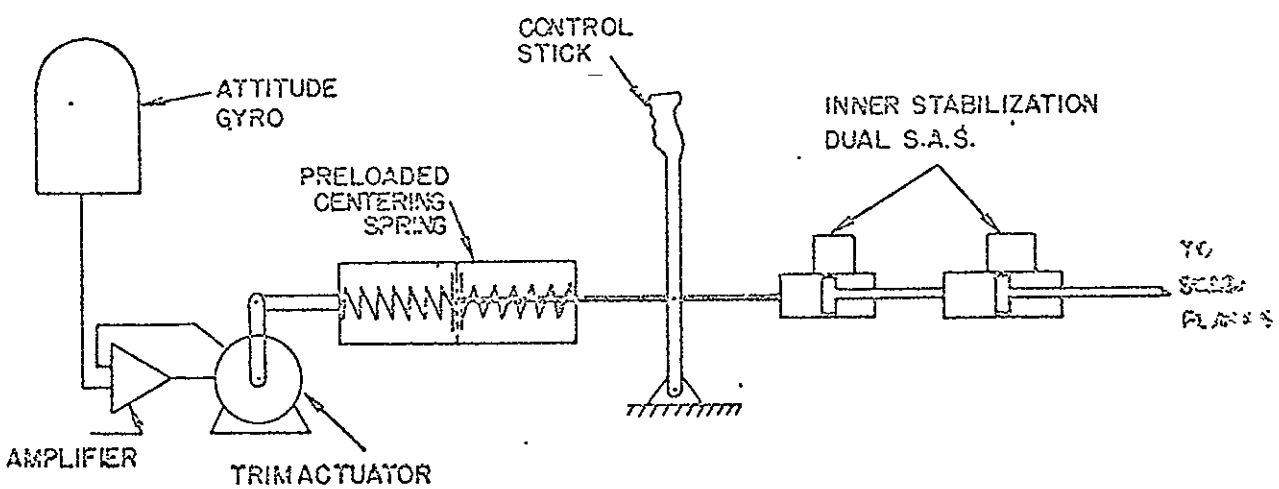

SCHEMATIC FIGURE 3
S.A.S. AND P.A.A.L. INSTALLATION

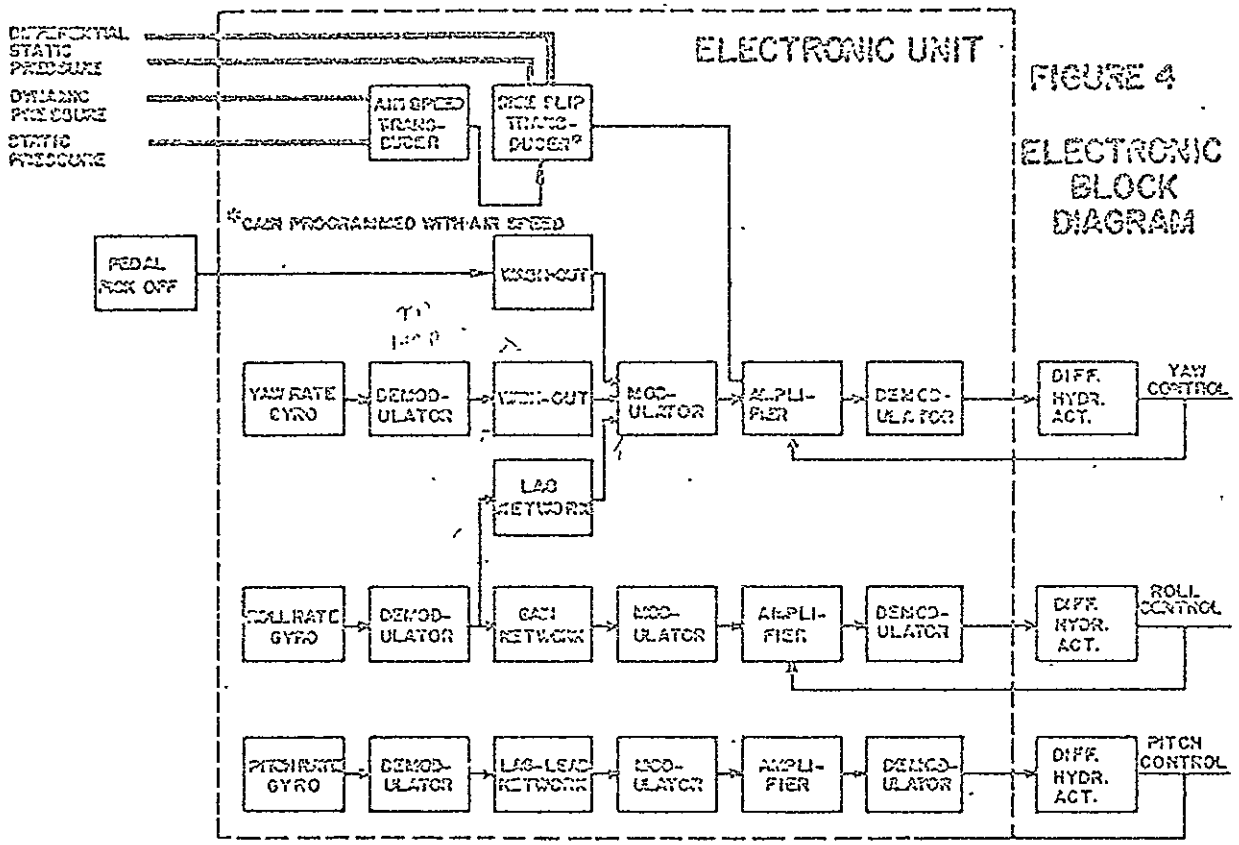

FIGURE 4

ELECTRONIC BLOCK DIAGRAM

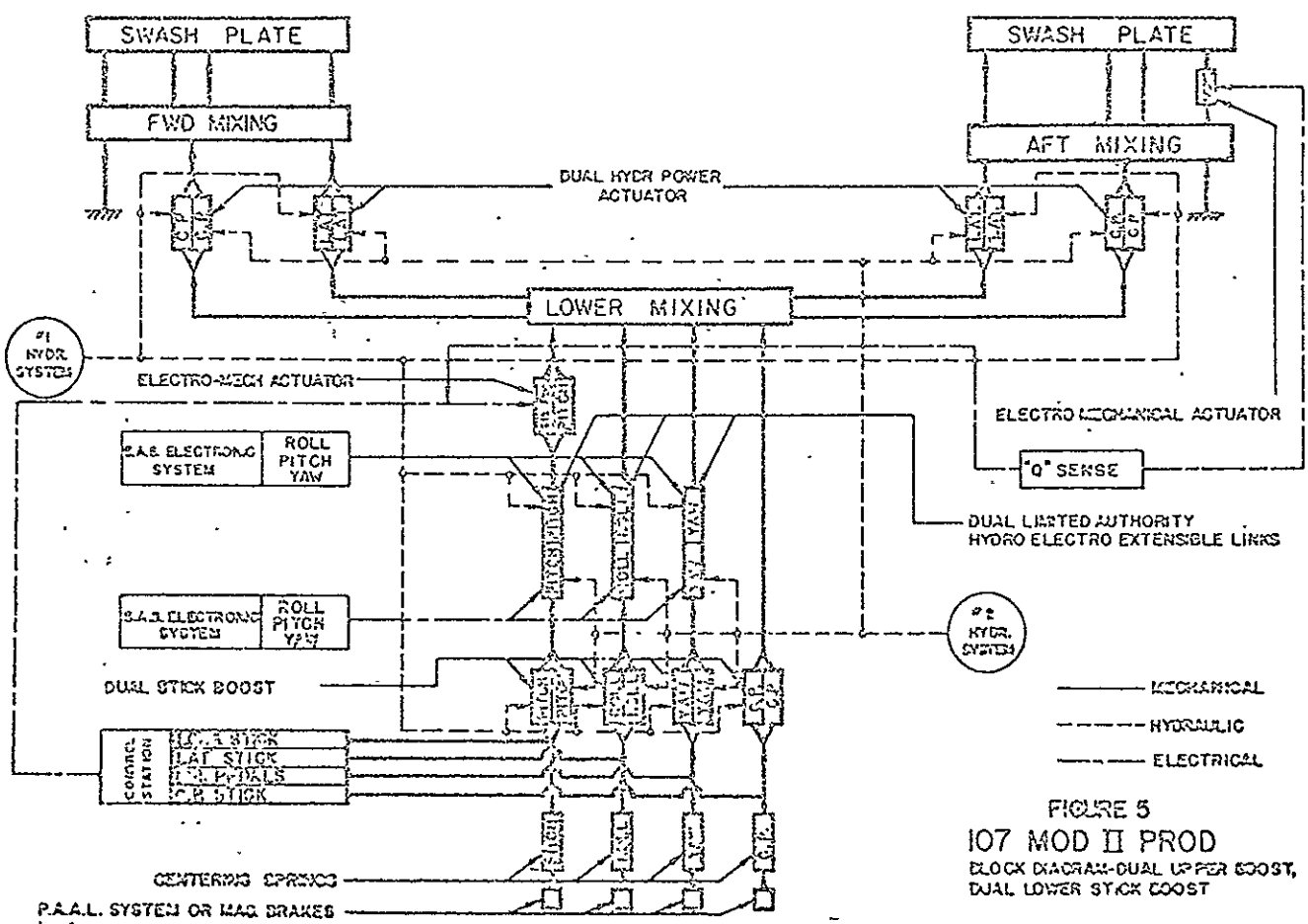

FIGURE 5

107 MOD II PROD

BLOCK DIAGRAM-DUAL UPPER BOOST, DUAL LOWER STICK BOOST

RUN 16

FIGURE 6
PITCH AXIS RESPONSE

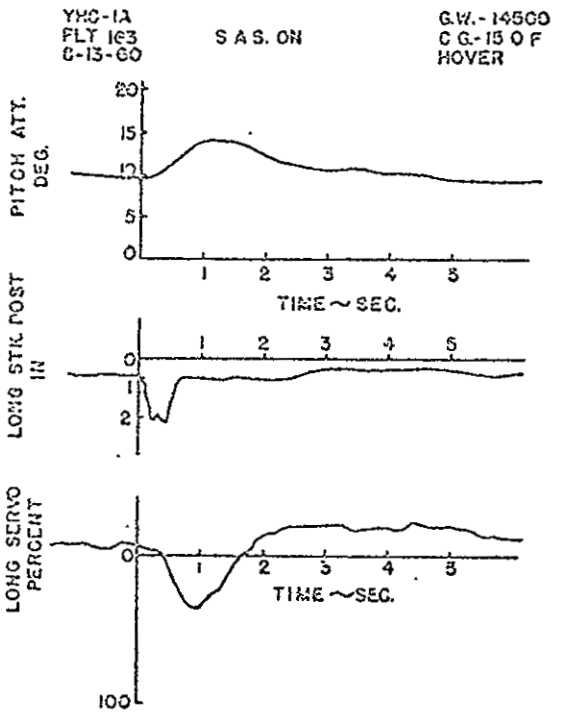

RUN 13

FIGURE 8
YAW AXIS RESPONSE

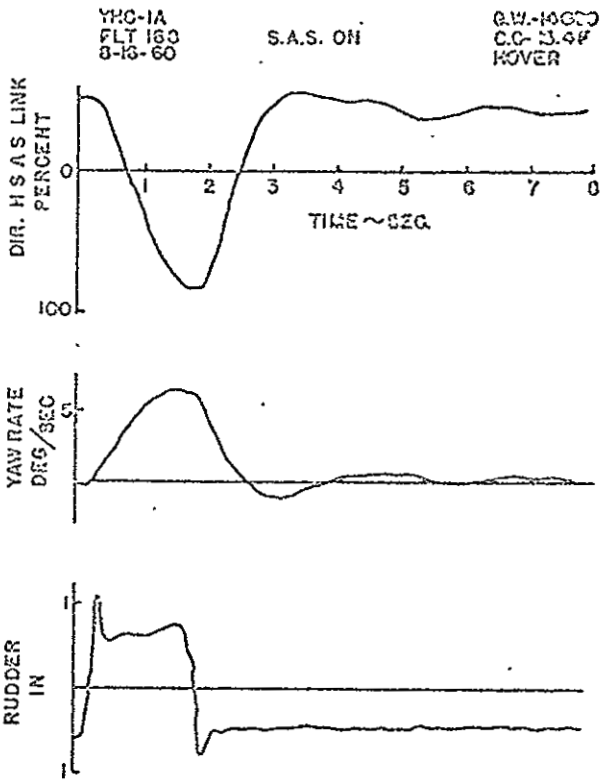

RUN 12

FIGURE 7
ROLL AXIS RESPONSE

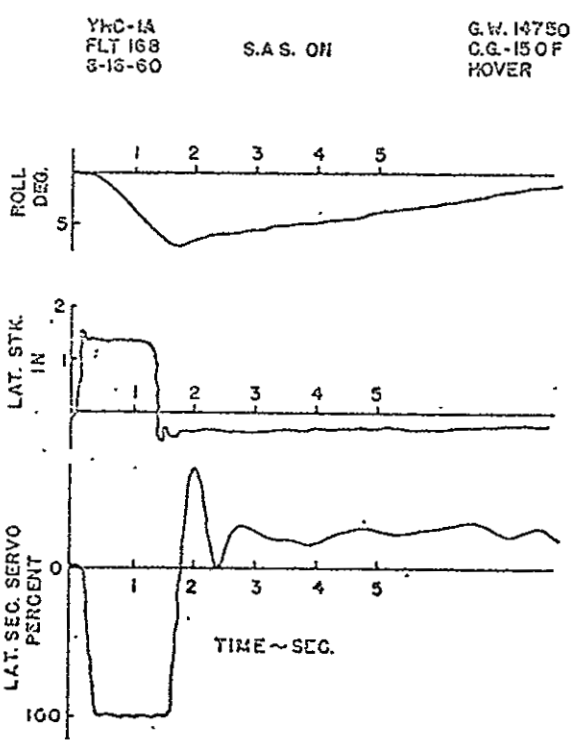

RUN 13

FIGURE 9

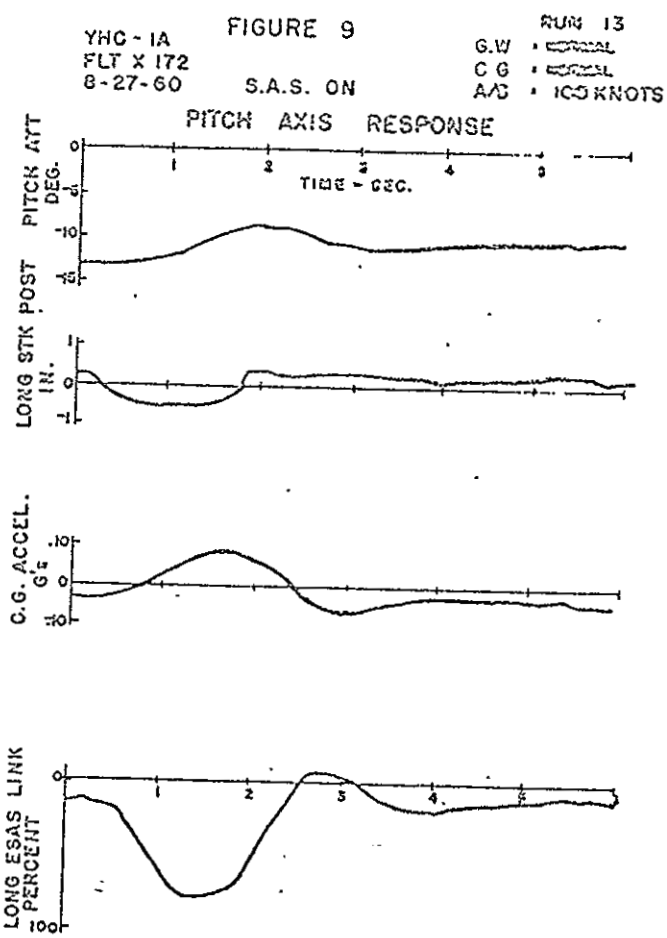

VERTOL 107 PROTOTYPE. FIGURE 10

FLT X 212

S.A.S ON

G.W. = 14040
C.G. = 2'1" FWD
A/S 100 KNOTS

ROLL . YAW RESPONSE

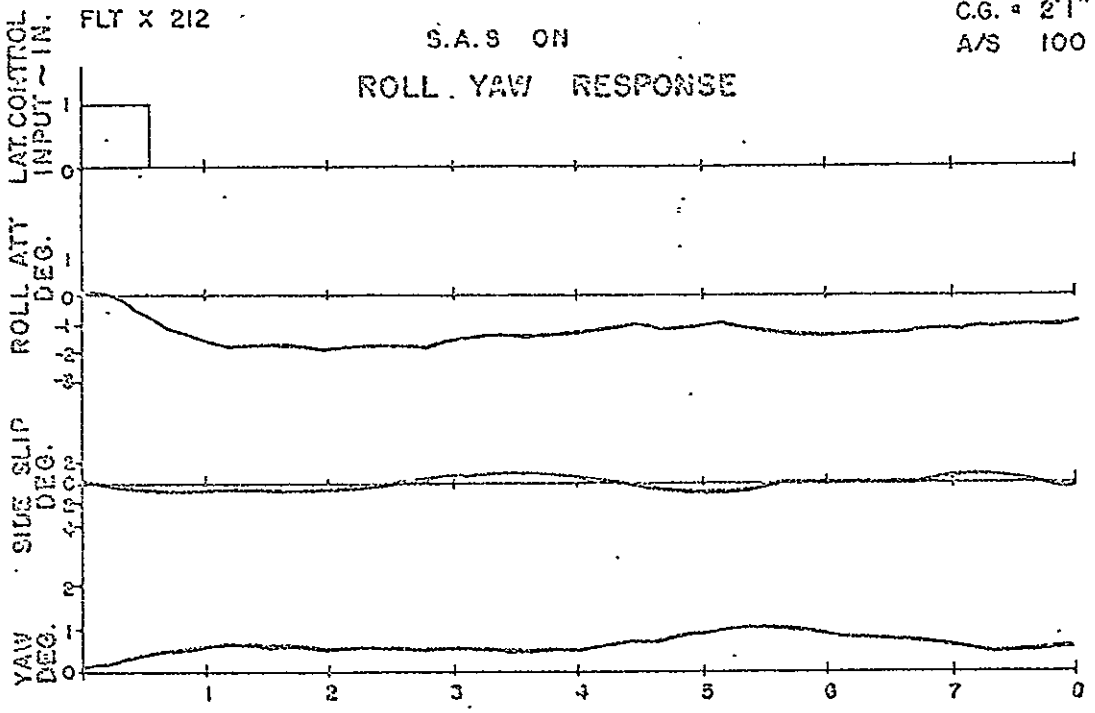

TIME ~ SEC.

VERTOL P.A.A.L. SYSTEM ACTUATOR

FIGURE 11

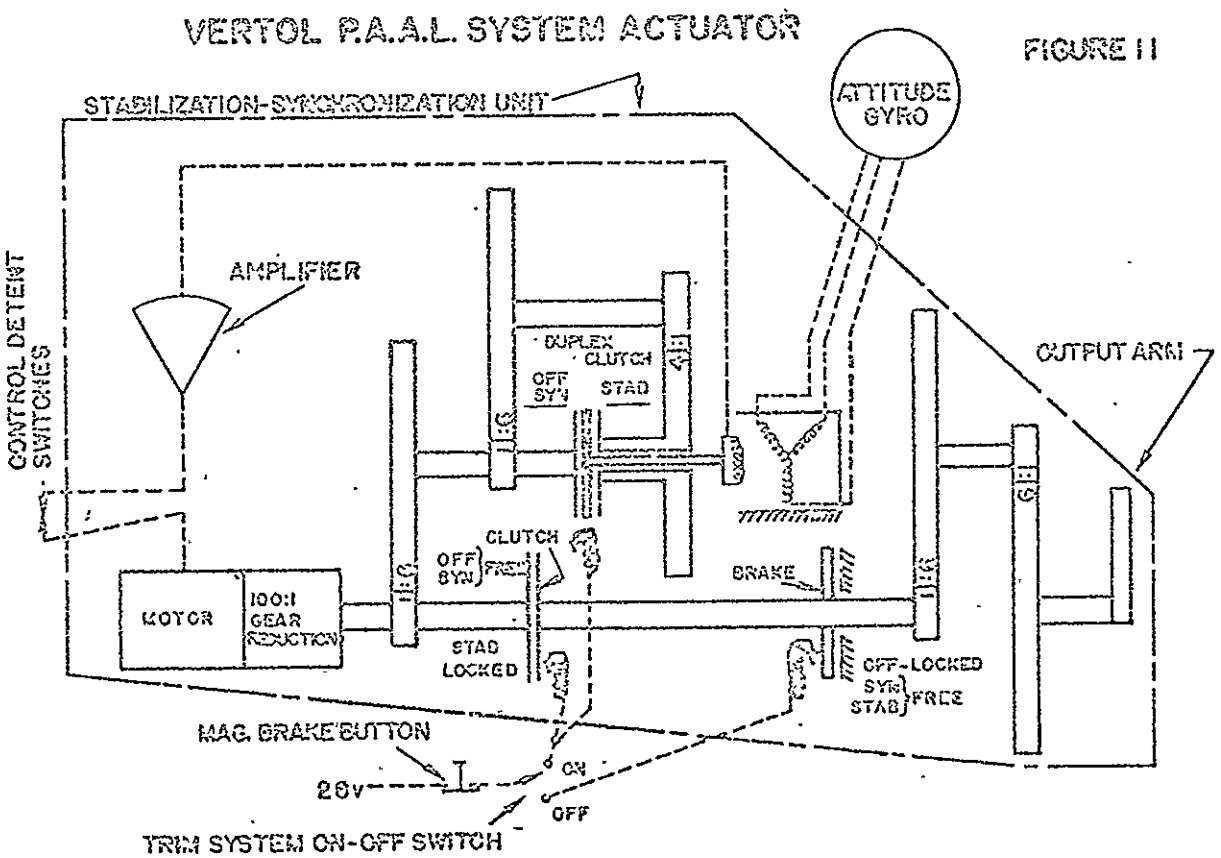

FAIL SAFE ACTUATOR

FIGURE 13

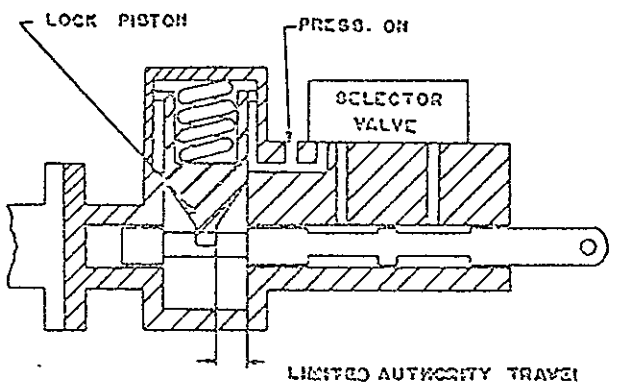

S A S ON

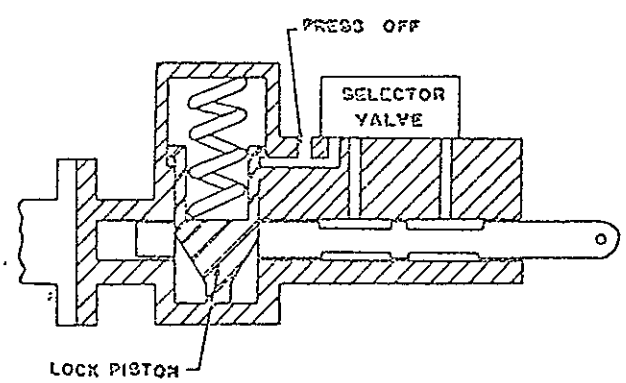

S.A.S. OFF

APPENDIX M

BIBLIOGRAPHY

1. Truxal, John C., Control System Synthesis, McGraw-Hill, N.Y. 1955.

2. Clark, Robert N., Introduction to Automatic Control Systems, Wiley, N.Y. 1962.

3. Laning and Battin, Random Processes in Automatic Control, McGraw-Hill, N.Y. 1956.

4. Kuo, Benjamin C., Analysis and Synthesis of Sampled-Data Control Systems, Prentice-Hall, N.J. 1963.

5. Tou, Julius T., Digital and Sampled-Data Control Systems, McGraw-Hill, N.Y. 1959.

6. Grabbe, Ramo, and Wooldridge, Handbook of Automation, Computation, and Control, Volume I, Wiley, N.Y. 1958.

7. Systems Technology, Inc., Analysis of Multiloop Vehicular Control Systems, ASD-TDR 62-1014, 1964.

8. Houbolt, J.C.; Steiner, R.; Pratt, K. G., Dynamic Response of Airplanes to Atmospheric Turbulence Including Flight Data on Input and Response, NASA TR R-199, June 1964.

9. Press, H.; Meadows, M. T.; Hadlock, I., A Reevaluation of Data on Atmospheric Turbulence and Airplane Gust Loads for Application in Spectral Calculations, NACA Report 1272, 1956.

10. Mazelsky, B.; Armez, Jr., On the Simulation of Random Excitations for Airplane Response Investigations on Analog Computers, IAS Preprint #686, January 1957.

11. Clementson, G. C., An Investigation of the Power Spectral Density of Atmospheric Turbulence, Ph.D. Thesis, Massachusetts Institute of Technology, Instrumentation Laboratory report 6445-T31, 1950.

12. Gessow and Myers, Aerodynamics of the Helicopter, MacMillan, N.Y., 1952.

13. Nikolsky, Alexander A., Helicopter Analysis, Wiley, N.Y., 1951.

14. Seckel, Edward, Stability and Control of Airplanes and Helicopters, Academic Press, N.Y., 1964.

15. Payne, P. R., Helicopter Dynamics and Aerodynamics, MacMillan, N.Y., 1959.

16. Proceedings of NASA Conference on V/STOL and STOL Aircraft, NASA Report No. SP-116, April 1966.

17. Wolkovitch, J., and R. P. Walton, "VTOL and Helicopter Approximate Transfer Functions and Closed Loop Handling Qualities", Systems Technology, Inc. Technical Report No. 128-1, June 1965.